Using next-generation multi-spectral FRRf to improve current estimates of marine primary production (MPP) within Australian waters

David J. Hughes

April 2018

A thesis submitted in fulfillment of the requirements for the degree of Doctor of Philosophy in Science

C3 Climate Change Cluster, School of Life Sciences, University of Technology Sydney

Certificate of Original Authorship

I certify that the work in this thesis has not previously been submitted for a degree nor has it been submitted as part of requirements for a degree.

I also certify that the thesis has been written by me. Any help that I have received in my research work and the preparation of the thesis itself has been appropriately acknowledged. In addition, I certify that all information sources and literature used are indicated in the thesis.

Production Note:
Signature removed prior to publication.

David J. Hughes

12/04/2018

Dedication

This thesis is dedicated to my parents, Peter and Rose, who shared their appreciation for the natural world with me from an early age, and sparked a lifelong interest in marine science.

Many times over the years they have encouraged me to follow the path that makes me happy and have supported me every step of the way. It is with their support that I embarked on this journey, and this thesis stands as a testament to the belief that they have shown in me.

Now I have reached the conclusion of this journey I look back with full appreciation for their love and support.

Acknowledgements

There are many people to thank for helping me along this journey. First and foremost, I thank my primary supervisor, David Suggett for introducing me to the challenging, but rewarding field of FRRf which ultimately led me to move to the other side of the world to embark on this PhD. Throughout my PhD you always took time out to answer questions, offer guidance and generally help me see the wood for the trees. You have been an inspiration and I hope to have the opportunity to work alongside you again in the future.

I would also like to thank my co-supervisors, Peter Ralph and Martina Doblin for their invaluable help, particularly for taking time out of their busy schedules to turn-around drafts of manuscripts at short notice.

Thanks to Paul Brooks, the vital cog in the machine at C3 who finds technical solutions to keep everybody's research (including mine) ticking along. Thanks to Paul, and Graeme Poleweski, my PhD experience was made a whole lot easier. Thanks also to Gemma, Sue, Phil, Milan, Joey, Dale, and Vinnie for technical support and assistance along the way.

To members of my lab group: Lisa, Sam, Caitlin, Emma, Mickael, and Fernanda for all of your help and moral support along the way. The same applies to Arjun, Ric, Rendy, Leo, Bonnie, Trent, Fabio and Marco A. for the numerous chats (strictly scientific of course) over coffee.

Paul Van Ruth and Mark Doubell for inviting me to collaborate onboard the RV *Investigator* for 3 weeks of research in the Great Australian Bight and for making me feel part of their team – an experience that I will remember long after my PhD.

Marco #1, Marco #2 and Deepa for the good times crammed into the radiation lab onboard the RV *Investigator* for 3 weeks - I'm sure none of us will forget that experience in a hurry. To the crews of the RV *Investigator* and RV *Zelda Faith* for all of their support during oceanographic fieldwork.

My research was only made possible thanks to financial support from the C3 Climate Change Cluster and from UTS via the President's scholarship.

Last, but not least, a special thanks to Deepa Varkey who has been my rock and a pillar of strength to get me through these final few months leading up to submission. I look forward to resuming a normal life with you again…

Table of Contents

List of Figures

List of Tables

List of Supplementary Figures

List of Supplementary Tables

List of Abbreviations

AEF	Alternative electron flow
ANACC	Australian national algal culture collection
ANOVA	Analysis of variance
ATP	Adenosine triphosphate
Bac	Bacillariophyceae
C	Carbon
CCM	Carbon concentrating mechanism
CDOM	Coloured dissolved organic matter
CEF-PSI(II)	Cyclic electron flow around PSI(II)
CO_2	Carbon dioxide
Chl	Chlorophyceae
Chl-*a*	Chlorophyll *a*
Cry	Crptophyceae
CTD	Conductivity, temperature and depth
Cya	Cyanobacterium/Cyanophyceae
dbRDA	Distance-based redundancy analysis
DCMU	3-(3,4-dichlorophenyl)-1,1-dimethylurea
Dia	Diatom
DIC	Dissolved inorganic carbon
Din	Dinophyceae
DistLM	Distance-based linear modeling
DOC	Dissolved organic carbon
DPM	Disintegrations per minute
EAC	East Australian Current
Eus	Eustigmatophyceae
FDOM	Fluorescent dissolved organic matter
FDP	Flavodiiron protein
FIRe	Flash Induction and Relaxation fluorometry
Fla	Flagellate
Flv	Flavoproteins
FRRf	Fast Repetition Rate fluorometry
FY	Fluorescence Yield
GAP	Glyceraldehyde 3-phosphate
GC	Gas chromatography
GPP	Gross primary production
Hap	Haptophyte
HCl	Hydrochloric acid
$HgCl_2$	Mercuric chloride
HPLC	High-performance liquid chromatography
IMOS	Integrated Marine Observing System
LED	Light emitting diode

LEF	Linear electron flow
MDS	Multidimensional scaling
MIMS	Membrane inlet mass spectrometry
MLD	Mixed layer depth
MPP	Marine primary production
N	Nitrogen
N_2	Atmospheric Nitrogen
$NADP^+(H)$	Nicotinamide adenine dinucleotide phosphate
$NaH^{14}CO_3$	^{14}C-labelled Sodium bicarbonate
NaH_2PO_4	Sodium phosphate dibasic
NE	North east
NH_4^+	Ammonium
NH_4NO_3	Ammonium nitrate
NO_2^-	Nitrite
NO_3^-	Nitrate
NPP	Net primary production
NPQ	Non-photochemical quenching
NPQ_{NSV}	NPQ(normalised Stern-Volmer coefficient)
NSW	New South Wales
O_2	Oxygen
OCP	Orange carotenoid protein
P	Phosphorus
Pabs	Particulate absorption spectra
PAM	Pulse amplitude modulated fluorometry
PAR	Photosynthetically active radiation
PCA	Principal component analysis
PE	Photosynthetic-irradiance
Pel	Pelagophyceae
PH	Port Hacking
Pmf	Proton motive force
PO_4^{3-}	Phosphate
POC	Particulate organic carbon
PON	Particulate organic nitrogen
POP	Particulate organic phosphorus
PP	Primary production
PQ	Plastoquinol
PQ	Photosynthetic quotient
Pry	Prymnesiophyceae
PSI	Photosystem I
PSII	Photosystem II
PSU	Practical salinity unit
PSU	Photosynthetic unit
PTOX	Plastiquinol terminal oxidase
Q_A	Quinone-A electron acceptor

q_E	Energy-dependent Quenching
ROS	reactive oxygen species
rpm	Revolutions per minute
RuBisCO	Ribulose-1,5-bisphosphate carboxylase/oxygenase
S	Sulphur
Scf	Spectral correction factor
Si	Silicate
SiO_4	Silicate
SST	Sea surface temperature
ST	Single turnover
SVP	Surface velocity program
TOC	Total organic carbon
V	Cell volume

List of Symbols

a^{Chl}	Spectral light absorption
a_{LHII}	PSII absorption coefficient of the light-harvesting pigments
$A(\lambda)$	Wavelength-dependent absorbance
β	Pathlength amplification factor
C	Fraction of [RCII] in the closed state
d^{-1}	Daily division rate
ΔpH	Proton gradient
E	Irradiance
E_K	Light saturation parameter
E_{LED}	Intensity of the fluorometers 450 nm measuring beam
$\mathrm{ETR_{PSII}}$	Electron Transport Rate through PSII
Φ_{PSII}'	quantum yield of photochemistry under actinic light
F'	Fluorescence yield under actinic light at time t
F_0	Minimum PSII fluorescence yield (dark-acclimated state) where all PSII reaction centres are open
F_0'	Minimum PSII fluorescence yield (light-acclimated state) where all PSII reaction centres are open
F_m	Maximum PSII fluorescence yield (dark-acclimated state) where all PSII reaction centres are closed
F_m'	Maximum PSII fluorescence yield (light-acclimated state) where all PSII reaction centres are closed
F_t	Steady-state fluorescence
F_v	Maximum variable PSII fluorescence yield (dark-acclimated state)
F_v'	Variable fluorescence yield under actinic light
$\mathrm{F_v/F_m}$	Maximum photochemical efficiency (dark-acclimated state)
$\mathrm{F_v'/F_m'}$	Maximum photochemical efficiency (light-acclimated state)
$\mathrm{F_q'/F_m'}$	Effective photochemical efficiency under actinic light
$\mathrm{F_q'/F_v'}$	PSII efficiency factor (under actinic light
K_C	Electron requirement for carbon fixation
K_R	Instrument-specific constant
L	Optical pathlength of filter particulates
λ	Wavelength
μ	Growth rate
n_{PSII}	Assumed ratio of PSII reaction centres per unit chlorophyll-*a*
qE	Energy-dependent quenching
qJ	FRRf connectivity model (assumes partial connectivity between RCIIs)
qP	Photochemical quenching parameter
[RCII]	Concentration of functional PSII reaction centres
$[\mathrm{RCII}]^{(\mathrm{FRRf})}$	Concentration of [RCII] as estimated by FRRf
ρ	PSII Connectivity Factor

ρ'	PSII Connectivity Factor under actinic light
ROS	Reactive Oxygen Species
σ_{PSII}	Functional absorption cross-section of PSII
$\sigma_{PSII}(')$	Functional absorption cross-section of PSII (under actinic light)
τ_{PSII}	Turnover time of PSII
Y	Fractional yield
YF	Fluorescence yield
YPSII	Photochemical yield of PSII

Summary

Bio-optical tools remain key technologies to address a long-standing goal in oceanography: to improve understanding of how marine primary productivity (MPP) varies over space and time. A major goal for one particular technique, Fast Repetition Rate fluorometry (FRRf), is to retrieve highly resolute patterns of carbon (C) uptake *in situ* to improve satellite retrieved predictions of MPP. However, this goal hinges upon the application of a highly-variable, yet poorly-understood conversion factor to scale FRRf-derived electron transport rates (ETRs) to rates of C-uptake. Understanding of the conversion factor, termed the "electron requirement for carbon fixation" (K_C) is limited, in particularly for Australian waters where K_C has rarely been measured.

This thesis focuses on coupled ETR – C-uptake measurements, to examine how key factors drive variability in K_C, utilising both laboratory and field studies to isolate the respective influences of growth environment and phytoplankton taxonomy. I performed nutrient addition bioassays upon natural phytoplankton assemblages to demonstrate for the first time how macronutrient availability (N, P and Si) regulates K_C at an Australian coastal reference station when nutrient concentrations are low during summer. To examine taxonomic variability of K_C together with metrics influencing phytoplankton growth and physiology (cell size and non-photochemical quenching, NPQ), I grew phytoplankton covering a broad range of taxonomic and size classes within a controlled laboratory setting where environmental variability could be excluded. Finally, to examine how well K_C could be predicted in a highly-dynamic system with multiple environmental stressors and phytoplankton assemblages, I performed a novel high-throughput assessment of K_C (n = 80) along the eastern Australian coast spanning multiple water masses including the Tasman Sea and the East Australian Current

(EAC). Prevailing environmental variables, physiological (non-photochemical heat dissipation, NPQ_{NSV}) and phytoplankton community structure (size-fractionated Chl-*a*) were also measured for each sample to allow evaluation of their respective performance in empirically modelling K_C variance.

This thesis highlights the importance in characterising both environmental and taxonomic factors to most robustly retrieve K_C, but also demonstrates that a single FRRf parameter (NPQ_{NSV}) may reliably explain ~50% of variability in eastern Australian waters. These new findings potentially provide new and unprecedented capacity to retrieve C-fixation rate from FRRf-based productivity assessments, but ultimately require further validation that may be possible through re-visiting past FRRf data sets. These findings are then considered to propose a roadmap to enable broader implementation and uptake of FRRf for widespread assessments of marine (and freshwater) primary productivity into the future.

Declaration of the Contribution to Each Chapter

Chapter 2

This chapter has been submitted for publication in Limnology and Oceanography as:

Hughes DJ, Varkey D, Doblin M.A, Ingleton T, McInnes A, Ralph P.J, Van Dongen-Vogels V, Suggett D.J (2017) Impact of nitrogen availability upon the electron requirement for carbon fixation in Australian coastal phytoplankton communities. Currently under review. Experimental design was by DJH with help from DJS. Fieldwork was conducted by DJH, VVDV and TI. Laboratory sample analysis was performed by DH with help from DS. Data analysis and interpretation was done by DJH with help from DV and DJS. Writing of the manuscript was completed by DJH with help from DJS, DV, MAD and PJR.

Chapter 3

The experiments of this study were designed by me, with help from Assoc. Prof. David Suggett (UTS). I was responsible for the majority of laboratory work, data analysis and interpretation, and the writing-up of the manuscript. Dr. Maria Giannini (UTS) and Arjun Verma (UTS) grew and provided several phytoplankton strains used in this experiment. Dr. Joseph Crosswell (CSIRO) provided assistance with analysis of dissolved inorganic carbon. Dr. Deepa Varkey (Macquarie University) provided support with R-software. Assoc. Professor David Suggett, Prof. Peter Ralph (UTS), Assoc. Professor Martina Doblin (UTS) and Dr. Deepa Varkey provided detailed feedback on the manuscript at various stages.

Chapter 4

The data presented in this chapter reflects a joint laboratory effort. I was responsible for the experimental design, methodological development, data interpretation, and write-up of the manuscript with help from Assoc. Professor David Suggett (UTS). I performed the coupled ^{14}C/FRRf incubations, and jointly conducted size-fractionated Chl-a analysis with Assoc. Professor David Suggett (UTS). Assoc. Professor David Suggett collected multispectral FRRf measurements. Dr. Joseph Crosswell (CSIRO) performed analysis of dissolved inorganic carbon. Assoc. Professor Martina Doblin (UTS), Prof. Peter Ralph (UTS) and Assoc. Professor David Suggett were instrumental in securing ship-time.

Chapter 6

This opinion paper reflects a joint effort. I was responsible for writing the majority of the original manuscript which was then significantly improved by contributions from Assoc. Professor David Suggett (UTS), Dr Doug Campbell (Mount Allison University), Professor Mark Moore (Univeristy of Southampton). Dr Evelyn Lawrenz and Prof. Ondrej Prasil (Czech Academy of Sciences) performed time-resolved measurements of ^{14}C-incubations and provided significant intellectual input into the manuscript. Assoc. Prof. Martina Doblin and Marco Alvarez (UTS) performed short vs long-term ^{14}C incubations and provided comprehensive feedback on the manuscript.

1 Chapter 1

General Introduction

Unicellular phytoplankton are responsible for the vast majority (~95%) of marine primary productivity (MPP) (Geider et al. 2001). Their photosynthetic conversion of inorganic carbon (C), and other nutrients, into organic compounds supports virtually all life in the oceans, sets the upper limit for sustainable fisheries harvest and profoundly influences global biogeochemical cycles (Falkowski et al. 1998). Collectively, these ubiquitous microorganisms account for half of primary production on Earth, fixing ~30-50 billion tons of C per year (Falkowski, 1994) and thus, play a key role in regulating our climate via the drawdown of atmospheric CO_2 and simultaneous release of biogenic volatile gases (Hoegh-Guldberg and Bruno, 2010; Kostadinov et al. 2010). Thus, the capacity to accurately determine MPP is recognised as a key goal for management of marine resources to monitor the health of the marine environment and understand global ecosystem functioning (Beardall et al. 2009). Despite this, the magnitude and variability of MPP remains poorly characterised, in part due to methodological constraints and as such, global models of MPP contain a large degree of uncertainty (Chavez et al. 2011; Saba et al. 2011; Laufkötter et al. 2015).

Satellite remote-sensing of ocean colour is currently the most powerful tool available to measure MPP across the marine environment, which comprises a total surface area >360,000,000 km^2 (Saba et al. 2011). However, satellites do not directly measure photosynthetic rates, but instead estimate Chlorophyll-a (Chl-*a* - the pigment molecule central to all oxygenic phytoplankton) concentration via ocean colour. In turn, phytoplankton photosynthetic rates can be modelled factoring in knowledge of

additional environmental variables such as sea surface temperature (SST). However satellite-based models of MPP rely upon "ground-truthing" from *in-situ*, discrete measurements of photosynthetic rates which are sparse in number, can date back nearly a century and may reflect anywhere between gross or net primary production (GPP and NPP respectively), dependent upon disparities in methodology (Bailey and Werdell, 2006; Chavez et al. 2011; Regaudie-de-Gioux et al. 2014). Furthermore, measurements are often spatio-temporally biased, with few data existing for coastal regions and the southern hemisphere in general (Cheah et al. 2011; Everett and Doblin, 2015), thus including Australian waters.

To date, the most widely-utilised method to ground-truth satellite models of NPP is that of the ^{14}C-bicarbonate uptake method (henceforth referred to as the ^{14}C-method, Steemann-Nielsen, 1952; see also Lewis and Smith, 1983) which quantifies photosynthetic rates by tracing the incorporation of radio-labelled inorganic C into phytoplankton cells during *ex-situ* incubations (Beardall et al. 2009). Estimates of photosynthetic rates generated via the ^{14}C-method have generally been considered to represent the "gold standard" benchmark against which the majority of satellite-based MPP models are calibrated, despite persistent methodological concerns (see Longhurst et al. 1995; Melrose et al. 2006). An often-cited criticism of the ^{14}C-method concerns the length of incubation, as variable timeframes can capture a photosynthetic rate reflecting anywhere along a continuum from GPP to NPP (Beardall et al. 2009; see also Halsey et al. 2010, 2011, 2013). In theory, shorter incubation times (conventionally interpreted by oceanographers to be within the timeframe of several hours, but discussed later in Section 1.5.2) should approximate GPP, whilst lengthy incubations, e.g. over a full diel period should approximate something much closer to NPP (Dring and Jewson, 1982). However, a historical lack of standardisation surrounding the

choice of incubation lengths used, together with additional methodological protocols (see also Section 1.5) has effectively limited how well ^{14}C-uptake rates can be reconciled across broad spatial scales (Regaudie-de-Gioux et al. 2014). Thus, persistent uncertainty regarding the process actually captured by the ^{14}C method (i.e. GPP, NPP or somewhere in-between), the relatively low sampling resolution afforded by the length incubation process and increasing regulations surrounding the use of radioisotopes in the field (Mateo et al. 2001; Robinson et al. 2014), has led to increased exploration of alternative methods to estimate MPP free from such constraints.

Indeed, oceanographers have increasingly gravitated towards a class of bio- optical instrumentation that 'actively' probes photosynthesis; notably, Chl-*a* fluorometry. In active-fluorometry, controlled excitation protocols can perturb the signature of fluorescence emitted by Chl-*a* as a means to estimate the instantaneous rate of photosynthesis (e.g. Suggett et al. 2010). Active Chl-*a* fluorometers can therefore be placed alongside numerous other autonomous sensors describing physical, chemical and biological properties of the water column (or surface waters), enabling unprecedented insight into how environmental and taxonomic variability influence MPP (Suggett et al. 2006; Lawrenz et al. 2013).

1.1 Estimating MPP with Fast Repetition Rate Fluorometry (FRRf)

Active Chl-*a* fluorometry describes instrumentation and protocols designed to actively probe the photochemical status of the oxygen-evolving complex at photosystem II (PSII) (for a full description see Huot and Babin, 2010). Briefly, virtually all (>95%) Chl-*a* fluorescence emanates from the core chlorophyll molecule at PSII (P680) at room temperature as a result of energy transfer between various photosynthetic complexes (see Krause and Weis, 1993); importantly light absorbed by the PSII antennae is passed

to P680 where it undergoes one of three "fates": (i) driving charge separation at P680 resulting in splitting of water to generate an electron for subsequent photochemical electron transfer, or is returned to the antennae where it is re-emitted at longer wavelengths (lowered energy) as (ii) heat or (iii) fluorescence. Assessing the probability of absorbed energy emitted via these three pathways can therefore inform the extent to which excitons are used for photochemistry versus non-photochemical down-regulation (i.e. dissipated as heat).

Electrons extracted from water at PSII can flow via PSI photochemistry through to NADPH during a series of electron transfer reactions, a process referred to as linear electron transport (Rochaix, 2011). This process is coupled with proton pumping into the thylakoid lumen, generating proton motive force (pmf) which can be harnessed to produce energy (ATP), which together with NADPH fuels the Calvin-Benson-Bassham cycle (hereafter referred to as the Calvin Cycle) during carbon-fixation (see Behrenfeld et al. 2008).

Fast Repetition Rate fluorometry (FRRf, Kolber et al. 1998) is a specific type of active Chl-*a* fluorometry, so-called because it delivers a series of closely-spaced excitation flashes to transiently close all PSII reaction centres, stimulating a fluorescence yield transient (Kromkamp and Foster, 2003). Complete PSII closure occurs within a timeframe of <200 μs, fast enough to reduce the first acceptor molecule within the photosynthetic electron transport chain (Q_A) once only, and thus is referred to as a "single- turnover" (ST) protocol (Kromkamp and Forster 2003; Suggett et al. 2003). From this ST fluorescence transient (Fig 1.1), a number of photosynthetic parameters associated with PSII can be derived by fitting a biophysical model describing photochemistry (Kolber et al. 1998). In turn, these parameters can be used to estimate

the linear photosynthetic electron transport rate (ETR_{PSII}) (Fig. 1.2). Strictly, since generation of electrons at PSII results from splitting of water to produce O_2, FRRf-based photochemistry rates (ETR_{PSII}) should therefore be indicative of gross O_2 evolution (Genty et al. 1989) (discussed further in Section 1.2).

FRRf has been the widely-applied variant of active fluorometry to probe phytoplankton photosynthetic rates *in-situ* (Suggett et al. 2009; Oxborough et al. 2012), because its high-sensitivity makes it well-suited to oceanographic research even in low biomass, oligotrophic waters (Laney, 2003; Röttgers, 2007). Data can be acquired at unprecedented resolution (a highly-averaged induction curve requires <1 s) with additional capability to measure photophysiological descriptors such as the functional absorption cross-section of PSII (σ_{PSII}) which allows for calculation of photochemical flux through each PSII reaction centre (Oxborough et al. 2012, see section 1.2).

Crucially, a recently-developed algorithm (Oxborough et al. 2012; later modified by Murphy et al. 2017 to include a correction factor accounting for possible photoinibition) enables FRRf to measure MPP without the need to include ancillary measurements or use assumed constants (discussed further in Section 1.5). As such, FRRf has vast potential as an autonomous productivity sensor for marine waters, particularly for dynamic regions where biomass can be highly variable, including coastal waters or during periods of dynamic phytoplankton blooms.

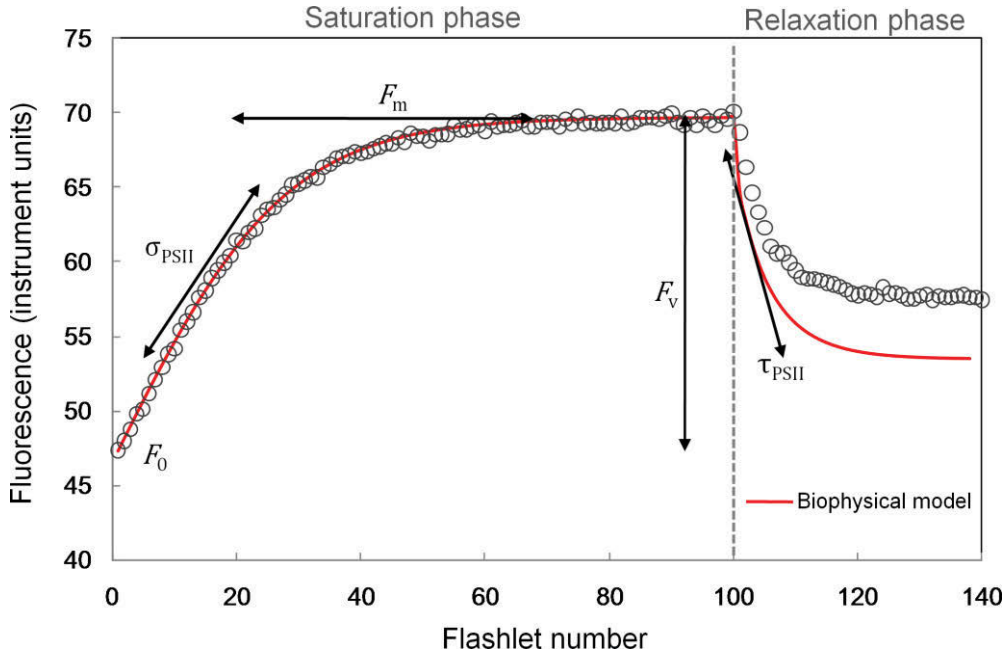

Figure 1.1 Fluorescent transient derived from a single-turnover (ST) FRRf measurement using a culture of the marine diatom, *Ditylum brightwelli*. Each open circle represents the fluorescence yield (instrument units) from each excitation flashlet. The FRRf was programmed to deliver a ST saturation phase of PSII from 100 flashlets (1 µs pulse with a 2 µs interval), to sequentially close all PSII reaction centres and stimulate an increase from minimal (F_0) to maximum (F_m) fluorescence; followed by a relaxation phase of 40 flashlets (1 µs pulse with a 50 µs interval) to monitor decay kinetics (indicating re-opening of PSII) and thus derive PSII turnover time (τ_{PSII}). The rate of increase between F_0 and F_m can be used to calculate the functional absorption cross-section of PSII (σ_{PSII})

1.2 Determination of the Electron Transport Rate (ETR) by FRRf

Linear electron flow (LEF) is the primary pathway of photosynthesis and involves the coupling of the light-driven charge separation events that occur at photosystems I (PSI) and II (PSII). Electrons extracted from water at PSII are transferred along the electron transport chain to PSI via the plastiquinone pool (PQ pool) and cytochrome b_6f complex (Cyt b_6f). From PSI, electrons are then transferred to ferredoxin, and eventually $NADP^+$ to generate NADPH (Rochaix, 2011). This transfer of electrons results in the simultaneous pumping of protons from the stroma into the thylakoid lumen, building

proton motive force (pmf) which can be harnessed to generate ATP (Hald et al. 2008). NADPH and ATP generated by LEF can subsequently be used to fuel C-fixation via the Calvin-Benson cycle (e.g. Woodrow and Berry, 1988; Behrenfeld et al. 2008). Given that FRRf measures the electron transfer rate from charge separation at PSII it is therefore an indicator of the maximum potential to drive generation of photosynthetically-derived energy (ATP) and reductant (NADPH) which is available for C-fixation (Fisher and Halsey, 2016). As with other bio-optical algorithms describing productivity (e.g. Behrenfeld and Falkowski, 1997), photosynthetic ETR_{PSII} is determined from a common mathematical construct: the product of light intensity, how much of this light is absorbed and the proportion of this absorbed light which is subsequently used to drive photochemistry; specifically, irradiance (E), the PSII absorption coefficient of the light-harvesting pigments (a_{LHII}) and the quantum yield of photochemistry under actinic light (ϕ_{PSII}) (Eq. 1):

$$\mathrm{ETR_{PSII}} = E \cdot a_{\mathrm{LHII}} \cdot \Phi_{\mathrm{PSII}} \quad (1)$$

Several different approaches exist with which to parameterise a_{LHII} and ϕ_{PSII} (these will be discussed further in Section 1.5) which has resulted in an array of different algorithms with which to calculate ETR_{PSII} from FRRf fluorescence parameters (Suggett et al. 2010). The most commonly used (Lawrenz et al. 2013; Robinson et al. 2014) is the biophysical "sigma-based" algorithm originally developed by Kolber and Falkowski (1993) (Eq. 2).

$$\mathrm{ETR_{PSII}} = E \cdot \sigma_{\mathrm{PSII}}' \cdot (1/[F_\mathrm{v}/F_\mathrm{m}]) \cdot [\mathrm{RCII}] \cdot (1 - C) \quad (2)$$

$$a_{\mathrm{LHII}} = \sigma_{\mathrm{PSII}} \cdot (1/[F_\mathrm{v}/F_\mathrm{m}]) \cdot [\mathrm{RCII}]$$

$$\Phi_{\mathrm{PSII}}' = [\sigma_{\mathrm{PSII}}'/\sigma_{\mathrm{PSII}}] \cdot (1 - C)$$

where E is the irradiance (photons m^{-2} s^{-1}), σ_{PSII}' is the functional absorption cross-section of PSII (nm^2 $quanta^{-1}$), [RCII] is the concentration of functional reaction centres (mol RCII m^{-3}), C is the fraction of [RCII] in the closed state. The inclusion of the factor $1/[F_v/F_m]$ (where $F_v/F_m = [F_m - F_0]/F_m$) accounts for the non-radiative loss of energy associated with σ_{PSII}' (Kolber et al. 1998; Suggett et al. 2009; Oxborough et al. 2012). Both [RCII] and (1 - C) are required to measure gross photosynthesis (see Kolber and Falkowski, 1993), yielding ETR (e^- m^{-3} s^{-1}). Eq. 2 (and other derivatives) assumes an efficiency of one charge-separation event per photon absorbed (Kolber and Falkowski, 1993). Until recently [RCII] had to either be assumed, derived or laboriously measured (see Suggett et al. 2004), which has proven impractical for the majority of oceanographic studies; however, fluorescence algorithm developments (Oxborough et al. 2012; Murphy et al. 2017) allow for $[RCII]^{(FRRf)}$ to be estimated from FRRf parameters as follows:

$$[RCII]^{(FRRf)} = \frac{KR}{E_{LED}} \cdot \frac{F_0}{\sigma_{PSII}} \quad (3)$$

where KR defines an instrument-specific constant that scales F_0 to σ_{PSII}, E_{LED} is the photon flux density from the FRRf's excitation LED (photons m^{-2} s^{-1}). KR/E_{LED} (m^{-1}) requires a one-time calibration per instrument (using an O_2 flash-yield system) against a sample with known Chl-*a* concentration (Oxborough et al. 2012; Robinson et al. 2014; Silsbe et al. 2015). Once an FRR fluorometer has been calibrated in this fashion, $[RCII]^{(FRRf)}$ can be estimated independently and fed into Eq. 2. Alternatively, Eq. 2 and 3 can be integrated to yield the "absorption algorithm" proposed by Oxborough et al. (2012), which effectively removes the need for σ_{PSII} (σ_{PSII}'), which can be difficult to resolve under high light, together with the need to choose the connectivity model inherent to (1-C); specifically:

$$ETR = \mathrm{E} \cdot \alpha_{\mathrm{LHII}} \cdot \Phi_{\mathrm{PSII}} \left(\text{where } \Phi_{\mathrm{PSII}} = F_{\mathrm{q}}'/F_{\mathrm{m}}' = [F_{\mathrm{m}}' - F']/F_{\mathrm{m}}'\right) \quad (4)$$

$$= \mathrm{E} \cdot (\sigma_{\mathrm{PSII}} \cdot (1/[F_{\mathrm{v}}/F_{\mathrm{m}}]) \cdot [(KR/E_{LED}) \cdot F_0/\sigma_{\mathrm{PSII}}]) \cdot [F_{\mathrm{m}}' - F']/F_{\mathrm{m}}'$$

$$= \mathrm{E} \cdot ([F_{\mathrm{m}} \cdot F_0]/[F_{\mathrm{m}} - F_0]) \cdot ([F_{\mathrm{m}}' - F']/F_{\mathrm{m}}') \cdot (KR/E_{LED})$$

1.3 The electron requirement for carbon fixation, (K_C)

FRRf has potential to revolutionise the way productivity can be quantified *in-situ*, where its unparalleled sampling rate allows for a detailed profiling of the spatio-temporal variability of MPP not possible via conventional methods. The additional bonus of being able to simultaneously measure photophysiological parameters, together with spectrally-discriminating between phytoplankton taxa (see MacIntyre et al. 2010) via next-generation "multispectral FRRf" further strengthens the case for FRRf as a viable means to address global deficiencies in estimating MPP.

However, the majority of key stakeholders interested in MPP measurements require that primary productivity be expressed in the photosynthetic "currency" of fixed-C, not of electrons (i.e. ETR_{PSII}) (Suggett et al. 2009). Therefore, despite electrons being a potentially useful standalone photosynthetic currency in its own right (see Chapter 6), the inference of C fluxes from FRRf-measurements remains a key goal. The ability to convert from ETR_{PSIIs} to C-fixation rates, requires the use of a poorly-understood parameter termed "the electron requirement for carbon fixation" (denoted K_C, see Kromkamp et al. 2008; Lawrenz et al. 2013) describing the number of electrons invested into C biomass. Throughout this thesis, K_C is used as a descriptor as the bulk conversion of electrons (derived from FRRf measurements) into carbon biomass (measured from short-term ^{14}C incubation) and thus, inherently contains potential methodological bias induced from both techniques (discussed further in sections 1.5).

Theoretically, a minimum reference ratio is considered as 4 mol e^- (mol C)$^{-1}$, on the basis that 4 electrons are extracted from 2 H_2O molecules in the production of 1 O_2 molecule and subsequent fixation of 1 CO_2 molecule (Genty et al. 1989; Suggett et al. 2009).

ETR_{PSII} and C-fixation rates have been repeatedly demonstrated to correlate well for phytoplankton in the laboratory (e.g. Fujiki et al. 2007; Suggett et al. 2009) and for natural assemblages (e.g. Kolber and Falkowski, 1993; Suggett et al. 2006; Corno et al. 2006; Kromkamp et al. 2008; Schuback et al. 2015, 2016, 2017; Zhu et al. 2016, 2017), however the slopes of the relationships often differ, thus reflecting (i) natural variability in K_C between studies, or (ii) variability induced by methodological biases between different protocols, or (iii) a combination of both. Deviations from the theoretical minimum have been observed in response to environmental "stress" such as high light (Moore et al. 2006; Brading et al. 2013; Zhu et al. 2016, 2017) and nutrient limitation (Kolber et al. 1988, 1994; Napoleon et al. 2013; Schuback et al. 2015, 2016) (also see Lawrenz et al. 2013). Furthermore, a taxonomic influence upon K_C has been demonstrated by Suggett et al. (2009) reporting K_C values ranging between ~4-12 mol e^- (mol C)$^{-1}$ for 6 phytoplankton taxa in steady-state, nutrient-replete growth (see also Napoleon et al. 2013).

In recognition that K_C is far from a constant value, apparently being regulated by both the environment, and taxonomy, recent efforts have been focussed towards gaining a predictive understanding of this critical parameter. Lawrenz et al. (2013) synthesised all available field data to date and found that K_C was indeed highly-variable, ranging from ~3-65 mol e^- (mol C)$^{-1}$, but demonstrating that it could also be correlated with environmental variables known to regulate MPP such as light, temperature, salinity and macronutrient availability (albeit with a varying degree of success depending upon

geographic location). Their study also showed that coastal sites to generally exhibit the lowest measured K_C values, presumably reflecting a lack of light or nutrient stress, or both. They concluded that variance in K_C probably reflected subtle differences in community composition and/or physiological condition for any given sample and thus was ultimately a product of local biological/environmental conditions. Since then, strong relationships have been established between K_C and light at Ariake Bay, Japan (Zhu et al. 2016, 2017), and between K_C and non-photochemical quenching (NPQ) (Schuback et al. 2015, 2016) for iron-limited waters of the subarctic Pacific Ocean. In contrast, Robinson et al. (2014) showed that K_C variability in eastern Australian coastal waters was better explained by the phytoplankton community composition rather than environmental condition. Certainly, it is apparent that multiple factors are responsible for driving variance in K_C; therefore this chapter will address some of the most common physiological, taxonomic and methodological processes potentially underlying such variability.

1.4 Physiological processes that influence K_C

ETR_{PSII} measured by FRRf is indicative of the potential for LEF to generate ATP and NADPH (Section 1.2). Under steady-state (balanced) growth, the conversion of light energy into chemical energy is optimal, and thus ATP and NADPH generation by LEF should closely match that for C-fixation (Foyer et al. 2012). However, photosynthesis is a dynamically-regulated process with additional pathways and networks that can operate to maintain photosynthetic performance during unbalanced growth, e.g. during transient light fluctuations and nutrient starvation (Johnson and Alric, 2013). These additional functions may act to: a) safely dissipate excess excitation energy (Niyogi, 1999) and b) adjust the intracellular ATP:NADPH ratio according to the rate of utilisation by cellular metabolism (Foyer et al. 2012). In fact, because ATP and NADPH are the primary

energetic and reductive currencies of the cell respectively, demands for one, or both, can come from a variety of processes within the cell. The Calvin-Benson cycle, for example, requires precisely 3 ATP per 2 NADPH molecules for C-fixation, i.e. a fixed ratio of 9:6 (Alric et al. 2010). The reductive assimilation of nitrogen (N) and the process of photorespiration (both discussed below) also require ATP and NADPH, but at different ratios to that of the Calvin-Benson cycle. Furthermore, numerous intracellular processes may solely demand ATP, thus decreasing the intracellular ATP:NADPH ratio. LEF only produces ATP and NADPH at a fixed ratio of 9:7 and thus consumption from multiple sources can easily lead to an imbalanced availability of the two forms of assimilatory power. Stoichiometric adjustment is therefore essential because even small discrepancies between the rate of ATP:NADPH consumption relative to production can quickly affect intracellular adenylate and redox status, negatively impacting electron transport and associated reactions (Noctor and Foyer, 2000).

Cells must also dissipate excess excitation energy since no phytoplankton cell is able to fully utilise all photons absorbed, especially during exposure to full sunlight (Zigman et al. 2012). Photosynthesis is a combination of extremely fast light-harvesting reactions occurring in the photosystems, and much-slower biochemical processes that fix CO_2 downstream, hence a build-up of excitation energy can accumulate quickly within the electron transport chain (McDonald et al. 2011). Such a build-up may prevent excited singlet states of chlorophyll from transferring their excitation energy, increasing the probability of inter-system-crossing to triplet-states of chlorophyll (Carbonera et al. 2012). Triplet-state chlorophyll can react with O_2 to generate reactive oxygen species (ROS), including singlet oxygen ($^1O_2$) – a highly unstable molecule that can photo-oxidatively damage PSII reaction centres (RCIIs) (Krieger-Liszkay, 2005), leading to photoinhibition (Ragni et al. 2008).

For marine phytoplankton, the capacity to dissipate excess energy is especially critical. In the marine environment, irradiance continually fluctuates over a range of timescales, from wave-flicker and wave-lensing (< seconds), to the passage of clouds and turbulence (seconds to minutes), and the day-night cycles and deep mixing (hours) (Falkowski, 1984). Unsurprisingly, phytoplankton therefore demonstrate extreme flexibility in their capacity to adjust electron flow in response to environmental change (Cardol, 2011), utilising alternative electron flows (AEFs) which do not result in C-fixation and thus increase K_C. Such AEFs (Fig. 1.2) are used for photoprotection (Ralph et al. 2010), or to generate additional ATP. This chapter will therefore discuss how these mechanisms are influenced by specific environmental conditions and their relevance for key phytoplankton taxa together with their influence upon K_C.

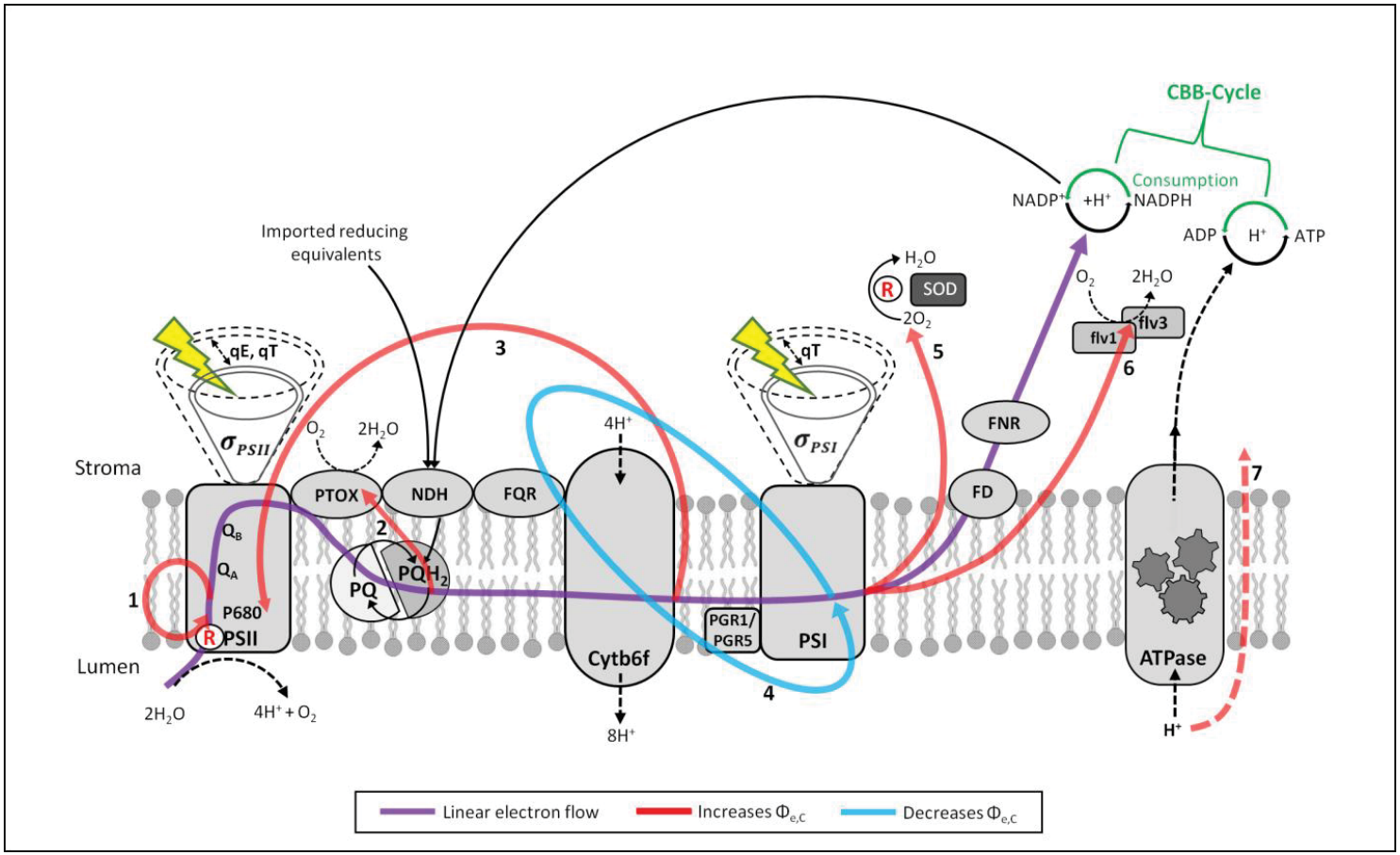

Figure 1.2. Schematic of photosynthetic linear electron flow (LEF) of oxygenic photosynthesis through to ATP/NADPH productions. Also depicted are the alternative electron flows (AEFs): 1) Plastiquinol terminal oxidase (PTOX), 2) Cyclic electron flow around PSII, 3) Cyclic electron flow around PSI, 4) Mehler reaction, 5) Flavodiiron protein (Flv)-mediated alternative electron flow. Also depicted are 6) slippage reactions. Directional arrows indicate the flow of electrons or protons and colour represents the effect upon K_C (red= increase, green=decrease). Energy-dependent non-photochemical quenching processes (qE) and state-transitions are also depicted, and their effect upon the functional absorption cross-section of photosystems I and II ($\sigma_{PSI/II}$).

1.4.1 Nitrogen reduction

Unlike higher plants, phytoplankton cells have a limited capacity to store organic C in the form of carbohydrates, so a large proportion of their cellular content consists of additional macromolecules (proteins, lipids and nucleic acids) which require the assimilation of nitrogen from an external source during biosynthesis (Anderson, 1995; Finkel et al. 2016). Biosynthesis reactions dictate that the available nitrogen source must be reduced to ammonium (NH_4^+) prior to assimilation at the cost of photosynthetically-derived electrons, ATP and reductant. Thus, the higher the oxidation state of the nitrogen source assimilated, the more electrons must be invested in reduction, increasing K_C (see Jakob et al. 2007). For example, nitrate (NO_3^-), (a stable form of nitrogen most readily available to all phytoplankton in the marine environment) has a higher oxidation state (+5) than nitrite (NO_2^-) (+3), thus requiring greater electron expenditure to achieve NH_4^+ (-3 oxidation state) by reduction. Electron donors for the assimilatory enzymes are usually NAD(P)H or Fd, whilst ATP:NADPH consumption varies depending on the nitrogen source (Kramer and Evans, 2011). In the event that NH_4^+ is directly available to the phytoplankton as a source of N, minimal electron expenditure is required prior to biosynthesis, thus potentially favouring lower K_C values.

1.4.2 N_2 fixation

Fixation of atmospheric N_2 is also performed by diazotrophic cyanobacteria; however this process requires a significant expenditure of both ATP and reductant: a minimum of 16 ATP molecules and 6-8 electrons per N_2 molecule fixed (Postgate, 1974; Scherer et al. 1988). Such a large energy demand is inevitably coupled to an energy-producing reaction such as photosynthesis, or mitochondrial respiration (Vitousek et al. 2002). However, the extreme sensitivity of the enzyme nitrogenase to O_2 means that N_2

fixation is often spatially or temporally separated from photosynthesis (Fay, 1992). This distinction may prove critical for K_C measurements because for phytoplankton that fix N_2 at night (i.e. temporal separation) it is most likely that the required energy will be supplied via mitochondrial respiration (Scherer et al. 1988), thus not likely influencing short-term K_C measurements during the day. Conversely, for cyanobacteria that fix N_2 during the day within compartmentalised heterocysts (spatial separation), much of the required energy is likely supplied by photosynthesis (Scherer et al. 1988) thus most likely leading to an increased K_C. The key bloom-forming genera in Australian waters, *Trichodesmium,* (which lacks heterocysts) can fix N_2 during either the day, or night, or both - thus it is unclear how this process may impact variability of FRRf-based productivity estimates. Furthermore, *Trichodesmium* spp. possess phycolbilipigmnents with rather unsual absorption peaks compared to other phytoplankton taxa (notably with peaks located at 495, 545 and 565nm, see Fujita and Shimura, 1974), and therefore FRRf instruments containing only a single excitation LED (e.g. blue only) may fail to adequately drive PSII reaction centre closure, potentially leading to underestimation of ETRs (e.g. Robinson el al. 2014).

1.4.3 Mehler Ascorbate Peroxidase (MAP) activity

MAP activity refers to an alternative electron pathway in which electrons from reduced ferredoxin at the donor side of PSI are used to photoreduce O_2 instead of $NADP^+$ (the usual terminal electron acceptor in the photosynthetic electron transport chain) (Flameling and Kromkamp, 1998). During this photoreduction of O_2, superoxide radicals are produced which are then disproportionated to H_2O_2 and O_2 with the aid of the enzyme, superoxide dismutase (SOD). H_2O_2 is a highly-damaging form of ROS and must be quickly detoxified to H_2O via the ascorbate-peroxidase pathway, resulting in

the formation of monodehydroascorbate (MDHA) and the subsequent regeneration of ascorbate via the oxidation of glutathione (Badger et al. 2000). Oxidised glutathione is then reduced back to glutathione using electrons donated by NADPH, and thus MAP activity is tightly-coupled with the glutathione system (Krueger et al. 2014). The complete set of reactions has been termed the water-water cycle (WWC) (Asada, 2000). Whilst the WWC acts as a conduit to funnel electrons from PSI back to water, it is also coupled to vectorial proton transport, and therefore contributes to the establishment of pmf (Heber, 2005), thus potentially generating ATP, but not NADPH - thus increasing K_C. The majority of pmf generated by this pathway is likely used for the activation of NPQ, rather than ATP production however, as WWC is thought to serve primarily as a photoprotective mechanism, restoring redox poise when the electron transport chain is over-reduced (Ort and Baker, 2002; Rochaix, 2011). If PSI electron acceptors become fully reduced during excess light, the diversion of electrons to the photoreduction of O_2 via MAP can effectively restart a "stalled" electron transport chain. Indeed, MAP activity tends to occur when intracellular O_2 concentrations are high and the supply of reductant exceeds the requirements of the Calvin-Benson cycle (Flameling and Kromkamp, 1998), thus consistent with conditions expected during exposure to high light.

MAP activity has been documented for a wide range of marine phytoplankton taxa such as cyanobacteria (Kana, 1992; Kana, 1993), chlorophytes (Rees et al. 1992) and diatoms (Lomas et al. 2000). The proportion of electrons diverted to MAP activity (and thus, the impact upon K_C) however may vary considerably between phytoplankton taxa. Kana (1993) reported that > 25% of total electron flow may be diverted to MAP activity in *Trichodesmium* sp., whilst Rees et al. (1992) proposed a similar figure for *Dunaliella tertiolecta* under high light. In contrast, Lomas et al. (2000) suggested that for marine

diatoms MAP activity plays a minor photoprotective role, accounting for only a small proportion of total electron flow. However, few studies have attempted to quantify the extent or variability of MAP activity within marine phytoplankton, making it difficult to make broad assertions regarding the significance of this pathway between higher taxonomic classes.

In terms of environmental regulation, MAP may be more significant in Fe-replete waters as this pathway effectively occurs downstream of PSI (the synthesis of which tends to become downregulated under Fe-limitation), and is also thought to be particularly important during N-limitation (see Lewitus and Kana, 1995). In conditions which favour cyanpbacterial diazotrophic N_2 fixation, upregulation of MAP activity may increase light-dependent respiration as an important strategty to protect the enzyme nitrogenase from potential irreversible inactivation by O_2 (Milligan et al. 2007).

1.4.4 Cyclic Electron Flow around PSI (CEF-PSI)

CEF-PSI (Heber, 2005) is the primary mechanism by which photosynthetic organisms overcome the shortage of ATP required for C-fixation due to the fixed 9:7 ratio of ATP:NAPDH production by LEF (Allen, 2003). This process is modulated by PSI in a manner similar to MAP initiation; however electrons from reduced Fd (or NADPH) are recycled back to the cyt b_6f complex via plastoquinone (PQ)(Rumeau et al. 2007; Munekage et al. 2004). This pathway generates pmf, which is then harnessed by ATPase to generate ATP (Takahashi et al. 2013). As the 12 protons generated by LEF (assuming 8 photons divided equally between PSI and PSII) are insufficient to fully rotate ATPase to synthesise 3 ATP molecules, CEF-PSI makes up this shortfall (see Allen, 2003; Alric, 2010). Generally, 13-15 protons are needed to induce one full rotation of the ATPase complex, dependent upon the phytoplankton taxa (Alric, 2010),

so a CEF-PSI flow rate at 6-16% of LEF should provide sufficient ATP synthesis required for C-fixation without the need for additional photon capture (Alric, 2010). Potentially, by alleviating the need for additional photon capture (i.e. more ETR_{PSII}) per C-fixed, CEF-PSI should theoretically lower K_C. To date, CEF-PSI has been studied predominantly in chlorophytes and higher plants; but is widely accepted to be an essential component of photosynthesis during optimal, stress-free conditions for all autotrophs (Allen, 2003; Munekage et al. 2004; Alric, 2010). Consequently, the contribution of CEF-PSI under "normal" conditions should theoretically influence K_C to the same extent across phytoplankton taxa. During environmental stress however, the potential taxonomic-specific role of CEF-PSI is unclear. Certainly, CEF-PSI builds pmf and thus may play an important role in the activation of non-photochemical quenching (NPQ) during high light (Munekage et al. 2004). Studies of CEF-PSI in marine phytoplankton are few to date, although Thamatrakoln et al. (2013) recently demonstrated that CEF-PSI may play an important role in low-light, iron-limited conditions for the coastal marine diatom, *Thalassiosira pseudonana*. Specifically, clones that overexpressed TpDSP1 (a protein strongly linked to increased CEF-PSI activity) exhibited a two-fold increase in ETR and a reduced quantum requirement for growth compared to clones that did not. Whilst this response was clone-specific, it perhaps indicates potential for CEF-PSI to influence K_C in phytoplankton cells under specific environmental conditions. Estimating the extent of this influence will likely prove challenging in the immediate future because the precise mechanisms that induce CEF-PSI remain ambiguous (Takahashi et al. 2013).

1.4.5 Cyclic Electron flow around PSII (CEF-PSII)

CEF-PSII diverts electrons from Cytochrome b_{559} (Cyt b_{559}) back to the core Chl-*a*

molecule (P680); this effective "cycling" of electrons from the donor to acceptor side of PSII results in re-oxidation of the PQ pool, generating neither ATP or NADPH. The precise electron pathway was first proposed by Heber et al. (1979) as **P680 → PQ → Cyt b_{559} → Chl z+ → P680^{+}** (from studies of spinach chloroplasts) but is yet to be conclusively identified at the molecular level (Miyake and Okamura, 2003). Typically, CEF-PSII operation has been inferred by applying ST excitation flashes to cells on a bare-platinum, O_2 electrode - simultaneously measuring O_2 flash yields with the quantum yield of fluorescence (Falkowski et al. 1988). This technique has been applied to measure CEF-PSII in freshwater chlorophytes (Prasil et al. 1996) and marine diatoms (Feikema et al. 2006) but whether they share the same electron pathway as proposed by Heber et al. (1979) remains unclear. Some evidence that CEF-PSII may ultimately be taxa-dependent comes from observations that the triggering mechanisms for different taxa appear variable, requiring only a reduced PQ pool in diatoms (Feikema et al. 2006), but also requiring establishment of a proton gradient (ΔpH) within higher plant chloroplasts (Miyake and Yokota, 2001). Despite the lack of molecular evidence, there is general consensus that CEF-PSII operates concurrently with LEF to act as a photoprotective mechanism by reducing excitation pressure upon PSII (Miyake and Yokota, 2001; Miyake and Okamura, 2003). By reversibly disengaging water-splitting from photochemical charge separation, CEF-PSII alleviates donor-side photoinhibition of PSII, oxidising the (reduced) PQ pool and thus, prevents the accumulation of electrons within the electron transport chain and thus allows a greater portion of PSII reaction centres to remain open (Prasil et al. 1996). CEF-PSII increases K_C since it allows a greater flux of electrons through PSII, but generates neither ATP nor NADPH, and thus does not contribute to C-fixation. However, important unknowns include: a) the maximum proportion of electrons that can be diverted to CEF-PSII relative to LEF,

b) the taxa-dependent variability of CEF-PSII across marine phytoplankton and c) how environmental conditions (in addition to light) may influence CEF-PSII operation.

1.4.6 Plastoquinol Terminal Oxidase (PTOX) - Chlororespiration

PTOX describes an alternative electron pathway in which a PTOX enzyme, located within the thylakoid membranes, catalyses the reduction of O_2 to H_2O using electrons donated from the PQ pool (Mackey et al. 2008; McDonald et al. 2011). By using electrons from the PQ pool, PTOX operates independently of either Cyt b_6f or PSI, functioning as an electron sink under conditions where the acceptor side of PSI is limited (McDonald et al. 2011). In the PTOX pathway, the flow of electrons from H_2O (extracted at PSII) back to regenerated H_2O helps to establish ΔpH (by consuming stromal protons during the oxidation of PQH_2), but generates no NADPH and thus increases K_C. Arguably, PTOX is one of the most-studied AEFs in phytoplankton in recent years and it is clear that a significant proportion of PSII-derived electrons may be diverted to PTOX by picophytoplankton in high-light, low-nutrient ocean environments (Bailey and Grossman, 2008). Such oligotrophic waters are often deplete in macronutrients (N and P), but can also be characterised by virtually undetectable levels of Fe (Grossman et al. 2010). Fe-limitation poses a significant problem for autotrophs because this element is essential for the synthesis and repair of photosynthetic apparatus (Mackey et al. 2008). In terms of Fe-expenditure, costly photosynthetic components to synthesise are PSI and Cyt b_6f, requiring 12 and 6 Fe atoms per complex respectively (Strzepek and Harrison, 2004). During Fe-limiting conditions, phytoplankton therefore reduce the proportion of both components relative to the more-affordable PSII complex (requiring only 4 Fe atoms to synthesise) (Strzepek and Harrison, 2004). For example, comparisons of photosystem stoichiometery for the diatom genus Thalassiosira, has

demonstrated a much higher (~10:1) PSII:PSI ratio for the oceanic species *T. oceanica* diatoms compared to its coastal counterpart, *T. weissflogii* (~2:1) (Strzepek and Harrison, 2004). Such a lower PSI:PSII ratio results in fewer electron acceptors downstream of PSII; a situation potentially conducive to photoinhibition, particularly in the open ocean where surface irradiance can reach as high as 2000 µmol photons m^{-2} s^{-1} (see Partensky et al. 1999). PTOX is therefore a particularly useful pathway for Fe-limited cells because it bypasses both Cyt b_6f and PSI in the reduction of O_2, allowing a significant proportion of PSII reaction centres to remain open (even during high light), (Bailey et al. 2008; Grossman et al. 2010; Mackey et al. 2008). PTOX appears particularly important for the picocyanobacteria *Prochlorococcus* and *Synechococcus,* which numerically dominate phytoplankton communities in oceanic communities along with prasinophytes such as *Ostreococcus* (Partensky et al. 1999; Mackey et al. 2008). PTOX can account for a significant proportion of total PSII electron flow in the aforementioned taxa (Cardol et al. 2011), thus K_C could be expected to be higher in oligotrophic waters. Indeed, Mackey et al. (2008) found that whilst C-fixation saturated at low light levels (~150 µmol photons m^{-2} s^{-1}) for oceanic populations of *Synechococcus,* a large fraction of PSII reaction centres continued to remain open, even under high light (~2000 µmol photons m^{-2} s^{-1}). The nature and extent with which PTOX operates for other phytoplankton communities more characteristic of variable coastal environments is unknown. Collectively, PTOX and redox reactions from from NADPH to oxygen mediated by the enzyme family NAD(P)H dehydrogenases, are referred to as Chlororespiration. However the latter is unlikely a significant factor considering that it only occurs at extremely low light levels (Kromkamp and Forster, 2003). It may however, provide an important role in modulating the activity of cyclic electron flow around PSI, particularly in cyanobacteria (Peltier and Cournac, 2002) and thus may

indirectly influence K_C.

1.4.7 Flavodiiron proteins

Flavodiiron (Flv) proteins have been recently identified to mediate electron flows from PSII directly to O_2 in cyanobacteria, and from PSI to O_2 in most photoautotrophs except angiosperms (Allahverdiyeva et al. 2015; Ilík et al. 2017). Such Flv electron flows appear particularly important during transitions from darkness to light exposure, leading to electron transport that transiently outpaces the capacity for C-fixation. Thus, it is highly-probable that Flv-mediated electron flows lead to increased K_C under fluctuating light regimes, e.g. in rapidly-mixing waters (see Hoppe et al. 2015).

1.4.8 Photorespiration

Photorespiration describes a process whereby RuBisCO catalyses the fixation of O_2 rather than CO_2, producing 1 molecule of 2-phosphoglycolate (unusable by the Calvin-Benson cycle), and the subsequent recovery of this product to the useable metabolic intermediate, 3-phosphoglyceric acid (PGA) (Wingler et al. 2000). Recovery involves the substantial recycling of reduced N (particularly NH_4^+), which must be detoxified via reassimilation into organic molecules (Linka and Weber, 2005). Whilst photorespiration provides a useful means to neutralise excessive build-up of O_2 that can become potentially toxic, photorespiration is both expensive and inefficient, costing a total of 5 ATP and 3 NADPH molecules per oxygenation event, and losing approximately 25% of fixed-C as released CO_2 (Badger et al. 2000). Photorespiration exceeds the cost of a carboxylation event by precisely 2 ATP and 1 NADPH molecules, which translates to the expenditure of more photosynthetically-derived electrons in order to fix less C; thus increasing K_C (but see Section 1.4.9 below). Interestingly, the relative inefficiency of photorespiration meant that it was once considered a wasteful side-reaction, however

now it is hypothesised to function as a safety-valve, preventing the build-up of intracellular reductant levels when carbon assimilation is low (Ort and Baker, 2002).

1.4.9 Carbon Concentrating Mechanisms (CCMs)

Despite the *potential* importance of photorespiration to K_C it is unlikely to play a significant role for the majority of microalgae, which despite possessing C_3 biochemistry, use CCMs to effectively suppress photorespiration (Beardall, 1989). CCMs are found in the majority of marine phytoplankton, and are utilised by both prokaryotes and eukaryotes (Rost et al. 2003). CCMs are designed to overcome the low-affinity for CO_2 of RuBisCO (the main carboxylating enzyme) by increasing the intracellular concentration of CO_2 relative to the surrounding environment. Significant differences in both the catalytic efficiency (Badger et al. 1998), and affinity for CO_2 (Tortell et al. 2000) of RuBisCO exist between the major algal and cyanobacterial groups. Such taxonomic separation may arise from evolutionary divergence, with RuBisCO from geologically-older phytoplankton taxa (e.g. cyanobacteria) exhibiting a lower affinity for CO_2 compared to recently-evolved taxa such as diatoms (Tortell et al. 2000). CCMs incur a metabolic cost to the cell (i.e. the consumption of ATP) and therefore potentially exert a taxa-specific, influence upon K_C. It could be reasoned that geologically-older taxa investing more resources into their CCMs would, accordingly, spend more electrons per unit C-fixed (over time) resulting in higher K_C. Whilst there are no studies that have directly examined this potential relationship and therefore the exact energetic costs remain unclear, it is feasible that CCMs would likely incur metabolic costs in the form of ATP consumption, loss of chemiosmotic potential or upregulation of cyclic electron flows (Raven et al. 2014).

1.4.10 Electron and proton "slippage"

Slippage refers to a less-than-theoretical stoichiometry in an energy transduction process, usually resulting from intrinsic uncoupling (Quigg et al. 2006) of which there are two relevant examples that have been observed for microalgae. Firstly, "proton slippage" refers to the uncoupled dissipation of ΔpH occurring when protons can "slip" through ATPase without the generation of ATP (Evron and Avron, 1990; Nelson et al. 2002) or, alternatively, leak directly across the thylakoid membrane, avoiding the ATPase complex entirely (Fuks and Homblé, 1996). Secondly, "electron slippage" describes the decay of unstable intermediate states (S_0-S_4) of the O_2-evolving complex (OEC) and Q_A/Q_B charge recombination (Quigg et al. 2006). Slippage reactions likely become proportionally more significant at lower light levels (~1 μmol photons m^{-2} s^{-1}) (Foyer et al. 2012) and thus, are unlikely to influence K_C measurements in the field.

1.4.11 Non-Photochemical Quenching (NPQ)

NPQ is a complex signature of energy dissipation from PSII via mechanisms other than photochemistry; as such, it may reflect the operation of AEFs which potentially influence K_C, such as MAP and CEF-PSI. Indeed, recent studies have demonstrated strong correlation between NPQ and K_C (Schuback et al. 2015, 2016; Hughes et al. in press, Chapter 2; see also Chapter 4).

1.5 Methodological influences upon K_C variance

Several key methodological constraints should be considered when attempting to untangle the respective influences of environment and taxa upon K_C (Suggett et al. 2009; Lawrenz et al. 2013; Robinson et al. 2014) and are discussed below.

1.5.1 PSII quantification

Prior to the recent algorithm developments by Oxborough et al. (2012), FRRf-research was severely-limited by the need to either i) independently measure the number of PSII reaction centres [RCII], or ii) use an assumed constant to estimate [RCII] from Chl-*a* measurements (see Suggett et al. 2004, 2011). ETR_{PSII} calculations inherently require an estimate of the absorption coefficient of light- harvesting complex II (a_{LHCII}), which is partly derived from σ_{PSII} (Eq.2, Section 1.2). However, σ_{PSII} only describes the effective light absorption for PSII photochemistry *relative* to the number of [RCII], thus the need to quantify RCII (and derive a_{PSII}) via one of several methods (see Silsbe et al. 2015). Directly measuring [RCII] is conventionally performed using O_2 flash-yields, a highly-accurate, but notoriously time-consuming process (Moore et al. 2006; Suggett et al. 2009). Consequently, many studies have opted to estimate a_{PSII} by assuming a constant photosynthetic unit size (n_{PSII}) of either 0.002 or 0.003 mol [RCII] (mol Chl-*a*)$^{-1}$ for eukaryotes and prokaryotes respectively (Kolber and Falkowski, 1993). However, the accuracy of this approach is questionable (see Suggett et al. 2004) due to the fact that measurements of n_{PSII} from oceanic phytoplankton samples often show considerable taxonomic variability (Suggett et al. 2010). Furthermore, this approach requires ancillary measurements of Chl-*a* thus constraining the spatio-temporal resolution of the ETR_{PSII} measurements (Silsbe et al. 2015). For previous studies that have used the fixed-n_{PSII} approach to evaluate ETR against ^{14}C-uptake, reconciling K_C variability due to environmental and/or taxonomic variability may not always be possible. The algorithm published by Oxborough et al. (2012) which enables the derivation of [RCII] solely from fluorescence parameters which has shown great promise to date, however being relatively new remains to be evaluated over a wide range of environmental conditions and phytoplankton taxa (but see Murphy et al. 2017).

1.5.2 Instrument correction factors

Perhaps the most critical methodological element for FRRf measurements is the need to accurately measure light absorption by PSII (a_{PSII}), which is obtained from σ_{PSII} (Suggett et al. 2009). Because σ_{PSII} is weighted to the spectral quality of the FRRf excitation LED, a spectral correction to that of the ambient light driving photosynthesis is required (Suggett et al. 2001). Failure to spectrally correct can lead to large errors in ETR_{PSII} measurements (and thus K_C). For example, lack of spectral correction, together with other instrument correction factors (e.g. sample blanks) can introduce up to 100% error (e.g. Laney 2004, 2008).

1.5.3 ^{14}C-fixation rates

The ^{14}C method (and the more recently ^{13}C-method, Hama et al. 1983) are commonly viewed as the benchmark of phytoplankton productivity measurements since they directly track C-incorporation. Regardless, the ^{14}C-method especially, has faced considerable methodological scrutiny since its introduction (see Marra, 2009). There still exists considerable uncertainty surrounding the complicated relationship between incubation length and the cellular residency time and metabolic processing of fixed-C. In theory, short-term incubations that allow little time for fixed-^{14}C to be respired or excreted (released as dissolved organic carbon, DOC) should approximate GPP, whereas longer (e.g. dawn-dusk) incubations allow for fixed-^{14}C to be respired, thus measurements tend to approximate net primary production (NPP) (Dring and Jewson, 1982). In this context, NPP is defined as GPP minus light-enhanced mitochondrial respiration and photorespiration (e.g. Halsey and Jones, 2015), reflecting production rates predominately from the photosynthetic activity of the phytoplankton community. Furthermore, any fixed-C assimilated is defined as contributing to particulate organic

carbon (POC) production versus that excreted as DOC.

Laboratory experiments typically show GPP to be approximately three-fold higher than NPP, (see Halsey and Jones, 2015), and therefore K_C (ETR_{PSII}/C-fixation) increases with incubation length as C-uptake moves from GPP towards NPP, with the timeframe being influenced by both phytoplankton species, and the dominant growth phase of the population (see Lopez-Sandoval et al. 2014). However, the distinction between short and long incubations (i.e. those capturing GPP and NPP respectively) is not always clear-cut, as demonstrated by Halsey et al. (2010, 2011, 2013). During their studies, even very short incubations (~20 min) were demonstrated to yield C-fixation rates anywhere between GPP and NPP, determined by growth rate-dependent variability in the lifetimes of recently-incorporated ^{14}C. Such differences reflect the rate and extent with which GPP-derived energy and reductant are used to fuel cellular maintenance (Halsey et al. 2010, 2013).

Considerable uncertainty in K_C may therefore exist when using incubation lengths where it is not possible to establish where the process being measured sits along the scale from GPP to NPP (see Milligan et al. 2015). This is particularly true for field studies where natural phytoplankton communities can exhibit highly-variable growth rates, which are difficult to measure. The majority of studies that have measured K_C in the field have used incubation lengths in the region of 1-4 hr based on the (most likely incorrect) assumption that the measured C-fixation rates represented GPP (Lawrenz et al. 2013), and far less commonly from longer (e.g. 12-24 hr) incubations designed to quantify NPP (Zhu et al. 2016, 2017). The inherent uncertainty surrounding the process captured by 1-4 hr incubations clearly limits our ability to reconcile the observed

variability of K_C for natural assemblages across broad spatial scales (Lawrenz et al. 2013).

Preferably, measurements of ^{14}C-uptake and ETR_{PSII} should be performed on the same sample simultaneously to minimise errors associated with sample heterogeneity and handling protocols (Lawrenz et al. 2013). This also removes the need for spectral correction (discussed above). Critically, ^{14}C-uptake incubations should be as short as feasible in order to derive the closest approximation to GPP. Lengthy incubation times that allow for the recycling of ^{14}C within the sample would result in an increased (and hence inaccurate) K_C.

1.5.4 Miscellaneous

Until recently, the majority of FRRf fluorometers were designed with only blue excitation LEDs (generally 450-470 nm wavelengths). This methodological limitation has often meant that the productivity of cyanobacterial populations (e.g. *Prochlorococcus*) is not always well-characterised, due to the FRRf failing to fully close [RCII] during the application of a single-turnover flash (see Kaiblinger and Dokulil, 2006).

1.6 Research objectives and thesis outline

As it stands, we do not necessarily possess the required tools to develop sufficient mechanistic understanding of the cellular processes responsible for decoupling ETR_{PSII} and C-fixation, in order to reliably predict K_C. The most successful attempts to predict and understand K_C variability to date have resulted from empirical-based approaches (Lawrenz et al. 2013; Schuback et al. 2015, 2016; Zhu et al. 2015, 2016). However, the extent to which K_C can be predicted from such approaches, and indeed the variables

required to develop empirical models appears highly-specific to each geographical region (Lawrenz et al. 2013). Currently, virtually no data exists for Australian waters and thus the capacity to employ FRRf to measure marine primary production in this region is severely-limited. My research within this thesis will therefore address this key knowledge gap by focussing on parallel measurements of FRRf electron transfer rates (ETR_{PSII}), and ^{14}C-fixation rates, to better understand, and ultimately develop empirical algorithms to predict the ***electron requirement for carbon fixation*** (K_C) in Australian waters. Through examination of natural phytoplankton assemblages and laboratory-grown phytoplankton cultures, I investigated the respective influence of environmental condition (of factors known to influence productivity) versus taxonomic identity in regulating K_C.

The primary goal of this thesis is to improve knowledge of K_C and understand and quantify how K_C varies predictably with changes in environmental conditions or phytoplankton community composition. In doing so, this new knowledge will ultimately improve capacity with which FRRf can be applied to retrieve high-resolution estimates of C-fixation within Australian waters. Current understanding of environmental and taxonomic regulation of K_C variability is extremely limited, and whilst correlations between K_C and environmental variables (particularly nutrient availability) have been demonstrated for field studies, our interpretation is confounded by the fact that: i) it is virtually impossible to isolate the effect of any single environmental variable upon K_C in the field, where multiple environmental stressors operate simultaneously; and ii) taxonomic information is rarely available to support observations of K_C.

In **Chapter 2**, the aim was to examine the influence of macronutrient availability upon K_C and isolate the respective roles of taxonomy and environment in driving any

observed variance. I first isolated the effects of macronutrient availability upon K_C regulation by collecting samples from a physically-dynamic Australian coastal reference station and performing multi-factorial nutrient-addition bioassays (N, P and Si, and all combinations) during summer when nutrient availability was low. By quantifying both photophysiological parameters and taxonomic composition through microscopy, I was able to determine the respective influences of physiology and taxonomy upon K_C regulation in response to differing states of nutrient availability, simultaneously assessing the viability of using a fluorescence-based proxy for the extent of non-photochemical quenching (NPQ_{NSV}) as an empirical predictor of K_C.

Attempts to understand K_C variability driven purely from changes in taxonomy have been limited to a few studies examining a handful of phytoplankton stains. Therefore, **Chapter 3** moved to the laboratory to perform a systematic screening of K_C across multiple species of phytoplankton (n = 17). The aim of this chapter was to determine the extent to which taxonomic variation regulates K_C under steady-state, nutrient-replete growth (i.e. with no environmental stressors). Furthermore, I aimed to identify whether K_C was regulated by an overarching trait governing photosynthetic performance (in this case, cell size). This was complemented by a subsequent meta-analysis that incorporated these new data with all past published data (n = 5) from controlled laboratory growth experiments. As it remained unclear whether taxonomic influence upon K_C arises from class-specific differences in phytoplankton, or is related to taxonomically independent changes in physiological traits (e.g. cell size, which is considered a master trait governing photosynthetic performance), this was assessed by incorporating strains spanning multiple orders of magnitude in cell volume/size. This approach capitalised on the use of, matched FRRf-^{14}C "dual incubations" performed at the growth irradiance, thus allowing robust assessment of K_C variability free from

methodological and environmental influence.

In **Chapter 4**, I returned to the field, in order to determine how well K_C could be empirically modelled from knowledge of prevailing environmental conditions along an environmental gradient, spanning oligotrophic offshore waters to the physically-dynamic eastern Australian coast. The aim was to develop the first empirical model to predict K_C within Australian waters. Capitalising on findings from Chapters 2 and 3, I performed 80 small volume "dual incubations" during a 3-week research voyage from Sydney to Brisbane, spanning the Tasman Sea and East Australian Current (EAC). In addition to the high-throughput approach of coupled FRRf-^{14}C measurements, I measured size-fractionated Chl-*a,* as a broad descriptor of community composition to evaluate if this improved retrieval of K_C beyond knowledge of prevailing environmental conditions alone. Finally, I re-assessed the performance of NPQ_{NSV} as a predictor of K_C, asking the question whether knowledge of a purely physiological parameter (perhaps reflective of environmental history) explains more variability in K_C than prevailing environmental conditions alone, or in fact whether a combination of both approaches is needed to best predict K_C.

I conclude the thesis with **Chapter 5**, which contains a brief discussion of the key concepts emerging from Chapters 2-4 and considers them in the context of proposing future research directions. However, in doing so, it became apparent that whilst some of these proposals are indeed novel and arise directly from this research, at least some of them could (and indeed should) have been implemented as "best practice" in prior years amongst the broader FRRf user community. After several insightful discussions with my supervisor and other leading FRRf specialists, there was clear consensus that FRRf-research was not living up to its potential for this very reason, and that a clear roadmap

was needed to overcome persistent issues that have hindered the usefulness and application of FRRf datasets to date. Thus, to synthesise both historical and novel proposals to FRRf research, an idea for an opinion paper evolved that has captured these discussions with numerous colleagues over the course of my PhD. I have therefore included as **Chapter 6**, the final draft of an opinion paper titled "**FRRf Roadmaps and Detours**: **Active chlorophyll-*a* assessments of primary productivity across marine and freshwater systems**", integrating the findings of my novel research within this thesis into a broader guide and discussion targeted to oceanographers and limnologists.

1.7 References

Allahverdiyeva, Y., J. Isojärvi, P. Zhang, and E.-M. Aro. 2015. Cyanobacterial oxygenic photosynthesis is protected by flavodiiron proteins. Life 5(1): 716-743.

Allahverdiyeva, Y. and others. 2013. Flavodiiron proteins Flv1 and Flv3 enable cyanobacterial growth and photosynthesis under fluctuating light. Proc. Natl. Acad. Sci. 110(10): 4111-4116.

Allen, J. F. 2003. Cyclic, pseudocyclic and noncyclic photophosphorylation: new links in the chain. Trends Plant Sci. 8(1): 15-19.

Alric, J. 2010. Cyclic electron flow around photosystem I in unicellular green algae. Photosynth. Res. 106(1-2): 47-56.

Alric, J., J. Lavergne, and F. Rappaport. 2010. Redox and ATP control of photosynthetic cyclic electron flow in *Chlamydomonas reinhardtii* (I) aerobic conditions. Biochim. Biophys. Acta, Bioenerg. 1797(1): 44-51.

Anderson, L. A. 1995. On the hydrogen and oxygen content of marine phytoplankton. Deep Sea Res., Part I. 42(9): 1675-1680.

Asada, K. 2000. The water–water cycle as alternative photon and electron sinks. Philos. Trans. R. Soc., B. 355(1402): 1419-1431.

Badger, M. R., T. J. Andrews, S. Whitney, M. Ludwig, D. C. Yellowlees, W. Leggat, and G. D. Price. 1998. The diversity and coevolution of Rubisco, plastids, pyrenoids, and chloroplast-based CO_2-concentrating mechanisms in algae. Can. J. Bot. 76(6): 1052-1071.

Badger, M. R., S. Von Caemmerer, S. Ruuska, and H. Nakano. 2000. Electron flow to oxygen in higher plants and algae: rates and control of direct photoreduction (Mehler reaction) and rubisco oxygenase. Philos. Trans. R. Soc., B. 355(1402): 1433-1446.

Bailey, S., and A. Grossman. 2008. Photoprotection in cyanobacteria: regulation of light harvesting. Photochem. Photobiol. 84(6): 1410-1420.

Beardall, J. 1989. Photosynthesis and photorespiration in marine phytoplankton. Aquat. Bot. 34(1-3): 105-130.

Beardall, J., S. Stojkovic, and S. Larsen. 2009. Living in a high CO_2 world: impacts of global climate change on marine phytoplankton. Plant Ecol. Divers. 2(2): 191-205.

Behrenfeld, M. J., and P. G. Falkowski. 1997. Photosynthetic rates derived from satellite-based chlorophyll concentration. Limnol. Oceanogr. 42(1): 1-20.

Behrenfeld, M. J., K. H. Halsey, and A. J. Milligan. 2008. Evolved physiological responses of phytoplankton to their integrated growth environment. Philos. Trans. R. Soc., B. 363(1504): 2687-2703.

Brading, P., M. E. Warner, D. J. Smith, and D. J. Suggett. 2013. Contrasting modes of inorganic carbon acquisition amongst *Symbiodinium* (Dinophyceae) phylotypes. New Phytol. 200(2): 432-442.

Carbonera, D., C. Gerotto, B. Posocco, G. M. Giacometti, and T. Morosinotto. 2012. NPQ activation reduces chlorophyll triplet state formation in the moss *Physcomitrella patens*. Biochim. Biophys. Acta, Bioenerg. 1817(9): 1608-1615.

Cardol, P., G. Forti, and G. Finazzi. 2011. Regulation of electron transport in microalgae. Biochim. Biophys. Acta, Bioenerg. 1807(8): 912-918.

Chavez, F. P., M. Messié, and J. T. Pennington. 2011. Marine primary production in relation to climate variability and change. Annu. Rev. Mar. Sci. 3: 227-260.

Cheah, W., A. Mcminn, F. B. Griffiths, K. J. Westwood, S. W. Wright, E. Molina, J. P. Webb, and R. Van Den Enden. 2011. Assessing Sub-Antarctic Zone primary productivity from fast repetition rate fluorometry. Deep Sea Res., Part II. 58(21): 2179-2188.

Corno, G., R. M. Letelier, M. R. Abbott, and D. M. Karl. 2006. Assessing primary production variability in the North Pacific Subtropical Gyre: a comparison of fast repetition rate fluorometry and ^{14}C measurements. J. Phycol. 42(1): 51-60.

Dring, M. J., and D. H. Jewson. 1982. What does ^{14}C uptake by phytoplankton really measure? A theoretical modelling approach. Philos. Trans. R. Soc., B. 214(1196): 351-368

Everett, J. D., and M. A. Doblin. 2015. Characterising primary productivity measurements across a dynamic western boundary current region. Deep Sea Res., Part I. 100: 105-116.

Evron, Y., and M. Avron. 1990. Characterization of an alkaline pH-dependent proton 'slip'in the ATP synthase of lettuce thylakoids. Biochim. Biophys. Acta, Bioenerg. 1019(2): 115-120.

Falkowski, P. G. 1984. Physiological responses of phytoplankton to natural light regimes. J. Plankton Res. 6(2): 295-307.

Falkowski, P. G., Z. Kolber, and Y. Fujita. 1988. Effect of redox state on the dynamics Photosystem II during steady-state photosynthesis in eucaryotic algae. Biochim. Biophys. Acta, Bioenerg. 933(3): 432-443.

Feikema, W. O., M. A. Marosvölgyi, J. Lavaud, and H. J. Van Gorkom. 2006. Cyclic electron transfer in photosystem II in the marine diatom *Phaeodactylum tricornutum*. Biochim. Biophys. Acta, Bioenerg. 1757(7): 829-834.

Finkel, Z. V., M. J. Follows, J. D. Liefer, C. M. Brown, I. Benner, and A. J. Irwin. 2016. Phylogenetic diversity in the macromolecular composition of microalgae. PLoS One 11(5): e0155977.

Fisher, N. L., and K. H. Halsey. 2016. Mechanisms that increase the growth efficiency of diatoms in low light. Photosynth. Res. 129(2): 183-197.

Flameling, I. A., and J. Kromkamp. 1998. Light dependence of quantum yields for PSII charge separation and oxygen evolution in eucaryotic algae. Limnol. Oceanogr. 43(2): 284-297.

Foyer, C. H., J. Neukermans, G. Queval, G. Noctor, and J. Harbinson. 2012. Photosynthetic control of electron transport and the regulation of gene expression. J. Exp. Bot. 63(4): 1637-1661.

Fujiki, T., T. Suzue, H. Kimoto, and T. Saino. 2007. Photosynthetic electron transport in *Dunaliella tertiolecta* (Chlorophyceae) measured by fast repetition rate fluorometry: relation to carbon assimilation. J. Plankton Res. 29(2): 199-208.

Fuks, B., and F. Homblé. 1996. Mechanism of proton permeation through chloroplast lipid membranes. Plant Physiol. 112(2): 759-766.

Genty, B., J.-M. Briantais, and N. R. Baker. 1989. The relationship between the quantum yield of photosynthetic electron transport and quenching of chlorophyll fluorescence. Biochim. Biophys. Acta, Gen. Sub. 990(1): 87-92.

Grossman, A. R., K. R. Mackey, and S. Bailey. 2010. A perspective on photosynthesis in the oligotrophic oceans: hypotheses concerning alternate routes of electron flow. J. Phycol. 46(4): 629-634.

Hald, S., M. Pribil, D. Leister, P. Gallois, and G. N. Johnson. 2008. Competition between linear and cyclic electron flow in plants deficient in Photosystem I. Biochim. Biophys. Acta, Bioenerg. 1777(9): 1173-1183.

Halsey, K. H., and B. M. Jones. 2015. Phytoplankton strategies for photosynthetic energy allocation. Annu. Rev. Mar. Sci. 7: 265-297.

Halsey, K. H., A. J. Milligan, and M. J. Behrenfeld. 2010. Physiological optimization underlies growth rate-independent chlorophyll-specific gross and net primary production. Photosynth. Res. 103(2): 125-137.

Halsey, K. H., A. J. Milligan, and M. J. Behrenfeld. 2011. Linking time-dependent carbon-fixation efficiencies in *Dunaliella tertiolecta* (chlorophyceae) to underlying metabolic pathways. J. Phycol. 47(1): 66-76.

Halsey, K. H., R. T. O'malley, J. R. Graff, A. J. Milligan, and M. J. Behrenfeld. 2013. A common partitioning strategy for photosynthetic products in evolutionarily distinct phytoplankton species. New Phytol. 198(4): 1030-1038.

Hama, T., T. Miyazaki, Y. Ogawa, T. Iwakuma, M. Takahashi, A. Otsuki, and S. Ichimura. 1983. Measurement of photosynthetic production of a marine phytoplankton population using a stable ^{13}C isotope. Mar. Biol. 73(1): 31-36.

Heber, U. 2005. Irrungen, Wirrungen? The Mehler reaction in relation to cyclic electron transport in C3 plants, p 551-559. In Govindjee, J. T. Beatty, H. Gest and J. F. Allen [eds.], Discoveries in Photosynthesis. Springer.

Heber, U., M. Kirk, and N. Boardman. 1979. Photoreactions of cytochrome b-559 and cyclic electron flow in photosystem II of intact chloroplasts. Biochim. Biophys. Acta, Bioenerg. 546(2): 292-306.

Hoegh-Guldberg, O., and J. F. Bruno. 2010. The impact of climate change on the world's marine ecosystems. Science 328(5985): 1523-1528.

Hill, R., and F. A. Y. Bendall. 1960. "Function of the two cytochrome components in chloroplasts: a working hypothesis." Nature 186(4719): 136.

Hoppe, C. J., L. M. Holtz, S. Trimborn, and B. Rost. 2015. Ocean acidification decreases the light-use efficiency in an Antarctic diatom under dynamic but not constant light. New Phytol. 207(1): 159-171.

Hughes, D.J., Varkey, D., Doblin, M.A., Ingleton, T., Mcinnes, A., Ralph, P.J., van Dongen-Vogels, V and D.J Suggett. 2018. Impact of nitrogen availability upon

the electron requirement for carbon fixation in Australian coastal phytoplankton communities (In Press). Limnol. Oceanogr. DOI: 10.1002/lno.10814

Huot, Y., and M. Babin. (2010). Overview of fluorescence protocols: theory, basic concepts, and practice, p. 31-74. In D. Suggett, O. Prášil and M. Borowitzka [eds.], Chlorophyll a fluorescence in aquatic sciences: Methods and applications. Springer.

Ilík, P. and others. 2017. Alternative electron transport mediated by flavodiiron proteins is operational in organisms from cyanobacteria up to gymnosperms. New Phytol. 214(3): 967-972.

Jakob, T., H. Wagner, K. Stehfest, and C. Wilhelm. 2007. A complete energy balance from photons to new biomass reveals a light-and nutrient-dependent variability in the metabolic costs of carbon assimilation. J. Exp. Bot. 58(8): 2101-2112.

Johnson, X., and J. Alric. 2013. Central carbon metabolism and electron transport in *Chlamydomonas reinhardtii*: metabolic constraints for carbon partitioning between oil and starch. Eukaryotic Cell 12(6): 776-793.

Kaiblinger, C., and M. T. Dokulil. 2006. Application of fast repetition rate fluorometry to phytoplankton photosynthetic parameters in freshwaters. Photosynth. Res. 88(1): 19-30.

Kana, T. M. 1992. Relationship between photosynthetic oxygen cycling and carbon assimilation in *Synechococcus* WH7803 (Cyanophyta). J. Phycol. 28(3): 304-308.

Kana, T. M. 1993. Rapid oxygen cycling in *Trichodesmium thiebautii*. Limnol. Oceanogr. 38(1): 18-24.

Kolber, Z., and P. G. Falkowski. 1993. Use of active fluorescence to estimate phytoplankton photosynthesis *in situ*. Limnol. Oceanogr. 38(8): 1646-1665.

Kolber, Z., J. Zehr, and P. Falkowski. 1988. Effects of growth irradiance and nitrogen limitation on photosynthetic energy conversion in photosystem II. Plant Physiol. 88(3): 923-929.

Kolber, Z. S., O. Prášil, and P. G. Falkowski. 1998. Measurements of variable chlorophyll fluorescence using fast repetition rate techniques: defining methodology and experimental protocols. Biochim. Biophys. Acta, Bioenerg. 1367(1): 88-106.

Kostadinov, T., D. Siegel, and S. Maritorena. 2010. Global variability of phytoplankton functional types from space: assessment via the particle size distribution. Biogeosciences 7(10): 3239-3257.

Kramer, D. M., and J. R. Evans. 2011. The importance of energy balance in improving photosynthetic productivity. Plant Physiol. 155(1): 70-78.

Krause, G. H., and E. Weis 1991. Chlorophyll fluorescence and photosynthesis: the basics. Annu. Rev. Plant Physiol. 42(1): 313-349.

Krieger-Liszkay, A. 2004. Singlet oxygen production in photosynthesis. J. Exp. Bot. 56(411): 337-346.

Kromkamp, J. C., N. A. Dijkman, J. Peene, S. G. Simis, and H. J. Gons. 2008. Estimating phytoplankton primary production in Lake IJsselmeer (The Netherlands) using variable fluorescence (PAM-FRRF) and C-uptake techniques. Eur. J. Phycol. 43(4): 327-344.

Kromkamp, J. C., and R. M. Forster. 2003. The use of variable fluorescence measurements in aquatic ecosystems: differences between multiple and single turnover measuring protocols and suggested terminology. Eur. J. Phycol. 38(2): 103-112.

Krueger, T., S. Becker, S. Pontasch, S. Dove, O. Hoegh-Guldberg, W. Leggat, P. L. Fisher, and S. K. Davy. 2014. Antioxidant plasticity and thermal sensitivity in four types of *Symbiodinium* sp. J. Phycol. 50(6): 1035-1047.

Laney, S. 2003. Assessing the error in photosynthetic properties determined by fast repetition rate fluorometry. Limnol. Oceanogr. 48(6): 2234-2242.

Laufkötter, C. and others. 2015. Drivers and uncertainties of future global marine primary production in marine ecosystem models. Biogeosciences 12: 6955-6984.

Lawrenz, E. and others. 2013. Predicting the electron requirement for carbon fixation in seas and oceans. PLoS One 8(3): e58137.

Lewis, M. R., and J. C. Smith. 1983. A small volume, short-incubation-time method for measurement of photosynthesis as a function of incident irradiance. Mar. Ecol.: Prog. Ser. 13: 99-102.

Lewitus, A. J., and T. M. Kana. 1995. Light respiration in six estuarine phytoplankton species: contrasts under photoautotrophic and mixotrophic growth conditions. J. Phycol. 31(5): 754-761.

Linka, M., and A. P. Weber. 2005. Shuffling ammonia between mitochondria and plastids during photorespiration. Trends Plant Sci. 10(10): 461-465.

Lomas, M. W., C. J. Rumbley, and P. M. Glibert. 2000. Ammonium release by nitrogen sufficient diatoms in response to rapid increases in irradiance. J. Plankton Res. 22(12): 2351-2366.

Longhurst, A., S. Sathyendranath, T. Platt, and C. Caverhill. 1995. An estimate of global primary production in the ocean from satellite radiometer data. J. Plankton Res. 17(6): 1245-1271.

López-Sandoval, D. C., T. Rodríguez-Ramos, P. Cermeño, C. Sobrino, and E. Marañón. 2014. Photosynthesis and respiration in marine phytoplankton: relationship with cell size, taxonomic affiliation, and growth phase. J. Exp. Mar. Biol. Ecol. 457: 151-159.

MacIntyre, H. L., E. Lawrenz, and T. L. Richardson. 2010. Taxonomic discrimination of phytoplankton by spectral fluorescence, p. 129-19. In D. Suggett, O. Prášil and M. Borowitzka [eds.], Chlorophyll a fluorescence in aquatic sciences: Methods and applications. Springer.

Mackey, K. R., A. Paytan, A. R. Grossman, and S. Bailey. 2008. A photosynthetic strategy for coping in a high-light, low-nutrient environment. Limnol. Oceanogr. 53(3): 900-913.

Mateo, M. A., P. Renom, M. A. Hemminga, and J. Peene. 2001. Measurement of seagrass production using the ^{13}C stable isotope compared with classical O_2 and ^{14}C methods. Mar. Ecol.: Prog. Ser. 223: 157-165.

Mcdonald, A. E., A. G. Ivanov, R. Bode, D. P. Maxwell, S. R. Rodermel, and N. P. Hüner. 2011. Flexibility in photosynthetic electron transport: the physiological role of plastoquinol terminal oxidase (PTOX). Biochim. Biophys. Acta, Bioenerg. 1807(8): 954-967.

Melrose, D. C., C. A. Oviatt, J. E. O'reilly, and M. S. Berman. 2006. Comparisons of fast repetition rate fluorescence estimated primary production and ^{14}C uptake by phytoplankton. Mar. Ecol.: Prog. Ser. 311: 37-46.

Milligan, A. J., Berman-Frank, I., Gerchman, Y., Dismukes, G. C., P.G Falkowski. 2007. Light-dependent oxygen consumption in nitrogen-fixing cyanobacteria plays a key role in nitrogenase protection. J. Phycol. 43(5): 845-852.

Milligan, A. J., K. H. Halsey, and M. J. Behrenfeld. 2015. Advancing interpretations of ^{14}C-uptake measurements in the context of phytoplankton physiology and ecology. J. Plankton Res. 37(4): 692-698.

Miyake, C., and M. Okamura. 2003. Cyclic electron flow within PSII protects PSII from its photoinhibition in thylakoid membranes from spinach chloroplasts. Plant Cell Physiol. 44(4): 457-462.

Miyake, C., and A. Yokota. 2001. Cyclic flow of electrons within PSII in thylakoid membranes. Plant Cell Physiol. 42(5): 508-515.

Moore, C. M. and others. 2003. Physical controls on phytoplankton physiology and production at a shelf sea front: a fast repetition-rate fluorometer based field study. Mar. Ecol.: Prog. Ser. 259: 29-45.

Moore, C. M., D. J. Suggett, A. E. Hickman, Y.-N. Kim, J. F. Tweddle, J. Sharples, R. J. Geider, and P. M. Holligan. 2006. Phytoplankton photoacclimation and photoadaptation in response to environmental gradients in a shelf sea. Limnol. Oceanogr. 51(2): 936-949.

Munekage, Y., M. Hashimoto, C. Miyake, and K.-I. Tomizawa. 2004. Cyclic electron flow around photosystem I is essential for photosynthesis. Nature 429(6991): 579.

Murphy, C. D. and others. 2017. Quantitating active Photosystem II reaction center content from fluorescence induction transients. Limnol. Oceanogr.: Methods 15(1): 54-69.

Napoleon, C., V. Raimbault, and P. Claquin. 2013. Influence of nutrient stress on the relationships between PAM measurements and carbon incorporation in four phytoplankton species. PLoS One 8(6): e66423.

Nelson, N., A. Sacher, and H. Nelson. 2002. Opinion: The significance of molecular slips in transport systems. Nat. Rev. Mol. Cell Biol. 3(11): 876.

Steeman-Nielsen, E. 1952. The use of radioactive carbon (C^{14}) for measuring organic production in the sea. ICES J. Mar. Sci. 18(2): 117-140.

Niyogi, K. K. 1999. Photoprotection revisited: genetic and molecular approaches. Annu. Rev. Plant Biol. 50(1): 333-359.

Ort, D. R., and N. R. Baker. 2002. A photoprotective role for O_2 as an alternative electron sink in photosynthesis? Curr. Opin. Plant Biol. 5(3): 193-198.

Oxborough, K., C. M. Moore, D. J. Suggett, T. Lawson, H. G. Chan, and R. J. Geider. 2012. Direct estimation of functional PSII reaction center concentration and PSII electron flux on a volume basis: a new approach to the analysis of Fast Repetition Rate fluorometry (FRRf) data. Limnol. Oceanogr.: Methods 10(3): 142-154.

Partensky, F., W. R. Hess, and D. Vaulot. 1999. *Prochlorococcus*, a marine photosynthetic prokaryote of global significance. Microbiol. Mol. Biol. Rev. 63(1): 106-127.

Peltier, G., and L. Cournac. 2002. Chlororespiration. Annu. Rev. Plant Biol. 53(1): 523-550.

Postgate, J. R. 1974. New advances and future potential in biological nitrogen fixation. J. Appl. Microbiol. 37(2): 185-202.

Prasil, O., Z. Kolber, J. A. Berry, and P. G. Falkowski. 1996. Cyclic electron flow around photosystem II in vivo. Photosynth. Res. 48(3): 395-410.

Quigg, A., K. Kevekordes, J. A. Raven, and J. Beardall. 2006. Limitations on microalgal growth at very low photon fluence rates: the role of energy slippage. Photosynth. Res. 88(3): 299-310.

Ragni, M., R. L. Airs, N. Leonardos, and R. J. Geider. 2008. Photoinhibition of PSII in *Emiliania huxleyi* (Haptophyta) under high light stress: the roles of photoacclimation, photoprotection, and photorepair. J. Phycol. 44(3): 670-683.

Ralph, P. J., C. Wilhelm, J. Lavaud, T. Jakob, K. Petrou, and S. A. Kranz. 2010. Fluorescence as a tool to understand changes in photosynthetic electron flow regulation, p. 75-89. In D. Suggett, O. Prášil and M. Borowitzka [eds.], Chlorophyll a fluorescence in aquatic sciences: Methods and applications. Springer.

Raven, J. A., J. Beardall, and M. Giordano. 2014. Energy costs of carbon dioxide concentrating mechanisms in aquatic organisms. Photosynth. Res. 121(2-3): 111-124.

Rees, D., C. B. Lee, D. J. Gilmour, and P. Horton. 1992. Mechanisms for controlling balance between light input and utilisation in the salt tolerant alga *Dunaliella* C_9AA. Photosynth. Res. 32(3): 181-191.

Regaudie-De-Gioux, A., S. Lasternas, S. Agustí, and C. M. Duarte. 2014. Comparing marine primary production estimates through different methods and development of conversion equations. Front. Mar. Sci. 1: 19.

Robinson, C., D. Suggett, N. Cherukuru, P. Ralph, and M. Doblin. 2014. Performance of Fast Repetition Rate fluorometry based estimates of primary productivity in coastal waters. Journal of Marine Systems 139: 299-310.

Rochaix, J., D. 2011. Assembly of the photosynthetic apparatus. Plant physiology 155(4): 1493-1500.

Rost, B., U. Riebesell, S. Burkhardt, and D. Sültemeyer. 2003. Carbon acquisition of bloom-forming marine phytoplankton. Limnol. Oceanogr. 48(1): 55-67.

Röttgers, R. 2007. Comparison of different variable chlorophyll a fluorescence techniques to determine photosynthetic parameters of natural phytoplankton. Deep Sea Res., Part I. 54(3): 437-451.

Rumeau, D., G. Peltier, and L. Cournac. 2007. Chlororespiration and cyclic electron flow around PSI during photosynthesis and plant stress response. Plant, Cell Environ. 30(9): 1041-1051.

Saba, V. and others. 2011. An evaluation of ocean color model estimates of marine primary productivity in coastal and pelagic regions across the globe. Biogeosciences 8: 489-503.

Scherer, S., H. Almon, and P. Böger. 1988. Interaction of photosynthesis, respiration and nitrogen fixation in cyanobacteria. Photosynth. Res. 15(2): 95-114.

Schuback, N., M. Flecken, M. T. Maldonado, and P. D. Tortell. 2016. Diurnal variation in the coupling of photosynthetic electron transport and carbon fixation in iron-limited phytoplankton in the NE subarctic Pacific. Biogeosciences 13(4): 1019-1035.

Schuback, N., C. J. Hoppe, J. É. Tremblay, M. T. Maldonado, and P. D. Tortell. 2017. Primary productivity and the coupling of photosynthetic electron transport and carbon fixation in the Arctic Ocean. Limnol. Oceanogr. 62(3): 898-921.

Schuback, N., C. Schallenberg, C. Duckham, M. T. Maldonado, and P. D. Tortell. 2015. Interacting effects of light and iron availability on the coupling of photosynthetic electron transport and CO_2-assimilation in marine phytoplankton. PloS One 10(7): e0133235.

Shimura, S., & Fujita, Y. (1975). Phycoerythrin and photosynthesis of the pelagic blue-green alga *Trichodesmium thiebautii* in the waters of Kuroshio, Japan. Mar. Biol 31(2), 121-128

Silsbe, G. M. and others. 2015. Toward autonomous measurements of photosynthetic electron transport rates: an evaluation of active fluorescence-based measurements of photochemistry. Limnol. Oceanogr.: Methods 13(3): 138-155.

Strzepek, R. F., and P. J. Harrison. 2004. Photosynthetic architecture differs in coastal and oceanic diatoms. Nature 431(7009): 689.

Suggett, D. J., H. L. Macintyre, and R. J. Geider. 2004. Evaluation of biophysical and optical determinations of light absorption by photosystem II in phytoplankton. Limnol. Oceanogr.: Methods 2(10): 316-332.

Suggett, D. J., H. L. Macintyre, T. M. Kana, and R. J. Geider. 2009. Comparing electron transport with gas exchange: parameterising exchange rates between alternative photosynthetic currencies for eukaryotic phytoplankton. Aquat. Microb. Ecol. 56(2-3): 147-162.

Suggett, D. J., C. M. Moore, E. Marañón, C. Omachi, R. A. Varela, J. Aiken, and P. M. Holligan. 2006. Photosynthetic electron turnover in the tropical and subtropical Atlantic Ocean. Deep Sea Res., Part II. 53(14): 1573-1592.

Suggett, D. J., K. Oxborough, N. R. Baker, H. L. Macintyre, T. M. Kana, and R. J. Geider. 2003. Fast repetition rate and pulse amplitude modulation chlorophyll a fluorescence measurements for assessment of photosynthetic electron transport in marine phytoplankton. Eur. J. Phycol. 38(4): 371-384.

Suggett, D. J., O. Prášil, and M. A. Borowitzka. 2010. Chlorophyll a fluorescence in aquatic sciences: methods and applications. Springer.

Takahashi, H., S. Clowez, F.-A. Wollman, O. Vallon, and F. Rappaport. 2013. Cyclic electron flow is redox-controlled but independent of state transition. Nat. Commun. 4: 1954.

Thamatrakoln, K. and others. 2013. Death-specific protein in a marine diatom regulates photosynthetic responses to iron and light availability. Proc. Natl. Acad. Sci. 110(50): 20123-20128.

Tortell, P. D. 2000. Evolutionary and ecological perspectives on carbon acquisition in phytoplankton. Limnol. Oceanogr. 45(3): 744-750.

Vitousek, P. M. and others. 2002. Towards an ecological understanding of biological nitrogen fixation. Biogeochemistry 57(1): 1-45.

Woodrow, I. E., and J. A. Berry. 1988. Enzymatic regulation of photosynthetic CO2, fixation in C3 plants. Annu. Rev. Plant Physiol. Plant Mol. Biol. 39(1): 533-594.

Wingler, A., P. J. Lea, W. P. Quick, and R. C. Leegood. 2000. Photorespiration: metabolic pathways and their role in stress protection. Philos. Trans. R. Soc., B. 355(1402): 1517-1529.

Zhu, Y., J. Ishizaka, S. Tripathy, S. Wang, Y. Mino, T. Matsuno, and D. Suggett. 2016. Variation of the photosynthetic electron transfer rate and electron requirement for daily net carbon fixation in Ariake Bay, Japan. J. Oceanogr. 72(5): 761-776.

Zhu, Y., J. Ishizaka, S. C. Tripathy, S. Wang, C. Sukigara, J. Goes, T. Matsuno, and D. J. Suggett. 2017. Relationship between light, community composition and the electron requirement for carbon fixation in natural phytoplankton. Mar. Ecol.: Prog. Ser. 580: 83-100.

Zigman, M., Z. Dubinsky, and D. Iluz. 2012. The xanthophyll cycle in aquatic phototrophs and its role in the mitigation of photoinhibition and photodynamic damage, p. . In M. Najafpour [ed.], Applied Photosynthesis. InTech.

2 Chapter 2:

Impact of nitrogen availability upon the electron requirement for carbon fixation in Australian coastal phytoplankton communities

Accepted for publication as: Hughes, D.J., Varkey, D., Doblin, M.A., Ingleton, T., Mcinnes, A., Ralph, P.J., van Dongen-Vogels, V., and Suggett, D.J. (2018). Impact of nitrogen availability upon the electron requirement for carbon fixation in Australian coastal phytoplankton communities. (in press) Limnol. Oceanogr. DOI: 10.1002/lno.10814

[1] Climate Change Cluster, University of Technology Sydney, Broadway 2007, NSW, Australia

[2]Department of Chemistry and Biomolecular Sciences, Macquarie University, NSW, Australia, 2109

[3]Waters and Coastal Science, New South Wales Office of Environment and Heritage, Department of Premier and Cabinet, Sydney, Australia

*Corresponding author: David.Suggett@uts.edu.au

2.1 Abstract

Nitrogen (N) availability affects phytoplankton photosynthetic performance and regulates marine primary production (MPP) across the global coast and oceans. Bio-optical tools including Fast Repetition Rate fluorometry (FRRf) are particularly well suited to examine MPP variability in coastal regions subjected to dynamic spatio-temporal fluctuations in nutrient availability. FRRf determines photosynthesis as an electron transport rate through Photosystem II (ETR_{PSII}), requiring knowledge of an additional parameter, the electron requirement for carbon fixation (K_C), to retrieve rates of CO_2-fixation. K_C strongly depends upon environmental conditions regulating photosynthesis, yet the importance of N-availability to this parameter has not been examined. Here, we use nutrient bioassays to isolate how N (relative to other macronutrients P, Si) regulates K_C of phytoplankton communities from the Australian coast during summer, when N-availability is often highly variable. K_C consistently responded to N-amendment, exhibiting up to a threefold reduction and hence an apparent increase in the extent with which electrons were used to drive C-fixation. However, the process driving this consistent reduction was dependent upon initial conditions. When diatoms dominated assemblages and N was undetectable (e.g. post bloom), K_C decreased predominantly via a physiological adjustment of the existing community to N-amendment. Conversely, for mixed assemblages, N-addition achieved a similar reduction in K_C through a change in community structure towards diatom domination. We generate new understanding and parameterisation of K_C that is particularly critical to advance how FRRf can be applied to examine C-uptake throughout the global ocean where nitrogen availability is highly variable and thus frequently limits primary productivity.

[Production note:

This chapter is not included in this digital copy due to copyright restrictions.]

Hughes, D.J., Varkey, D., Doblin, M.A., Ingleton, T., Mcinnes, A., Ralph, P.J., van Dongen-Vogels, V., and Suggett, D.J. (2018). Impact of nitrogen availability upon the electron requirement for carbon fixation in Australian coastal phytoplankton communities. (In Press). Limnol. Oceanogr. DOI: 10.1002/lno.10814

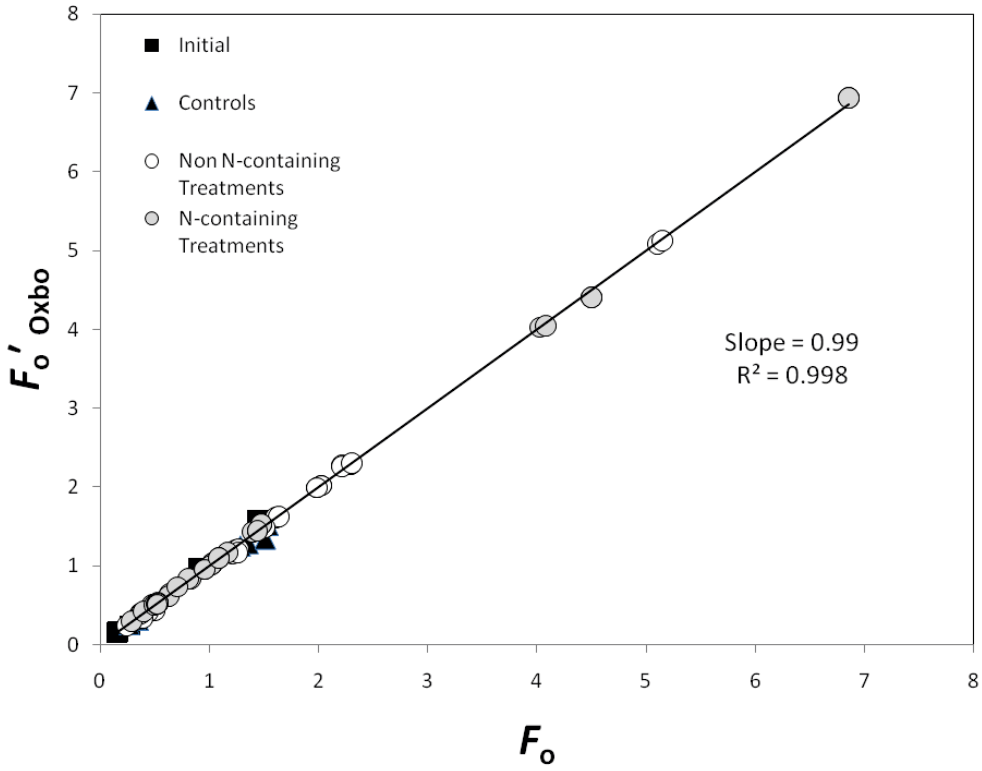

Supplementary Figure S2.1 Measured values of dark-acclimated minimal fluorescence (F_0) plotted against calculated values of minimal fluorescence in the light-acclimated state ($F_0'_{OXBO}$ - derived as per Oxborough and Baker, 1997) for initial, control and nutrient treatments for the three months (Dec-Feb) sampled. Values for $F_0'_{OXBO}$ represent an average value from a 6 min incubation period.

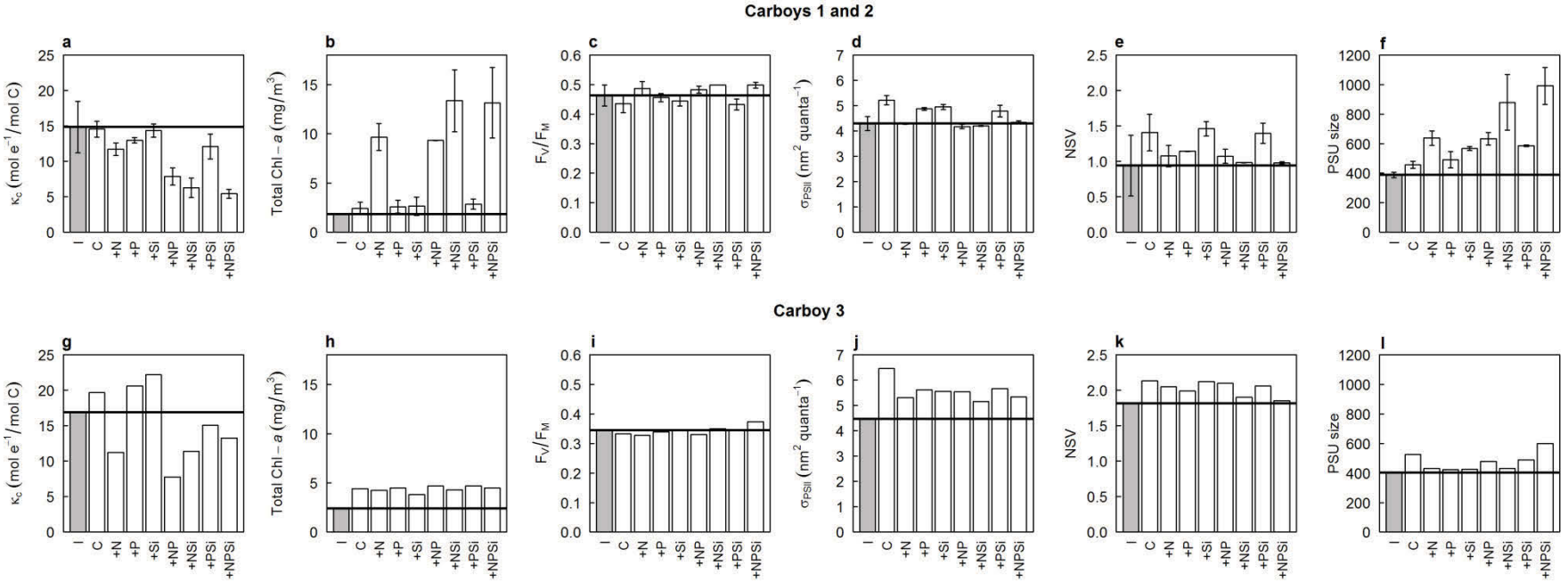

Supplementary Figure S2.2 Breakdown of February data, separating carboys 1 and 2 (a-f), from carboy 3 (g-l). Carboys 1 and 2 were generally dominated by diatoms (*Leptocylindrus* spp.), whilst Carboy 3 was characterised by the dominant presence of an unidentified nanoflagellate. Carboy 3 is further characterised by: a K_C response to N-amendment which mirrors that of carboys 1-2 but has generally higher values, together with a considerably lower F_v/F_m and a higher induction of NPQ_{NSV}. Photosynthetic unit (PSU) size responds to N-amendment for the diatom-dominated carboys 1-2 in parallel with a reduced K_C, however whilst N-amendment appears to reduce K_C for carboy 3 (nanoflaglellate-dominated) there is no obvious response in PSU size. This suggests that observed PSU size responses were driven primarily by increases in Chl-*a* synthesis rather than the Oxborough et al. (2012) algorithm underperforming during nutrient-limited conditions leading to possible overestimation of $[RCII]^{(FRRf)}$.

3 Chapter 3:

Identifying a role for taxonomy in explaining variability in the electron requirement for carbon fixation across phytoplankton

David J. Hughes[1], Maria Fernanda Colo Giannini[1,2], Arjun Verma[1], Joseph R Crosswell[1,3], Martina A. Doblin[1], Peter J. Ralph[1], Deepa Varkey[1,4] and David J. Suggett[1*]

[1] Climate Change Cluster, University of Technology Sydney, Broadway 2007, NSW, Australia

[2] Laboratorio Aquarela, Centro de Biologia Marinha (CEBIMar/USP) – Universidade de Sao Paulo, Rodovia Manoel Hypolito Rego, km 131.5, Sao Sebastiao, SP, Brazil

[3] CSIRO Oceans and Atmosphere, Brisbane, Queensland, Australia

[4]Department of Chemistry and Biomolecular Sciences, Macquarie University, NSW, Australia, 2109

*Corresponding author: David.Suggett@uts.edu.au

3.1 Abstract

FRRf has become increasingly adopted by oceanographers as a means to improve understanding of marine primary productivity. A component of this interest has been the desire to improve knowledge of carbon uptake patterns over space and time, but fundamentally requires the application of a factor to convert FRRf-measured electron transport rates to carbon fixation rates. Whilst recent studies have sought to understand variation of K_C across broad environmental scales, a possible role for phytoplankton taxonomy has not been specifically explored. We therefore grew a wide range of phytoplankton strains (n = 17) spanning multiple taxonomic and size-classes, and examined K_C under controlled laboratory conditions. These data were further considered alongside data mined from past studies (n = 5, across 4 taxonomic classes) to evaluate the extent to which variation of K_C could be explained by taxonomy as opposed to generic metrics influencing growth and physiological performance (e.g. cell size and NPQ). We hypothesised that K_C would follow a predictable pattern, whereby higher values would be observed for taxa with greater energetic requirements for cellular maintenance (and thus lower μ). As expected, K_C exhibited considerable variability, from ~4-10 mol e^- (mol C)$^{-1}$ from the 17 cultures, and indeed was negatively correlated with growth rate (R^2 = 0.7, $p < 0.01$). Diatoms and cryptophytes generally exhibited a lower K_C compared to dinoflagellates during steady-state, nutrient-replete culture conditions. Broader analysis that also included past published data did not find significant relationships between K_C and class, or growth rate, but did highlight that cell size potentially plays a role in explaining K_C variability. Together, this new analysis has revealed empirical relationships between K_C and growth rate and biovolume; consequently, given recent improvements in quantifying phytoplankton growth rates and cell size, these empirical relationships hold promise to improve capability to predict K_C which is needed to scale up the application of FRRf-based productivity studies to improve knowledge of C-cycling.

3.2 Introduction

Marine primary production (MPP) is a fundamental ecosystem process that supports food webs and regulates the global climate. For decades, various approaches have been applied to quantify phytoplankton photosynthesis, which is by far the single largest contributor to MPP across the world's oceans (Regaudie-de-Gioux et al. 2014). However, many of these approaches evaluate different components of photosynthesis, often over variable timeframes, and thus yield measurements in different units or photosynthetic "currencies" (Suggett et al. 2009a). Resolving estimates of MPP between approaches is thus not a trivial exercise, being further compounded by inherent assumptions and caveats specific to each method (Marra, 2012; Regaudie-de-Gioux et al. 2014).

Use of ^{14}C bottle incubations (Steeman-Nielsen, 1952) to trace the incorporation of radio-labelled carbon into organic matter, has long been considered the aquatic "gold-standard" method, despite well-recognised methodological flaws (Melrose et al. 2006; Marra, 2009), and underpins the calibration of virtually all satellite algorithms that yield MPP from ocean colour (Quay et al. 2010). However, the desire to improve understanding of carbon (C) sequestration from the atmosphere to oceans in the face of a rapidly-changing climate has resulted in renewed efforts to develop conversion factors allowing for retrieval of C-fixation rates from alternative photosynthetic currencies that can be measured with greater resolution and precision. For example, the photosynthetic quotient (PQ, see Laws, 1991), describing the molar ratio of O_2-evolved to CO_2-fixed during photosynthesis has been widely applied to aquatic productivity studies utilising the O_2-bottle method since the mid-1980s.

Poor sampling resolution ultimately afforded by incubation-dependent techniques that track C-fixation (or O_2 evolution) can lead to bias and uncertainties within satellite-based MPP models, resulting from insufficient synchronous *in-situ* photosynthetic rates to robustly "ground-truth" ocean colour algorithms (Behrenfeld et al. 2005; Jacox et al. 2015). Oceanographers have therefore increasingly turned towards bio-optical techniques such as Fast Repetition Rate fluorometry (FRRf, Kolber et al. 1998) in order to tackle this chronic issue of data-scarcity. FRRf and analogous chlorophyll fluorescence-induction techniques, actively probe the photochemical status of the oxygen-evolving complex at photosystem II (PSII) (see Huot and Babin, 2010), to estimate electron transport rate through PSII (ETR_{PSII}), introducing another photosynthetic currency (i.e. electrons generated from water-splitting during photosynthesis). Retrieving rates of C-fixation from FRRf-based estimates of MPP therefore requires a specific conversion factor, termed the "electron requirement for carbon fixation", K_C (Lawrenz et al. 2013; Hancke et al. 2015), describing the number of electrons required to synthesise one mole of C biomass.

The theoretical lower limit for K_C is 4 mol e^- [mol C]$^{-1}$ (see Kolber and Falkowski, 1993) based on the minimum number of electrons derived from 2 H_2O molecules in the production of 1 O_2 molecule (Suggett et al. 2009a). However, this lower limit assumes that all electrons are transferred to $NAPH^+$ via photosystem I (PSI), a pathway referred to as *linear electron flow* which generates energy (ATP), together with the reductant required to fix C during the Calvin Cycle (Behrenfeld et al. 2008). PSII electrons can also flow to diverse alternative electron sinks that either: i) do not result in C-fixation, e.g. nutrient reduction or cyclic electron flow, or ii) fix carbon less efficiently per electron, e.g. photorespiration. Thus, ETR_{PSII} represents the total number of electrons available to multiple electron sinks, and K_C summarises the net distribution of electrons

between C-fixing and non C-fixing pathways. Phytoplankton in particular, exhibit extreme flexibility in their capacity to adjust photosynthetic electron flow in response to highly-dynamic environments (Cardol et al. 2011). When conditions for photosynthesis are optimal (e.g. when light is limiting and downstream electron acceptors are not limited by CO_2-availability or nutrient stress), linear electron flow dominates (McDonald et al. 2011), and thus K_C is expected to be closer to the theoretical minimum. Under less-optimal conditions, phytoplankton cells employ alternative electron pathways which do not fix C, but instead act as photoprotective sinks (Roberty et al. 2014), or mechanisms to generate more ATP relative to NADPH (Cardol et al. 2011; Fisher and Halsey, 2016); allowing cells to meet increased energy requirements for cellular maintenance, or power nutrient-acquisition processes including carbon concentrating mechanisms (CCMs) (Langner et al. 2009; Halsey et al. 2010, 2015). These non C-fixing pathways thus decouple ETR_{PSII} from C-fixation and increase K_C. As such, measured values of K_C often exceed the theoretical minimum, with a global mean of ~11 mol e^- (mol C)$^{-1}$, and often correlates with environmental variables known to regulate photosynthesis (Lawrenz et al. 2013; Schuback et al. 2015, 2016, 2017; Hughes et al. in press., see Chapter 2), albeit with considerable variability. Gaining a predictive understanding of K_C variability thus remains an ongoing and key challenge for FRRf–based attempts to quantify MPP.

Interestingly, recent field studies focussed on examining K_C variability in response to light and nutrient availability (Lawrenz et al. 2013; Schuback et al. 2015, 2016, 2017; Zhu et al. 2016; Hughes et al. in press., Chapter 2), have also established a link between K_C and the extent of non-photochemical quenching (NPQ). NPQ reflects the dissipation of excess excitation energy prior to charge-separation at PSII, and thus is likely complimented by photoprotective mechanisms such as alternative electron flows acting

downstram of PSII, which ultimately act to increase K_C and thus potentially explaining this observed relationship (Schuback et al. 2015; 2016). However, NPQ mechanisms may vary considerably between key phytoplankton groups; for example diatoms and chlorphytes rely on notably different xanthophylls for energy-dependent quenching (qE, see Lavaud and Groth, 2006), whilst cyanobacteria utilise an orange caretonoid protein (OCP, see Kirilovsky, 2007). Thus, it is unclear whether the link between NPQ and K_C is driven by mainly by environmental influence (as examined by the aforementioned studies) or whether there is also a potential taxonomic component at play. In fact, whilst most recent efforts in the field have generally focussed on examining K_C variability in response to environmental conditions, laboratory studies examining a handful of phytoplankton strains (e.g. Suggett et al. 2009a; Napoleon et al. 2013) have offered compelling evidence for potential taxonomic regulation of K_C – indeed, this idea that has gained further traction through field observations (Suggett et al. 2006; Lawrenz et al. 2013; Robinson et al. 2014). However, identifying taxa-specific trends from field studies is difficult, because taxonomic dominance by broad functional groups is often closely tied-to (selected-for via) specific environmental conditions (e.g. Finkel et al. 2009). Thus, as it stands there is not enough power within existing data to conclusively determine i) if, and to what extent, taxonomic variation regulates K_C, ii) the taxonomic resolution needed to explain such variability, or iii) whether an overarching trait governing photosynthetic performance (e.g. cell size or non-photochemical quenching [NPQ] capacity) associated with changes in taxa can prove a common metric to explain variability in K_C.

To address this key knowledge gap we grew a broad range of phytoplankton strains spanning multiple taxonomic and size -classes, and examined K_C under controlled laboratory conditions. We hypothesised that K_C would follow a predictable taxonomic

pattern, whereby higher values would be observed for taxa with greater energetic requirements for cellular maintenance (and thus lower growth rates). We further combined our new observations with data mined from the extended literature to evaluate the extent to which variation of K_C could be explained by taxonomy, versus additional metrics including cell size and non-photochemical quenching (NPQ). Such knowledge is needed to fundamentally improve the accuracy with which FRRf measurements can be scaled-up for remote sensing purposes, particularly as capacity to resolve phytoplankton groups and size classes from satellite data is fast improving (see Bracher et al. 2017).

Table 3.1 Summary of phytoplankton strains used in this study, indicating taxonomic class and cell volume (μm^3). The grey shaded area represents strains that were sampled opportunistically in addition to the main study (note the different growth conditions).

Class	Species	Cell Volume (μm^3)	Temperature (ºC)	PAR (growth)	Media
Bacillariophyceae	*Ditylum brightwelli* CS-131	54521.28	20	60	f/2
	Nitzschia closterium CS-5	206.16	20	60	f/2
	Thalassiosira pseudonana CS-173	81.90	20	60	f/2
	Thalassiosira weissflogii CCMP1336	1469.02	20	60	f/2
Chlorophyceae	*Dunaliella tertiolecta* CCMP1320	292.50	20	60	f/2
	Tetraselmis sp. CS-91	291.65	20	60	f/2
	Tetraselmis sp. CS-352	1977.40	20	60	f/2
Cyanophyceae	*Synechococcus* sp. CS-94	1.35	20	60	f/2
Eustigmatophyceae	*Nannochloropsis oculata* CS-179	14.12	20	60	f/2
Prymnesiophyceae	*Emiliania huxleyi* CS-370	102.37	20	60	f/2
	Phaeocystis pouchetti CS-165	596.91	20	60	f/2
Cryptophyceae	*Rhodomonas salina* CS-692	168.50	20	60	f/2
Dinophyceae	*Ostreopsis siamensis* F3	30752.12	20	60	f/10
	Ostreopsis siamensis MW3	31556.26	20	60	f/10
	Symbiodinium SCF082 (D1a)	1124.00	26	180	IMK
	Symbiodinium SCF058-04 (C123)	1586.00	26	180	IMK
	Symbiodinium SCF055-06 (C124)	1123.00	26	180	IMK

3.3 Materials and Methods

3.3.1 Phytoplankton culturing

We examined a range of phytoplankton taxa, encompassing 7 taxonomic classes and a wide range of cell sizes/volumes (Table 3.1). Measurements were initially performed on 12 species of non-axenic phytoplankton cultures obtained from the Australian National Algal Culture Collection (ANACC) , representing 5 eukaryotic microalgal classes: *Dunaliella tertiolecta* CCMP1320*, Tetraselmis* sp. CS-91 and *Tetraselmis* sp. CS-352 (Chlorophyceae); *Thalassiosira weissflogii* CCMP1336*, T. pseudonana* CS-173, *Nitzschia closterium* CS-5 and *Ditylum brightwelli* CS-131 (Bacillariophyceae); *Nannochloropsis oculata* (Eustigmatophyceae); *Phaeocystis pouchetti* CS-165 and *Emiliania huxleyi* CS-370 (Prymnesiophyceae); *Rhodomonas salina* CS-692 (Cryptophyceae) and the one prokaryotic group, *Synechococcus* sp. CS-94 (Cyanophyceae). All cultures were grown in a temperature-controlled incubator (Steridium model: E500, Brisbane, Australia) at 20°C (See Table 3.1) within 75 mL flasks (Falcon T75, Sigma-Aldrich Pty Ltd, Castle Hill, Australia) and maintained in semi-continuous batch mode via periodic serial dilutions when required (Wood et al. 2005). Strains were grown in f/2 enriched seawater (Guillard and Ryther, 1962), prepared with 0.2 μm filtered natural seawater, plus additional silicate (Si) for Bacillariophyceae (diatoms). Salinity was maintained at 35 PSU for all cultures, and PAR of 60 ± 10 μmol photons m^{-2} s^{-1}, provided by T5 cool-white fluorescent lighting (24W, Combrite SD224-40**)** set to a 12:12 hour photoperiod. Cultures were acclimated to growth conditions for approximately 3 months before sampling commenced. After acclimation, samples were collected during mid-exponential growth for: Fast Repetition Rate fluorometry (FRRf) photophysiology and photosynthetic-irradiance (PE) response, Chlorophyll-*a* (Chl-*a*) determination, particulate organic carbon and nitrogen content

(POC, PON), cell density and biovolume analysis, spectral light absorption (a^{Chl}) and measurements of K_C, detailed below.

3.3.2 Additional opportunistic sampling

On several occasions, we were able to perform opportunistic measurements of K_C (plus ancillary measurements where available) on additional strains being used in experimental work overlapping the duration of our study. Specifically, 6 further strains from the eukaryotic group Dinophyceae: the toxin-producing benthic dinoflagellate, *Ostreopsis siamensis* (strains MW3 and F3, isolated by A. Verma in NSW, Australia) and the symbiotic dinoflagellate, *Symbiodinium* (strains SCF082 (clade D1a), SCF058-04 (clade C123) and SCF055-06 (clade C124). Dinoflagellate strains were also maintained in balanced growth via semi-batch culturing, but were grown under different environmental conditions (see Table 3.1).

3.3.3 Growth rates and cell size

Growth was calculated from daily measurements of *in-vivo* fluorescence over a total period of ca. 3 months, using Fast Repetition Rate fluorometry (FRRf) to monitor minimal fluorescence (F_0) as a proxy for Chl-*a* concentration (as per Suggett et al. 2009). Growth rates (μ) were calculated through linear regression of the natural log of F_0 against time, where the slope of the regression line describes daily division rate (d^{-1}). Growth rates calculated from F_0 were periodically validated against cell counts from samples preserved daily throughout the experimental period in Lugol's alkaline solution (to a final concentration of 1%), with the exception of *Synechococcus* sp. Overall, growth rates determined from F_0 showed strong correlations for all 12 strains grown (range of R^2: 0.71 – 0.92, mean R^2 = 0.87; data not shown). For most species, a minimum of 50 cells were imaged via microscopy and measured using ImageJ software

(US National Institutes of Health). Cell volume (μm^3) was determined from the equation describing the volume of the closest-matching geometric shape to that of the cell as per Sun and Liu (2003).

3.3.4 Chl-*a* analysis

Chl-*a* for all samples was determined by filtering 15 mL aliquots onto a Whatman GF/F filter (0.7 µm nominal pore size) before immediate extraction of pigments in 90% acetone and storage at 4°C in darkness. For the >10 µm fraction, a similar procedure was conducted, but instead using 10 µm polycarbonate filters (Merck Millipore, Bayswater, VIC, Australia). After 48 hr of extraction in acetone, Chl-*a* was determined fluorometrically using a Trilogy fluorometer fitted with Chl-*a* non-acidification module (Turner Designs, California, USA) and calibrated against pure Chl-*a* standards (Sigma-Aldrich Pty Ltd).

3.3.5 POC and PON analysis

20 mL aliquots were filtered onto pre-combusted GF/F filters (0.7 µm pore size) under low vacuum (~50 mm Hg), dried for 48 hr at 60°C, packaged in pre-combusted aluminium foil and stored in darkness inside an air-tight ziplock bag containing silica gel packets. Subsequent analysis of POC and PON content was conducted at the Research Corporation of the University of Hawaii, using an elemental analyser (MAT Conflo IV, Thermo Finnigan, California USA) coupled to a mass spectrometer (Delta+ XP, Thermo Finnigan), however no value is reported for *Synechococcus* sp. (CS-94) because this sample was unfortunately lost prior to analysis.

3.3.6 Fast Repetition Rate fluorometry (FRRf) photophysiology

A FastOcean MKIII Fast Repetition Rate Fluorometer (FRRf) (Serial number: 12-8679-007) attached to a FastACT docking base (Chelsea Technologies Group, London, UK) was programmed to deliver single turnover (ST) saturation of PSII from 100 flashlets (1 μs pulse with a 2 μs interval between flashes), followed by a relaxation phase of 40 flashlets (1 μs pulse with a 50 μs interval between flashes). A total of 20 sequences were performed per acquisition with an interval of 150 ms between sequences. For all eukaryotic phytoplankton in this study, the blue LED (450 nm) was the sole excitation source used, whilst a combination of blue + red LEDs (450 nm + 624 nm) was applied to *Synechococcus* to drive closure of PSII reaction centres. The biophysical model of Kolber et al. (1998) was fitted to all FRRf acquisitions using the instrument-bundled FastPRO software (V.1.5.2) to determine minimum (F_0, F') and maximum fluorescence (F_m, F_m'), functional absorption cross-section of PSII ($\sigma_{PSII,}$ σ_{PSII}') and PSII connectivity factor (ρ, ρ′) (where the prime notation denotes that samples were measured during exposure to actinic light). FastPRO software was also used to subtract baseline fluorescence (obtained from 0.2 μm filtered samples) from the total variable fluorescence signal.

3.3.7 Electron transport rate (ETR_{PSII})

FRRf-derived photosynthetic electron transport rates ($ETR_{PSII,}$ electrons m^{-3} s^{-1}) were determined using the biophysical "sigma-based" algorithm originally developed by Kolber and Falkowski (1993).

$$ETR_{PSII} = E \cdot \sigma_{PSII}' \cdot (1/[F_v/F_m]) \cdot [RCII]^{(FRRf)} \cdot (1\text{-}C) \quad (3)$$

where E is irradiance (photons m^{-2} s^{-1}), σ_{PSII}' is the functional absorption cross-section of PSII under actinic light (nm^{-2} $quanta^{-1}$), $[RCII]^{(FRRf)}$ is the concentration of PSII reaction centres (mol RCII m^{-3}), estimated fluorometrically according to Oxborough et al. (2012):

$$[RCII]^{(FRRf)} = \frac{K_R}{E_{LED}} \times \frac{F_o}{\sigma_{PSII}} \quad (4)$$

where K_R is an instrument-specific constant (photons m^{-3} s^{-1}) and E_{LED} is the intensity of the fluorometer's 450 nm measuring beam (photons m^{-2} s^{-1}). C is the fraction of [RCII] in the closed state, calculated here as 1-qP (qP = $(F'-F_0')/(F_m'-F_0')$. Inclusion of the factor $1/[F_v'/F_m']$ (where $F_v'/F_m' = [F_m' - F_0']/F_m'$) accounts for the non-radiative loss of energy associated with σ_{PSII}' (Kolber et al. 1998; Suggett et al. 2009a; Oxborough et al. 2012). Both [RCII] and (1-C) are necessary in order to measure gross photosynthesis (Kolber and Falkowski, 1993), yielding ETR_{PSII} with units of electrons m^{-3} s^{-1}, assuming an efficiency of one charge-separation event per photon absorbed (see Kolber and Falkowski, 1993). All measurements of σ_{PSII}' were spectrally-adjusted to account for the bias of light absorption towards the 450 nm FRRf excitation LED. For this, absorption spectra for each sample was measured using the quantitative filter pad technique (Roesler, 1998), with absorbance measured from 400-750 nm using a fibre-optic spectrometer (UV/VIS, Ocean Optics, Florida, USA) against a separate sample blank. Measured absorbance spectra were scatter-corrected and converted into Chl-*a* specific absorption coefficients (a^{Chl}) as:

$$a^{Chl}(\lambda) = \frac{2.303 \cdot A(\lambda)}{L \cdot \beta \cdot Chl - a} \quad (3)$$

where $A(\lambda)$ represents the wavelength-dependent absorbance, L is the optical pathlength of filter particulates (sample volume filtered [m^3] / filter clearance area [m^2]) and β the

pathlength amplification factor (see Roesler, 1998). From this we obtained spectrally-resolved values of PSII effective absorption, $\sigma_{PSII}'(\lambda)$ as:

$$\sigma_{\mathrm{PSII}}{}'(\lambda) = \left(\sigma_{\mathrm{PSII}}{}'(450) \Big/ \alpha^{Chl(\lambda)}(450) \right) . \alpha^{Chl(\lambda)} \quad (4)$$

Values of $\sigma_{PSII}'(\lambda)$ were then spectrally-adjusted to the spectra of the actinic light source within the FRRf optical head (cool white LED) as,

$$\overline{\sigma_{\mathrm{PSII}}{}'} = \left(\sum_{400}^{700} \sigma_{\mathrm{PSII}}^{'(\lambda)} . E(\lambda) \right) \Delta\lambda \Big/ \sum_{400}^{700} E(\lambda)\Delta\lambda \quad (5)$$

3.3.8 FRRf photosynthesis-irradiance (PE) curves

Steady-state fluorescence light curves were performed using an identical protocol as described in Suggett et al. (2015). The model of Platt et al. (1980) was then fit to the data using Sigmaplot curve-fitting software (Version 12.5, Systat Software Inc, California, USA). Least squares non-linear regression analysis of the model fit was performed to derive the maximum rate of photosynthesis, ETR_{PSII}^{max} and the light utilisation efficiency, α (electrons m^{-3} s^{-1}), allowing for subsequent calculation of the light saturation parameter, E_K (ETR_{PSII}^{max}/ α) with units of µmol photons m^{-2} s^{-1}.

3.3.9 Simultaneous FRRf-^{14}C incubations (K_C)

We followed the recommendations of Suggett et al. (2009a) and measured both ETR_{PSII} and ^{14}C-uptake simultaneously (i.e. a "dual incubation") upon the same sample, thus avoiding discrepancies between spectral quality and intensity of the light source driving photosynthesis in separate incubations. This was achieved by incubating radiolabelled samples within the optical head of the FastOcean FRRf and using the FRRf's cool-white

LED array to supply actinic light to the sample (see Supplementary Fig. S3.1). Not only does the dual incubation method avoid the need to apply spectral correction factors which can be error-prone, but also avoids potential issues with sample heterogeneity (Lawrenz et al. 2013).

To quantify ^{14}C-uptake, we adopted the small-volume method of Lewis and Smith (1983) with several modifications. For each strain, triplicate 3 mL samples were placed in a borosilicate test-tube and spiked to a final concentration of 0.4 μCi mL^{-1} $NaH^{14}CO_3$ (Perkin-Elmer, Melbourne, Australia). The radio-labelled sample was then incubated for 20 min inside the FRRf at a single irradiance corresponding to the growth conditions of that specific strain (i.e. 60 or 180 μmol photons m^{-2} s^{-1}) and ETR_{PSII} was determined every 5 s during this period. At the end of the incubation period, the sample was removed and immediately acidified with 150 μL of 6 M HCl to drive remaining unfixed inorganic C to CO_2. Samples were then agitated gently on an orbital shaker (100 rpm) and left to de-gas for 24 hr prior to fixation with 10 mL scintillation fluid (Ultima Gold LLT, Perkin Elmer). Fixed samples were shaken vigorously for several minutes and left to stand for 3 hr before measuring disintegrations per minute (DPM) via liquid scintillation counting (Tri-Carb 2810 TR, Perkin-Elmer) using automatic quench correction and a count time of 5 min. ^{14}C-uptake was calculated on a volumetric basis from the concentration of dissolved inorganic carbon (DIC) and the amount of ^{14}C isotope incorporated during the incubation as per Knap et al. (1996). 20 mL aliquots for DIC analysis were taken from parallel samples grown under identical conditions. Each sample was transferred to a glass scintillation vial, preserved with $HgCl_2$ at a final concentration of 0.5%, double-wrapped in parafilm to prevent gas exchange and stored in darkness until subsequent analysis of DIC using a dissolved gas analyser (Picarro 1301, Picarro Instruments, California, USA). Both ETR_{PSII} and ^{14}C-uptake were scaled

to hourly-integrated rates as per Suggett et al. (2009a) so that K_C (mol e^- [mol C]$^{-1}$) could be determined as:

$$K_C = {}^{\mathrm{ETR_{PSII}}}/_{\text{14C uptake rate}} \quad (7)$$

3.3.10 Additional FRRf-based parameterisation

For all cultures and conditions, non-photochemical quenching of fluorescence was calculated as the normalised Stern-Volmer coefficient (NPQ_{NSV}) as per McKew et al. (2013) during the simultaneous ^{14}C-FRRf incubations and represents an integrated value over the entire incubation period. In addition, PSU size (mol Chl-*a* [mol RCII]$^{-1}$) was calculated from $[RCII]^{(FRRf)}$ and measured Chl-*a* concentration as per Oxborough et al. (2012) as:

$$\text{PSU Size} = {}^{\mathrm{Chl-a}}/_{[\mathrm{RCII}]} \quad (8)$$

3.3.11 Meta-analysis

We searched the literature for parallel measurements of ETR_{PSII} and ^{14}C-uptake upon laboratory-grown phytoplankton cultures. Principle component analysis (PCA) was used to visually assess patterns in K_C (Supplementary Fig. S3.2). Upon initial inspection, it was evident that methodological inconsistencies between studies were potentially driving variability in K_C. Thus, to remove methodological bias from our pooled assessment of K_C, we applied stringent screening criteria to ensure consistency with our existing data set. Specifically, data was only included if the following were met: i) phytoplankton were grown under nutrient-replete conditions, ii) ETR_{PSII} was measured by single-turnover instrumentation protocols (see Kromkamp and Forster (2003) for more detail) iii) ^{14}C incubations were derived from short incubations <30 min

(to allow little time for respiration of C-fixed), iv) the concentration of functional PSII reaction centres [RCII] was determined, rather than assumed using a constant relative to measured Chl-*a* concentration, v) K_C was measured at irradiances representing light-limited photosynthesis (i.e. where $E/E_K <= 1$ – we revisit this point later in the results section) and vi) appropriate spectral correction factors were applied (see above).

3.3.12 Statistical Analysis

A one-way analysis of variance (ANOVA) was used to test for species-specific differences in K_C, using a Tukey test when significant differences were detected. A two-way ANOVA was performed to test for differences, and possible interactive effects, between taxonomic class and size class (based on cell volume), which were regarded as fixed factors. When significant differences were found, a Tukey test was performed. All K_C data were $\log_{10}$ transformed prior to statistical analysis to improve assumptions for ANOVA (IBM SPSS v20.0). Neither the Levene's test for homogeneity of variance, nor Shapiro-Wilk test for normality was violated. Relationships between K_C and both growth rate, and NPQ_{NSV} were assessed by linear regression (R-software v. 3.2.1). Factors explaining variation in growth rates between strains were assessed using distance-based redundancy analysis (dbRDA) ordination plots (PRIMER v6.0, PRIMER-E, Plymouth, UK) using K_C, POC:PON and cell volume as predictive variables. Principle component analysis (PCA, PRIMER v6.0) was used to identify patterns in data collated during the meta-analysis of the wider literature. Upon incorporating the additional data from the meta-analysis, the Levene's test for homogeneity of variance was violated despite transformation. Thus, differences in K_C between taxonomic, and size, classes were evaluated using the non-parametric Kruskal-Wallis test and Dunn's post-hoc test with Bonferroni correction.

3.4 Results

3.4.1 Phytoplankton growth, elemental stoichiometry and photophysiology

Growth rates varied considerably between strains, ranging from 0.24 (*Tetraselmis sp.*) to 0.84 (*N. closterium*). Diatoms, together with *Synechococcus* sp, consistently exhibited the highest growth rates (0.75 - 0.84), compared to chlorophytes which were generally low (0.24 - 0.57), with prymnesiophytes intermediate (0.51 – 0.71) (Table 3.2). Growth rates for strains measured "opportunistically" are not reported here because we do not have sufficient fluorometry data prior to sampling from which to derive a comparable growth rate. Measured POC:PON ratios ranged from 4.97 to 9.59 across the 12 taxa grown in the main study (Table 3.2). Diatoms had notably lower POC:PON ratios than most other classes, with all but *D. brightwelli* exhibiting values <6, together with the cryptophyte, *R. salina*.

Generally, as expected (see Suggett et al. 2009b, 2015), we observed an inverse covariation between F_vF_m and σ_{PSII} associated with cell volume (Table 3.2, Supplementary Fig. S3.3), with the exception of the dinoflagellates which, had relatively low F_v/F_m values together with larger σ_{PSII} despite their large cell volumes (Table 3.2). *Synechococcus* sp. also appeared to contradict this trend, most likely since the low value for σ_{PSII} reflects the unique combination of excitation LEDs employed in the FRRf protocol for this strain (450 nm + 630 nm). Photosynthetic unit (PSU) ranged from 254.8 - 842.5 mol Chl-*a* (mol RCII)$^{-1}$, however most (14 out of 17) strains had a PSU size between 300 - 650 mol Chl-*a* (mol RCII)$^{-1}$ (Table 3.2). The cyanobacterium *Synechococcus* exhibited the smallest PSU size, likely since more Chl-*a* is typically associated with PSI rather than PSII as opposed to the eukaryotic strains in this study (Pakrasi et al. 1985).

Table 3.2 Mean (± SE) values of daily growth rate (μ, d^{-1}), particulate organic carbon to nitrogen ratio (POC:PON, dimensionless), maximum PSII photochemical efficiency (F_v/F_m, dimensionless), functional absorption cross-section of PSII (σ_{PSII}, nm^2 $quanta^{-1}$), turnover time of PSII (τ_{PSII}, ms), light saturation parameter (E_K, μmol photons m^{-2} s^{-1}), the incubation irradiance relative to E_K (E/E_K, dimensionless), the size of the photosynthetic unit (PSU size, mol Chl-*a* [mol RCII]$^{-1}$) calculated as per Oxborough (2012) and the spectral correction factor (s.c.f) for each strain used in this study. The grey shaded area represents strains that were sampled opportunistically in addition to the main study, thus some measurements were not performed (-).

Species	μ	POC:PON	Cell Volume	F_v/F_m	σ_{PSII}	τ_{PSII}	E_K	E/E_K	PSU size	S.c.f
D. tertiolecta	0.35 (0.01)	6.43	292.5 (21.5)	0.51	2.98	611.0	151.8 (7.1)	0.27	565.6 (143.9)	2.65
Tetraselmis sp. (CS-91)	0.57 (0.01	6.46	300.9 (17.1)	0.56	2.99	696.3	157.5 (2.7)	0.28	306.5 (7.5)	2.03
Tetraselmis sp. (CS-352)	0.24 (0.01)	4.97	1569.6 (45.4)	0.60	1.82	701.6	354.8 (64.4)	0.11	339.3 (23.6)	2.53
N. oculata	0.28 (0.02)	8.58	14.1 (1.1)	0.53	3.52	689.6	144.1 (5.9)	0.30	543.1 (58.6)	2.20
T. weissflogii	0.76 (0.02)	5.05	1718.3 (28.2)	0.58	3.44	585.4	205.6 (13.2)	0.27	642.3 (25.6)	1.92
T. pseudonana	0.74 (0.01)	5.18	131.8 (9.1)	0.54	4.05	551.8	140.9 (12.5)	0.31	447.1 (26.7)	2.16
N. closterium	0.84 (0.05)	5.77	206.2 (15.2)	0.53	3.63	562.3	137.8 (9.53)	0.32	501.9 (92.2)	2.03
D. brightwelli	0.77 (0.03)	6.62	54521.3	0.49	3.71	571.8	159.9 (14.35)	0.30	472.6 (79.3)	1.78
Synechococcus (CS-94)	0.82 (0.05)	Lost	1.35	0.49	1.79	619.1	132.8 (17.2)	0.37	254.8 (11.0)	1.59
E. huxleyi	0.71 (0.02)	9.59	102.4 (11.8)	0.47	6.86	521.9	58.8 (4.4)	0.89	636.9 (30.1)	2.44
P. pouchetti	0.51 (0.02)	6.67	596.9 (41.0)	0.46	5.06	594.9	65.03 (2.1)	0.84	507.0 (9.1)	2.26
R. salina	0.39 (0.01)	5.11	168.5 (8.7)	0.50	2.62	745.75	52.2 (7.8)	1.11	457.6 (32.9)	1.44
O. siamensis (MW3)	-	-	31556.3	0.44	3.73	589.6	131.9 (6.05)	0.33	842.5 (60.1)	2.40*
O. siamensis (F3)	-	-	30752.1	0.46	3.54	611.3	124.78 (2.3)	0.35	552.5 (6.6)	2.40*
Symbiodinium (D1a)	-	-	1124	0.40	4.28	597	195.2 (9.9)	0.92	350.5 (24.3)	2.25*
Symbiodinium (C123)	-	-	1586	0.43	4.59	582	212.5 (8.6)	0.85	267.7 (3.2)	2.25*
Symbiodinium (C124)	-	-	1123	0.41	4.53	570	222.0 (6.5)	0.81	338.7 (11.8)	2.25*

Interestingly, the light-saturation parameter, E_K (i.e. the irradiance at which photosynthesis becomes light-saturated), when spectrally-corrected to match the growth conditions, was between 130 - 200 μmol photons m^{-2} s^{-1} for the majority of strains, thus up to three-fold higher than growth irradiance (60-180 μmol photons m^{-2} s^{-1}, Table 3.2). Only three strains (*R. salina* and both prymnesiophytes) exhibited E_K values close to growth irradiance, ranging from 52.2 - 58.8 μmol photons m^{-2} s^{-1}, whilst the single largest E_K value in this study (~350 μmol photons m^{-2} s^{-1}) was measured in *Tetraselmis* sp (CS-352). Consequently, because ETR_{PSII} and ^{14}C-uptake incubations were performed at irradiance levels close to growth conditions, the irradiance (E) relative to E_K, (i.e. E/E_K) was <1 for most strains except *R. salina* (1.26), *E. huxleyi* (1.12) and *P. pouchetti* (1.01), thus virtually all K_C values reported in this study correspond to light-limited photosynthesis (Table 3.2).

3.4.2 Simultaneous ^{14}C-uptake and ETR_{PSII} incubations (K_C)

The mean measured value of K_C for this study was 5.7 ± 0.3 mol e^- (mol C)$^{-1}$ (n = 48), but ranged from 3.85 to 10.73 mol e^- (mol C)$^{-1}$; with *T. weissflogii* and *R. salina* exhibiting K_C values fractionally below the theoretical minimum of 4 mol e^- (mol C)$^{-1}$ (Fig. 3.1). Measured K_C for *Symbiodinium* D1a was significantly higher (10.7 mol e^- [mol C]$^{-1}$) than all other strains in this study (ANOVA, $p < 0.05$), whilst the values for *P. pouchetti* and *N. oculata* were also larger (7.8 and 7.26 mol e^- [mol C]$^{-1}$, respectively) than a number of other strains (ANOVA, $p < 0.05$) (Fig. 3.1). For the remaining strains, K_C values were ~4-5 mol e^- (mol C)$^{-1}$ and not statistically distinguishable from one another (Fig. 3.1). Overall, dinoflagellates and prymnesiophytes exhibited a greater range of K_C values compared to other classes (Fig. 3.2a), indicating that taxonomic class alone was not a reliable predictor for K_C for these

groups. Nevertheless, statistically-significant differences in K_C values were evident between taxonomic classes ($p < 0.01$), with both diatoms, and cryptophytes exhibiting lower values than dinoflagellates (both $p < 0.05$) (Fig. 3.2a). When binned into arbitrary size classes, K_C was not significantly different (albeit close to significant: $p = 0.056$) (Fig. 3.2b); however there was a significant interaction between both taxonomic class and size class (ANOVA, $p < 0.01$).

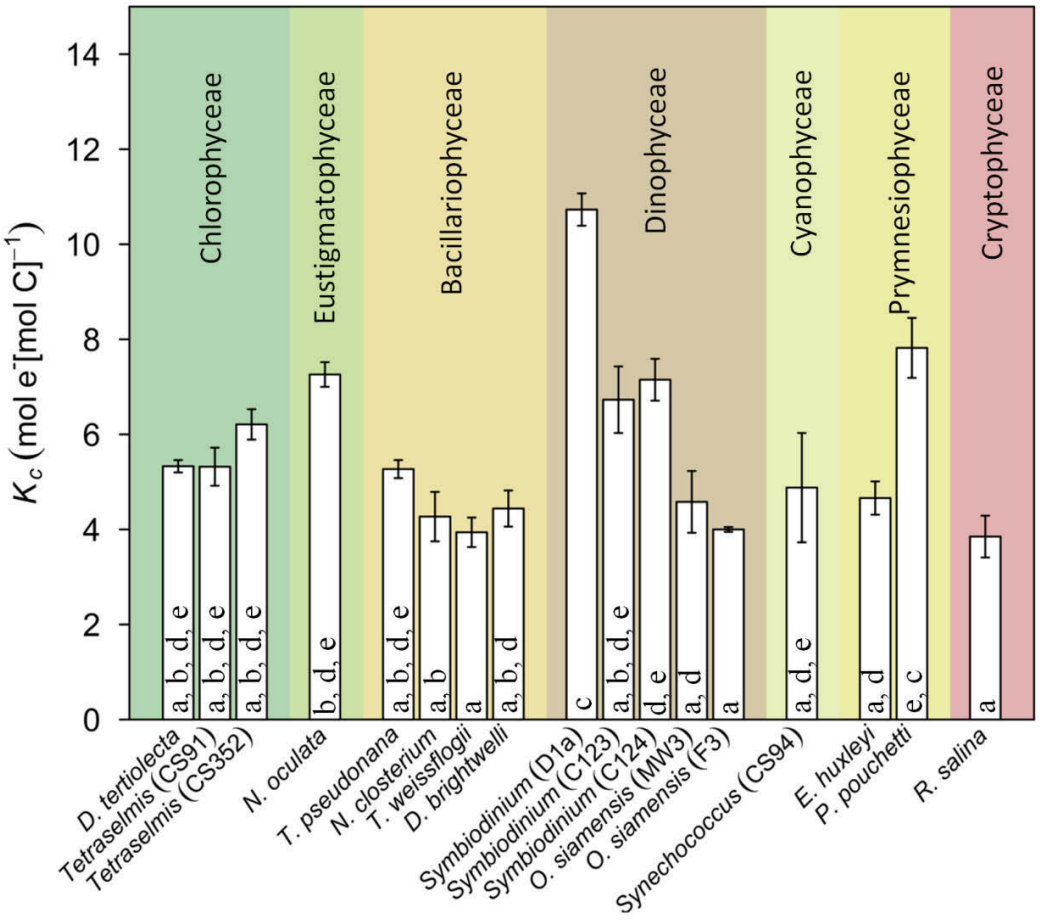

Figure 3.1 Measured values of the electron requirement for carbon fixation (mol e^- [mol C]$^{-1}$), K_C for the 17 phytoplankton strains examined in this study. The background colour corresponds to taxonomic class (also labelled). Error bars indicate standard errors and letters indicate means that are statistically indistinguishable ($\alpha = 0.05$) (ANOVA).

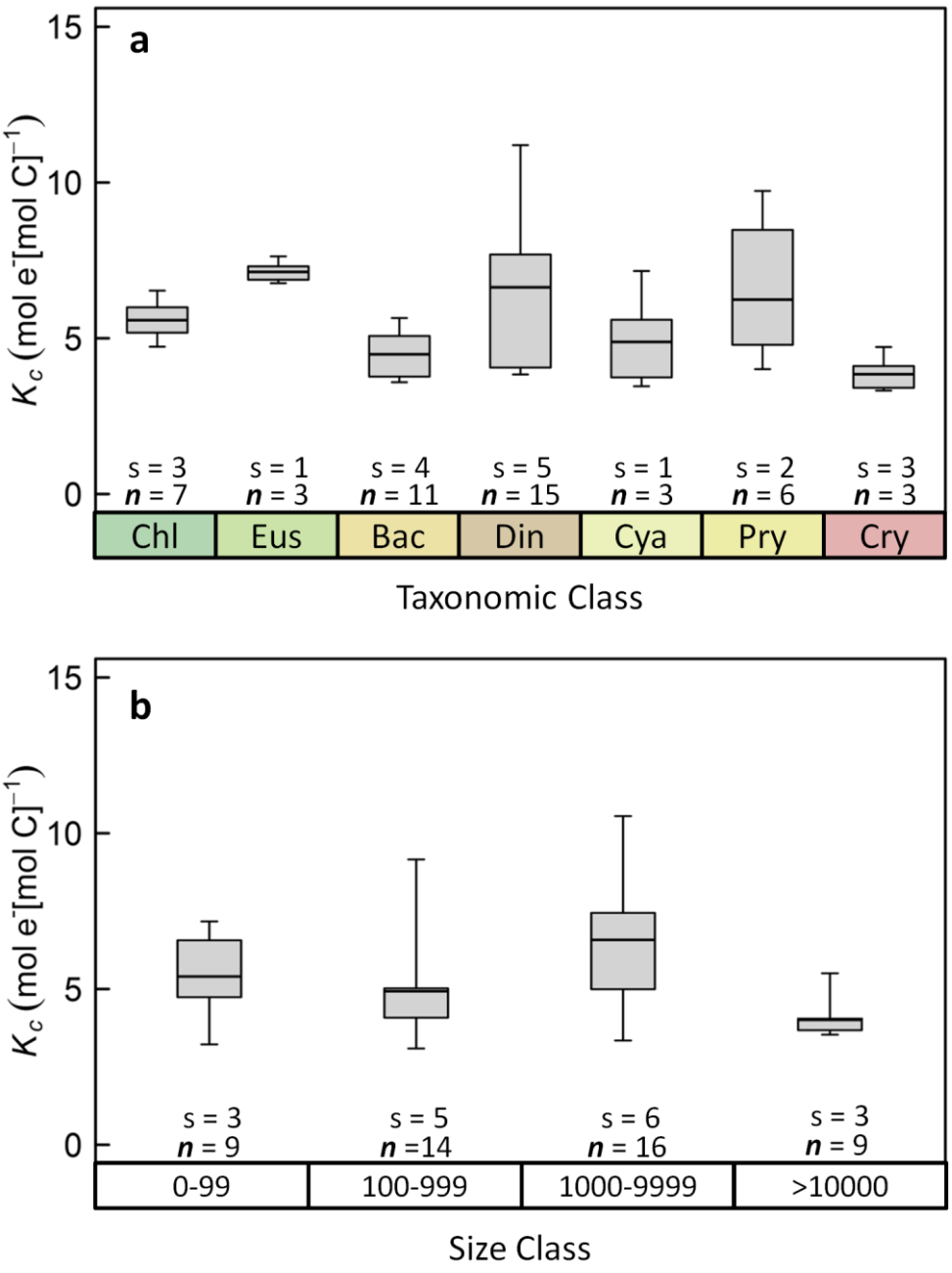

Figure 3.2 Boxplot of the electron requirement for carbon fixation, K_C for the 17 phytoplankton strains examined in this study (n = 48), grouped by **a**) taxonomic class – abbreviated by the first 3 letters of the class name: **Chl**orophyceae, **Eus**tigmatophyceae, **Bac**illariophyceae, **Din**ophyceae, **Cya**nophyceae, **Pry**mnesiophyceae and **Cry**ptophyceae, and **b**) arbitrary bins of cell volume (μm^3). The length of the box corresponds to the inter-quartile range, whilst whiskers indicate the range of the data in each cluster respectively.

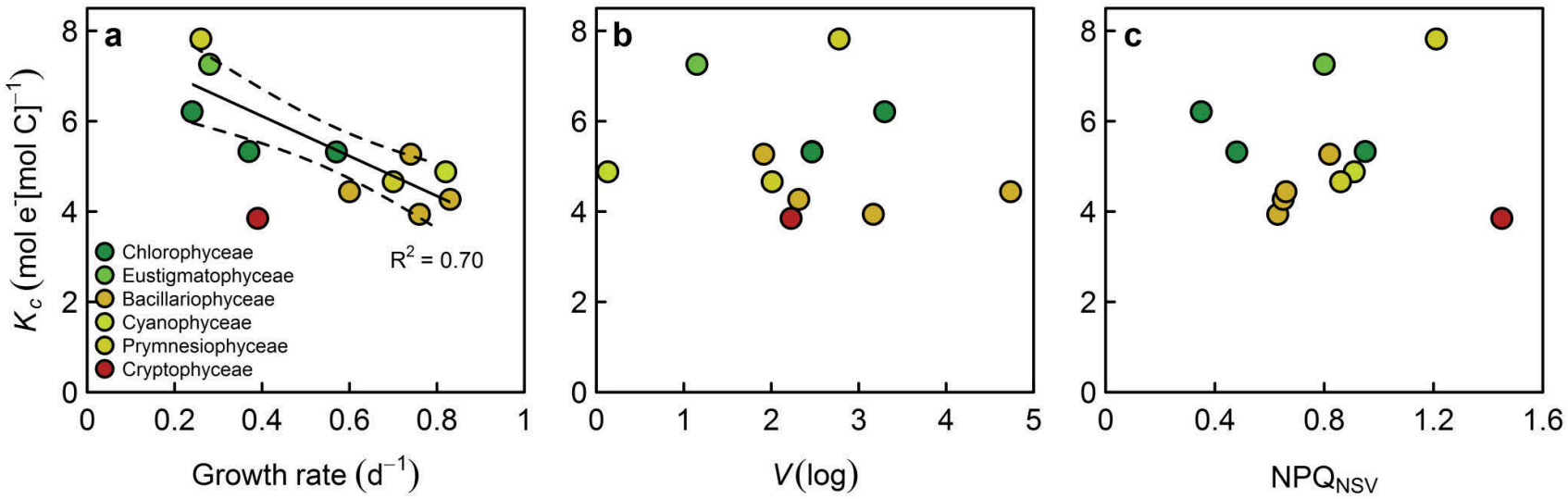

Figure 3.3 Relationship between the electron requirement for carbon fixation, K_C (mol e$^-$ [mol C]$^{-1}$), and corresponding measures of a) phytoplankton growth rate (d^{-1}), b) log-normalised cell volume (V[log]) and c) non-photochemical quenching, estimated as the normalised Stern-Volmer coefficient (McKew et al. 2013), denoted here as NPQ$_{NSV}$ (dimensionless) for all strains grown in the main study (i.e. excluding strains sampled "opportunistically" where growth data was unavailable. The cryptophyte, *R. salina* (red circle) has been excluded from the regression in panel a – if included the relationship weakens ($R^2 = 0.49$, $p < 0.05$), generating a regression equation of $y = -3.73 + 7.31$.

3.4.3 Relationship between K_C and other metrics

Consistent with our original hypothesis, we observed a significant inverse relationship between K_C and growth rate ($R^2 = 0.49$, $p < 0.05$, Fig. 3.3a); however, *R. salina* clearly contributed to lack of convergence of a linear fit, and the relationship improved considerably once this strain was removed ($R^2 = 0.71$, Fig. 3.3a). Linear regression returned no significant relationship between K_C and either NPQ_{NSV} ($p = 0.26$, Fig. 3.3b), or cell volume ($p = 0.28$, Fig. 3.3c). Given the apparent uncoupling between K_C and growth rate (particularly in the case of *R. salina*), we further examined whether a greater extent of variability of growth rate could be explained from K_C, combined with additional variables associated with biophysical constraints (cell volume) and elemental composition (POC:PON ratio) that govern the efficiency with which light energy is converted to biomass (see Litchman et al. 2007). Approximately 55% of variability in growth rates for all strains combined was explained using all 3 variables, thus offering only a slight improvement over K_C alone; again, removal of *R. salina* improved this to 76% (Fig. 3.4). Thus overall, the inclusion of additional variables resulted in only a marginally improved ability to reconcile variability between K_C and growth rates.

3.4.4 Resolving further trends in K_C by including meta-data

Incorporation of data mined from the extended literature (Supplementary Table S3.1), increased the total number of observations to $n = 72$ (from our study alone, $n = 48$), representing K_C measurements from taxonomic classes we evaluated (Chlorophyceae, Bacillariophyceae, Dinophyceae and Cryptophyceae), plus one new class (Pelagophyceae). All of these additional data fell into just two of our four arbitrarily-defined size classes, 100-999 μm^3 and 1000-9999 μm^3. These additional data introduced variability of K_C within most taxonomic classes (Fig. 3.5a) compared to our

original data set (Fig. 3.2a). Dinoflagellates continued to exhibit the widest range of K_C values (~4-22 mol e^- [mol C]$^{-1}$) whilst diatoms were still characterised by a narrower range of K_C values (~4-10 mol e^- [mol C]$^{-1}$); however the two classes (which together comprised the most observations in this study) were no longer statistically distinguishable (Kruskal-Wallis, $p = 0.07$). In fact, the only significant difference in K_C was found between diatoms and the newly-added class, Pelagophyceae (Kruskal-Wallis, $p < 0.01$).

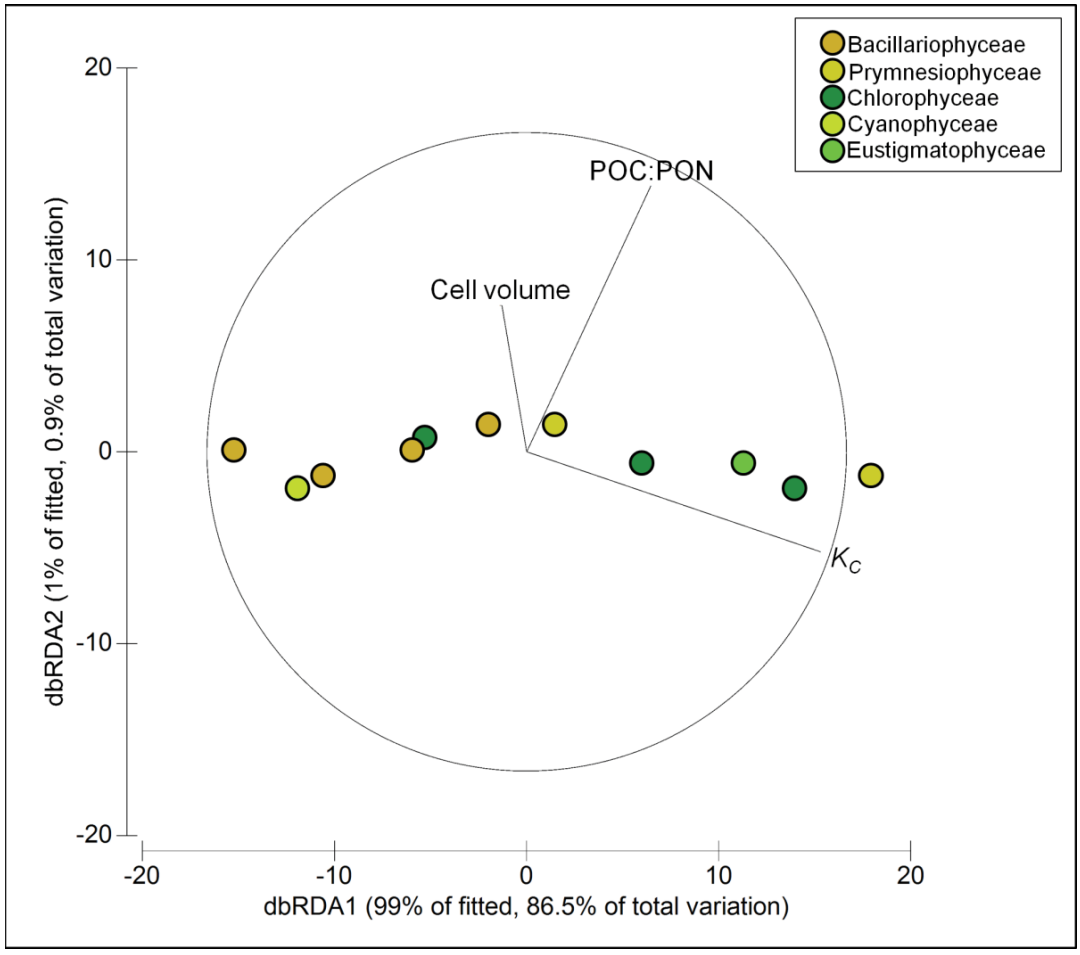

Figure 3.4 Distance-based redundancy (dbRDA) plot illustrating the DistLM model based on the phytoplankton growth rate, and selected predictive variables: Cell volume, POC:PON ratio and the electron requirement for carbon fixation (K_C). Symbols represent the different phytoplankton classes (see key). Note: *R. salina* is excluded from this analysis (see results section).

Consideration of the full meta-data allowed for statistical differences to be determined across the three larger arbitrary size classes (i.e. excluding the 0-99 μm^3 class), with the 1000-9999 μm^3 class having significantly higher K_C than the either the 100-999 μm^3 class (Kruskal-Wallis, $p < 0.01$) and the >10000 μm^3 class (Kruskal-Wallis, $p < 0.001$) (Fig. 3.5b). However linear regression returned no significant relationship between K_C and either growth rate, cell volume or NPQ_{NSV} or cell volume (Fig. 3.6a-c).

3.5 Discussion

Studies are increasingly turning towards examining and modelling K_C in order to retrieve estimates of C-fixation from FRRf-assessments of phytoplankton photosynthetic rates (as ETR_{PSII}). However, these studies have been predominately empirically-based from measurements upon natural phytoplankton communities, where it is difficult to reconcile conflated regulatory effects of taxa and environment upon K_C. By growing 17 species of phytoplankton taxa under controlled laboratory conditions, and mining data from existing studies, we demonstrate taxonomic regulation of K_C at both the species, and class level and further show growth rate to be an important factor explaining K_C variability. Whilst this is still an empirical descriptor, by isolating factors that appear to drive this, we demonstrate that diatoms and cryptophytes have a lower K_C compared to dinoflagellates during steady-state, nutrient-replete growth. The subsequent meta-analysis also highlighted a potential role for cell volume in determining K_C variability, but this requires further investigation. We discuss these observations in the following sections and how they can potentially improve our ability to apply FRRf for the widespread assessment of MPP.

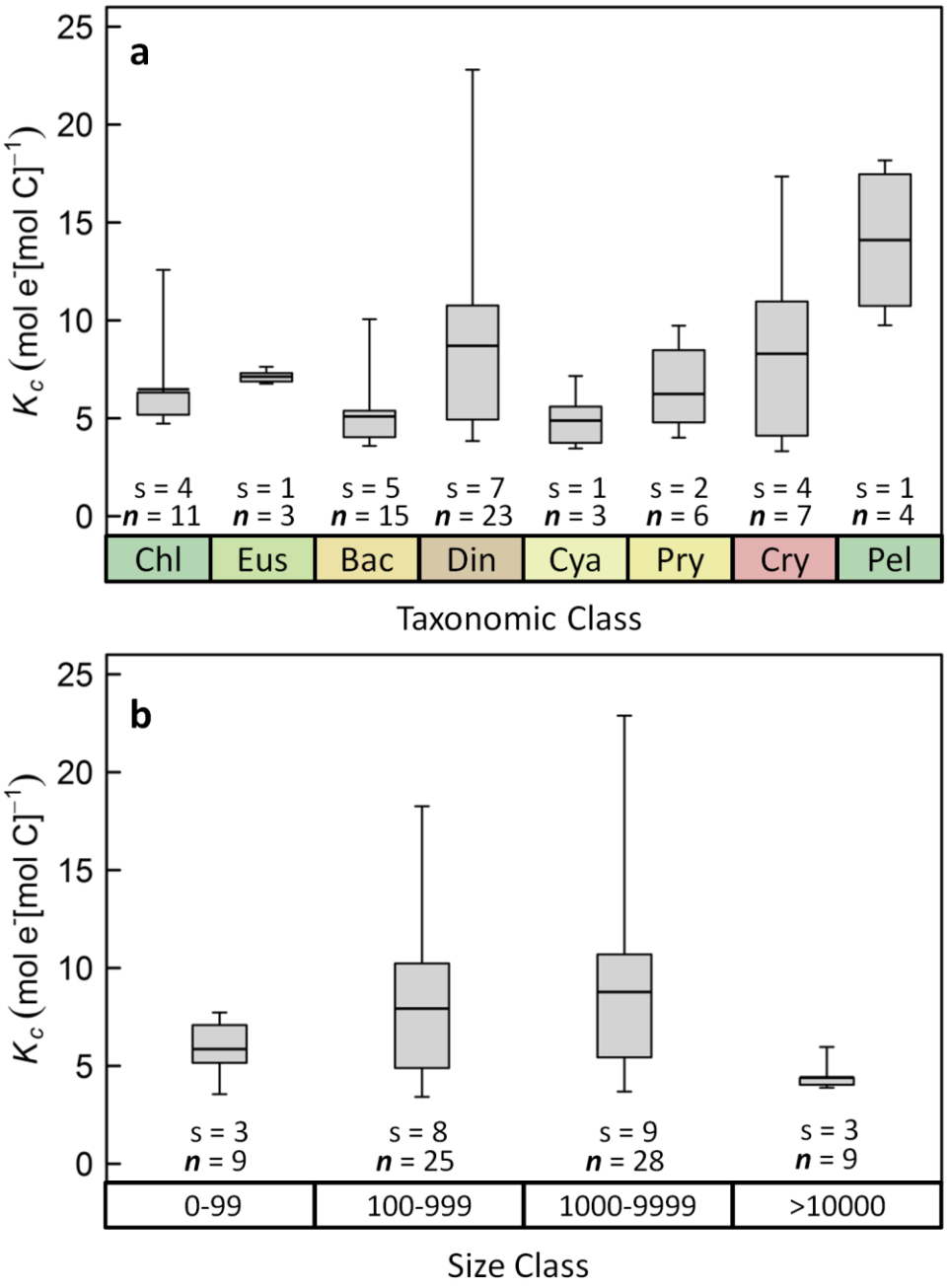

Figure 3.5 Boxplot of the electron requirement for carbon fixation (mol e^- [mol C]$^{-1}$), K_C including data from meta-analysis together with all strains measured during this study, (n = 71), grouped by a) taxonomic class – abbreviated by the first three letters of the class name as outlined in Fig. 3.2 with an additional class, Pelagophyceae, and b) arbitrary size-class bins, based upon cell volume (µm^3). The length of the box corresponds to the inter-quartile range, whilst the whiskers indicate the range of the data. The solid line denotes the mean, whilst n and s indicate the number of values and strains sampled respectively.

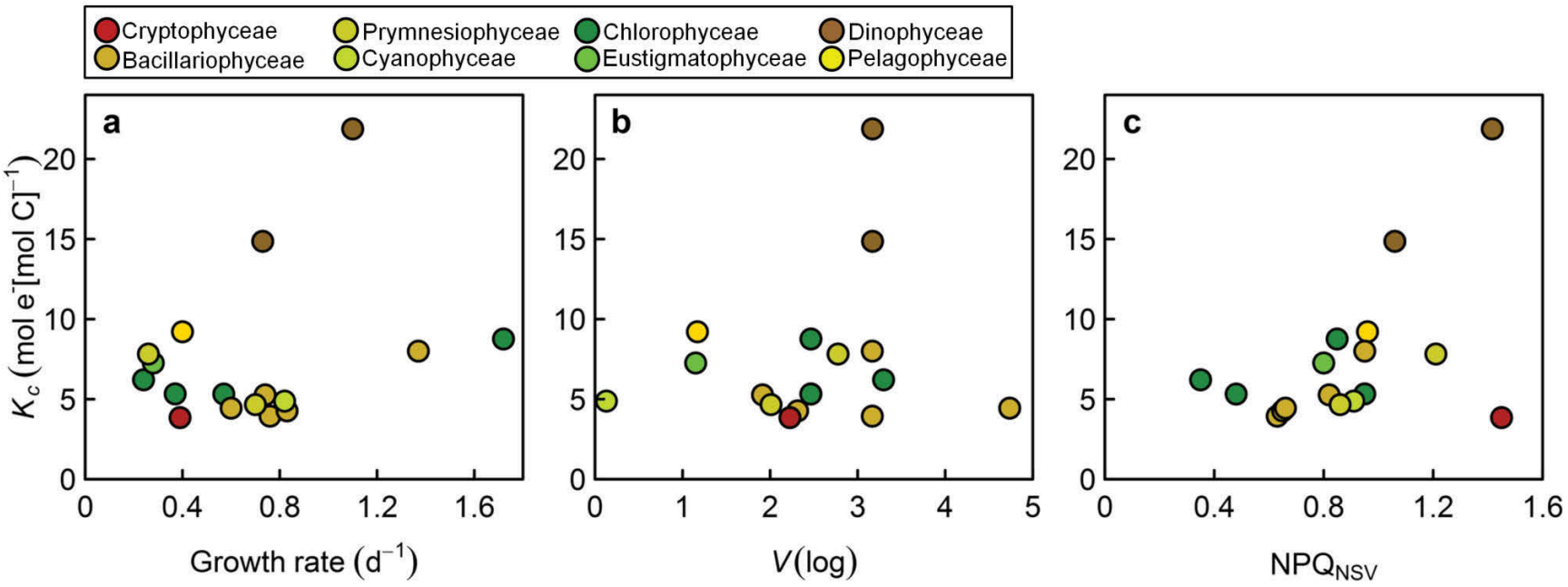

Figure 3.6 Relationship between the electron requirement for carbon fixation, K_C (mol e$^-$ [mol C]$^{-1}$), and corresponding measures of a) phytoplankton growth rate (d^{-1}), b) log-normalised cell volume (V[log]) and c) non-photochemical quenching, estimated as the normalised Stern-Volmer coefficient (McKew et al. 2013), denoted here as NPQ$_{NSV}$ (dimensionless) for all strains grown in the main study (i.e. excluding strains sampled "opportunistically" where growth data was unavailable, together with meta-analysis data.

3.5.1 Species-specific variability in K_C

We observed K_C values ranging from ~3.8-10.5 mol e^- (mol C)$^{-1}$ from the phytoplankton cultures, which fall within the range of values reported by the (few) laboratory studies to date (Suggett et al. 2009a; Brading et al. 2011; see Supplementary Table S3.1), and well within the range of observations from the field (Lawrenz et al. 2013; Robinson et al. 2014). In agreement with previous findings (Suggett et al. 2009a; Napoleon et al. 2013), our study identified species-specific differences in K_C, with *Symbiodinium* D1a, *N. oculata*, and *P. pouchetti* exhibiting higher K_C values than other strains. Our measured K_C for *Symbiodinium* D1a (10.7 mol e^- [mol C]$^{-1}$) was higher than those reported by Brading et al. (2013) for other *Symbiodinium* strains (A13 and A20) under light-limited photosynthesis (~5 mol e^- [mol C]$^{-1}$). Our findings that strains from the same clade (in our case, clade C) exhibit a similar K_C, supports observations by Brading et al. (2013) for clade A strains. To our knowledge no study has reported K_C for *N. oculata*, or *P. pouchetti*, thus it is not possible to evaluate our K_C values against previous measurements. However, for all remaining strains, K_C values (~4-6 mol e^- [mol C]$^{-1}$) agreed well with the theoretical minimum value of 4-5 mol e^- (mol C)$^{-1}$ (see Suggett et al. 2009a), indicating a close-coupling of ETR_{PSII} to C-fixation.

The observed inverse relationship between growth rate and K_C in this study supported our original hypothesis that taxa investing electrons more efficiently into fixed-C (i.e. those with a low K_C), can sustain higher rates of growth. As the ratio of GPP to NPP remains fairly constant irrespective of growth rate (Halsey et al. 2010) this is not unexpected, and was demonstrated particularly well by diatoms, which consistently exhibited high growth rates together with the lowest overall K_C values of ~4 mol e^- (mol C)$^{-1}$. Such an outcome appears logical, considering the favourable growth conditions,

i.e. nutrient-replete and a constant, relatively low irradiance. Under such optimal conditions, linear electron flow, which generates the ATP and NADPH needed for carbon-assimilation (and thus, ultimately for cellular growth) is expected to be the dominant component of ETR_{PSII}, with little competition from alternative (i.e. non C-fixing) electron sinks (McDonald et al. 2011).

The nutrient replete and light limited growth conditions used in our study likely also explains why the overall range of K_C values measured (~4-10 mol e^- [mol C]$^{-1}$), was conservative compared to field observations (~2-50 mol e^- [mol C]$^{-1}$). In their natural environment, phytoplankton cells regularly experience non steady-state environmental conditions, with transient fluctuations in both light and nutrient availability, and thus persist under more "extreme" conditions than those here. Numerous field (Moore et al. 2006; Schuback et al 2015, 2017; Zhu et al 2016) and laboratory (Suggett et al. 2009a; Brading et al. 2013) studies have shown excess light to be a strong factor decoupling ETR_{PSII} and rates of C-fixation. In the present study, K_C was measured at an irradiance approximating growth conditions, representing light-limited photosynthesis (i.e. $E/E_K < 1$) for the majority of strains. However, in nature, irradiance can fluctuate over a range of time-scales (Falkowski, 1984), and thus phytoplankton cells are often subjected to extended periods of light-saturated photosynthesis (i.e. where $E/E_K > 1$) (Moore et al. 2006). Thus, it is unlikely that our observations would hold true under a dynamic light field, where energy dissipation mechanisms (including non C-fixing pathways which increase K_C) play an important role in regulating photosynthetic performance (e.g. Cardol et al. 2011). Currently, little is known as to how K_C may ultimately scale to a daily mean value under such a fluctuating light regime (but see Hoppe et al. 2015; Zhu et al. 2016), and this represents an important direction for future research. Certainly, it is highly likely that taxa-specific differences would be a key factor here, as

demonstrated by Wagner et al (2006) who showed that the diatom, *Phaeodactylum tricornutum* was nearly twice as efficient at converting absorbed photons into biomass than the chlorophyte, *Chlorella vulgaris* when grown under fluctuating light, attributing this difference to the highly-efficient NPQ of the diatom.

3.5.2 Class-dependent variability in K_C

Our study found that dinoflagellates exhibited higher K_C values than diatoms, and cryptophytes, an observation consistent with Suggett et al. (2009a) but contrary to findings of Napoleon et al. (2013). The latter study reported differences in K_C for both diatoms (*Pseudo-nitzschia pungens* and *Asterionellopsis glacialis*), and dinoflagellates (*Heterocapsa* sp. and *Karenia mikimitoi*), between species but not classes; however the mechanism driving this variability remains unclear. Although the statistical differences between classes (Fig. 3.2) disappeared with the variance introduced by the inclusion of meta-data (Fig. 3.5), K_C for diatoms was still confined to a relatively narrow range of values despite the increased number of observations (n = 23) and they were the only class found to exhibit significantly lower K_C than any other phytoplankton class (in this case, Pelagophytes). Suggett et al. (2006) has previously shown that increased K_C value occurred during the spring bloom transition from diatoms to (dino)flagellates, whilst Hughes et al (in press., Chapter 2) recently demonstrated via nutrient-enrichment bioassays, that a decrease in K_C was largely driven by a taxonomic shift from co-domination of diatoms and dinoflagellates, towards a diatom-only assemblage. Studies thus appear to consistently report low K_C values for diatoms (Suggett et al. 2009a; Hoppe et al. 2015) perhaps suggesting that lower conversion factors (i.e. K_C) could be routinely applied to diatom-dominated assemblages to retrieve C-fixation rates from ETR_{PSII} (at least under specific environmental conditions: e.g. where nutrients are replete and irradiance is limiting).

Overall, our range of K_C values both within, and between taxonomic classes, appears consistent with previous studies of diatoms, chlorophytes and dinoflagellates under conditions of balanced, nutrient-replete growth (Suggett et al. 2009a; Brading et al. 2013; Hoppe et al. 2015). Variability of K_C between classes is presumably driven by variable demands for energy (ATP) and reductant (NADPH) to maintain optimal growth (Halsey et al. 2015), thus potentially reflecting adaptive strategies to maintain photosynthetic fitness, such as differences in light-harvesting or light-utilisation which have their origins in evolutionary history. Indeed, it has recently been shown that adaptations in light-harvesting apparatus partially explain phylogenetic differences in the proportions of macromolecular pools (i.e. carbohydrates, lipids and proteins) between classes, consistent with observed C:N ratios in the field (see Finkel et al. 2016). Incorporation of N into biomass typically consumes electrons for reductive assimilation of an external N source (see Anderson, 1995), thus K_C is expected to increase in parallel with cellular nitrogen content (Jakob et al. 2007). However, in our study C:N ratio did not appear to be a factor driving K_C variability, as the lowest measured POC:PON ratios (i.e. a higher proportion of N per C biomass) often corresponded to strains with lowest K_C values (e.g. *R. salina*). It is however possible that taxa with larger pools of protein, would have a larger K_C due to the increased cellular maintenance costs for protein turnover (e.g. Quigg and Beardall, 2003), which can be directly coupled to the use of photo-produced ATP, instead of via respiration. Whilst this notion would warrant testing, the relative production of ATP from photosynthetic versus respiratory metabolism would be difficult to quantity (Quigg and Beardall, 2003). We can rule out differences in K_C arising from structurally-impacted photosynthetic apparatus affecting linear electron transport efficiency arising from nutrient-stress (as per Napoleon et al. 2013) since all strains were maintained under nutrient-replete conditions. However, we

do note that the relatively low POC:PON ratios reported in this study means that we should consider the possibility that some strains may have been subjected to a degree of C-limitation, e.g. perhaps due to excessive drawdown of dissolved CO_2 which outpaced CCM capacity.

In addition to adaptive strategies of light-harvesting, variability in K_C could also be expected to be driven by taxonomic differences in the downstream efficiency of CO_2-assimilation itself. Dinoflagellates are the only phytoplankton class in this study to possess form II of RuBisCO, characterised by poor CO_2/O_2 discrimination, and thus conducive to the occurrence of photorespiration (see Brading et al. 2013). However, it remains unclear whether photorespiration is significant for microalgae or is instead overcome by the expenditure of photo-produced ATP to fuel carbon-concentrating mechanisms (e.g. Badger et al. 1980); although as either scenario would ultimately increase $K_{C,}$ this provides a possible explanation for measured differences between dinoflagellates and diatoms during this study that clearly warrants more targeted investigation.

3.5.3 An overarching explanation for K_C variability through cell size

Cell size is considered a "master trait" that constrains many physiological and ecological characteristics, including photosynthetic performance (Finkel et al. 2009), whereby cell size influences PSII light absorption efficiency (Ciotti et al. 2002), photochemical conversion efficiency (Suggett et al. 2009b) and, thus, photosynthetic electron transport (Moore et al. 2005; Suggett et al. 2009a; Rattan et al. 2012). Generally, when normalised to cell size, photosynthetic rates tend to be lower for phytoplankton of larger size classes (Bouman et al. 2005; Barnes et al. 2015), as surface-area-to-volume ratio imposes biophysical constraints upon light absorption and

nutrient-uptake (see Marra et al. 2007). Interestingly, we found that K_C scaled to growth rate, suggesting biophysical constraints over K_C, yet we did not observe the expected relationship between cell volume and growth rate that would be expected due to constraints of cell size.

Generally, a reduction in growth rate corresponding to increasing cell size is documented for phytoplankton (Geider et al. 1986), thus our observations would appear to support that K_C was not subjected to biophysical constraints of cell size. However, we also point out that it has been previously demonstrated that growth rate may be taxa-dependent, with diatoms and dinoflagellates of equivalent size exhibiting up to a three-fold difference in cellular division rate under identical conditions (Banse, 1982). Thus, it remains unclear whether biophysical constraints imposed by cell size may ultimately play a major role explaining the observed variability in K_C between size classes. Further study, focussing on a single taxonomic group spanning multiple orders of magnitude in cell-size (e.g. diatoms – see Key et al. 2010) would be required to conclusively separate the effects of taxonomic class from cell size upon K_C regulation.

Given the relationship between growth rate and K_C but not cell volume, it raises the interesting question as to whether growth rates in our study were a proxy for optimality of growth conditions for each strain, and whether this may be responsible for driving variability in K_C. Variation in phytoplankton growth rates has been shown to affect the lifetimes of newly-fixed carbon Halsey et al. (2010, 2011, 2013) leading to a variable C-uptake rate somewhere between gross primary production (GPP) and net primary production (GPP) captured by very short incubations (20 – 60 min), reflecting different extents to which energy and reductant were utilised for cellular maintenance. Specifically, faster growing cells were found to invest newly-fixed carbon into polysaccharides with a longer turnover time (hours), compared to slower growing cells

that instead invested the majority of carbon into glyceraldehyde-3-phospate (GAP) which was respired within a much shorter timeframe (20 minutes, see Halsey et al. 2011, 2013).

Differences in growth rates were achieved via nutrient limitation by Halsey et al (2010, 2011, 2013), which is obviously not the case for our study; however, it remains unclear whether there were additional factors not measured/considered here that may have resulted in sub-optimal growth rates (thereby introducing variability of K_C) and how significant this would likely have been for the incubation lengths used in our study (20 min). Light may be one such factor, as many stains used in this study were grown under a single irradiance despite differences in cell size which may influence the size of the effective cross-section for photochemistry (Key et al. 2010), and ultimately the amount of photosynthetic energy available for growth.

A notable exception to the generally close-coupling of K_C and cellular growth rate was observed for the cryptophyte, *R. salina*, which despite having one of the lowest K_C values (~4 mol e^- [mol C]$^{-1}$), also exhibited a low growth rate during the study (0.39 d^{-1}). The small volume ^{14}C-method used in this study measured total organic carbon (TOC) fixed, and does not discriminate between particulate and dissolved organic carbon (POC and DOC respectively), thus any extracellular release of ^{14}C-fixed as DOC remained unaccounted-for. Recent work by Fukuzaki et al. (2014) examining a range of taxa, found a closely-related cryptophyte species (*Rhodomonas ovalis)* to be a prolific producer of fluorescent dissolved organic matter (FDOM, of which DOC is likely the largest component), thus possibly explaining why *R. salina* did not fit the general trend of other species examined.

3.5.4 NPQ_{NSV} provides limited predictive capability for K_C

In efforts to identify empirical relationships between K_C and (more easily measured) biophysical properties, we observed poor correspondence between NPQ_{NSV} and K_C, an outcome that appears to contradict recent observations from natural phytoplankton communities (Schuback et al. 2015, 2016, 2017; Zhu et al 2016; Hughes et al. subm, Chapter 2). Such an empirical relationship presumably depends upon a mechanistic link between the upregulation of alternative electron pathways in response to high excitation pressure (which increases K_C) and the simultaneous generation of ΔpH that may activate thermal-dissipation mechanisms in the PSII antenna (detected as an increased NPQ_{NSV} signature) (Schuback et al. 2015; Nawrocki et al. 2015). Thus, it is perhaps unsurprising that we found no correlation between NPQ_{NSV} and K_C in our study since incubations were predominately performed during conditions of low excitation pressure (i.e. light-limited photosynthesis, E/E_K <1).

Field observations of a correlation between K_C and NPQ_{NSV} often appear to be driven by cells experiencing dynamic stress to nutrient availability (Schuback et al. 2016; Hughes et al. in press., Chapter 2) or light exposure (Zhu et al. 2016). Whilst our cells were maintained under steady-state conditions, we still measured a fairly large range of NPQ_{NSV} values (0.35-1.81) across all strains, indicating some degree of taxonomic control over this fluorescence parameter. NPQ_{NSV} quantifies the thermal dissipation of absorbed energy, but the regulation and mechanisms by which this is accomplished, varies considerably between higher taxa (Kaňa et al. 2012). For example, NPQ in diatoms is characterised by a diadinoxanthin-based xanthophyll cycle which is rapidly triggered by ΔpH (Lavaud and Groth, 2006), compared to the violaxanthin-based

xanthophyll cycle found in chlorophytes over which ΔpH has less control (Finazzi et al. 2006), or the entirely different NPQ found in cyanobacteria associated with the orange carotenoid protein (OCP, Kiriliovsky et al. 2007). Furthermore, size-scaling of photophysiological parameters, including NPQ have been observed under exposure to high light with metabolic costs that vary accordingly (Key et al. 2010). Presumably, differences in metabolic costs could reasonably be expected to manifest as a difference in K_C, yet would only be apparent if cells were transiently exposed to high light conditions. Therefore, a better relationship between K_C and NPQ would be expected for natural communities (e.g. Schuback et al 2016; Hughes et al. in press) rather during laboratory studies where a single incubation irradiance is used, such as this study.

In comparison to the NPQ_{NSV} values measured in this study, Hughes et al. (in press., Chapter 2) measured a similar range of NPQ_{NSV} for a predominately diatom-dominated assemblage, however this corresponded to a much larger range of K_C values (~4-16 mol e^- [mol C]$^{-1}$), in various nutritional (and hence photophysiological) states. Indeed, it is becoming increasingly clear that the slopes of the relationship reported between K_C and NPQ_{NSV} are often highly variable between studies, potentially complicating our ability to utilise NPQ_{NSV} as a standalone predictor of K_C without further understanding the cause of this variance. The taxonomic variability in NPQ_{NSV} highlighted here may explain at least some of that variability across prior recent field studies, and requires further investigation. It would be particularly valuable to determine if a minimum, taxa-specific "threshold" for NPQ_{NSV} exists that could be used to identify K_C values close to the theoretical minimum regardless of variability in slopes.

3.6 Conclusions

By conducting a novel assessment of K_C variability across taxa from both new and prior culture-based studies, we have highlighted that inter-class differences, together with cell volume may be important factors contributing to observed variability of K_C. Our empirical observations of co-variance between growth rate and K_C potentially provides a new means with which K_C could be predicted, a process desperately needed to scale up the application of FFRf-based productivity studies to improve knowledge of C-cycling. Improved measures in determining phytoplankton growth rates (Behrenfeld et al. 2008) and cell size (Bracher et al. 2017) may become key elements in realising this goal. Past studies have considered K_C variance from environmental parameters, but we have shown that broader traits indicative of fitness, e.g. growth rate and cell size, co-vary with K_C. Whilst we cannot fully resolve the mechanisms responsible explaining this co-variance, our data provides new insight to explore potential cellular properties regulating K_C across taxa.

3.7 References

Anderson, L. A. 1995. On the hydrogen and oxygen content of marine phytoplankton. Deep Sea Res., Part I. 42(9): 1675-1680.

Badger, M. R., A. Kaplan, and J. A. Berry. 1980. Internal inorganic carbon pool of *Chlamydomonas reinhardtii* Evidence for a carbon dioxide-concentrating mechanism. Plant Physiol. 66(3): 407-413.

Banse, K. 1982. Cell volumes, maximal growth rates of unicellular algae and ciliates, and the role of ciliates in the marine pelagial. Limnol. Oceanogr. 27(6): 1059-1071.

Barnes, M. K., G. H. Tilstone, T. J. Smyth, C. E. Widdicombe, J. Gloël, C. Robinson, J. Kaiser, and D. J. Suggett. 2015. Drivers and effects of *Karenia mikimotoi* blooms in the western English Channel. Prog. Oceanogr. 137: 456-469.

Behrenfeld, M. J., E. Boss, D. A. Siegel, and D. M. Shea. 2005. Carbon-based ocean productivity and phytoplankton physiology from space. Global Biogeochem. Cycles 19(1): GB1006, doi:10.1029/2004GB002299.

Behrenfeld, M. J., K. H. Halsey, and A. J. Milligan. 2008. Evolved physiological responses of phytoplankton to their integrated growth environment. Philos. Trans. R. Soc., B 363(1504): 2687-2703.

Bouman, H., T. Platt, S. Sathyendranath, and V. Stuart. 2005. Dependence of light-saturated photosynthesis on temperature and community structure. Deep Sea Res., Part I. 52(7): 1284-1299.

Bracher, A. and others. 2017. Obtaining phytoplankton diversity from ocean color: a scientific roadmap for future development. Front. Mar. Sci. 4: 55.

Brading, P., M. E. Warner, P. Davey, D. J. Smith, E. P. Achterberg, and D. J. Suggett. 2011. Differential effects of ocean acidification on growth and photosynthesis among phylotypes of *Symbiodinium* (Dinophyceae). Limnol. Oceanogr. 56(3): 927-938.

Brading, P., M. E. Warner, D. J. Smith, and D. J. Suggett. 2013. Contrasting modes of inorganic carbon acquisition amongst *Symbiodinium* (Dinophyceae) phylotypes. New Phytol. 200(2): 432-442.

Cardol, P., G. Forti, and G. Finazzi. 2011. Regulation of electron transport in microalgae. Biochim. Biophys. Acta, Bioenerg. 1807(8): 912-918.

Ciotti, A. M., M. R. Lewis, and J. J. Cullen. 2002. Assessment of the relationships between dominant cell size in natural phytoplankton communities and the spectral shape of the absorption coefficient. Limnol. Oceanogr. 47(2): 404-417.

Falkowski, P. G. 1984. Physiological responses of phytoplankton to natural light regimes. J. Plankton Res. 6(2): 295-307.

Finazzi, G., G. N. Johnson, L. Dall'osto, F. Zito, G. Bonente, R. Bassi, and F.-A. Wollman. 2006. Nonphotochemical quenching of chlorophyll fluorescence in *Chlamydomonas reinhardtii*. Biochemistry 45(5): 1490-1498.

Finkel, Z. V., J. Beardall, K. J. Flynn, A. Quigg, T. a. V. Rees, and J. A. Raven. 2009. Phytoplankton in a changing world: cell size and elemental stoichiometry. J. Plankton Res. 32(1): 119-137.

Finkel, Z. V., M. J. Follows, J. D. Liefer, C. M. Brown, I. Benner, and A. J. Irwin. 2016. Phylogenetic diversity in the macromolecular composition of microalgae. PloS one 11(5): e0155977.

Fisher, N. L., and K. H. Halsey. 2016. Mechanisms that increase the growth efficiency of diatoms in low light. Photosynth. Res. 129(2): 183-197.

Fujiki, T., T. Suzue, H. Kimoto, and T. Saino. 2007. Photosynthetic electron transport in *Dunaliella tertiolecta* (Chlorophyceae) measured by fast repetition rate fluorometry: relation to carbon assimilation. J. Plankton Res. 29(2)**:** 199-208.

Fukuzaki, K., I. Imai, K. Fukushima, K.-I. Ishii, S. Sawayama, and T. Yoshioka. 2014. Fluorescent characteristics of dissolved organic matter produced by bloom-forming coastal phytoplankton. J. Plankton Res. 36(3): 685-694.

Geider, R. J., T. Platt, and J. A. Raven. 1986. Size dependence of growth and photosynthesis in diatoms: a synthesis. Mar. Ecol.: Prog. Ser. 30: 93-104.

Guillard, R. R., and J. H. Ryther. 1962. Studies of marine planktonic diatoms: I. *Cyclotella nana* Hustedt, and *Detonula confervacea* (cleve) Gran. Can. J. Microbiol. 8(2): 229-239.

Halsey, K. H., and B. M. Jones. 2015. Phytoplankton strategies for photosynthetic energy allocation. Annu. Rev. Mar. Sci. 7: 265-297.

Halsey, K. H., A. J. Milligan, and M. J. Behrenfeld. 2010. Physiological optimization underlies growth rate-independent chlorophyll-specific gross and net primary production. Photosynth. Res. 103(2): 125-137.

Halsey, K. H., A. J. Milligan, and M. J. Behrenfeld. 2011. Linking time-dependent carbon-fixation efficiencies in *Dunaliella tertiolecta* (chlorophyceae) to underlying metabolic pathways. J. Phycol. 47(1): 66-76.

Halsey, K. H., R. T. O'malley, J. R. Graff, A. J. Milligan, and M. J. Behrenfeld. 2013. A common partitioning strategy for photosynthetic products in evolutionarily distinct phytoplankton species. New Phytol. 198(4): 1030-1038.

Hancke, K., T. Dalsgaard, M. K. Sejr, S. Markager, and R. N. Glud. 2015. Phytoplankton productivity in an Arctic Fjord (West Greenland): estimating electron requirements for carbon fixation and oxygen production. PloS One 10(7): e0133275.

Hoppe, C. J. M., L.-M. Holtz, S. Trimborn, and B. Rost. 2015. Ocean acidification decreases the light-use efficiency in an Antarctic diatom under dynamic but not constant light. New Phytol. 207(1): 159-171.

Hughes, D.J., Varkey, D., Doblin, M.A., Ingleton, T., Mcinnes, A., Ralph, P.J., van Dongen-Vogels, V and D.J Suggett. 2018. Impact of nitrogen availability upon the electron requirement for carbon fixation in Australian coastal phytoplankton communities (In Press). Limnol. Oceanogr. DOI: 10.1002/lno.10814

Huot, Y., and M. Babin. (2010). Overview of fluorescence protocols: theory, basic concepts, and practice, p. 31-74. In D. Suggett, O. Prášil and M. Borowitzka [eds.], Chlorophyll a fluorescence in aquatic sciences: Methods and applications. Springer.

Jacox, M. G., C. A. Edwards, M. Kahru, D. L. Rudnick, and R. M. Kudela. 2015. The potential for improving remote primary productivity estimates through subsurface chlorophyll and irradiance measurement. Deep Sea Res., Part II. 112: 107-116.

Jakob, T., H. Wagner, K. Stehfest, and C. Wilhelm. 2007. A complete energy balance from photons to new biomass reveals a light-and nutrient-dependent variability in the metabolic costs of carbon assimilation. J. Exp. Bot. 58(8): 2101-2112.

Kaňa, R., E. Kotabová, R. Sobotka, and O. Prášil. 2012. Non-photochemical quenching in cryptophyte alga *Rhodomonas salina* is located in Chlorophyll a/c antennae. PLoS One 7(1): e29700.

Key, T., McCarthy, A., Campbell, D. A., Six, C., Roy, S., and Z.V. Finkel. 2010. Cell size trade-offs govern light exploitation strategies in marine phytoplankton. Environ. Microbiol., 12(1), 95-104.

Kirilovsky, D., and A. Wilson. 2007. A new photoactive protein acting as a sensor of light intensity: the Orange Carotenoid Protein (OCP). Photosynth. Res. 91(2-3): 291-292.

Knap, A., A. Michaels, A. Close, H. Ducklow, and A. Dickson. 1996. Protocols for the Joint Global Ocean Flux Study (JGOFS) core measurements.

Kolber, Z., and P. G. Falkowski. 1993. Use of active fluorescence to estimate phytoplankton photosynthesis *in situ*. Limnol. Oceanogr. 38(8): 1646-1665.

Kolber, Z. S., O. Prášil, and P. G. Falkowski. 1998. Measurements of variable chlorophyll fluorescence using fast repetition rate techniques: defining methodology and experimental protocols. Biochim. Biophys. Acta, Bioenerg. 1367(1–3): 88-106.=

Kromkamp, J. C., and R. M. Forster. 2003. The use of variable fluorescence measurements in aquatic ecosystems: differences between multiple and single turnover measuring protocols and suggested terminology. Eur. J. Phycol. 38(2): 103-112.

Langner, U., T. Jakob, K. Stehfest, and C. Wilhelm. 2009. An energy balance from absorbed photons to new biomass for *Chlamydomonas reinhardtii* and *Chlamydomonas acidophila* under neutral and extremely acidic growth conditions. Plant, Cell Environ. 32(3): 250-258.

Lavaud, J., and P. G. Kroth. 2006. In diatoms, the transthylakoid proton gradient regulates the photoprotective non-photochemical fluorescence quenching beyond its control on the xanthophyll cycle. Plant Cell Physiol. 47(7): 1010-1016.

Lawrenz, E. and others. 2013. Predicting the electron requirement for carbon fixation in seas and oceans. PLoS One 8(3): e58137.

Laws, E. A. 1991. Photosynthetic quotients, new production and net community production in the open ocean. Deep Sea Res., Part I. 38(1): 143-167.

Lewis, M. R., and J. C. Smith. 1983. A small volume, short-incubation-time method for measurement of photosynthesis as a function of incident irradiance. Mar. Ecol.: Prog. Ser. 13: 99-102.

Litchman, E., C. A. Klausmeier, O. M. Schofield, and P. G. Falkowski. 2007. The role of functional traits and trade-offs in structuring phytoplankton communities: scaling from cellular to ecosystem level. Ecol. Lett. 10(12): 1170-1181.

Marra, J. 2009. Net and gross productivity: weighing in with ^{14}C. Aquat. Microb. Ecol. 56(2-3): 123-131.

Marra, J. 2012. Comment on "Measuring primary production rates in the ocean: Enigmatic results between incubation and non-incubation methods at Station ALOHA" by PD Quay et al. Global Biogeochem. Cycles 26(2): GB2031, doi:10.1029/2011GB004087.

Marra, J., C. C. Trees, and J. E. O'reilly. 2007. Phytoplankton pigment absorption: a strong predictor of primary productivity in the surface ocean. Deep Sea Res., Part I. 54(2): 155-163.

Mcdonald, A. E., A. G. Ivanov, R. Bode, D. P. Maxwell, S. R. Rodermel, and N. P. Hüner. 2011. Flexibility in photosynthetic electron transport: the physiological role of plastoquinol terminal oxidase (PTOX). Biochim. Biophys. Acta, Bioenerg. 1807(8): 954-967.

Mckew, B. A. and others. 2013. The trade-off between the light-harvesting and photoprotective functions of fucoxanthin-chlorophyll proteins dominates light acclimation in *Emiliania huxleyi* (clone CCMP 1516). New Phytol. 200(1): 74-85.

Melrose, D. C., C. A. Oviatt, J. E. O'reilly, and M. S. Berman. 2006. Comparisons of fast repetition rate fluorescence estimated primary production and ^{14}C uptake by phytoplankton. Mar. Ecol.: Prog. Ser. 311: 37-46.

Moore, C. M., D. J. Suggett, A. E. Hickman, Y.-N. Kim, J. F. Tweddle, J. Sharples, R. J. Geider, and P. M. Holligan. 2006. Phytoplankton photoacclimation and photoadaptation in response to environmental gradients in a shelf sea. Limnol. Oceanogr. 51(2): 936-949.

Napoleon, C., V. Raimbault, and P. Claquin. 2013. Influence of nutrient stress on the relationships between PAM measurements and carbon incorporation in four phytoplankton species. PLoS One 8(6): e66423.

Nawrocki, W. J., N. J. Tourasse, A. Taly, F. Rappaport, and F.-A. Wollman. 2015. The plastid terminal oxidase: its elusive function points to multiple contributions to plastid physiology. Annu. Rev. Plant Biol. 66: 49-74.

Oxborough, K. 2012. FastPro8 GUI and FRRf3 systems documentation. West Molesey, UK: Chelsea Technologies Group Ltd.

Oxborough, K., C. M. Moore, D. J. Suggett, T. Lawson, H. G. Chan, and R. J. Geider. 2012. Direct estimation of functional PSII reaction center concentration and PSII electron flux on a volume basis: a new approach to the analysis of Fast

Repetition Rate fluorometry (FRRf) data. Limnol. Oceanogr.: Methods 10(3): 142-154.

Pakrasi, H. B., H. C. Riethman, and L. A. Sherman. 1985. Organization of pigment proteins in the photosystem II complex of the cyanobacterium *Anacystis nidulans* R2. P Proc. Natl. Acad. Sci. U. S. A. 82(20): 6903-6907.

Platt, T., C. Gallegos, and W. Harrison. 1980. Photoinhibition of photosynthesis in natural assemblages of marine phytoplankton. J. Mar. Res. 38: 103-111.

Quay, P., C. Peacock, K. Björkman, and D. Karl. 2010. Measuring primary production rates in the ocean: Enigmatic results between incubation and non-incubation methods at Station ALOHA. Global Biogeochem. Cycles 24(3): GB3014, doi:10.1029/2009GB003665.

Quigg, A., and J. Beardall. 2003. Protein turnover in relation to maintenance metabolism at low photon flux in two marine microalgae. Plant, Cell Environ. 26(5): 693-703.

Rattan, K. J., W. D. Taylor, and R. E. Smith. 2012. Nutrient status of phytoplankton across a trophic gradient in Lake Erie: evidence from new fluorescence methods. Can. J. Fish. Aquat. Sci. 69(1): 94-111.

Regaudie-De-Gioux, A., S. Lasternas, S. Agustí, and C. M. Duarte. 2014. Comparing marine primary production estimates through different methods and development of conversion equations. Front. Mar. Sci. 1: 19.

Roberty, S., B. Bailleul, N. Berne, F. Franck, and P. Cardol. 2014. PSI Mehler reaction is the main alternative photosynthetic electron pathway in *Symbiodinium* sp., symbiotic dinoflagellates of cnidarians. New Phytol. 204(1): 81-91.

Robinson, C., D. J. Suggett, N. Cherukuru, P. J. Ralph, and M. A. Doblin. 2014. Performance of Fast Repetition Rate fluorometry based estimates of primary productivity in coastal waters. J. Mar. Syst. 139: 299-310.

Roesler, C. S. 1998. Theoretical and experimental approaches to improve the accuracy of particulate absorption coefficients derived from the quantitative filter technique. Limnol. Oceanogr. 43(7): 1649-1660.

Schuback, N., M. Flecken, M. T. Maldonado, and P. D. Tortell. 2016. Diurnal variation in the coupling of photosynthetic electron transport and carbon fixation in iron-limited phytoplankton in the NE subarctic Pacific. Biogeosciences 13(4): 1019-1035.

Schuback, N., C. J. Hoppe, J. É. Tremblay, M. T. Maldonado, and P. D. Tortell. 2017. Primary productivity and the coupling of photosynthetic electron transport and carbon fixation in the Arctic Ocean. Limnol. Oceanogr. 62: 898-921.

Schuback, N., C. Schallenberg, C. Duckham, M. T. Maldonado, and P. D. Tortell. 2015. Interacting effects of light and iron availability on the coupling of photosynthetic electron transport and CO_2-assimilation in marine phytoplankton. PLoS One 10(7): e0133235.

Steeman-Nielsen, E. 1952. The use of radioactive carbon (C^{14}) for measuring organic production in the sea. ICES J. Mar. Sci. 18(2): 117-140.

Suggett, D. J., S. Goyen, C. Evenhuis, M. Szabó, D. T. Pettay, M. E. Warner, and P. J. Ralph. 2015. Functional diversity of photobiological traits within the genus *Symbiodinium* appears to be governed by the interaction of cell size with cladal designation. New Phytol. 208(2): 370-381.

Suggett, D. J., S. C. Maberly, and R. J. Geider. 2006. Gross photosynthesis and lake community metabolism during the spring phytoplankton bloom. Limnol. Oceanogr. 51(5): 2064-2076.

Suggett, D. J., H. L. Macintyre, T. M. Kana, and R. J. Geider. 2009a. Comparing electron transport with gas exchange: parameterising exchange rates between alternative photosynthetic currencies for eukaryotic phytoplankton. Aquat. Microb. Ecol. 56(2-3): 147-162.

Suggett, D. J., C. M. Moore, A. E. Hickman, and R. J. Geider. 2009b. Interpretation of fast repetition rate (FRR) fluorescence: signatures of phytoplankton community structure versus physiological state. Mar. Ecol.: Prog. Ser. 376: 1-19.

Sun, J., and D. Liu. 2003. Geometric models for calculating cell biovolume and surface area for phytoplankton. J. Plankton Res. 25(11): 1331-1346.

Wagner, H., T. Jakob, and C. Wilhelm. 2006. Balancing the energy flow from captured light to biomass under fluctuating light conditions. New Phytol. 169(1): 95-108.

Wood, A. M., R. Everroad, and L. Wingard. 2005. Measuring growth rates in microalgal cultures, p. 269-285. In R. A. Andersen [ed.], Algal Culturing Techniques: A Book for All Phycologists. Elsevier.

Zhu, Y., J. Ishizaka, S. C. Tripathy, S. Wang, Y. Mino, T. Matsuno, and D. J. Suggett. 2016. Variation of the photosynthetic electron transfer rate and electron requirement for daily net carbon fixation in Ariake Bay, Japan. J. Oceanogr. 72(5): 761-776.

Supplementary Table S3.1 Provisional meta analysis data

Class	Species	μ	PAR (growth)	PAR (incubation)	E/E_K	Salinity (ppt)	Temperature (ºC)	Photoperiod (hr)	n	Reference
Bacillariophyceae	*Thalassiosira weissflogii* (CCMP1047)	0.24 1.37	18 80	372.57 442.33	1.52 2.49	30	20	24	2	Suggett et al. 2009a
	Chaetoceros debilis	-	90	-	0.65	33	3	16	1	Hoppe et al. 2015
Chlorophyceae	*Dunaliella tertiolecta* (CCMP1320)	0.28 1.72 2.42	18 80 300	401.72 510.17 414.22	3.80 3.09 0.78	30	20	24	3	Suggett et al. 2009a
		-	30 30 90 90 270 270	-	0.5 2 0.5 2 0.5 2	33	20	12	6	Fujiki et al. 2007
	Pycnococcus provasolii (CCMP1203)	0.31 0.73 0.87	18 80 300	438.79 428.28 493.35	4.06 5.32 2.83	30	20	24	3	Suggett et al. 2009a
Cryptophyceae	*Storeatula major* Choptank Isolate (HP9001)	0.27 1.01 1.40	18 80 300	364.37 397.29 362.05	2.43 4.03 1.17	15	20	24	3	Suggett et al. 2009a
Dinophyceae	*Prorocentrum minimum* Choptank Isolate (PM-1)	0.24 0.73 1.10	18 80 300	372.57 388.44 362.05	1.65 2.08 0.96	15	20	24	3	Suggett et al. 2009a
	Symbiodinium (A20)	0.43	350 350	10-1330 (PE)	<1 >1	33	26	14	2	Brading et al. 2013
	Symbiodinium (A13)	0.29	350 350	10-1330 (PE)	<1 >1	33	26	14	2	Brading et al. 2013
Pelagophyceae	*Aureococcus anophagefferens* (CCMP1790)	0.22 0.4	18 80	353.86 279.99	4.10 3.54	30	20	24	2	Suggett et al. 2009a

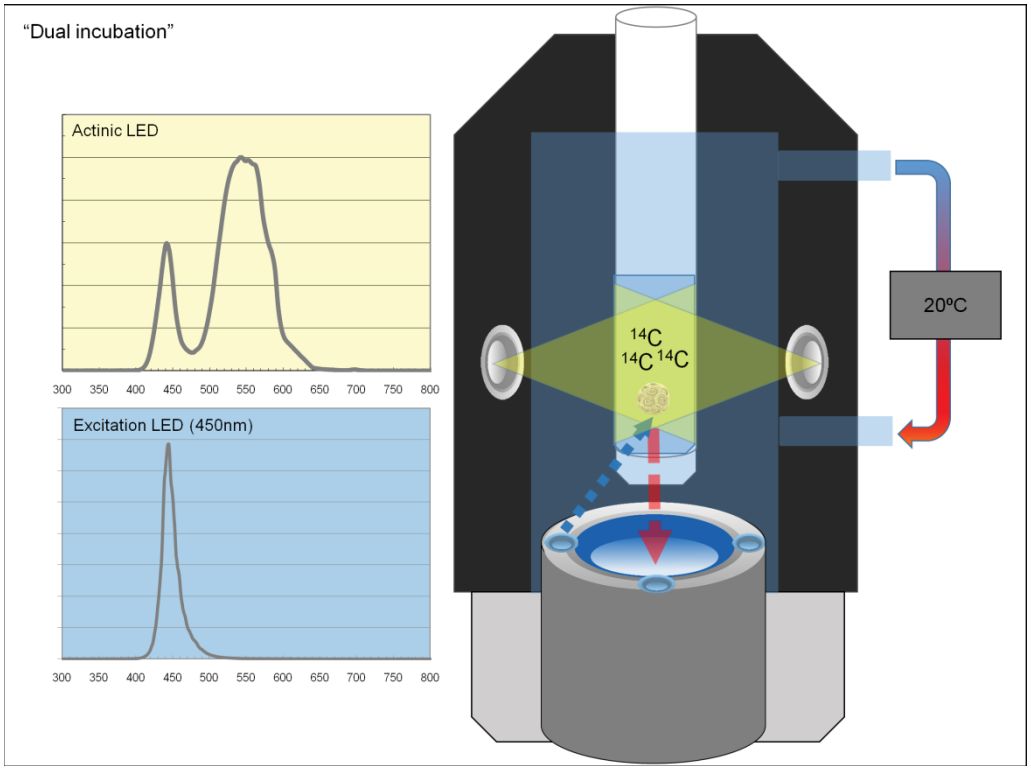

Supplementary Figure S3.1 Schematic of a "dual" incubation, used to measure ETR_{PSII} and ^{14}C-incorporation for a sample simultaneously. 3 mL of phytoplankton culture or seawater sample is radio-labelled inside the FRRf-specific test tube, which is then loaded into the FRRf optical head where the cool-white LED (see actinic LED spectra) provides a pre-determined irradiance level. ETR_{PSII} is continuously measured via the 450 nm blue excitation LED (spectral output shown). Upon completion of the incubation, the sample is removed and processed to measure ^{14}C-uptake. Sample temperature is maintained via a water jacket inside the optical head which is plumbed to a heater-chiller (in this example set to 20 ºC).

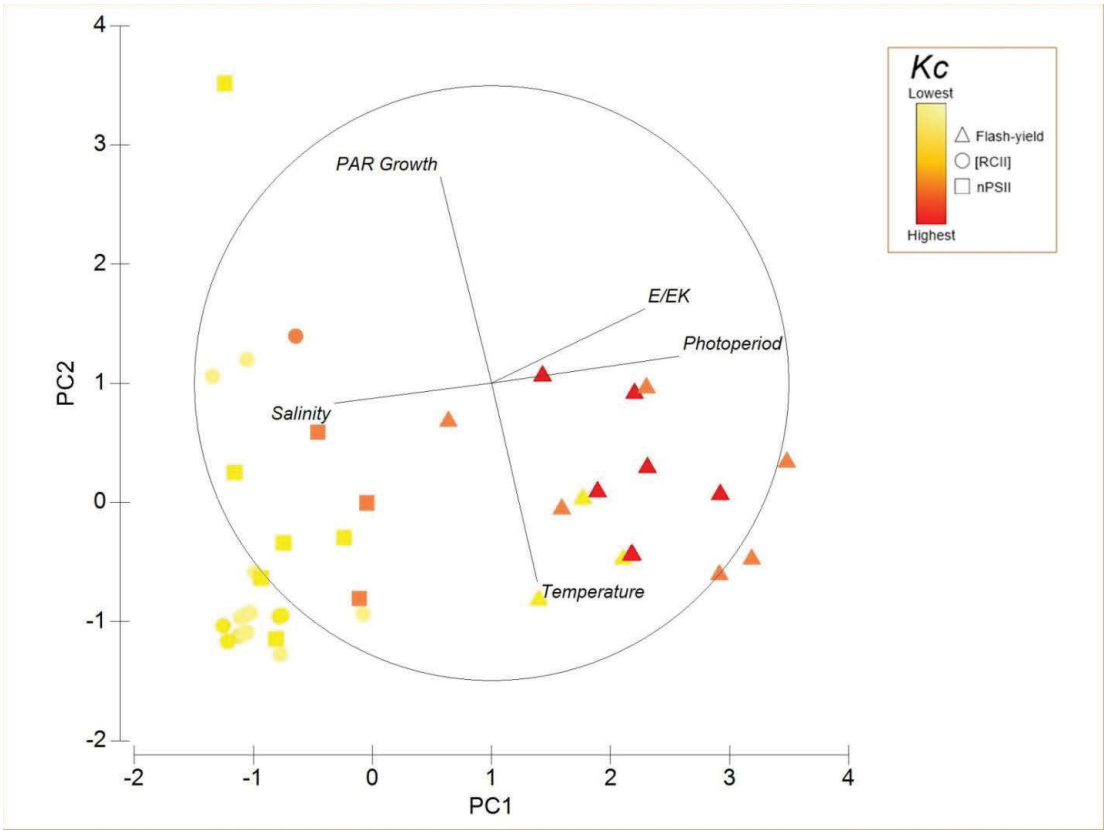

Supplementary Figure S3.2 Principle component analysis (PCA) of metadata, showing the variability in K_C explained by experimental growth conditions. The colour of each point represents K_C value as a scale from lowest (yellow) to highest (red). The shape of the symbol depicts the approach used to quantify/estimate PSII reaction centre content [RCII], triangle = direct measurement via O_2 flash-yield, circle = fluorometric estimate of RCII ($[RCII]_{FRRf}$) according to Oxborough et al. (2012), square = assumed constant value (n_{PSII}). Groupings of high K_C values appears to correspond to O_2 flash-yield assessment, with low values predominately associated with n_{PSII} and $[RCII]_{FRRf}$.

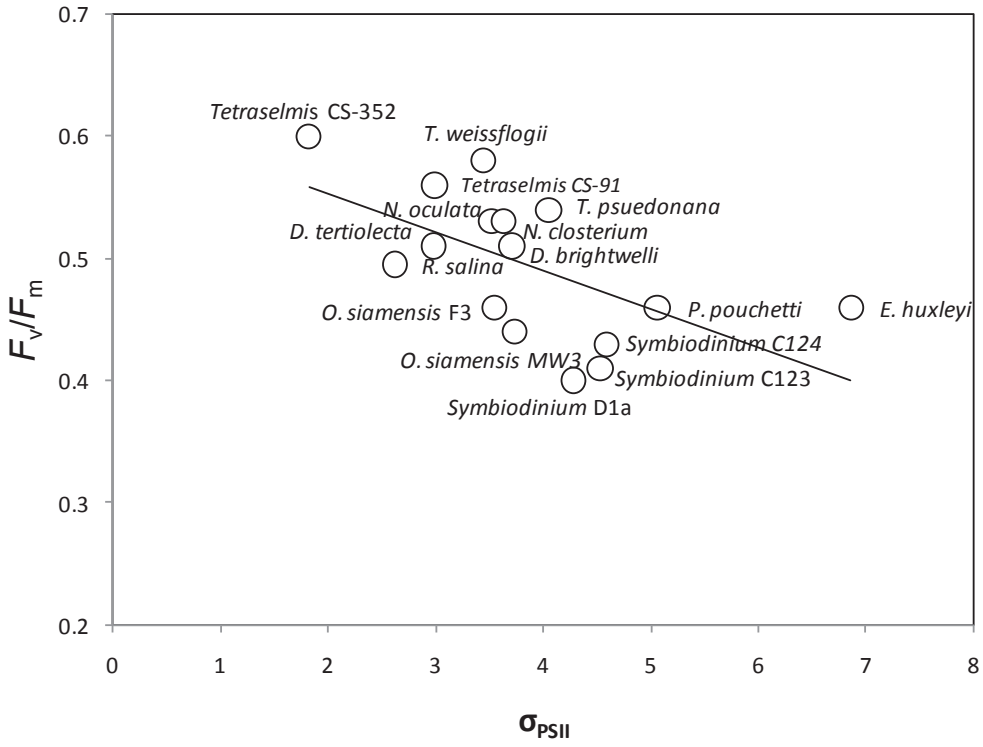

Supplementary Figure S3.3 Fast Repetition Rate fluorometry (FRRf) measurements of PSII maximum photochemical efficiency (F_v/F_m, dimensionless) and the functional absorption cross-section of PSII (σ_{PSII}, nm^2 $quanta^{-1}$) using the blue excitation LED (450 nm) for all strains examined during this study with the exception of *Synechococcus* (excluded due to having a unique LED protocol [blue + orange LEDs]). Values shown represent means from triplicate measurements prior to measurement of the electron requirement for carbon fixation (K_C).

4 Chapter 4:

Variability of phytoplankton electron requirement for C-fixation across physically-dynamic ocean waters of eastern Australia

David J. Hughes[1], Martina A. Doblin[1], Joseph R. Crosswell[1,2], Peter J. Ralph[1] and David J. Suggett[1*]

[1] Climate Change Cluster, University of Technology Sydney, Broadway 2007, NSW, Australia

[2] CSIRO Oceans and Atmosphere, Brisbane, Queensland, Australia

*Corresponding author: David.Suggett@uts.edu.au

4.1 Abstract

Chlorophyll-*a* fluorescence induction generates highly resolute broad-scale datasets of productivity as Photosystem II electron transport rates (ETR_{PSII}). Consequently, studies attempting to predict the "electron requirement for carbon fixation" (termed K_C) that describes the inter-dependency between ETR_{PSII} and C-uptake to retrieve highly resolute patterns of C-uptake have steadily gained popularity. Even so, it is still particularly unclear whether and how K_C follows predictable patterns for datasets that span complex oceanographic gradients. We therefore used a high-throughput coupled ETR_{PSII} (from Fast Repetition Rate fluorometry) – C-uptake technique to produce a semi-continuous dataset of K_C (n = 80), predominantly from surface waters, along the eastern Australian coast from Brisbane to the Tasman Sea, including near-shore waters of the East Australian Current. Environmental conditions along this transect could be generally grouped into warmer, more nutrient-rich waters dominated by larger size fractionated Chl-*a* (>10 μm) versus cooler nutrient-poor waters dominated by smaller size-fractionated Chl-*a* (< 2 μm). Whilst K_C was higher overall for the warmer water samples, differences in environmental conditions (plus predominant cell size) failed to explain more than 30% variance of K_C. Instead, normalised Stern-Volmer non-photochemical quenching (NPQ_{NSV}; = F_0'/F_v') appeared to explain as much as 55% variance of K_C. NPQ_{NSV} accounts for changes in both long-term driven acclimation in non-radiative decay quasi-instantaneous PSII downregulation, and thus may explain why K_C can be best predicted by a physiological descriptor, particularly across physically-dynamic environmental regimes. Our observations of a strong empirical relationship between K_C and NPQ_{NSV}, as well as those recently demonstrated for Fe- and N-limited ocean regions, suggest that FRRf-based ETR algorithms could be adjusted to account for the specific relationship describing the dependency between K_C

and NPQ_{NSV} (Fig. 4.6) to retrieve C-fixation rates but clearly warrants further validation.

4.2 Introduction

Accurately quantifying marine primary production (MPP) at sufficient spatial and temporal scales needed to develop algorithms that retrieve carbon (C)-fixation rates from satellite products represents a long-standing goal for oceanographers (Lee et al. 2015). Chlorophyll fluorescence induction tools, such as Fast Repetition Rate fluorometry (FRRf, Kolber et al. 1998), provide a means to realise this goal, where FRRf-derived Photosystem II electron transport rates (ETR_{PSII}) can be robustly converted to C-fixation rates according to the "electron requirement for carbon fixation" (termed K_C; Lawrenz et al. 2013; Hancke et al. 2015). Whilst multiple studies have now demonstrated an empirical relationship between ETR_{PSII} and both gross (Suggett et al. 2009a; Robinson et al. 2014; Napoleon et al. 2013; Schuback et al. 2015), and net (Hoppe et al. 2015; Zhu et al. 2016) C-fixation, K_C has in fact been shown to be highly variable, often far exceeding the theoretical minimum stoichiometry of 4 e^- $(mol\ C)^{-1}$ (see Kolber and Falkowski, 1993). Such variability reflects (i) re-routing of ETR_{PSII} to non C-fixing pathways (e.g. Fisher and Halsey, 2016), (ii) consumption of photo-produced ATP and reductant for metabolisms other than cellular growth (e.g. Halsey and Jones, 2015), (iii) growth-rate dependent variability in the lifetime of fixed-C (Halsey et al. 2011) and/or (iv) methodological bias in the determination of ETR_{PSII} or C-fixation (Suggett et al. 2009a; Lawrenz et al. 2013).

Resolving variability of K_C over space and time remains a major challenge, and it is unclear whether and how K_C follows predictable patterns and thus can be readily applied to broad FRRf data sets that often span complex oceanographic gradients.

Through a comprehensive meta-analysis of parallel ETR_{PSII} and C-fixation measurements, Lawrenz et al. (2013) established the existence of empirical relationships between K_C and prevailing environmental variables known to regulate photosynthesis (e.g. light, inorganic nutrients and temperature); however the strength of these relationships varied considerably depending upon geographic location. More recent campaigns have similarly evidenced that a large proportion of K_C variability can be explained by corresponding changes in variability of light across sites in the South China Sea (Zhu et al. 2016, 2017) or inorganic nitrogen over time at an oligotrophic coastal reference station in eastern Australia (Hughes et al. in press., Chapter 2). Intriguingly, these recent studies demonstrated a role for the prevailing phytoplankton taxonomy in moderating the covariance between K_C and environmental conditions. Past controlled laboratory culture experiments (Suggett et al. 2009a; Napoleon et al. 2013; also see Chapter 3) and field evaluations (Suggett et al. 2006, Lawrenz et al. 2013; Robinson et al. 2014; Zhu et al. 2017; Hughes et al. in press., Chapter 2) have indeed indicated that K_C can be highly variable across phytoplankton taxa. However, isolating the relative role of environment versus taxonomy has remained elusive given the fact that phytoplankton functional groups are often selected-for via specific environmental variables (see Finkel et al. 2009; also Hughes et al. in press., Chapter 2).

Variability of K_C is inherently driven by physiological 're-wiring' of the efficiency with which electrons are used to drive carbon uptake (Halsey et al. 2011; Fisher and Halsey, 2016). Thus, to overcome potential conflating roles of environment and taxonomy on regulation of K_C, Schuback et al. (2015, 2016, 2017) recently considered use of a physiological trait metric as a potentially overarching predictor for K_C. These authors demonstrated the existence of an empirical relationship between the extent of non-photochemical quenching (NPQ) and K_C, likely driven by a positive feedback between

the upregulation of non C-fixing pathways and ΔpH-activation of thermal dissipation mechanisms within the photosystem II (PSII) antennae (Nawrocki et al. 2015). This relationship appears robust for iron-limited conditions, and appears to hold under N-limitation (see Hughes et al. in press., Chapter 2), yet remains generally untested for complex coastal waters where both environmental conditions, and phytoplankton community composition are highly dynamic. Non-photochemical quenching describes the dynamic downregulation of PSII photochemistry and thus captures a snapshot of the prevailing physiological status of cellular excitation energy dissipation; however, other variables such as cell size, which frequently operate as 'master traits' capturing efficiency of resource acquisition and utilisation independently of phytoplankton taxonomic identity (Key et al. 2010; Finkel et al. 2009; see also Suggett et al. 2015, 2017), appear to show promise in broadly explaining variance in K_C (Zhu et al. 2017; Chapter 3).

Currently it remains unclear whether variance of K_C can in fact be explained from relatively easily retrieved phytoplankton properties that potentially capture both environmental and taxonomic variance across physically complex oceanographic gradients. To address this goal, we employed a high-throughput coupled FRRf (ETR_{PSII}) – C-incorporation technique to yield a unique semi-continuous data set of K_C (n = 80), predominantly from surface waters, along the eastern Australian coast spanning Brisbane to the Tasman Sea and including near-shore waters of the East Australian Current (EAC). These water bodies comprise strong latitudinal gradients of temperature (~15-23ºC) and nutrients (0-3 μM dissolved nitrate), moderated by eddies generated by the EAC that transiently incur nutrient-rich cooler waters onto the continental shelf (Oke and Middleton, 2001). We examine the extent to which variance of K_C can be explained by variance in the prevailing environmental conditions. However, based on

recent observations from laboratory cultures (Chapter 3) and contrasting water types in the South China Sea (Zhu et al. 2016, 2017) and Sydney coasts (Robinson et al. 2014), we further tested how well K_C variance could, in fact, be explained by a broad descriptor of the capacity to acquire and utilise resources; specifically, the predominant cell size fraction (measured as size-fractionated chlorophyll-*a* (Chl-*a*) since it is routinely incorporated into oceanographic studies) versus NPQ_{NSV}.

4.3 Materials and Methods

4.3.1 Seawater Samples

A total of 80 coupled FRRf and 14C-uptake samples were collected along the eastern coast of Australia between August 31 and September 22, 2016 onboard the RV *Investigator* (voyage number: IN2016_v04, departing from Sydney and arriving in Brisbane, Fig. 4.1). Discrete seawater samples were collected from surface waters (5-7 m depth), and from the sub-surface chlorophyll maximum (SSCM) via Conductivity Temperature Depth (CTD) casts (SeaBird SBE32, 24 bottle rosette sampler, Seabird Electronics, USA). The presence of a SSCM was identified from a vertical Chl-*a* fluorescence profile from a passive fluorometer attached to the CTD frame. Underway samples were collected from the pumped seawater supply system (7 m intake depth, non-filtered). In total, the data set comprised n = 64 surface samples and n = 14 SSCM samples.

4.3.2 Physico-chemical parameters

Salinity, temperature and oxygen were determined for each discrete sample from probes attached to the CTD sensor (SeaBird SBE911 dual conductivity and temperature sensor, SBE43 dissolved O_2 sensor) or the pumped underway seawater supply (Seabird SBE21

SeaCAT thermosalinograph, Aanderaa 3835 O_2 Optode). Analysis of dissolved inorganic nutrient concentrations (ammonium (NH_4^+), nitrate (NO_3^-), phosphate (PO_4^-) and silicate (Si) was conducted at sea immediately upon sample collection. Analysis was performed using a SEAL AA3HR segmented flow injection analyser with instrument detection limits of: 0.02, 0.2, 0.02 and 0.2 μM for NH_4^+, NO_3^-, PO_4^- and Si respectively. Dissolved inorganic carbon (DIC) was quantified using a dissolved gas analyser (Picarro 1301, Picarro Instruments, California, USA).

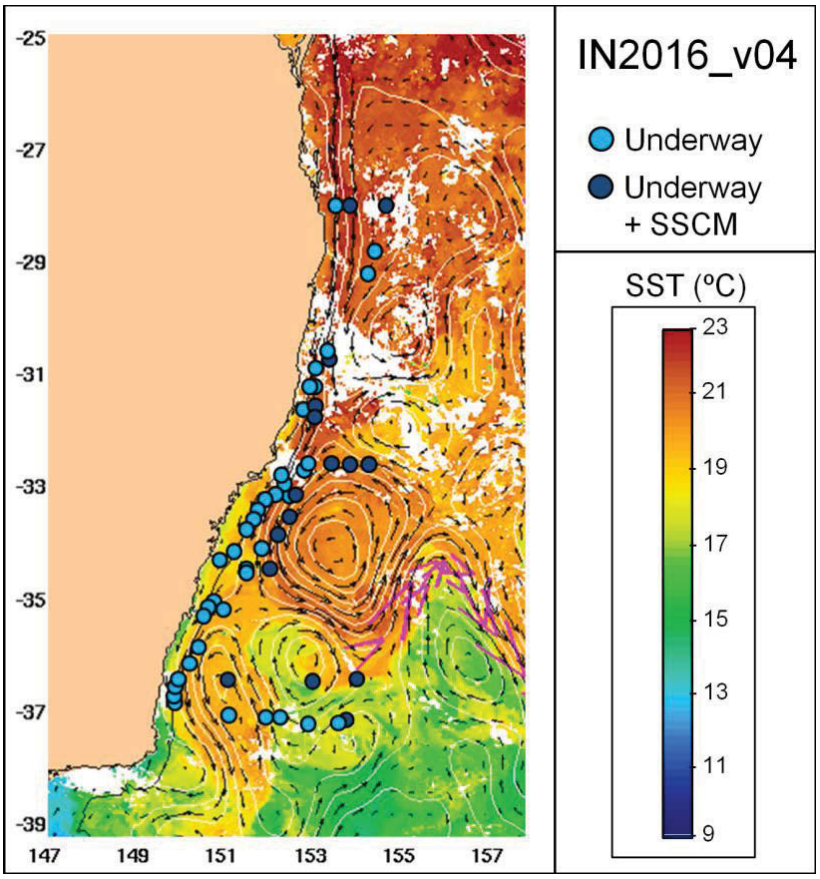

Figure 4.1 Study area and sampling locations. Light blue circles denote locations corresponding to underway sampling whilst the dark blue markers indicate Conductivity Temperature Depth casts (CTD) where the sub-surface Chlorophyll-*a* maximum (SSCM) was sampled in addition to surface water (n = 80 total samples). Sea surface temperature (SST) from satellite imagery is overlaid (data sourced from the IMOS data portal: (http://imos.aodn.org.au).

4.3.3 Size-fractionated Chl-*a*

Total Chl-*a* content was determined by filtering 250 mL of seawater under low vacuum (<50 mg Hg) through a Sterlitech GF/F filter (0.3 µm nominal pore size). Filters were then transferred to 20 mL glass vials and pigments were immediately extracted using 3 mL 90% acetone and stored in the dark at 4°C for 24 hours. For the 2-10 µm and >10 µm fractions, a similar procedure was conducted, using 2 µm GF/F filters (Microanalytix, Sydney, Australia) and 10 µm polycarbonate filters (Merck Millipore, Bayswater, VIC, Australia) respectively. Chl-*a* was then determined fluorometrically (Trilogy fluorometer serial number: 720000354, Turner Designs, California, USA), using a non-acidification Chl-*a* module (Turner Designs, USA), calibrated against a pure Chl-*a* standard (Sigma-Aldrich Pty Ltd).

4.3.4 Photophysiological characterisation and electron transport rates

A FastOcean MKIII FRRf (Serial number: 15-0087-004) attached to a FastACT II docking base (serial No. 12-8809-003, both Chelsea Technologies Group, London, UK) was programmed to deliver single turnover (ST) saturation of PSII from 100 flashlets (1 µs pulse, with an interval of 2 µs between flashes), followed by a relaxation phase of 40 flashlets (1 µs pulse with an interval of 50 µs between flashes). A total of 100 sequences were performed per acquisition, using an interval spacing of 150 ms between sequences. For all ST measurements, the blue LED (450 nm) was the sole excitation source used to drive closure of PSII reaction centres and generate fluorescence induction transients. The biophysical model of Kolber et al. (1998) was fitted to all fluorescent transients using FastPRO software (V.1.5.2) to determine minimum (F_0, F') and maximum fluorescence (F_m, F_m'), functional absorption cross-section of PSII (σ_{PSII}, σ_{PSII}') and the PSII connectivity factor (ρ, ρ′) (prime notation denotes that samples were measured

during exposure to actinic light). Baseline fluorescence was measured from 0.2 µm-filtered samples and subtracted from all samples using the FastPRO software.

For this study we calculated ETR on a volumetric basis (ETR_{PSII}, mol electrons m^{-3} s^{-1}) according to the "absorption" algorithm of Oxborough et al. (2012) (Eq. 1):

$$ETR_{\mathrm{PSII}} = \frac{F_{\mathrm{q}}'}{F_{\mathrm{m}}'} \cdot a_{\mathrm{LHII}} \cdot E \quad (1)$$

The absorption algorithm represents a modified version of the "sigma" algorithm (Kolber et al. 1998) which allows for parameterisation of a_{LHII} without σ_{PSII}' which can be difficult to measure reliably at high ambient irradiance (see Oxborough et al. 2012) (Eq. 2):

$$a_{\mathrm{LHII}} = \frac{F_{\mathrm{m}} \cdot F_0}{F_{\mathrm{m}} - F_0} \cdot \frac{\mathrm{K_R}}{E_{\mathrm{LED}}} \quad (2)$$

where K_R is an instrument-specific constant (photons m^{-3} s^{-1}) and E_{LED} represents the intensity of the fluorometer's 450 nm measuring beam (photons m^{-2} s^{-1}). This approach does not require the operator to make an assumption of the connectivity of PSII reaction centres (RCIIs) (see Kolber et al. 1998; Kramer et al. 2004) and thus the absorption algorithm can be alternatively expressed as per Eq. 3. Strictly, this derivation is denoted JV_{PSII}, since it is a flux (mol e^- m^{-3} s^{-1}) See Oxborough et al. 2012) but for consistency with the terminology in Eqs 1-2 and throughout the thesis, we continue to refer to this as ETR_{PSII}:

$$ETR_{\mathrm{PSII}} = \frac{F_{\mathrm{m}} \cdot F_0}{F_{\mathrm{m}} - F_0} \cdot \frac{F_{\mathrm{q}}'}{F_{\mathrm{m}}'} \cdot \frac{\mathrm{K_R}}{E_{\mathrm{LED}}} E \quad (3)$$

Measurements of σ_{PSII}' are spectrally-weighted towards the FRRf excitation LED (450 nm in this study) and thus were spectrally-adjusted using a correction factor informed by assessing the phytoplankton pigment group contributions to the FRRf signal. This was achieved by screening samples with a custom, multi-spectral FRRf (no serial number, Soliense Inc, California, USA) programmed to deliver "Flash, Length, Delay, Inc" of "100, 1.6, 5, 1" (excitation) and "80, 1.6, 20, 1.06" (relaxation), sequentially cycling through excitation LED wavelengths: 450 nm, 470 nm, 505 nm and 530 nm. FRRf acquisitions were averaged from 20-80 sequences (depending upon biomass). By comparing the ratio of PSII absorption (as σ_{PSII}) for each wavelength measured against previously-collected fluorescence excitation spectra (400-700 nm) from phytoplankton cultures pre-treated with 3-(3,4-dichlorophenyl)-1,1-dimethylurea (DCMU) where fluorescence emission was measured at 730 nm (see Suggett et al. 2009b; Wu et al. 2014) we selected the spectra most comparable to the specific sample and then used that complete spectra to calculate spectrally-resolved values of PSII effective absorption, $\sigma_{PSII}'(\lambda)$ as,

$$\sigma_{\mathrm{PSII}}{}'(\lambda) = \left(\sigma_{\mathrm{PSII}}{}'(450) \Big/ F_{730}(450) \right) . F_{730}(\lambda) \qquad (4)$$

Values of $\sigma_{PSII}'(\lambda)$ were then spectrally-adjusted to the actinic light source within the FRRf optical head as per Eq. 5.

$$\overrightarrow{\sigma_{\mathrm{PSII}}{}'} = \left(\sum_{400}^{700} \sigma_{\mathrm{PSII}}^{'(\lambda)} . E(\lambda) \right) \Delta\lambda \Big/ \sum_{400}^{700} E(\lambda) \Delta\lambda \qquad (5)$$

Rapid Light Curves (RLCs) were initially performed to approximate the light intensity for saturated electron transport (E_K) as a means to standardise subsequent incubations to

derive K_C (see following section), although we do acknowledge that RLCs may not allow sufficient time for photochemical and non-photochemical quenching to reach steady state (see Ralph and Gademann, 2005). For this, we used a similar protocol and instrument settings as described in Suggett et al. (2015), with the exception that each light step was held for only 20 s duration. The model of Platt et al. (1980) was then fit to the data (Sigmaplot v11.0, Systat Software Inc, California, USA). Least squares non-linear regression analysis of the model fit was performed to estimate the maximum rate of electron transport, ETR_{PSII}^{max}, the light utilisation efficiency, α (electrons m^{-3} s^{-1}) and thus the light saturation parameter, E_K (calculated as ETR_{PSII}^{max}/ α) with units of μmol photons m^{-2} s^{-1}.

4.3.5 High-throughput FRRf-^{14}C incubations (K_C)

A total of 80 small volume, incubations were performed, whereby ETR_{PSII} and ^{14}C-uptake were measured on the same sample simultaneously (i.e. a "dual incubation"). This approach avoids many errors associated with methodology that can be introduced with separate incubations (see Suggett et al. 2009a, Lawrenz et al. 2013). To achieve this, radio-labelled samples were incubated within the FRRf optical head itself, using the actinic white LED array to drive photosynthesis. Values of K_C have been shown to increase under saturating light intensities that yield ETR_{PSII}^{max} compared limiting irradiances that correspond to α (Brading et al. 2013). Therefore, to standardise incubation conditions, we opted to approximate the irradiance corresponding to the light-saturation parameter (E_K) for each sample, since E_K can be rudimentarily interpreted as a convenient indicator of photoacclimational status (Sakshaug et al. 1997). Due to constraints of instrumentation within the radiation laboratory, E_K was *estimated* visually from the raw RLC data (i.e. before the Platt et al. 1980 model fit - see

above). The FRRf white LED array was then programmed to deliver the closest corresponding irradiance level available. Incubation irradiances were subsequently expressed relative to the *calculated* E_K at a later time as: E/E_K (dimensionless). Generally the irradiances chosen represented good approximations of E_K (mean E/E_K = 1.15), although the full range of values was 0.7 – 1.7 (data not shown). Thus, the incubations in this study represent a reasonably-constrained continuum of light-limited (E/E_K <1) to light-saturated (E/E_K >1) conditions for photosynthesis.

To quantify ^{14}C-uptake, we adopted the small-volume method of Lewis and Smith (1983) with several modifications. Aliquots of 3 mL were placed in the FRRf test-tube and spiked to a final concentration of 0.4 μCi mL^{-1} NaH$^{14}CO_3$ (Perkin-Elmer, Melbourne, Australia). The radio-labelled sample was then incubated for 2 hr inside the FRRf at an irradiance approximating the light-saturation parameter (above) and ETR_{PSII} determined every 5 s during this period. Upon completion of the incubation, samples were removed and acidified with 150 μL of 6 M HCl to convert any remaining unfixed inorganic ^{14}C to $^{14}CO_2$. Samples were then left to de-gas for 24 hr before fixation with 10 mL scintillation fluid (Ultima Gold LLT, Perkin Elmer). Samples were then boxed and stored in a cool location for measurement upon return to University of Technology Sydney (UTS). At UTS, fixed samples were shaken vigorously for several minutes and left to stand overnight before liquid scintillation counting (Tri-Carb 2810 TR, Perkin-Elmer), selecting automatic quench correction and a count time of 5 min. ^{14}C-fixation (mol C m^{-3} hr^{-1}) was calculated from the concentration of dissolved inorganic carbon (DIC) and the amount of ^{14}C isotope incorporated during the incubation (see Knap et al. 1996). ETR_{PSII} was then scaled to hourly-integrated rates as per Suggett et al. (2009a) to allow determination of K_C (mol e$^-$ [mol C]$^{-1}$) as:

$$K_C = {}^{\mathrm{ETR_{PSII}}}/_{\text{14C uptake rate}} \quad (6)$$

4.3.6 NPQ_{NSV} and PSU size

NPQ of fluorescence was calculated as the normalised Stern-Volmer coefficient (denoted here as NPQ_{NSV}) as per McKew et al. (2013) (eq. 7), during the simultaneous ^{14}C-FRRf incubations and represents an integrated value over the duration of the incubation

$$\mathbf{NPQ_{NSV}} = \mathbf{1}/\left(\frac{\boldsymbol{F_v'}}{\boldsymbol{F_m'}}\right) - \mathbf{1} \quad (\mathbf{7})$$

The size of the photosynthetic unit (PSU, with units of mol Chl-*a* [mol RCII]) was calculated from a fluorometric estimate of RCII according to Oxborough et al. (2012) (see also Murphy et al. 2017) as:

$$\text{PSU Size} = {}^{\mathrm{Chl-a}}/_{\mathrm{[RCII]}} \quad (8)$$

4.3.7 Statistical analysis

All multivariate analysis was performed using the software package, PRIMER v6. (PRIMER-E, Plymouth, UK). Multidimensional scaling (MDS) plots were constructed to visualise patterns in physico-chemical variables. Hierarchical cluster analysis (HCA) with a SIMPROF test (p = 0.05) was performed on a Euclidean resemblance matrix of physico-chemical variables to identify groupings of similar hydrography. A Welch's t-test (unequal variances t-test) was used to test for statistical differences between data clusters identified by HCA after checking for normality using Kolmogorov-Smirnov test (Sigmaplot v11.0, Systat Software Inc, California, USA). Distance-based linear modelling (DistLM) was performed to examine how much variability in K_C could be

explained by core environmental variables (nutrients, temperature, salinity and E/E_K), NPQ_{NSV}, total Chl-*a* and size-fractionated Chl-*a* within clusters identified by HCA and for all data pooled. Predictor variables were selected individually (and in multiple combinations) using the forced inclusion criteria. To obtain the most parsimonious model, we also used the BEST selection procedure, choosing Akaike information criterion (AICc - corrected for small sample number), which incorporates a penalty factor for increasing the number of predictor variables (see Anderson et al. 2008). Prior to DistLM, the distribution of each physico-chemical variable was assessed using draftsman's plots and co-correlations were identified from Pearson's correlation matrices. Variables with skewed distribution were square-root transformed, and if pairs of variables had a Pearson's correlation co-efficient >0.8, 1 of the pair was excluded from the subsequent analysis. Distance-based redundancy analysis (dbRDA) plots were performed to enable two-dimensional visualisation of the BEST DistLM models.

4.4 Results

4.4.1 Physico-chemical characterisation

As expected, the sampled water masses were characterised by a distinct gradient of both nutrients and temperature (Fig. 4.2a-f). NO_3^-, PO_4^- and Si exhibited higher concentrations in coastal samples and the southern Tasman Sea, compared to the EAC and northernmost coastal/oceanic samples (Fig. 4.2b-d). NH_4^+concentrations were generally highest in coastal samples (up to 0.6 µM), but relatively low in the Tasman Sea and EAC where values occasionally fell below the detection limit (0.02 µM; Fig. 4.2a). Temperature exhibited a distinct latitudinal pattern, ranging from ~15ºC in the southern Tasman Sea to ~23.5 ºC for northernmost coastal samples, with a distinct thermal gradient also measured within the EAC, where surface temperatures cooled

with southward travel (Fig. 4.2f). Salinity remained largely consistent throughout (~35-35.8 ppt), although the highest values were measured within the EAC water mass (Fig. 4.2e).

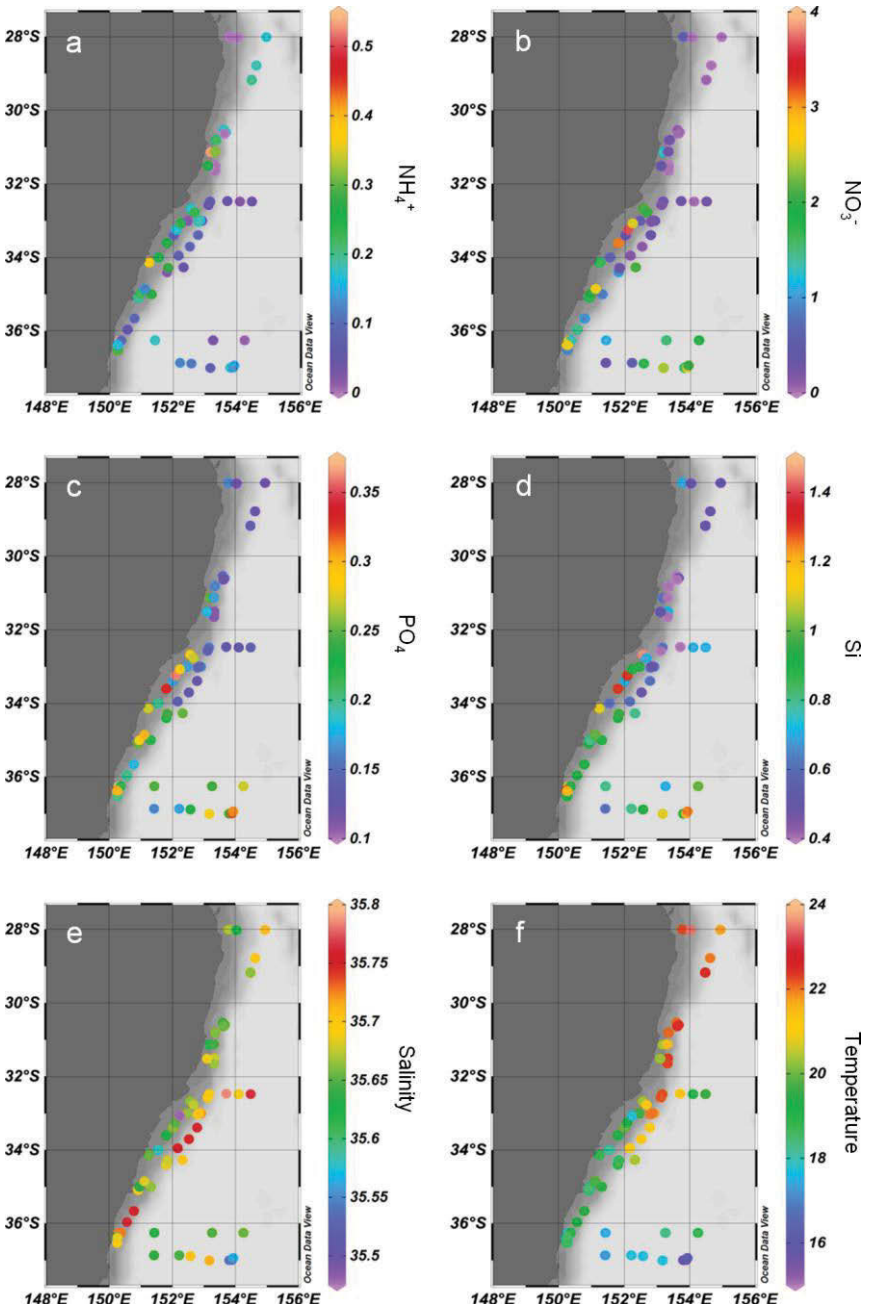

Figure 4.2 Physico-chemical characteristics of surface water sampled in coastal, East Australian Current (EAC) and Tasman Sea water masses measured from the RV *Investigator* (August – September 2016, IN2016_v04); (a) ammonium (NH_4^+), (b) nitrate (NO_3^-), (c) phosphate (PO_4^-), (d) silicate (Si) [all nutrient concentrations are reported as µM], (e) salinity (ppt) and (f) sea surface temperature (SST, °C).

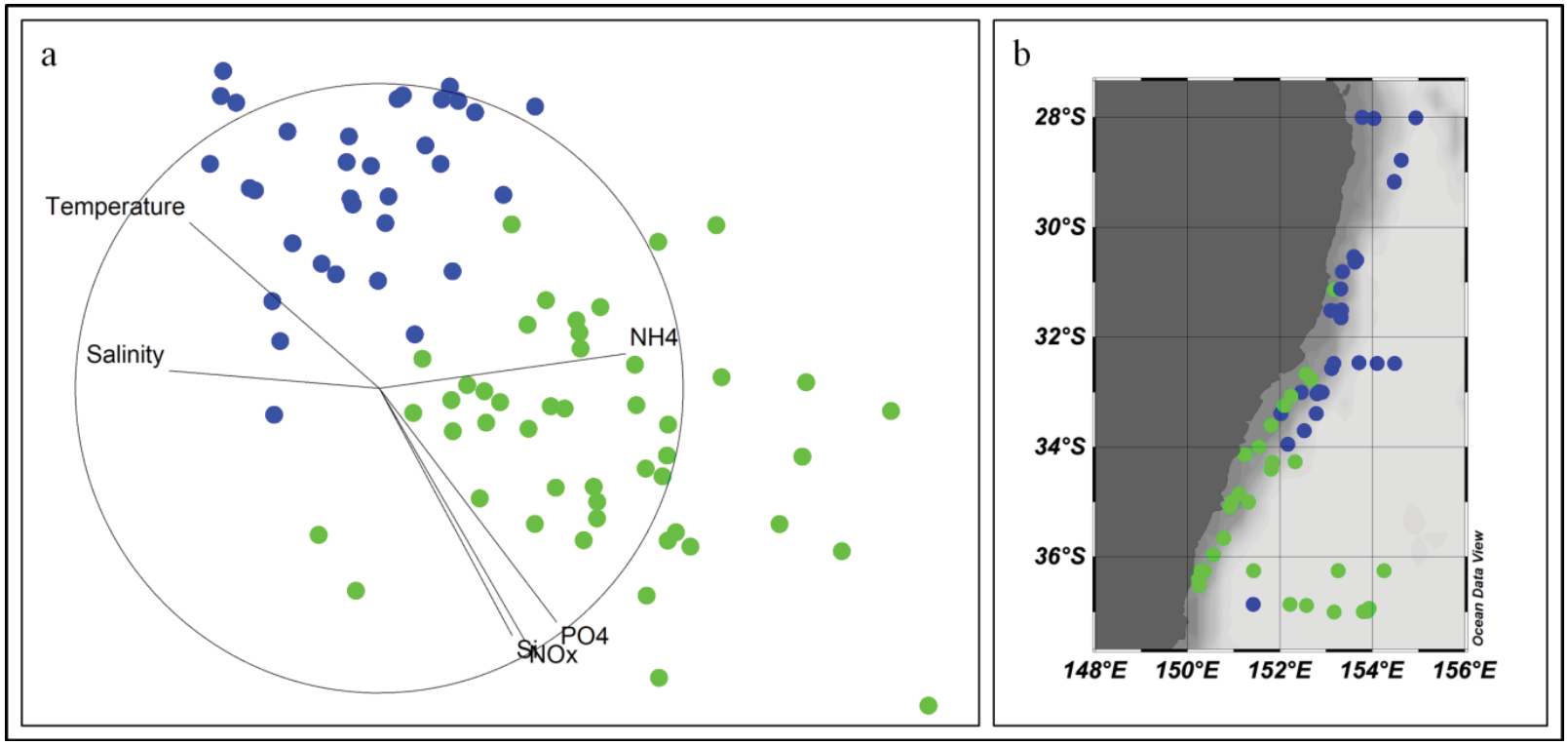

Figure 4.3 a) Multi-dimensional scaling (MDS) plot of physico-chemical (environmental) variables for samples collected from the RV *Investigator* (August – September 2016, IN2016_v04). Blue and green circles represent data clusters (a and b respectively), assigned according to hierarchical cluster analysis (CLUSTER, with SIMPROF test [$p = 0.05$]) performed upon a Euclidean resemblance matrix, generated from square-root transformed data; and **b)** latitudinal distribution of data clusters.

Table 4.1 Mean (± SE, standard error) of physico-chemical variables and biological parameters within Cluster A and B (see Fig. 4.3 for cluster information). Student's t-test results indicate statistical differences between clusters (* and ** denotes significance levels of 0.05 and <0.01 respectively).

	Cluster **A** (n = 33)	Cluster **B** (n = 47)	T-test statistic
Physico-chemical			
Temperature (ºC)	21.45(0.22)	18.60 (0.20)	p = < 0.001**
Salinity (ppt)	35.69 (0.01)	35.65 (0.01)	p = 0.002*
NH_4^+ (µM)	0.09 (0.02)	0.17 (0.02)	p = < 0.001**
NO_3^- (µM)	0.24 (0.03)	1.82 (0.12)	p = < 0.001**
PO_4^- (µM)	0.14 (0.01)	0.26 (0.01)	p = < 0.001**
Si (µM)	0.56 (0.02)	1.01 (0.03)	p = < 0.001**
Biological			
Chl-*a* < 2 µm (%)	35.23 (2.81)	20.01 (2.52)	p = < 0.001**
Chl-*a* 2-10 µm (%)	42.85 (2.14)	44.55 (2.70)	p = < 0.647
Chl-*a* > 10 µm (%)	21.91 (3.42)	35.44 (3.71)	p = 0.012*
Total Chl-*a* (mg m^{-3})	0.63 (0.06)	1.05 (0.13)	p = 0.008*
F_v/F_m	0.39 (0.02)	0.42 (0.01)	p = 0.096
$\sigma_{PSII(450)}$ (nm_2 $quanta^{-1}$)	5.40 (0.16)	5.12 (0.13)	p = 0.168
$E_{K\,(450)}$ (µmol photons m^{-2} s^{-1})	295.62 (21.77)	269.42 (20.36)	p = 0.196
NPQ_{NSV}	2.51 (0.26)	1.92 (0.10)	p = 0.019*
K_C (mol e^- [mol C]$^{-1}$)	18.96 (1.97)	14.23 (0.86)	p = 0.017*
CA (mg C [mg Chl-*a*] hr^{-1})	2.11 (0.18)	2.60 (0.18)	p = 0.034*
PSU size (mol Chl-*a* [mol RCII] $^{-1}$)	617.33 (26.24)	600.83 (28.55)	p = 0.695

MDS identified a distinct separation of data based on nutrients and temperature (Fig. 4.3a); thus, since previous studies modelling K_C variability have demonstrated improved predictive capacity by grouping samples according to similar hydrography (Lawrenz et al. 2013; Zhu et al. 2016, 2017), we adopted a similar approach. HCA identified two primary clusters (Supplementary Fig. S4.1): **Cluster a)** generally characterised by higher temperatures and lower nutrient availability, and **Cluster b**) by lower temperatures and high nutrient levels (Table 4.1, Fig. 4.3a), with a clear latitudinal

separation of the two clusters (Fig. 4.3b). Overall, 12 of the 17 SSCM samples were assigned to cluster b (data not shown). Binning these various data according to the 2 clusters identified revealed broad differences in the physiology inherent to the 2 prevailing water types sampled:

Mean K_C was lower and carbon assimilation number was higher in cluster a (14.2 mol e^- [mol C]$^{-1}$ and 2.6 mg C [mg Chl-*a*]$^{-1}$ hr^{-1} respectively) compared to cluster b (18.9 mol e^- [mol C]$^{-1}$ and 2.11 mg C [mg Chl-*a*]$^{-1}$ hr^{-1} respectively). Cluster b was further characterised by a significantly higher total Chl-*a* biomass, which was comprised of a greater proportion of the largest (>10 μm) Chl-*a* size fraction (35% - compared to 20% in cluster b) (Welch's t-test, Table 4.1). Conversely, the smallest size fraction (<2 μm) represented a greater proportion of total Chl-*a* for cluster b, yet there was effectively no difference in the proportion of the 2-10 μm size fraction between clusters (~ 45%), which was the overall dominant size fraction for both data clusters (Welch's t-test, Table 4.1). Photophysiological parameters were mostly statistically indistinguishable between clusters, with the exception of NPQ_{NSV} which was lower in cluster b (1.92) than cluster a (2.51) (Welch's t-test, Table 4.1). PSU size was also consistent between clusters, with a mean value (~600 mol Chl-*a* [mol RCII]), close to the commonly assumed value for eukaryotic-dominated phytoplankton assemblages (500 mol Chl-*a* [mol RCII] (Kolber and Falkowski, 1993; Supplementary Fig. S4.2).

4.4.2 K_C, biomass and photophysiology

K_C ranged from ~4.7 to 65 mol e^- (mol C)$^{-1}$, with a mean of ~16 mol e^- (mol C)$^{-1}$ (Fig. 4.4a). Thus, all observations were above the theoretical minimum of 4 mol e^- (mol C)$^{-1}$, and the upper values agreed well with a previous meta-analysis of global K_C data (Lawrenz et al. 2013). K_C was generally lowest in coastal waters, with virtually all

values falling below the mean measured across the entire data set (i.e. <16 mol e^- [mol C]$^{-1}$). The EAC and the Tasman Sea were both characterised by large variability in K_C (~10-65 mol e^- [mol C]$^{-1}$), and unlike physico-chemical variables (Fig. 4.2), no latitudinal pattern in K_C was evident. Carbon assimilation rate per unit Chl-*a* (carbon assimilation number) number ranged from 0.5 – 5.5 (mean: 2.2) mg C (mg Chl-*a*)$^{-1}$ hr^{-1} and was generally higher (>3 mg C [mg Chl-*a*]$^{-1}$ hr^{-1}) in coastal waters and the southern Tasman Sea, whilst lower values (<2.5 mg C [mg Chl-*a*]$^{-1}$ hr^{-1}) were consistently measured in the EAC (Fig. 4.4b). Overall, the generally low carbon assimilation numbers in this study would suggest that the 2 hr incubation time used to measure ^{14}C-incorporation most likely yielded productivity rates approximating NPP rather than GPP. Total Chl-*a* biomass ranged from ~0.1 to 3.5 mg m^{-3}, averaging ~0.8 mg m^{-3} during the study, with highest measured concentrations of Chl-*a* occurring within coastal waters and the southernmost Tasman Sea (Fig. 4.4c). The 2-10 μm Chl-*a* size fraction was the most dominant in this study, representing the largest contributor to total Chl-*a* in nearly half (42%) of all samples (Fig. 4.5b). Conversely, the <2 μm size fraction was least dominant, accounting for the majority of total Chl-*a* in only 15 out of 80 samples (19%), with the >10 μm size-fraction intermediate (~30% of samples) (Fig. 4.5b).

Values for the maximum photochemical efficiency (F_v/F_m) followed a similar pattern to Chl-*a* with larger values measured in coastal waters and the southern Tasman Sea (Fig. 4.4d). Conversely, the functional absorption cross-section of PSII (σ_{PSII}), was generally lowest in coastal waters (albeit with some variability), however the largest values recorded (>6 nm^2 quanta^{-1}) corresponded to the southern Tasman Sea water mass (Fig. 4.4e). Together, the dataset showed an inverse correlation between F_v/F_m and σ_{PSII}

(Supplementary Fig. S4.3) as commonly expected spanning broad environmental (and thus presumably taxonomic) gradients (e.g. Suggett et al. 2009b)

The light saturation parameter (E_K) spanned a wide range of values (~85-700 µmol photons m^{-2} s^{-1}) with a mean of ~270 µmol photons m^{-2} s^{-1}. E_K was consistently low (< 400 µmol photons m^{-2} s^{-1}) in both the southern Tasman Sea water mass and the EAC (with the exception of a single sample), but exhibited far greater variability in coastal waters (Fig. 4.4f).

4.4.3 Predicting K_C from physico-chemical versus taxonomic variables

Core environmental variables (Temperature, Salinity, NH_4^+, NO_3^-, PO_4^-, Si and E/E_K) only explained 22.7% of K_C variation across the entire data set (Table 4.2), indicating that prevailing environmental conditions were not strong predictors of K_C within this study area. When separated by cluster, the ability to explain variance in K_C improved to 29% for cluster a, but decreased slightly for cluster b (to 21.4%, see Table 4.2). Including knowledge of Chl-*a* improved the variance explained by the model within cluster a to 32.8%, but showed no improvement for cluster b (Table 4.2).

Inclusion of size-fractionated Chl-*a* only resulted in a moderate improvement of the model's performance, explaining 34.5% of K_C variance for cluster a, and 27.5% within cluster b (pooled data = 26.3%). Indeed, K_C did not appear to exhibit an obvious pattern relating to the proportion of total Chl-*a* from the three size classes (Fig. 4.5a), thus probably explaining the lack of model improvement. Interestingly however, when K_C values were binned into three sample groups based on their dominant Chl-*a* size-fraction (i.e. the largest individual contributor to overall Chl-*a* pigment), mean K_C decreased with increasing size fraction (Fig. 4.5b). K_C was thus lowest for assemblages dominated by cells/pigment in the >10 µm fraction (13.8 ± 1.2 mol e^- [mol C]$^{-1}$, n = 23),

increasing to 18.6 mol e^- [mol C]$^{-1}$, n = 15 for the < 2 μm fraction, with the 2-10 μm fraction intermediate (16.1 mol e^- [mol C]$^{-1}$) (Fig. 4.5b).

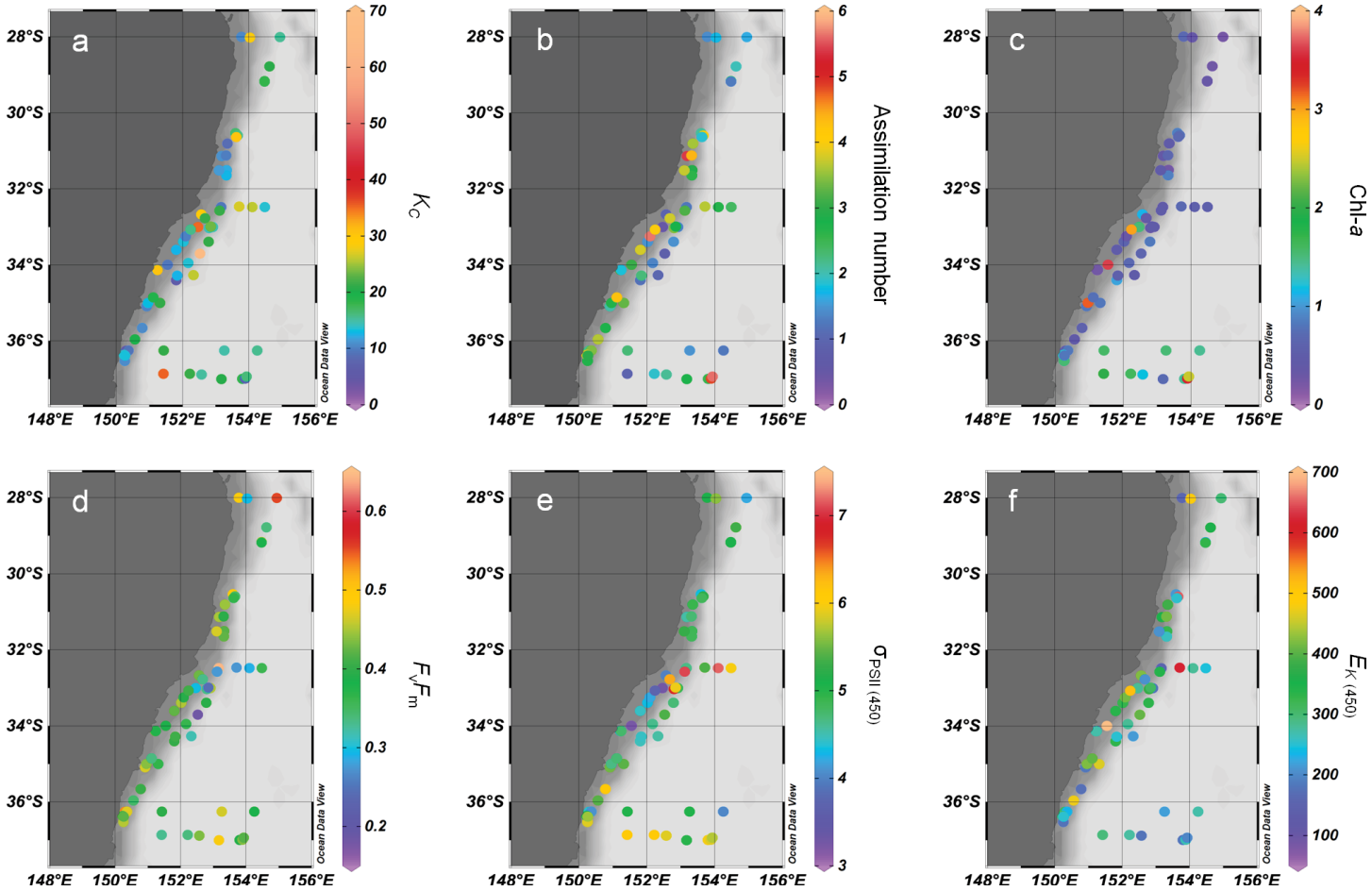

Figure 4.4 Biological characteristics of surface water sampled in coastal, East Australian Current (EAC) and Tasman Sea water masses measured from the RV *Investigator* (August – September 2016, IN2016_v04); (a) K_C, (mol e^- [mol C]$^{-1}$), (b) carbon assimilation number (mg C [mg Chl-*a*] hr^{-1}), (c) Chlorophyll-*a* (Chl-*a*) biomass (mg m^{-3}), (d) maximum photochemical efficiency (F_v/F_m, dimensionless), (e) functional absorption cross-section of PSII (σ_{PSII}, nm^2 quanta^{-1}) and (f) light-saturation parameter ($E_{K[450]}$, µmol photons m^{-2} s^{-1}).

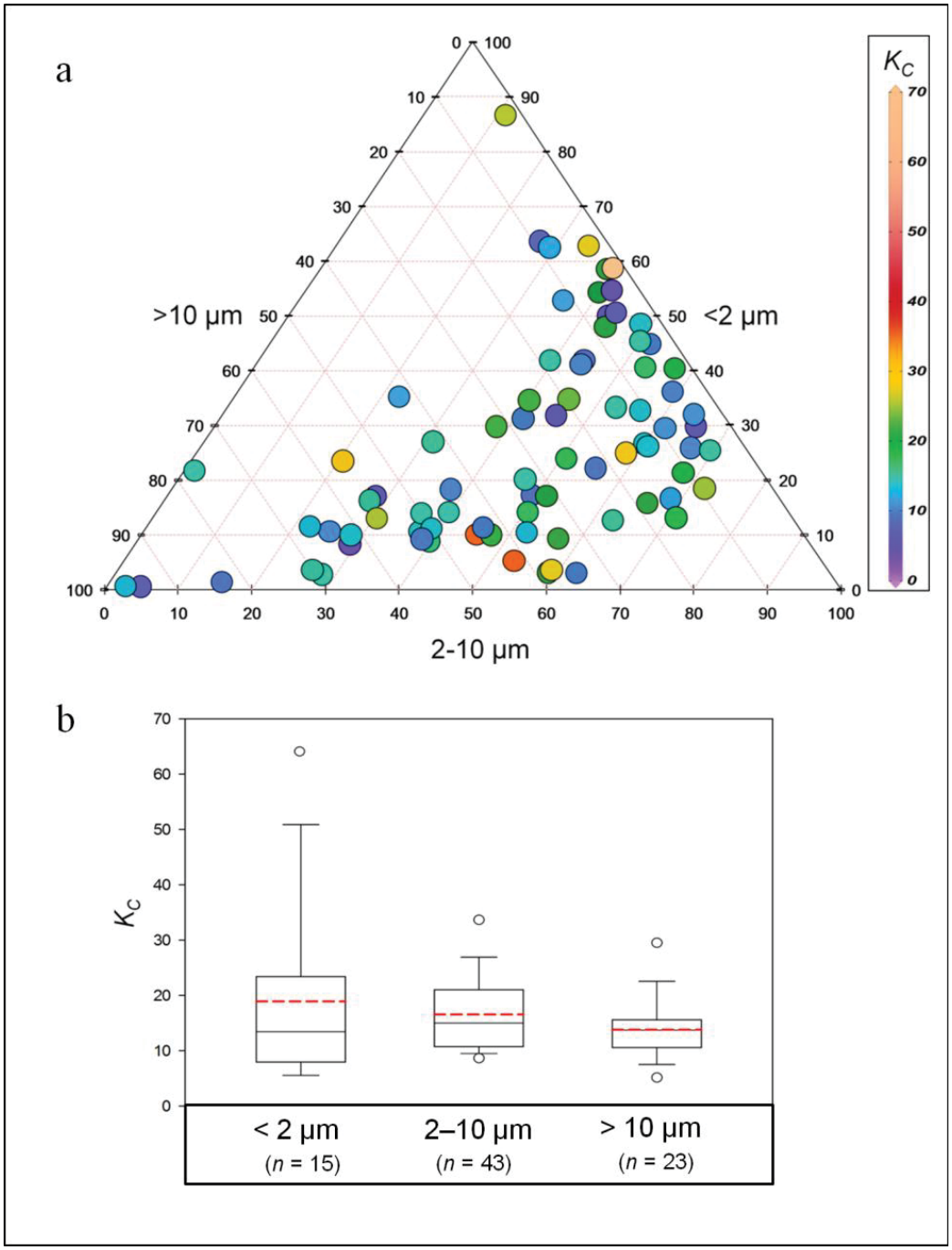

Figure 4.5 a) Simplex plot of K_C showing % contribution of Chl-*a* size fractions (<2 µm, 2-10 µm and >10 µm) for individual samples (n = 80); b) Box-plot of the electron requirement for carbon fixation, K_C (mol e^- [mol C]$^{-1}$) binned according to the dominant Chl-*a* size fraction (n = 81, note that one sample appears in both the <2 µm and 2-10 µm fractions due to equal dominance of both size fractions). For each cluster the median and mean values are indicated by the bold and red dashed lines respectively, the large box represent the 5th and 95th percentiles and the open circles denote outliers.

Linear regression showed that NPQ_{NSV} had the strongest relationship with K_C of all predictor variables in this study ($R^2 = 0.55$, $p < 0.01$, Fig. 4.6a) with almost identical slopes between clusters. Including NPQ_{NSV} as a predictor variable thus resulted in a substantial model improvement, explaining ~60% of K_C variance, when combined with core environmental variables, rising to 65-80% when knowledge of Chl-*a* and size-fractionated Chl-*a* were included (Table 4.2, Fig. 4.7). The most parsimonious (generated by BEST selection procedure) model explained 59 - 74.7% of variability for both clusters and for all data combined, with NPQ_{NSV} unsurprisingly representing the strongest predictive variable in each model (Fig. 4.7a-c).

Table 4.2 Percentage of variance in *Kc* explained by DistLM analysis for various combinations of predictor variables.

DistLM analysis (% variance explained)			
Predictors	All Data	Cluster a	Cluster b
Core Env.	22.7	29.2	21.4
Core Env., Chl-*a*	22.7	32.8	21.4
Core Env., Chl-*a*, S/F Chl-*a*	26.3	34.5	27.6
NPQ_{NSV}	55.2	59.6	52.7
$NPQ_{NSV,}$ Core Env.	62.2	61.3	61.5
NPQ_{NSV} , Core Env., Chl-*a*	62.3	75.9	61.5
All	**65.1**	**80.4**	**64.1**
BEST (Fig. 4.7)	65.0	75.4	59.3

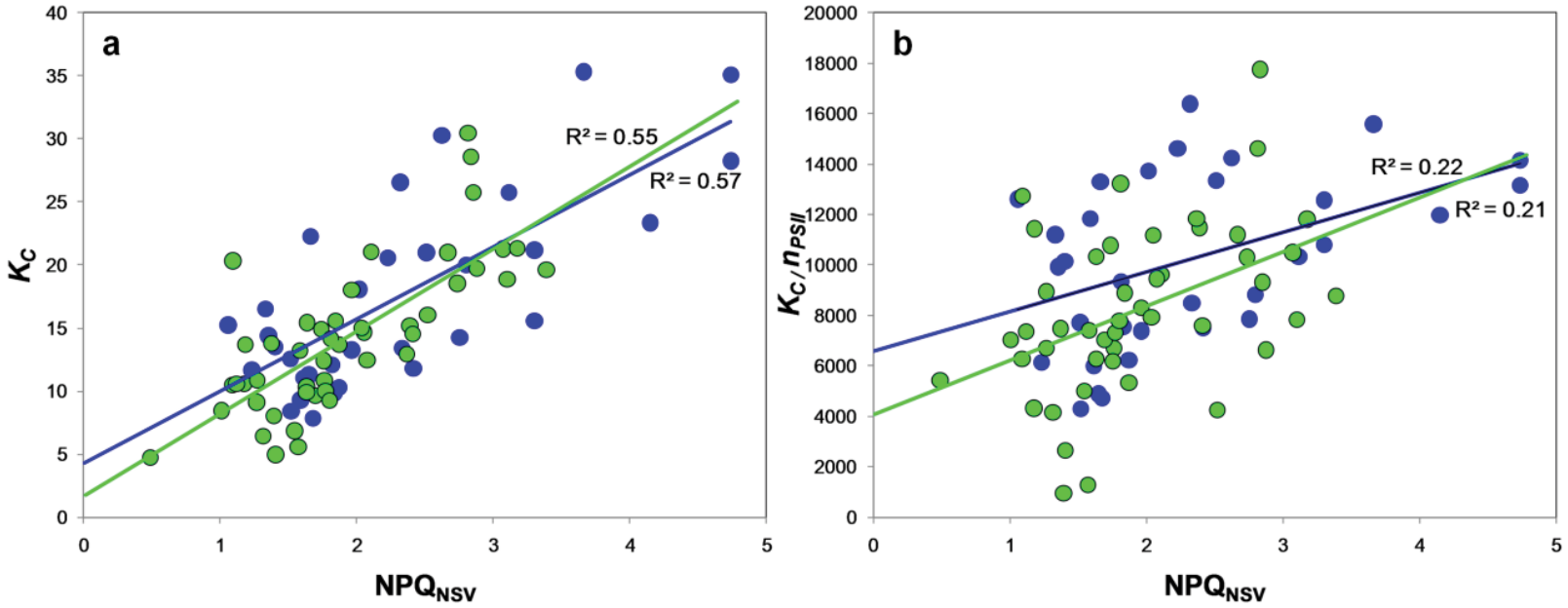

Figure 4.6 Relationship between **a)** the electron requirement for carbon fixation, K_C (mol e^- [mol C]$^{-1}$) and the expression of non-photochemical quenching (NPQ_{NSV}, calculated as per McKew et al. 2013) and **b)** K_C/nPSII against NPQ_{NSV} (i.e. without estimation of Photosynthetic Unit [PSU] size following the approach of Schuback et al. 2015). Data shown corresponds to clusters a and b (blue circles = cluster a; green circles = cluster b) based on physico-chemical variables (see Fig. 4.3, Table 4.1). The generated regression equation for all data combined was y = 6.176x + 2.699, R^2 = 0.58). NPQ_{NSV} reflects an integrated value over a period of 2 hr, at an irradiance approximating the light-saturation parameter (E_K) for each sample.

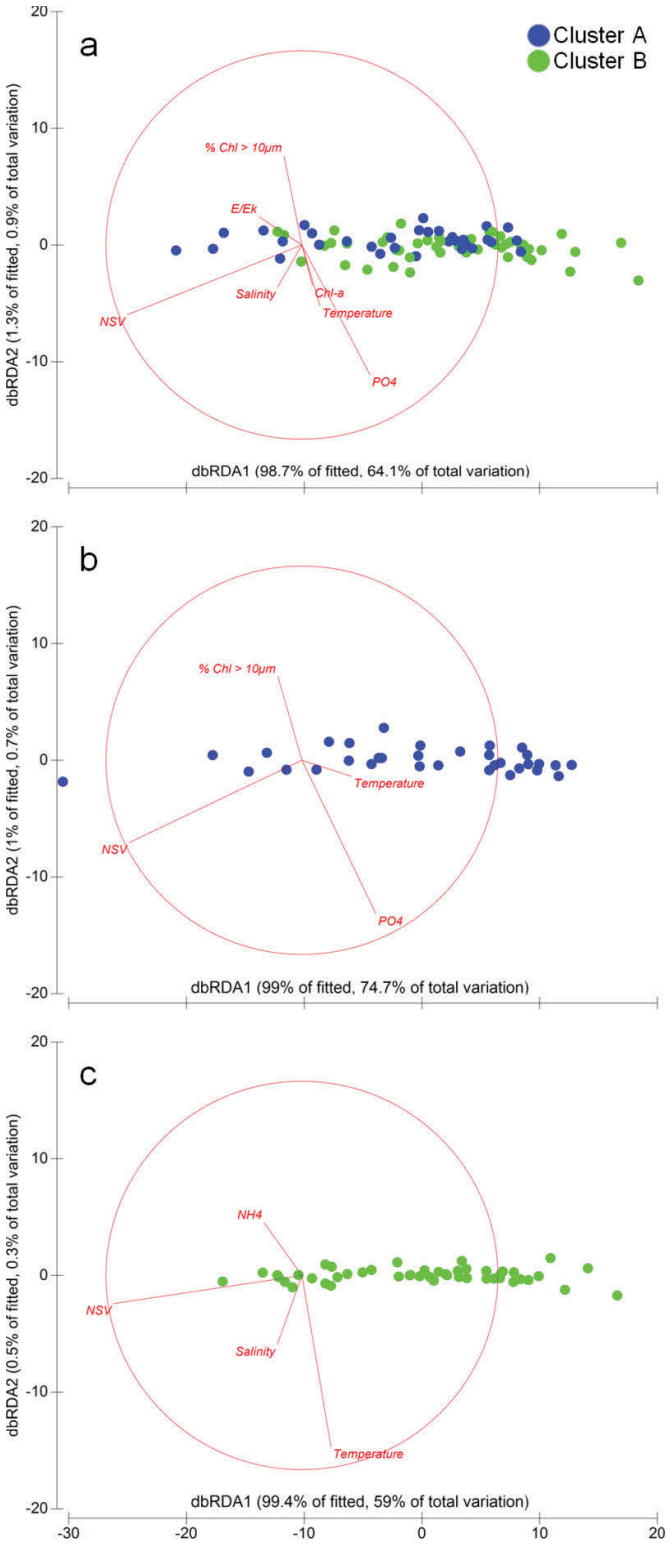

Figure 4.7 Distance-based redundancy analysis (dbRDA) for 2D visualisation of DistLM results explaining variability of the electron requirement for carbon fixation (K_C) from predictive variables (BEST analysis, see Table 4.2) for **a)** all data **b)** data in cluster a and **c)** data in cluster b (see Supplementary Fig. S4.1 for cluster details). Vector lengths and orientation are proportional to their respective contribution to the total variability in K_C.

4.5 Discussion

Field-based campaigns have increasingly demonstrated that variability of K_C (electron requirement for C-fixation) amongst natural phytoplankton communities can be explained by variance in prevailing environmental conditions (e.g. Lawrenz et al. 2013; Zhu et al. 2016, 2017), or more recently photophysiological parameters (NPQ_{NSV}; Schuback et al. 2015) and traits governing resource acquisition (Zhu et al. 2017). In this study, we conclusively demonstrate that NPQ_{NSV} was the better predictor of K_C variability than prevailing environmental conditions across the physically complex Tasman Sea and EAC system investigated using a high-throughput assessment of predominantly surface waters; specifically, NSV_{NPQ} explained ~55% of observed variation across the dataset versus ~25% for the environmental variables measured. The parameter NPQ_{NSV} accounts for changes in both long-term driven acclimation in non-radiative decay as well as quasi-instantaneous PSII downregulation (see McKew et al. 2013), the latter of which is also highly-dependent upon the environmental history of the cells (Dimier et al. 2007; Queval and Foyer, 2012; Giovagnetti et al. 2014). As such, it is perhaps not surprising that NPQ_{NSV} ultimately better predicts K_C since the environmental descriptors we used typically only account for prevailing and not historical environmental conditions. During this study, we attempted to use remotely sensed data (temperature, incident flux and Chl-*a* as a proxy for nutrient availability however this was restricted to certain time bins, and did not allow for K_C retrieval, presumably due to the fact that it did not capture historical conditions well (data not shown). We do, however, acknowledge that our model did not include knowledge of the diffuse attenuation coefficient for downwelling irradiance, K_d(PAR) as a predictor variable, simply due to the fact that the vast majority (>80%) of our data corresponded

to underway sampling, where *in-situ* irradiance measurements were not available. Whether this would have improved predictive retrieval of K_C, if included, is uncertain since this parameter was rarely identified to contribute significantly to empirical models developed by Lawrenz et al. (2013) during their global synthesis of K_C datasets. Nevertheless, light has been shown to be an effective predictor of K_C over longer time scales of C-assimilation (see Zhu et al. 2016, 2017) and hence historical conditions driving acclimation states between phytoplankton communities along complex environmental gradients (Moore et al. 2003, 2006). As such, omission of K_d[PAR] may ultimately have influenced the model outputs based on prevailing environmental conditions in this study.

In the meta-analysis by Lawrenz et al. (2013), the greatest proportion of K_C variance explained by prevailing conditions was ~70%, thus, far higher than was achieved during our study. However, this appeared to be the exception rather than the rule in their study, with some of their models performing far worse, being either not statistically significant, or explaining as little as 3% variability in K_C. In fact, when averaged across all regions, prevailing conditions explained ~25% of K_C variance in their meta-analysis (i.e. very similar to our study). In contrast, recent studies (Schuback et al. 2015, 2016; Hughes et al. subm, Chapter 2) have consistently demonstrated that 50-95% of K_C variance can be explained from knowledge of NPQ_{NSV}, thus collectively supporting our observations here that the parameter NPQ_{NSV} holds promise as a reliable, and consistent predictor of K_C variability in the field. There are however, several caveats to this conclusion which should be highlighted:

Firstly, the calculations reported by Schuback et al. (2015, 2016) conflate variability of K_C and the number of PSII reaction centres (n_{PSII}), whereas the present study inherently

accounts for n_{PSII} variability via calculation of [RCII] by the Oxborough et al. (2012) algorithm. Schuback et al. (2015, 2016) convincingly demonstrate that [RCII] content is unlikely to be contributing to variance in their data through the calculation of a "relative" PSU size, however the same does not hold true for our study (see also Hughes et al. subm, Chapter 2). When n_{PSII} was removed from our calculations (thus K_C / n_{PSII}), the predictive power of NPQ_{NSV} weakened by two-fold for pooled data in this study (R^2 = 0.21, p <0.01; Fig. 4.6b). This likely suggests that estimation of [RCII] is required across a more dynamic system such as the one examined in this study in order to utilise NPQ_{NSV} effectively as a predictor. Secondly, we have shown for unialgal strains grown under steady-state laboratory growth and incubated at growth irradiance that NPQ_{NSV} is not necessarily a reliable predictor of K_C (see Chapter 3). It therefore remains unclear whether this reflects the fact that NPQ_{NSV} is only a good K_C when multiple environmental stressors are at play, or if the relationship between NPQ_{NSV} and K_C breaks down under the influence of a dominant species-specific NPQ signature. Thus, further evaluation of this approach during dynamic conditions, particularly those that drive cells from balanced, to unbalanced, growth conditions is required. Thirdly, and perhaps most importantly, the slopes of the relationships between K_C and NPQ_{NSV} have been shown to differ considerably between studies (Schuback et al. 2015, 2016; Hughes et al. in press., Chapter 2). This phenomenon potentially limits the applicability of NPQ_{NSV} as a viable standalone predictor of K_C at any given space and time, unless we can better understand and predict the slope without use of parallel ^{14}C measurements.

4.5.1 Cell size does not appear to significantly aid retrieval of K_C

Phytoplankton cell size varies by 8 orders of magnitude, and represents a key property in phytoplankton governing a number of physiological characteristics, including photosynthetic performance (Sarthou et al. 2005; Finkel et al. 2009). Indeed, many traits potentially linked with photosynthetic performance such as PSII absorption efficiency, PSII efficiency and nutrient uptake rate have been shown to scale allometrically with cell volume (Ciotti et al. 2002; Suggett et al. 2015; Litchman et al. 2007). Cell volume-normalised photosynthetic rates have consequently been demonstrated to be lower for larger phytoplankton size classes (see Bouman et al. 2005; Barnes et al. 2015) as a result of biophysical constraints upon light absorption and nutrient-uptake, associated with reduced surface-area-to-volume ratios (see Marra et al. 2007). However, whilst trends in K_C were apparent when data were binned according to dominant size fraction, overall, the inclusion of cell size in our analysis did not establish a strong link between K_C and cell size and thus, provided only a slight improvement in retrieval of K_C, consistent with observations of Zhu et al. (2017).

At face value the lack of correspondence between K_C and cell size would suggest that overall, cell size was not a 'catch all' of physiological performance for the phytoplankton communities sampled across our physically-complex transect. This can potentially be interpreted as evidence for phytoplankton cells "breaking" central allometric scaling laws governing physiology (e.g. Suggett et al. 2017, and references therein). For example, swimming speed and sinking rates are minor traits that can be utilised by larger phytoplankton (>10 μm) to distort the boundary layer surrounding the cell, thus overcoming nutrient-uptake limitations imposed by cell size (Karp-Boss et al. 1996). Recent studies have in fact argued that for certain taxonomic groups, non-uniform scaling laws should be applied, which implicitly account for i) physiological

state, ii) taxonomic differences and iii) cell geometry (see Wirtz, 2011). Marine diatoms in particular, as a group, appear particularly good at overcoming biophysical constraints of cell size, and likely comprised a dominant component of phytoplankton communities within coastal samples during this study (see Alexander et al. 2015). Whilst many photophysiological parameters often scale with cell size for diatoms (Key et al. 2010), certain diatom species adopt the strategy of becoming disproportionately large through the use of non-limiting resources, incorporating vast vacuoles into their cell body and thus overcoming uptake and transport limitations (Litchman et al. 2007). Furthermore, pennate diatoms capitalise on cell elongation as a strategy to increase carboxylation capacity relative to photon harvesting, thus escaping uniform scaling laws (Wirtz, 2011). Indeed, this may explain why the slope describing the empirical size scaling of C-specific photosynthetic rates for marine diatoms is often far steeper than theoretical expectations (Finkel, 2001), and perhaps partly explains why we are unable to pick out strong trends for K_C and cell size in the present study. Clearly, without more detailed understanding of the specific taxonomic identity of the samples examined in our study, it is not currently possible to address this hypothesis.

We utilised size-fractionated Chl-*a* as a routinely-measured descriptor of phytoplankton community size structure during this study. Aside from the disadvantage of loss of information regarding species composition, the size-fractionated Chl-*a* method relies on the assumption that Chl-*a* biomass is directly related to primary productivity. However, the reliability of Chl-*a* as a pigment indicator for primary production (i.e. C-fixation) has been questioned (Bassett, 2015). In examining data from 27 studies, Bassett (2015) demonstrated that a strong relationship (defined as an $R^2 > 0.7$) between Chl-*a* biomass and ^{14}C production was evident for just 17% of the data, highlighting that contributions

to different size fractions amongst the Chl-*a* biomass does not necessarily translate to an equivalent proportion of total production, and may be strongly dependent upon physical and biological conditions (see also Pommier et al. 2008).

4.5.2 Using K_C to inform dynamics of the study region

In contrast to previous FRRf-based K_C field studies (e.g. Robinson et al. 2014; Zhu et al. 2017), we did not observe measurements of K_C below the theoretical minimum of 4 mol e^- (mol C)$^{-1}$. We suspect that this is partly due to the fact that methodological contributors were kept to a minimum through i) use of coupled FRRf-^{14}C incubations, ii) application of spectral correction factors, and iii) avoiding using assumed values of n_{PSII} (discussed by Robinson et al. 2009). Previous laboratory FRRf-based K_C studies that have similarly employed a "dual incubation" approach and removed these factors as potential sources of error (Suggett et al. 2009a) measured few values of K_C <4 (<5% of n = 48). The wide range of K_C values measured in our study (~4 - 65 mol e^- [mol C]$^{-1}$) likely reflects the well-documented spatial and temporal complexity of physico-chemical conditions within the study area (Baird et al. 2011; Hassler et al. 2011), and is consistent with data sets that also span broad changes in environmental condition (e.g. Lawrenz et al. 2013; Zhu et al. 2017).

Whilst the broad covariation between K_C and NPQ_{NSV} clearly captures the physically-complex system examined (see also Schuback et al. 2015), initial analysis of the prevailing environmental conditions identified two discrete environmental regimes. Specifically, these were characterised by warmer, low-nutrient water dominated by small cells versus cooler, nutrient-rich waters dominated by larger cells: our clusters a, and b. In turn, these were characterised by communities exhibiting a higher K_C in the nutrient-poor, small cell-dominated cluster a, thus appearing to support broader

observations of taxonomy with K_C (Robinson et al. 2014; Zhu et al. 2017). This is also consistent with the oceanography of the region, whereby the EAC is warm, low in nutrients and dominated by smaller cells (Hassler et al. 2011), whilst the Tasman Sea water mass is characterised by lower temperatures, higher nutrient availability, and a phytoplankton community often dominated by larger cells (Baird et al. 2008). Such an outcome is entirely consistent with previous work that has binned data into water masses (Lawrenz et al. 2013; Robinson et al. 2014) or environmental regime (Zhu et al. 2017); however, it also consistent with these various studies that environmental condition alone provides poor predictive retrieval of K_C (mean R^2 = ~25%). Thus, K_C appears to follow broad oceanographic trends with the prevailing environmental conditions measured, but ultimately requires a physiological descriptor of both prevailing (short-term dynamic physiological regulation) and historical conditions that drive acclimation states, such as NPQ_{NSV}. This presumably explains why cell size alone may also fail to provide a robust descriptor of K_C (Zhu et al. 2017; see also Chapter 3).

4.6 Conclusions

Using a unique high-throughput "dual incubation" FRRf approach to retrieve values of K_C, we have demonstrated co-variance between K_C and independently-measured environmental variables (notably temperature, salinity and PO_4^-), and to a greater extent physiologically-dependent variables (NPQ_{NSV}). The latter outcome suggests that for our dataset, a modification of Eq. 3 with the calculation of NPQ_{NSV} ($F_0'=F_v'$) (McKew et al. 2013) adjusted for the specific relationship describing the dependency between K_C and NPQ_{NSV} (Fig. 4.6) could redefine the FRRf algorithm to retrieve C-fixation rates within this study region however this clearly warrants further validation. A logical next step would therefore be the retrospective application of NPQ_{NSV} measurements to historic

FRRf – C-uptake data campaigns (e.g. those collated by Lawrenz et al. 2013) to allow additional comparison between the respective performance of NPQ_{NSV} and prevailing conditions in predicting K_C variability across a complex range of oceanic environments. Such a step is critically needed to permit further examination of the apparent discrepancy in the slopes of the relationship between K_C and NPQ_{NSV} (see Schuback et al. 2015; Hughes et al. in press., Chapter 2) and hence 'global' applicability of this approach through autonomous FRRf deployments.

4.7 References

Alexander, H., M. Rouco, S. T. Haley, S. T. Wilson, D. M. Karl, and S. T. Dyhrman. 2015. Functional group-specific traits drive phytoplankton dynamics in the oligotrophic ocean. Proc. Natl. Acad. Sci. U. S. A. 112(44): E5972-E5979.

Anderson, M., R. N. Gorley, and R. K. Clarke. 2008. Permanova+ for Primer: Guide to Software and Statistical Methods. Primer-E Limited.

Babin, S., J. Carton, T. Dickey, and J. Wiggert. 2004. Satellite evidence of hurricane-induced phytoplankton blooms in an oceanic desert. J. Geophys. Res.: Oceans 109, C03043.

Baird, M. E., J. D. Everett, and I. M. Suthers. 2011. Analysis of southeast Australian zooplankton observations of 1938–42 using synoptic oceanographic conditions. Deep Sea Res., Part II. 58(5): 699-711.

Baird, M. E., P. G. Timko, J. H. Middleton, T. J. Mullaney, D. R. Cox, and I. M. Suthers. 2008. Biological properties across the Tasman Front off southeast Australia. Deep Sea Res., Part I. 55(11)**:** 1438-1455.

Barnes, M. K., G. H. Tilstone, T. J. Smyth, C. E. Widdicombe, J. Gloël, C. Robinson, J. Kaiser, and D. J. Suggett. 2015. Drivers and effects of *Karenia mikimotoi* blooms in the western English Channel. Prog. Oceanogr. 137: 456-469.

Bassett, L. A. 2015. Size-fractionated relationships between phytoplankton production and biomass. Ph.D. thesis. Univ of South Carolina.

Bouman, H., T. Platt, S. Sathyendranath, and V. Stuart. 2005. Dependence of light-saturated photosynthesis on temperature and community structure. Deep Sea Res., Part I. 52(7): 1284-1299.

Brading, P., M. E. Warner, D. J. Smith, and D. J. Suggett. 2013. Contrasting modes of inorganic carbon acquisition amongst *Symbiodinium* (Dinophyceae) phylotypes. New Phytol. 200(2): 432-442.

Ciotti, A. M., M. R. Lewis, and J. J. Cullen. 2002. Assessment of the relationships between dominant cell size in natural phytoplankton communities and the spectral shape of the absorption coefficient. Limnol. Oceanogr. 47(2): 404-417.

Cullen, J. J., and R. F. Davis. 2003. The blank can make a big difference in oceanographic measurements. Limnol. Oceanogr. Bulletin 12(2): 29-35.

Dimier, C., F. Corato, F. Tramontano, and C. Brunet. 2007. Photoprotection and xanthophyll-cycle activity in three marine diatoms. J. Phycol. 43(5): 937-947.

Edwards, K. F., M. K. Thomas, C. A. Klausmeier, and E. Litchman. 2012. Allometric scaling and taxonomic variation in nutrient utilization traits and maximum growth rate of phytoplankton. Limnol. Oceanogr. 57(2): 554-566.

Finkel, Z. V. 2001. Light absorption and size scaling of light-limited metabolism in marine diatoms. Limnol. Oceanogr. 46(1): 86-94.

Finkel, Z. V., J. Beardall, K. J. Flynn, A. Quigg, T. a. V. Rees, and J. A. Raven. 2009. Phytoplankton in a changing world: cell size and elemental stoichiometry. J. Plankton Res. 32(1): 119-137.

Fisher, N. L., and K. H. Halsey. 2016. Mechanisms that increase the growth efficiency of diatoms in low light. Photosynth. Res. 129(2): 183-197.

Giovagnetti, V., S. Flori, F. Tramontano, J. Lavaud, and C. Brunet. 2014. The velocity of light intensity increase modulates the photoprotective response in coastal diatoms. PloS One 9(8): e103782.

Halsey, K. H., and B. M. Jones. 2015. Phytoplankton strategies for photosynthetic energy allocation. Annu. Rev. Mar. Sci. 7: 265-297.

Halsey, K. H., A. J. Milligan, and M. J. Behrenfeld. 2011. Linking time-dependent carbon-fixation efficiencies in *Dunaliella tertiolecta* (chlorophyceae) to underlying metabolic pathways. J. Phycol. 47(1): 66-76.

Hancke, K., T. Dalsgaard, M. K. Sejr, S. Markager, and R. N. Glud. 2015. Phytoplankton productivity in an Arctic Fjord (West Greenland): estimating electron requirements for carbon fixation and oxygen production. PloS One 10(7): e0133275.

Hassler, C., J. Djajadikarta, M. Doblin, J. Everett, and P. Thompson. 2011. Characterisation of water masses and phytoplankton nutrient limitation in the East Australian Current separation zone during spring 2008. Deep Sea Res., Part II. 58(5): 664-677.

Hippmann, A. A., N. Schuback, K.-M. Moon, J. P. Mccrow, A. E. Allen, L. J. Foster, B. R. Green, and M. T. Maldonado. 2017. Contrasting effects of copper limitation on the photosynthetic apparatus in two strains of the open ocean diatom *Thalassiosira oceanica*. PloS One 12(8): e0181753.

Hoppe, C. J. M., L.-M. Holtz, S. Trimborn, and B. Rost. 2015. Ocean acidification decreases the light-use efficiency in an Antarctic diatom under dynamic but not constant light. New Phytol. 207(1): 159-171.

Hughes, D.J., Varkey, D., Doblin, M.A., Ingleton, T., Mcinnes, A., Ralph, P.J., van Dongen-Vogels, V and D.J Suggett. 2018. Impact of nitrogen availability upon the electron requirement for carbon fixation in Australian coastal phytoplankton communities (In Press). Limnol. Oceanogr. DOI: 10.1002/lno.10814

Karp-Boss, L., E. Boss, and P. Jumars. 1996. Nutrient fluxes to planktonic osmotrophs in the presence of fluid motion. Oceanogr. Mar. Biol. 34: 71-108.

Key, T., A. Mccarthy, D. A. Campbell, C. Six, S. Roy, and Z. V. Finkel. 2010. Cell size trade-offs govern light exploitation strategies in marine phytoplankton. Environ. Microbiol. 12(1): 95-104.

Knap, A., A. Michaels, A. Close, H. Ducklow, and A. Dickson. 1996. Protocols for the Joint Global Ocean Flux Study (JGOFS) core measurements.

Kolber, Z., and P. G. Falkowski. 1993. Use of active fluorescence to estimate phytoplankton photosynthesis *in situ*. Limnol. Oceanogr. 38(8): 1646-1665.

Kolber, Z. S., O. Prášil, and P. G. Falkowski. 1998. Measurements of variable chlorophyll fluorescence using fast repetition rate techniques: defining methodology and experimental protocols. Biochim. Biophys. Acta, Bioenerg. 1367(1–3): 88-106.

Kramer, D. M., G. Johnson, O. Kiirats, and G. E. Edwards. 2004. New fluorescence parameters for the determination of Q_A redox state and excitation energy fluxes. Photosynth. Res. 79(2): 209-218.

Lawrenz, E. and others. 2013. Predicting the electron requirement for carbon fixation in seas and oceans. PLoS One 8(3): e58137.

Lee, Z., J. Marra, M. J. Perry, and M. Kahru. 2015. Estimating oceanic primary productivity from ocean color remote sensing: A strategic assessment. J. Mar. Syst. 149: 50-59.

Lewis, M. R., and J. C. Smith. 1983. A small volume, short-incubation-time method for measurement of photosynthesis as a function of incident irradiance. Mar. Ecol.: Prog. Ser. 13: 99-102.

Litchman, E., C. A. Klausmeier, O. M. Schofield, and P. G. Falkowski. 2007. The role of functional traits and trade-offs in structuring phytoplankton communities: scaling from cellular to ecosystem level. Ecol. Lett. 10(12): 1170-1181.

Marra, J., C. C. Trees, and J. E. O'reilly. 2007. Phytoplankton pigment absorption: a strong predictor of primary productivity in the surface ocean. Deep Sea Res., Part I. 54(2): 155-163.

Mckew, B. A. and others. 2013. The trade-off between the light-harvesting and photoprotective functions of fucoxanthin-chlorophyll proteins dominates light acclimation in *Emiliania huxleyi* (clone CCMP 1516). New Phytol. 200(1): 74-85.

Moore, C. M. and others. 2003. Physical controls on phytoplankton physiology and production at a shelf sea front: a fast repetition-rate fluorometer based field study. Mar. Ecol.: Prog. Ser. 259: 29-45.

Moore, C. M., D. J. Suggett, A. E. Hickman, Y.-N. Kim, J. F. Tweddle, J. Sharples, R. J. Geider, and P. M. Holligan. 2006. Phytoplankton photoacclimation and photoadaptation in response to environmental gradients in a shelf sea. Limnol. Oceanogr. 51(2): 936-949.

Murphy, C. D. and others. 2017. Quantitating active Photosystem II reaction center content from fluorescence induction transients. Limnol. Oceanogr.: Methods 15(1): 54-69.

Napoleon, C., V. Raimbault, and P. Claquin. 2013. Influence of nutrient stress on the relationships between PAM measurements and carbon incorporation in four phytoplankton species. PLoS One 8(6): e66423.

Nawrocki, W. J., N. J. Tourasse, A. Taly, F. Rappaport, and F.-A. Wollman. 2015. The plastid terminal oxidase: its elusive function points to multiple contributions to plastid physiology. Annu. Rev. Plant Biol. 66: 49-74.

Oke, P. R., and J. H. Middleton. 2001. Nutrient enrichment off Port Stephens: the role of the East Australian Current. Cont. Shelf Res. 21(6): 587-606.

Oxborough, K., C. M. Moore, D. J. Suggett, T. Lawson, H. G. Chan, and R. J. Geider. 2012. Direct estimation of functional PSII reaction center concentration and PSII electron flux on a volume basis: a new approach to the analysis of Fast

Repetition Rate fluorometry (FRRf) data. Limnol. Oceanogr.: Methods 10(3): 142-154.

Platt, T., C. Gallegos, and W. Harrison. 1980. Photoinhibition of photosynthesis in natural assemblages of marine phytoplankton. J. Mar. Res. 38: 103-111.

Pommier, J., M. Gosselin, and C. Michel. 2008. Size-fractionated phytoplankton production and biomass during the decline of the northwest Atlantic spring bloom. J. Plankton Res. 31(4): 429-446.

Queval, G., and C. H. Foyer. 2012. Redox regulation of photosynthetic gene expression. Philos. Trans. R. Soc., B 367(1608): 3475-3485.

Ralph, P. J., and R. Gademann. 2005. Rapid light curves: a powerful tool to assess photosynthetic activity. Aquat. Bot. 82(3): 222-237.

Robinson, C., D. J. Suggett, N. Cherukuru, P. J. Ralph, and M. A. Doblin. 2014. Performance of Fast Repetition Rate fluorometry based estimates of primary productivity in coastal waters. J. Mar. Syst. 139: 299-310.

Robinson, C. and others. 2009. Comparison of in vitro and *in situ* plankton production determinations. Aquat. Microb. Ecol. 54(1): 13-34.

Sakshaug, E. and others. 1997. Parameters of photosynthesis: definitions, theory and interpretation of results. J. Plankton Res. 19(11): 1637-1670.

Sarthou, G., K. R. Timmermans, S. Blain, and P. Tréguer. 2005. Growth physiology and fate of diatoms in the ocean: a review. J. Sea Res. 53(1): 25-42.

Schuback, N., M. Flecken, M. T. Maldonado, and P. D. Tortell. 2016. Diurnal variation in the coupling of photosynthetic electron transport and carbon fixation in iron-limited phytoplankton in the NE subarctic Pacific. Biogeosciences 13(4): 1019-1035.

Schuback, N., C. J. Hoppe, J. É. Tremblay, M. T. Maldonado, and P. D. Tortell. 2017. Primary productivity and the coupling of photosynthetic electron transport and carbon fixation in the Arctic Ocean. Limnol. Oceanogr. 62: 898-921.

Schuback, N., C. Schallenberg, C. Duckham, M. T. Maldonado, and P. D. Tortell. 2015. Interacting effects of light and iron availability on the coupling of photosynthetic electron transport and CO_2-assimilation in marine phytoplankton. PLoS One 10(7): e0133235.

Suggett, D. J., S. Goyen, C. Evenhuis, M. Szabó, D. T. Pettay, M. E. Warner, and P. J. Ralph. 2015. Functional diversity of photobiological traits within the genus *Symbiodinium* appears to be governed by the interaction of cell size with cladal designation. New Phytol. 208(2): 370-381.

Suggett, D. J., S. C. Maberly, and R. J. Geider. 2006. Gross photosynthesis and lake community metabolism during the spring phytoplankton bloom. Limnol. Oceanogr. 51(5): 2064-2076.

Suggett, D. J., H. L. Macintyre, T. M. Kana, and R. J. Geider. 2009. Comparing electron transport with gas exchange: parameterising exchange rates between alternative photosynthetic currencies for eukaryotic phytoplankton. Aquat. Microb. Ecol. 56(2-3): 147-162.

Suggett, D. J., C. M. Moore, A. E. Hickman, and R. J. Geider. 2009. Interpretation of fast repetition rate (FRR) fluorescence: signatures of phytoplankton community structure versus physiological state. Mar. Ecol.: Prog. Ser. 376: 1-19.

Suggett, D. J., M. E. Warner, and W. Leggat. 2017. Symbiotic dinoflagellate functional diversity mediates coral survival under ecological crisis. Trends Ecol. Evol. 32(10): 735-745.

Wirtz, K. W. 2011. Non-uniform scaling in phytoplankton growth rate due to intracellular light and CO_2 decline. J. Plankton Res. 33(9): 1325-1341.

Wu, Y., J. Jeans, D. J. Suggett, Z. V. Finkel, and D. A. Campbell. 2014. Large centric diatoms allocate more cellular nitrogen to photosynthesis to counter slower RUBISCO turnover rates. Front Mar. Sci. 1: 68.

Zhu, Y., J. Ishizaka, S. C. Tripathy, S. Wang, Y. Mino, T. Matsuno, and D. J. Suggett. 2016. Variation of the photosynthetic electron transfer rate and electron

requirement for daily net carbon fixation in Ariake Bay, Japan. J. Oceanogr. 72(5): 761-776.

Zhu, Y., J. Ishizaka, S. C. Tripathy, S. Wang, C. Sukigara, J. Goes, T. Matsuno, and D. J. Suggett. 2017. Relationship between light, community composition, and the electron requirement for carbon fixation in natural phytoplankton assemblages of the East China Sea. Mar. Ecol.: Prog. Ser. doi.org/10.3354/meps1231

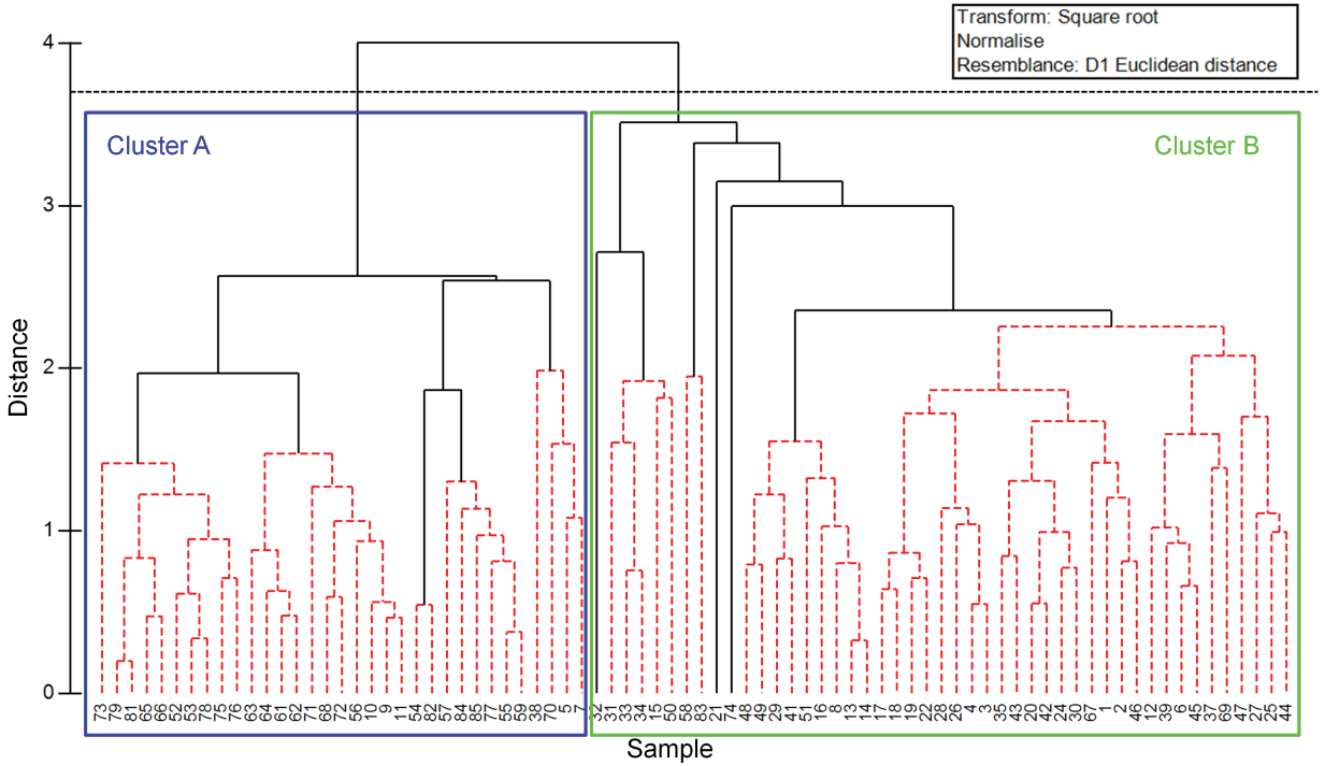

Supplementary Figure S4.1 Hierarchical cluster analysis (HCA) of samples (n = 80) based upon physico-chemical variables (temperature, salinity, NH_4^+, NO_x^-, PO_4^{3-} and Si). HCA identified two distinct hydrographic clusters, a and b (highlighted by blue and green sections respectively).

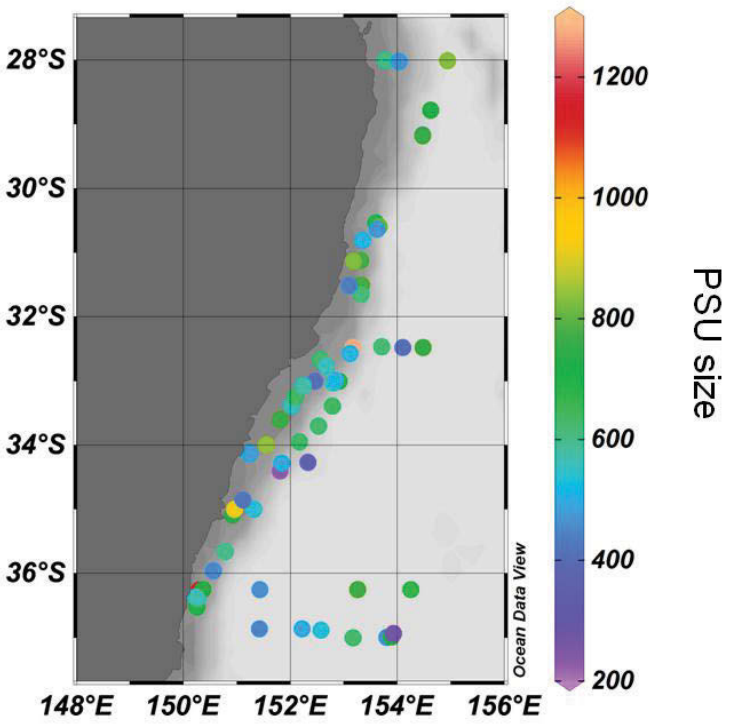

Supplementary Figure S4.2 Photosynthetic unit (PSU) size surface water sampled in coastal, East Australian Current (EAC) and Tasman Sea water masses measured from the RV *Investigator* (August – September 2016, IN2016_v04).

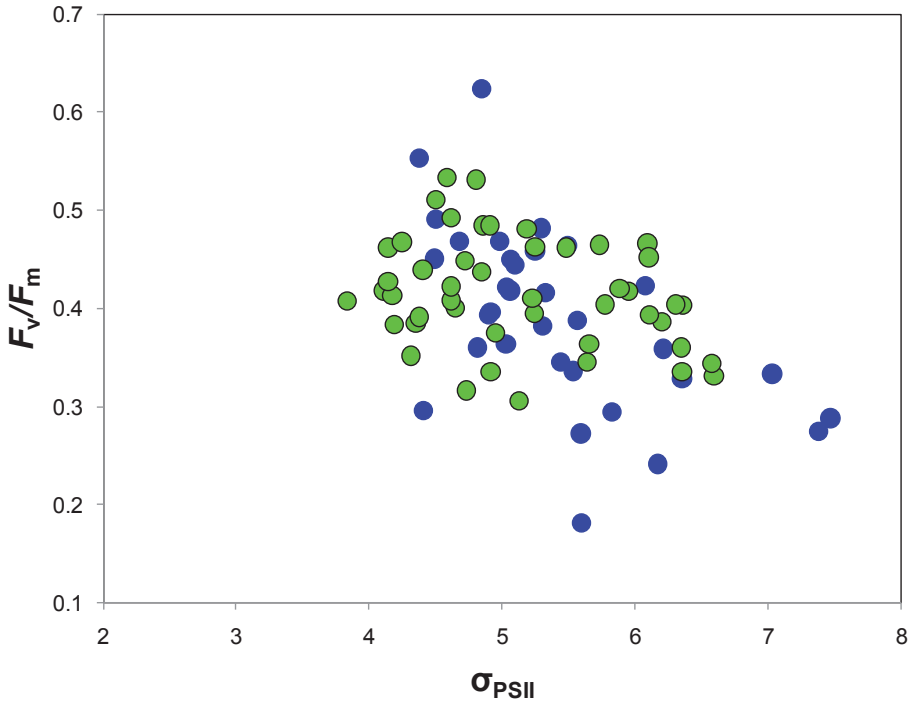

Supplementary Figure S4.3 Fast Repetition Rate fluorometry (FRRf) measurements of PSII maximum photochemical efficiency (F_v/F_m , dimensionless) and the functional absorption cross-section of PSII (σ_{PSII}, nm^2 $quanta^{-1}$) using the blue excitation LED (450 nm) for all samples examined during this study. Values shown represent single measurements from dark-acclimated samples (15 min) prior to measurement of the electron requirement for carbon fixation (K_C).

5 Chapter 5:

General discussion

Healthy functioning of Australia's coasts and oceans is to a large extent dependent upon marine primary production (MPP) – the majority of which is performed by unicellular, photosynthetic phytoplankton. Thus, the ability to accurately measure and predict *in-situ* photosynthetic rates by phytoplankton underpins our ability to effectively monitor and evaluate marine ecosystem health under the effects of global climate change. Central to these efforts is the move away from conventional, incubation-dependent measures of photosynthesis, towards the use of bio-optical tools including Fast Repetition Rate fluorometry (FRRf) to improve satellite-based models for monitoring and predicting future MPP.

Within this thesis I have directly addressed key knowledge gaps in understanding how the "electron requirement for carbon fixation" ($\boldsymbol{K_C}$), the fundamental parameter needed to scale FRRf-based measurements of electron transfer rate through PSII (ETR_{PSII}) to ecologically-meaningful rates of C-fixation, varies over space and time. I presented novel data to improve our knowledge of how K_C is regulated by the environment, specifically macronutrient (N, P and Si) availability, and examine how changes in phytoplankton community composition (i.e. taxonomy) may act in concert with physiological responses to explain variability in K_C. This combination of both laboratory and field studies, provided new insight into the respective roles of both environment and taxonomy and explored how this information can be used to empirically predict K_C within Australian waters. The key findings and implications for this research are briefly discussed in the following sections, and then synthesised within

future research directions as an opinion paper titled "**FRRf Roadmaps and Detours**: Active chlorophyll-*a* assessments of primary productivity across marine and freshwater systems" currently in final draft for submission.

Nitrogen (N) availability is known to be a key regulator of phytoplankton photosynthetic performance (and thus MPP) and phytoplankton community composition across coasts and oceans globally, yet the effects of N-availability upon K_C has never before been experimentally evaluated. This lack of knowledge partly stems from the fact that it is virtually impossible to isolate the effect of any one individual environmental variable when examining natural phytoplankton communities in the field. Furthermore, due to the fact that N regulates photosynthesis at the cellular level, and community structure at the ecosystem level, it remains unclear whether regulation of K_C operates through physiological versus taxonomic adjustment, or both.

The nutrient bioassay approach employed in **Chapter 2** demonstrated that N (and to a lesser degree P and Si) availability was a strong driver of K_C variability, with nutrient-addition lowering K_C, often to values close to the theoretical minimum. This response was achieved through a combination of photophysiological and/or taxonomic responses to N-amendment, depending on whether waters were sampled under nutrient limited conditions (typical for the time of year) or post transient bloom (nutrient-starved). Ultimately, both responses resulted in diatom-dominated assemblages as the community end-point. These experiments also highlighted a strong relationship between K_C and the extent of non-photochemical quenching (NPQ_{NSV}), thus adding to recent observations that had previously only considered this relationship under iron-limited conditions. The findings of Chapter 2 therefore not only allows for better parameterisation of K_C in coasts/oceans where N-availability may be highly-variable, but provided the first insight into how N-availability may regulate the bulk conversion of electrons into carbon

biomass. Alleviation from N-limitation was shown to significantly affect measured K_C via alleviation of photosynthetic stress, changes in community structure to favour taxa more efficient at converting electrons into carbon biomass (i.e. diatoms), or by increasing the lifetime of newly-fixed C products, thus resulting in an *apparent* reduction of K_C.

Field studies seeking to examine variability in K_C in natural phytoplankton communities have alluded to the role of taxonomy in regulating K_C. For example, Chapter 2 similarly demonstrated strong changes in K_C for water samples dominated by diatoms versus dinoflagellates. However, interpretation of K_C variance in the field is confounded by the myriad of environmental stressors present, together with the complications of interpreting a definitive taxonomic signature from a mixed assemblage. To date, few studies have measured K_C for phytoplankton strains grown under controlled laboratory conditions, and it remains unclear whether taxonomic influence upon K_C arises from higher-taxonomic differences between major classes of phytoplankton taxa, or from variation in key traits such as cell-size or growth rates.

Examination of 17 phytoplankton strains spanning multiple taxonomic and size-classes in **Chapter 3** addressed this data gap for the first time, providing evidence that diatoms generally appear to exhibit the lowest K_C values. These trends were further reinforced as part of an extended meta-analysis that integrated these data within existing literature reported values. Furthermore, across the entire data set, I observed a strong inverse correlation between growth rate and K_C. Whilst this data set yielded no significant relationships between K_C and taxonomic level (e.g. class), variation in cell size co-varied with variation in K_C. Knowledge of cell size (through size-fractionated Chl-*a*) was also shown to marginally improve predictive modelling of K_C (Chapter 4) from natural phytoplankton communities thus further demonstrating a role for cell size in the

regulation of K_C across taxa. Ultimately, these findings contribute to our understanding of how changes in phytoplankton taxonomic structure lead to changes in K_C, and thus a means to improve empirical models of K_C variability for natural phytoplankton assemblages.

Evidence for only a subtle role of phytoplankton taxonomy regulating K_C (Chapters 2 and 3) led to a further focus on taxonomic-independent measures of physiology, and specifically cell size and the non-photochemical quenching term NPQ_{NSV}. In **Chapter 4** I collected a unique data set to examine K_C variance in eastern Australian waters, and confirmed past findings (Lawrenz et al. 2013) that changes in environmental factors explain a relatively small proportion of K_C variance. However, these data, along with those in Chapter 2, enabled broad scale evaluation for a relationship between NPQ_{NSV} and K_C, which to date has only been considered in iron-limited waters (Schuback et al. 2015, 2016). Multivariate analysis of K_C variance (Chapter 4) indicated that this photophysiological parameter may indeed be a far better predictor of K_C variability than prevailing environmental conditions or phytoplankton taxonomic identity. This exciting outcome potentially paves the way for the construction of a modified equation to derive ETR_{PSII}, inherently accounting for the dependency between K_C and NPQ_{NSV} to allow for retrieval of C-fixation rates along the dynamic eastern Australian coast.

5.1 Future research perspectives

Inevitably, in addition to addressing knowledge gaps in FRRf-based research, this thesis has also raised several new questions, together with a number of historical issues which remain unaddressed despite two decades of research. Thus, to synthesise novel proposals to FRRf research arising directly from my thesis outcomes, together with historical proposals, I present **Chapter 6** as the final draft of an opinion paper "FRRf

Roadmaps and Detours: Active chlorophyll-*a* assessments of primary productivity across marine and freshwater systems":

6 Chapter 6:

Roadmaps and Detours: Active chlorophyll-*a* assessments of primary productivity across marine and freshwater systems

David J. Hughes[1], Douglas A. Campbell[2], Martina A. Doblin[1], Jacco C. Kromkamp[3,4], Evelyn Lawrenz[5], C. Mark Moore[6], Ondřej Prášil[5], Peter J. Ralph[1], Marco F. Alvarez[1], and David J. Suggett[1*]

[1] Climate Change Cluster, University of Technology Sydney, Broadway 2007, NSW, Australia

[2] Biology, Mount Allison University, Sackville, NB, Canada

[3] NIOZ Royal Netherlands Institute for Sea Research, Department of Estuarine and Delta Systems, and [4]Utrecht University, P.O. Box 140, 4401 NT Yerseke, the Netherlands

[5] Centre Algatech, Institute of Microbiology, Czech Academy of Sciences, Třeboň 379 81, Czech Republic

[6] Ocean and Earth Science, University of Southampton, National Oceanography Centre, Southampton, European Way, Southampton SO14 3ZH, UK

*Corresponding author: David.Suggett@uts.edu.au

6.1 Abstract

Assessing patterns of phytoplankton primary productivity over space and time has remained a key goal for oceanographers and limnologists for two centuries. The introduction of active chlorophyll-*a* based fluorometers several decades ago provided a potential means to realise this goal with unprecedented spatiotemporal resolution and scale. Wide adoption of one particular technique, Fast Repetition Rate fluorometry (FRRf), is particularly evident over the past 20 years, but has yet to live up to expectations as the go-to measurement of productivity. A major obstacle to broader scale implementation has been the conversion of FRRf-based photosynthesis, measured as rates of electron turnover, rates of CO_2-uptake that carry most relevance in studies of biogeochemical C fluxes. This key conversion suffers from methodological inconsistencies but also from our limited understanding of how the electron requirement for carbon fixation, (K_C) is influenced by both the environment, and by differences across phytoplankton groups. In this review and operational prospectus, we therefore design a "roadmap" to limit methodological bias associated with measurements of K_C, but also to develop a mechanistic understanding of the ecophysiology underlying this conversion factor. We re-evaluate core physiological processes governing how microalgae invest electron-derived energy and reductant into cellular-retained carbon versus alternative sinks. We propose a series of steps to facilitate the broader uptake and exploitation of FRRf, which could transform our knowledge of aquatic primary productivity. In so doing, we argue that it is time to revise our historic methodological focus on carbon as *the* currency of aquatic primary productivity, to better appreciate that electrons fundamentally drive ecosystem biogeochemistry, modulate cell-to-cell interactions, and ultimately modify community biomass and structure.

6.2 Introduction

Numerous active chlorophyll-*a* fluorescence techniques and instruments now exist to assay the physiological status and productivity of aquatic phototrophs, notably Pulse Amplitude Modulated fluorometry (PAM, Schreiber et al. 1986) and recently, PicoF Lifetime Fluorometry (Lin et al. 2016). However, Fast Repetition Rate fluorometry (FRRf; Kolber et al. 1998) and its variant, Flash Induction and Relaxation fluorometry (FIRe, Gorbunov and Falkowski, 2004), remains the approach most commonly used to assess natural phytoplankton communities (Suggett et al. 2003, 2009; Oxborough et al. 2012), in part because of its flexible operational biomass threshold, which enables sampling from oligotrophic "blue" waters of very low biomass to coastal waters and eutrophic lakes where chlorophyll-*a* (Chl-*a*) concentrations can be several orders of magnitude higher (Laney, 2003; Kromkamp and Forster, 2003; Suggett et al. 2006).

Fast Repetition Rate fluorometry (FRRf, Kolber et al. 1998) was introduced two decades ago, following the earlier Pump and Probe (Falkowski et al. 1986) fluorometer, as a bio-optical tool to quantify aquatic primary productivity (PP). The novel capability to non-invasively probe photosynthetic rates *in-situ* within seconds, freed investigators from long-standing constraints associated with conventional bottle incubations (Kolber and Falkowski, 1993; Falkowski and Kolber, 1995), and thus offered a means to transform global efforts examining the nature and variability of aquatic PP. Indeed, FRRf technology has since been developed for a range of applications, from single microalgal cells (Gorbunov et al. 1999) to corals and macrophytes (Gorbunov et al. 2001), as well as being deployed across all major oceans via research vessels and ships of opportunity to assess phytoplankton productivity (Suggett et al. 2001; Smyth et al. 2004; Fujiki et al. 2008).

Initial adoption of the technology was rapid, with publications based upon FRRf data becoming commonplace post-1998; however, most studies have used FRRf to analyse phytoplankton physiology and community structure (e.g. Behrenfeld and Kolber, 1999; Suggett et al. 2009b), rather than to derive PP *per se* (see Lawrenz et al. 2013). Regional-global scale aquatic PP estimates still contain large uncertainties, due to problems with both measurement techniques, and chronic under-sampling. Ultimately, these deficiencies limit the amount and reliability of discrete photosynthetic rate datasets, which today underpin our best current regional-global scale estimates of aquatic PP through (semi-) empirically calibrated algorithms applied to satellite-based ocean colour observations (Chavez et al. 2011; Moore et al. 2003; Saba et al. 2011). So, with FRRf instrumentation (and datasets) more accessible than ever: why has FRRf not become the ′go-to tool′ to fill this data void?

Evolution of FRRf-based research followed a path common to emergent technologies; initial widespread enthusiasm that has, over time, yielded to a pragmatic realisation of inherent uncertainties and constraints associated with both concept and application; which together, frequently undermined the interpretation and reconciliation of the datasets generated. Progress was effectively hampered by ever shifting focus from the power of the technique to understand photosynthesis, towards the limitations involved in attempting to quantify photosynthesis. For FRRf, a recurrent obstacle for estimating PP has been the "currency" in which FRRf quantifies rates of photosynthesis (Kromkamp et al. 2008; Suggett et al. 2009a).

Carbon is the most common photosynthetic "currency" used in studies of biogeochemical cycling. FRRf does not directly measure carbon-fixation, but instead quantifies gross photosynthesis as an electron transport rate (ETR_{PSII}) through photosystem II (PSII) (see Section 6.2) (Kolber and Falkowksi, 1993; Suggett et al.

2003; Oxborough et al. 2012). Fixed carbon is a fundamental currency representing energy and reductant exchange between ecosystem components, and clearly carries broad importance within the Earth system. However, generation of electrons and how they are used to synthesise energy can be considered as more fundamental drivers of biological metabolism and associated biogeochemical cycles (Grossman et al. 2010). From such a perspective, our focus upon the carbon currency, which partly stems from foundational studies using ^{14}C to measure carbon uptake in phytoplankton and plant leaves, somewhat obscures the key roles of photosynthetic reductant in driving single-cell N and S assimilation (Halsey and Jones, 2015; Wagner et al. 2017), reductive biosynthesis of macromolecules such as lipids (Finkel et al. 2016), and the generation of reactive oxygen species (ROS) that modulate cell-cell interactions and community structures (Morris et al. 2011). Yet, despite such key roles for electrons, energy and/or reductant as standalone currencies, the inference of C fluxes from FRRf type measurements remains an important goal.

The viability of FRRf for improved global PP estimates based upon C hinges on our ability to robustly convert from an ETR_{PSII} to a rate of carbon-fixed using a photosynthetic exchange rate, the electron requirement for carbon fixation, termed K_C (e.g. Suggett et al. 2009a; Lawrenz et al. 2013; Hancke et al. 2015). However, K_C may vary considerably due to physiological and taxonomic changes which are driven by external factors (see Section 6.5). Whilst recent efforts have attempted to empirically model K_C variation over space and time (Lawrenz et al. 2013; Schuback et al. 2015) with varying degrees of success, we continue to lack an integrated understanding of the mechanisms that regulate this conversion factor, thus much of the observed variability remains unexplained and prediction of accurate values problematic.

Despite persistent uncertainties in how ETR_{PSII} measurements can be scaled to carbon uptake rates, oceanographers and limnologists continue to widely incorporate FRRf-based techniques into biogeochemical and eco-physiological studies. The relative ease of semi-continuous data acquisition across immense temporal and spatial scales yields a vast quantity of data that offers unprecedented insight into taxonomic patterns (Raateoja et al. 2004; Suggett et al. 2009b; Robinson et al. 2014), physiological processes (Behrenfeld and Kolber, 1999; Behrenfeld et al. 2006; Moore et al. 2006; Ryan-Keogh et al. 2013; Royer et al. 2015) and phytoplankton abundance (Fujiki et al. 2008). However, the diverse array of FRRf protocols deployed ultimately hinder a more systematic exploitation of these ever-expanding data sets to better understand PP across studies, regions, conditions and taxa. For studies specifically examining K_C, further disparity in methods used to (i) quantify total or particulate carbon-uptake rates, including: incubation lengths, sample volumes, spectral quality of actinic light; and (ii) report the ancillary data needed to link K_C to environmental or taxonomic regimes, has further confounded our ability to separate the methodological biases from true natural variability for published values of K_C (Lawrenz et al. 2013).

With this research perspective, we begin by examining the range of K_C measurements reported to date and discuss how these relate to known underlying biological processes. We then evaluate current methodology used to derive K_C and provide a roadmap by which the aquatic research community can maximise value from FRRf-based platforms towards global evaluation of PP. We outline "best-practice" protocols, which capitalise upon recent breakthroughs in FRRf technology and theoretical concepts that can be consistently, and immediately, implemented into future observational campaigns. Finally, we discuss how a multidisciplinary research approach, focussed upon developing a fully *mechanistic* understanding of electron allocation under various

environmental and taxonomic regimes, is essential to develop predictive modelling of K_C based upon data extracted from FRRf measures, combined with standardised ancillary measures.

6.3 Fast Repetition Rate Fluorometry (FRRf) measurements of PP

Active Chl-*a* fluorometry comprises instrumentation and protocols to actively probe the photochemical status of Photosystem II (PSII), the complex that photo-oxidises water to generate electrons for reductive biosynthesis (for a full description of aquatic applications, see Huot and Babin, 2010).

Photons are initially absorbed by diverse pigment complexes serving PSII, with the resulting exciton passed among the photosynthetic pigments. According to Kramer et al. (2004) (see also Klughammer and Schreiber, 2008), the ultimate fates for this exciton are described by fractional yields (Y), which together sum to 1, comprising (i) re-emission as a longer wavelength photon detectable as fluorescence (YF), (ii) loss as heat through Non-Photochemical Quenching (NPQ) processes that are both non-regulated (YNO) and regulated (YNPQ), and/or (iii) arrival at a reaction centre as the initial photochemical step (YPSII) towards water oxidation and electron transport; this final step can potentially invoke photooxidation of the P680 chlorophyll thereby generating the P680+Phaeophytin- radical pair. Alternatively, the exciton can return to the antennae pigments (δ) where they are subjected a further time to fates (i)-(iii). Assessing the complementary probabilities of absorbed energy emission via these pathways therefore informs the extent to which excitons are used for photochemistry versus regulated or non-regulated dissipation as heat, generically termed NPQ. All of these yields are readily accessible from active Chl-*a* fluorometry measures. An additional small, but metabolically expensive, exciton fate leads to photoinactivation of PSII through

degradation of the reaction centre protein, D1 (e.g. see Campbell and Tyystjarvi, 2012; Vass, 2011).

FRRf delivers a series of closely-spaced excitation flashlets (see Kolber et al. 1998) to cumulatively and transiently close all PSII reaction centres typically within 50-200 μs, thereby ensuring that the first acceptor molecule within the photosynthetic electron transport chain (Q_A) is reduced only once for each PSII during a given flashlet series. As PSII reaction centres cumulatively receive a photon they become photochemically closed for a period of ~1000 μs until downstream processes remove the photochemically-generated electrons. Such temporary closure of the photochemical yield stimulates a transient increase in the complementary fluorescence yield, measured as a fluorescence rise. FRRf protocols are termed "single-turnover" (ST; Kolber et al. 1998; Kromkamp and Forster, 2003), which has important implications, for the mechanistic interpretation of the resulting fluorescence rise. One of the main advantages of the single turnover protocol is that it does not increase the redox state of the plastoquinone pool, making FRRf measurements less intrusive than instrumentation which induces multiple-turnovers PSII (i.e. PAM) (see Suggett et al. 2003). FIRe fluorescence is similar to FRRf, except that a single ST pulse is provided and the fluorescence yield rapidly sub-sampled to characterise the fluorescence rise. This approach potentially simplifies FRRf-type technology, where the flashlet train enables monitoring of the baseline between flashlets, if the excitation source is stable.

Table 6.1 Fast Repetition Rate fluorometry (FRRf) variables and parameters, their synonyms and derivations

Parameter	Definition	Synonym(s)	Derivation	Units
ETR_{PSII}	Electron Transport Rate through PSII	ETR	Various	Various
F_o	Minimum PSII fluorescence yield (dark-acclimated state) where all PSII reaction centres are open	$F_{0,}$ F_{min}		Dimensionless
F_o'	Minimum PSII fluorescence yield (light-acclimated state) where all PSII reaction centres are open		$F_o/((F_v/F_m)+(F_o/F_m'))$**	Dimensionless
F_m	Maximum PSII fluorescence yield (dark-acclimated state) where all PSII reaction centres are closed	F_{max}, ϕ_{Fm}		Dimensionless
F_m'	Maximum PSII fluorescence yield (light-acclimated state) where all PSII reaction centres are closed			Dimensionless
F'	Fluorescence yield under actinic light at time *t*	F, ϕ_f		
F_v	Maximum variable PSII fluorescence yield (dark-	ϕ_{Fv}	F_m-F_o	Dimensionless
F_v'	Variable fluorescence yield under actinic light		F_m'-F_o'	Dimensionless
F_v/F_m	Maximum photochemical efficiency (dark-acclimated	ϕ_{PSII}^{max}, ϕ_P^{max}, $\Delta\phi_m$	$(F_m$-$F_o)/F_m$	Dimensionless
F_v'/F_m'	Maximum photochemical efficiency (light-acclimated		$(F_m'$-$F_o')/F_m'$	Dimensionless
F_q'/F_m'	Effective photochemical efficiency under actinic light	$\phi_{PSII,}$ $\Delta F/F_m'$	$(F_m'$-$F')/F_m'$	Dimensionless
F_q'/F_v'	PSII efficiency factor (under actinic light)	qP	$(F_m'$-$F')/(F_m'$-$F_o')$	
n_{PSII}	Assumed ratio of PSII reaction centres per unit			mol RCII (mol Chl-
ϕ_{PSII}	Quantum yield of PSII			
NPQ	Non-Photochemical Quenching (Stern-Volmer)		$(F_m/F_m'$-1)	Dimensionless
NPQ_{NSV}	Normalised Stern-Volmer coefficient of quenching	NSV	(F_o'/F_v')	Dimensionless
$\sigma_{PSII}(')$	Functional absorption cross-section of PSII (under actinic	PSII cross-section		nm^2 $quanta^{-1}$
ρ	PSII Connectivity Factor			Dimensionless
$RCII_{[FRRf]}$	Estimate of functional PSII reaction centre concentration from fluorescence-based algorithm		$K_R/E_{LED} \cdot (F_o/\sigma_{PSII})$	Mol RCII m^3
qJ	FRRf connectivity model (assumes partial connectivity between RCIIs)		$((F'$-$F_o')/(1$-$p) \cdot (F_m'$-$F_o) + p \cdot (F'$-$F_o))$	
qP	Photochemical quenching parameter	F_q'/F_v'	$(F_m'$-$F')/(F_m'$-$F_o')$	
K_C	Electron requirement for carbon fixation	$\phi_{e:C}$, e:c, eC	mol e^-/mol C	mol e^-: mol C
τ	Turnover time of PSII	Tau		µs

By fitting the FRRf (FIRe) rise with a biophysical model describing photochemistry (Kolber et al. 1998; see also Laney, 2003; Laney et al. 2008) we can extract minimal fluorescence F_0, maximal fluorescence F_m, the effective absorption cross-section for PSII, σ_{PSII} and a connectivity coefficient, ρ, which describes the probability of an exciton from a closed centre being transferred to a remaining open PSII centre. It is important to note that the mechanistic meaning (and correct terminology) for these variables depends upon the state of the sample at the instant of the measurement. For example, if the FRRf rise is imposed upon a sample that is already under a level of actinic illumination the F_0 extracted from the FRRf fit is actually steady-state fluorescence, F'. Similarly, the F_m extracted from an illuminated sample will be some version of F_m'. From the core FRRf variables a number of derived photosynthetic parameters describing PSII activity can be constructed (see Table 6.1). These parameters can then in turn be used to estimate the rate at which electrons are generated by PSII (ETR_{PSII}), the initial step in both linear photosynthetic electron flow and in multiple forms of pseudo-cyclic electron fluxes from water back to oxygen to regenerate water (Kolber and Falkowski 1993; Suggett et al. 2003, 2011; Oxborough et al. 2012).

Subsequent to the rapid succession of excitation flashlets that drive PSII closure, FRR fluorometers also allow programming of probe flashes spaced far enough apart to allow progressive re-opening of the PSII centres. In this relaxation phase, each probe flash tracks the instantaneous fluorescence yield (intensity) of the PSII pool at that instant, and by complementary inference, tracks the photochemical-reopening of the PSII pool by downstream electron transport processes (Kolber et al. 1998). This re-opening can be described by up to three kinetic lifetimes, τ (μs), which are the reciprocals of exponential decay rates (μs^{-1}) of the fluorescence signal with time. These lifetimes

therefore track the rates and relative amplitudes of processes consuming photochemical electrons and thus, are potentially indicative of the status of photosynthetic machinery downstream of PSII. Even so, whilst routinely measured by Chl-*a* fluorescence induction techniques, τ is still rarely utilised despite immense potential to explore electron turnover processes (Behrenfeld et al. 1998) and productivity (Moore et al. 2006).

6.4 What is ETR_{PSII} and its relationship to CO_2-uptake?

Photosynthetic electron transfer begins with absorbed photons leading to photochemical charge separation, and the subsequent generation of electrons originating from photosynthetic water-splitting, through the PSII reaction centres (RCIIs). Splitting of water at PSII produces O_2 and hence ETR_{PSII} is considered to be proportional to gross O_2 evolution (Genty et al. 1989); whereby minimally 4 successive photochemical electron generating events are required to evolve 1 molecule of O_2 (e.g. Kolber and Falkowski, 1993). However, ETR_{PSII} fundamentally reflects the rate at which electrons from water-splitting flow away from PSII, quantified for a given sample under a given condition by τ_{PSII} (Table 6.1). Electrons leaving PSII may flow via PSI photochemistry through to NADPH as photosynthetic linear electron flow (LEF, see Fig. 6.1), which supplies the energy (ATP) and reductant (NADPH) needed to fuel the Calvin-Benson-Bassham cycle (hereafter referred to as the Calvin Cycle) during carbon-fixation (Behrenfeld et al. 2008). There are, however, diverse alternate flows for electrons leaving PSII, including paths which lead back to oxygen, thereby regenerating water (termed pseudo-cyclic electron flow) that do not directly result in carbon-fixation.

A photosynthetic currency of electrons is rarely considered in PP studies (Suggett et al. 2009a), where the preference is to scale ETR_{PSII} to the equivalent rate of carbon-fixation

using a photosynthetic exchange rate, K_C (mol e^- [mol C]$^{-1}$, i.e. ETR_{PSII}/CO_2-uptake). Thus, algebraically $K_C{}^{-1}$ accounts for the yield of electron extraction from water during O_2 evolution, theoretically 4 mol e^- [mol O_2]$^{-1}$ when neglecting charge-recombination processes (Kolber and Falkowski 1993; Vass, 2011), O_2-consuming processes associated with alternative electron flows (e.g. Cardol et al. 2011), as well as the additional energetic and reductant costs to assimilate CO_2 for every O_2 generated (the photosynthetic quotient (PQ), Laws, 1991). Based upon the assumption that 4 electrons are extracted from the splitting of two water molecules per molecule of O_2 evolved, and using the commonly applied PQ value of 1.25 (but see Williams, 1993; Laws 1991), the theoretical minimum reference ratio for K_C is assumed to be ~4-5 mol e^- [mol CO_2]$^{-1}$.

Whilst ETR_{PSII} and CO_2-uptake have been repeatedly shown to correlate well for microalgae monocultures in the laboratory (Fujiki et al. 2007; Suggett et al. 2009a) and phytoplankton communities in the field (e.g. Kolber and Falkowski 1993; Suggett et al. 2006; Corno et al. 2006; Kromkamp et al. 2008; Schuback et al. 2015, 2016, 2017; Zhu et al. 2016), the slopes of the relationships often differ, reflecting combinations of (i) natural variability in K_C across studies, and/or (ii) variability induced by methodological biases between different protocols. Significant divergence from the minimum reference ratio of ~5 mol e^- [mol CO_2]$^{-1}$ appears to be most common under saturating light (Flameling and Kromkamp, 1998; Moore et al. 2006; Brading et al. 2013; Zhu et al. 2016) and nutrient limitation (Kolber et al. 1988, 1994) (see Lawrenz et al. 2013). Suggett et al. (2009a) also demonstrated a strong taxonomic influence upon K_C through the comparison of simultaneous ETR_{PSII} and CO_2-uptake rates for 6 distinct phytoplankton taxa cultured under different steady-state growth conditions (see also Moore et al. 2006; Suggett et al. 2006; Robinson et al. 2014; Zhu et al. 2017), reporting K_C values ranging between 3.63-11.5 mol e^- (mol CO_2)$^{-1}$.

Mounting evidence that both environment and taxonomy influence K_C has turned our attention towards resolving, understanding and hence, ultimately predicting K_C variation. Lawrenz et al. (2013) led a comprehensive synthesis of available experimental field data demonstrating that K_C was highly plastic over space and time, reporting measurements ranging from 1.15-54.2, with a global mean of 10.9 (±6.91) mol e^- [mol C]$^{-1}$ (Table 6.2). Their analysis showed that K_C was empirically correlated with key environmental variables known to regulate primary productivity, including irradiance, temperature, salinity and nutrient availability; these effects were nonetheless highly variable between regions. Environments found to have the lowest K_C, thus closest to the theoretical minimum, were coastal stations that do not often suffer from severe nutrient and/or light stress. Much of the observed variability in K_C was therefore hypothesised to reflect differences in physiological status and/or taxonomic structure at any given location, ultimately arising from specific, local biotic and abiotic conditions. Importantly, this study focussed on largely short term ^{14}C incubations and somewhat standardised FRRf approaches in an attempt to minimise confounding influence from methodology.

Since Lawrenz et al. (2013), several further studies have determined K_C for laboratory cultures (Brading et al. 2013; Hoppe et al. 2015) and natural populations (Robinson et al. 2014; Schuback et al. 2015, 2016, 2017; Zhu et al. 2016, 2017) reporting K_C values falling within the range outlined by Lawrenz et al. (2013). In attempting to reconcile K_C with environmental conditions, Zhu et al. (2016) found a strong relationship (r^2 = 0.94) between irradiance and K_C for a specific nutrient-replete location (Ariake Bay, Japan) throughout a two-year period. Furthermore, Schuback et al. (2015, 2016) recently demonstrated that K_C was highly covariant with the extent of NPQ, perhaps reflective of the strong influence of iron-limitation upon both NPQ and electron to C coupling

throughout the NE subarctic Pacific. Finally, and in contrast to these recent studies demonstrating strong environmental regulation of K_C, Robinson et al. (2014) found that phytoplankton community composition, and not environmental conditions, explained more of their observed variance in K_C within a physically-dynamic coastal system.

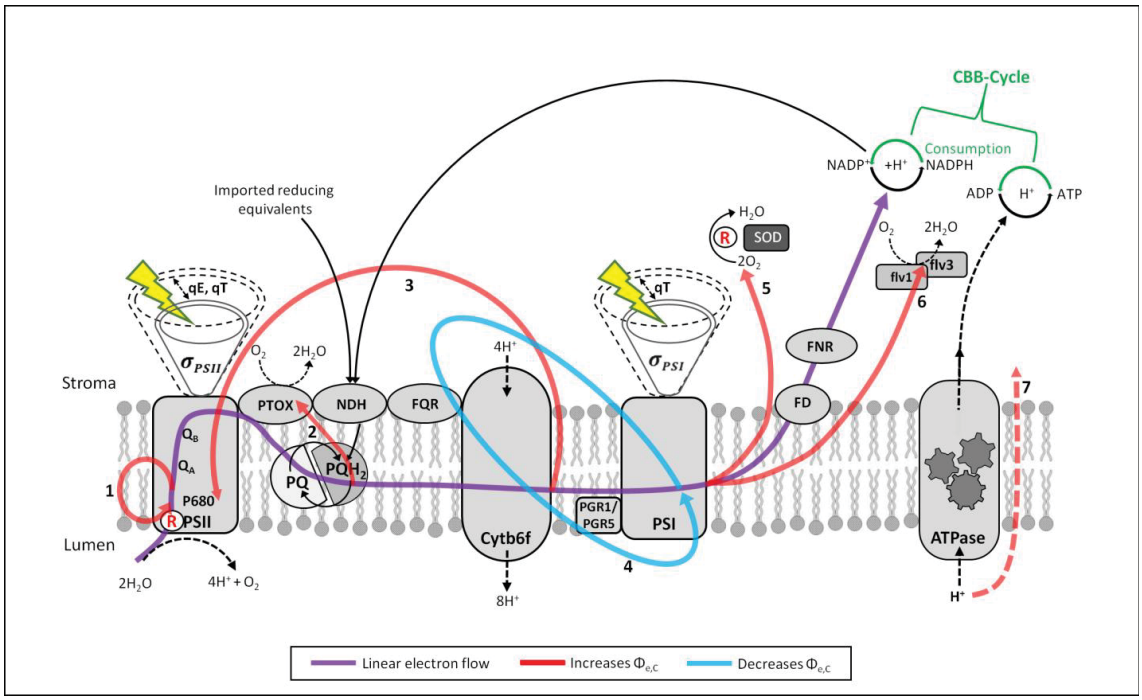

Figure 6.1 Schematic of photosynthetic linear electron flow (LEF, denoted by purple line) of oxygenic photosynthesis through to ATP/NADPH production, and C-fixation via the Calvin-Benson Bassham (CBB) cycle. Also depicted are additional processes which potentially influence Φe,C, coloured according to whether they ultimately increase (red) or decrease (blue) Φe,C: 1) charge recombination at PSII, 2) Plastiquinol terminal oxidase (PTOX), 3) Cyclic electron flow around PSII, 4) Cyclic electron flow around PSI, 5) Mehler reaction, 6) Flavodiiron protein (Flv)-mediated electron flows and 7) proton slippage reactions. Solid and dashed lines represent electron and proton fluxes, respectively. Energy-dependent non-photochemical quenching processes (qE) and state-transitions (qT) have reversible effects upon the functional absorption cross sections of photosystems I (qT) and II (qE, qT). Generation of reaction oxygen species (ROS) is also indicated via the red R within open circles, together with the superoxide dismutase (SOD) detoxification step following the Mehler reaction.

Table 6.2 Synthesis of K_C information (modified and updated from Lawrenz et al. 2013).

K_C	**Value (mol e^- mol C)$^{-1}$**	**Note**
Minimum stoichiometry	4	Assumes that 4 electrons are extracted from 2 H_2O molecules (evolving 1 molecule of O_2) and used to fix of 1 molecule of CO_2.
Commonly applied reference ratio	5-6	Regularly applied by studies when converting ETR_{PSII} to C-uptake, based upon the theoretical minimum, plus inclusion of the photosynthetic quotient used to account for nutrient assimilation.
Global Min	1.15	Values of K_C <4 are difficult to reconcile on a physiological basis and are most likely subject to methodological bias
Global Max	54.2	
Global Mean	10.9±6.91	Considerably higher (twofold) than assumed reference ratio
K_C <5 (% studies)	14.2	Indicates that an assumed reference ratio of 4-5 for K_C will result in an over-estimation of C-fixation rates in the majority of cases.
K_C >5 (% studies)	85.8	

Table 6.3. Summary of alternative electron flows (AEFs) and key electron-consuming pathways, reflecting their influence upon ATP, NAPDH and K_C with arrows representing ↑ increase and decrease to intracellular levels. Important environmental stimuli linked to each process are listed (where known) together with associated taxa, rate measurements and molecular proxies (where known).

Process	Primary Function(s)	Outcomes	Environmental Stimuli	Associated Taxa	Molecular proxies
Linear Electron Flow	ATP & NADPH generation	↟ATP ↟NADPH	Light	All autotrophs	
Alternative e^- Flows					
Cyclic Electron Flow (PSI)	ATP generation NPQ activation	↡ K_C ↟ATP	Light, Nutrient Limitation	All autotrophs, significant for chlorophytes (e.g. *C. reinhardtii)*	Ratio of PsaC to other representative photosynthetic components (Zorz et al. 2015)
Cyclic Electron Flow (PSII)	Photoprotection	↟ K_C	Saturating Light	Diatoms, Chlorophytes	
Mehler Reaction	Photoprotection, activation of NPQ ATP generation	↟ K_C ↟qE ↟ATP*	Saturating Light	May be important for *Trichodesmium spp.*	Flavoprotein in cyanobacteria (Helman et al. 2003); SOD and APX (Waring et al. 2010)
Alternative Oxidase	Photoprotection ATP generation	↟ K_C ↟ATP	Saturating Light		
Plastoquinol Terminal Oxidase (PTOX)	Photoprotection ATP generation	↟ K_C ↟ATP	Oligotrophy, Iron-Limitation Saturating Light	*Synechococcus*, *Prochlorococcus* & *Ostreococcus,* probably all phototrophs	PTOX expression (Bailey et al 2008; Cournac et al. 2000; Steglich et al. 2006)
Chlororespiration	ATP generation	↟ K_C ↟ATP	Low light, Dark exposure	Cyanobacteria, Dinoflagellates	
Other Processes					
Photorespiration	Subject to debate	↟ KC ↡ATP ↡ NADPH**		CCMs likely render this process irrelevant for majority of phytoplankton	
Malate/Oxaloacetate Shuttle		↟ K_C			Respiratory complex I and IV (Cardol et al. 2003); mitochondrial AOX (Allen et al. 2008)
Nutrient Reduction	Biosynthesis	↟ K_C ↡ATP	Nutrient availability/species	All phytoplankton taxa	Nutrient transporters
Carbon-Concentrating Mechanisms (CCMs)	Suppress photorespiration	↡ATP	Occurs continuously, however efficiency may vary across taxa	All phytoplankton taxa	

Table 6.4 General summary of the common approaches to measuring phytoplankton primary production including comparative strengths and limitations.

Method	Currency	Strengths	Limitations	References
^{14}C Method	Carbon (CO_2-uptake)	May reliably estimates NPP Highly sensitive Can measure dissolved (DOC) and particulate (POC) carbon fraction "Tried & tested" method (60+ years of data)	Timescale dependence between GPP and NPP "Bottle-effects" from incubation-dependent approach Limited sampling resolution ^{14}C is also taken-up by heterotrophic bacteria + AAnPs Fails to capture remineralised production	Steemann-Nielsen (1952)
^{13}C Method	Carbon (CO_2-uptake)	Reliably estimates NPP Highly sensitive Can be used *in-situ* (photosynthetic tracer)	Timescale dependence between GPP and NPP "Bottle effects" (for discrete incubations) Fails to capture remineralised production	Slawyk et al. (1977)
$^{18}O/^{16}O$ Method	Oxygen (O_2-evolution)	Reliably estimates GPP Estimates light respiration Highly sensitive	Does not measure NPP "Bottle effects" (for discrete incubations) Requires sophisticated equipment (e.g. MIMS)	
O_2 Bottle Method	Oxygen (O_2-evolution)	Can estimate GPP Can estimate Net Community Production (NCP)	"Bottle-effects" from incubation-dependent approach Needs photosynthetic quotient to derive CO_2-uptake rates. No separation of phototrophic and bacterial respiration	Trampe et al. (2015)
FRRf	Electrons (ETR_{PSII}) Inferred from Chl-*a* fluorescence	Unprecedented sampling resolution Incubation-free approach (*in-situ*) Highly sensitive Potential for stand-alone deployment Potential for spectral and kinetic resolution of contributions from different taxa	Lack of standardized methodological protocols Single-wavelength instruments may not drive full PSII closure of cyanobacterial taxa Potentially complicated methodology/terminology for newcomers Dependent upon ancillary measurements*	Kolber et al. (1998)

To date, these various studies have collectively reinforced the concept that K_C variability is strongly dependent upon the system in question, with environmental and/or taxonomic control of the underlying physiological processes. However, reconciling the fifty-fold variation for published K_C values across the world′s oceans based on empirical approaches alone (Lawrenz et al. 2013; Robinson et al. 2014; Schuback et al. 2015, 2016; Zhu et al. 2016, 2017) still seems a step too far. Instead, we ask if it is possible to better understand variance of K_C by mechanistically analysing how microalgae invest electron-derived energy and reductant into cellularly-retained fixed carbon versus diverse alternative sinks?

6.5 Physiological regulation of K_C

The parameter K_C interrelates two photosynthetic currencies (ETR_{PSII} and carbon-fixed), derived from disparate techniques that evaluate opposing ends of the photosynthetic pathway, which operate on significantly different time scales (Trampe et al. 2015). FRRf probes the initial light-harvesting and photochemical capacity of PSII to estimate ETR_{PSII} with the processes and measurements operating on timescales of ps to ms. ^{14}C-methods measure the balance between CO_2-uptake that occurs within the stroma downstream of PSI/PSII, during the metabolic reactions of the Calvin Cycle, with loss of labelled carbon to respiratory processes over the incubation period. Whilst operation of these metabolic reactions is as fast as those for the ETR, the measurement of CO_2-uptake is generally over scales of minutes to hours. Critically, because the two methods measure processes that are physically, temporally, mechanistically and kinetically separated, a suite of intervening physiological processes can operate to consume electrons, reductant and/or ATP (Suggett et al. 2009; Fisher and Halsey, 2016). Many of these processes dynamically regulate photosynthesis under conditions where instantaneous reductant generation exceeds the instantaneous sink for reductant through

C-fixation and other processes (Huner et al. 1998), including supraoptimal light, suppressed C-fixation capacity due to nutrient stress, or when light-harvesting transiently outpaces the response rate of the regulation of C fixation under rapidly fluctuating light (Ilík et al. 2017). A variable proportion of electrons may be diverted away from LEF towards alternative electron flows (AEFs) (Krall and Edwards, 1992; Miyake, 2010; Cardol et al. 2011), including the Mehler reaction (Heber, 2002; Asada, 1999; Claquin et al. 2004), "Mehler-like" reactions associated with Flavodiiron proteins (FDPs, also called flavoproteins, Flvs) of cyanobacteria and green algae (Allahverdiyeva et al. 2015), cyclic electron flow around PSI (CEF-PSI) (Heber, 2002) and PSII (CEF-PSII) (Prášil et al. 1996; Miyake et al. 2002; Lavaud et al. 2002) and chlororespiration via mid-stream oxidases such as the plastoquinol terminal oxidase (PTOX) (Bailey et al. 2008; Zehr and Kudela, 2009; Peltier et al. 2010; Berg et al. 2011) (Fig 6.1, Table 6.3).

AEFs can function in a photoprotective capacity (Ralph et al. 2010; Cardol et al. 2011) acting as alternative electron sinks to prevent harmful accumulation of reduced chemical species within the linear electron transport chain that can lead to damaging reactive oxygen species (ROS) formation (Foyer et al. 1994; Vass 2011; Murphy et al. 2017). AEFs can also play a role in the activation of NPQ, which increases thermal-dissipation of excess energy within the antenna bed to protect PSII from high light (Makino et al. 2002). AEFs will generally increase K_C (See Table 6.3) and can largely explain why measured K_C values are typically higher under high light when photosynthesis is light saturated (e.g. Brading et al. 2013; Zhu et al. 2016) since cells must activate processes that can counter ever-accumulating reductant pressure. Additionally, many AEFs will tend to increase the proton gradient across thylakoid membranes, generating the proton motive force (pmf), required for the activation of

synthesis of ATP in excess of the ATP:NADPH generated by LEF. Certain AEFs therefore allow phytoplankton to fine-tune intracellular ATP:NADPH stoichiometry to balance their respective consumption by various physiological processes (Cardol et al. 2011), and overcome the ATP-shortage problem (see Behrenfeld et al. 2008) balancing ATP:NAPDH consumption by C-fixation (Allen, 2003). Light-dependent generation of ATP by specialised proteins (Proteorhodopsin) is in fact critical for survival in some bacteria and archaea under resource limitation (Delong and Béjà, 2010). As such, generation of additional ATP by AEF may ultimately be a key mechanism required for cells to increase their competitive success, e.g. fuelling nutrient transporters in low nutrient conditions. AEF can thus decouple energy and reductant flow within photosynthetic organisms, providing a potentially important mechanism by which aquatic microbes balance the requirements for these two fundamental photosynthetic currencies. By diverting electrons to Mehler activity and PTOX, additional ATP is effectively generated, reducing the overall quantum yield of C-fixation to increase K_C. Similarly, ATP generated by CEF-PSI, which returns electrons to PSI rather than consuming them, would potentially reduce K_C. Of all AEFs, CEF-PSII is the least-understood, but may have significant ramifications for FRRf-based productivity estimates since this pathway results in the complete disengagement of ETR_{PSII} from the generation of both ATP and reductant (and therefore from C-fixation), akin to a "release valve" which dissipates excess excitation energy under high light (Falkowski et al. 1986; Prášil et al. 1996; Miyake and Okamura, 2003). Key unknowns include: (a) the maximum proportion of electrons that can be diverted to CEF-PSII relative to LEF, (b) the taxa-dependent variability of CEF-PSII across marine phytoplankton, although it appears especially pronounced in diatoms (Lavaud, 2007), and (c) how environmental

conditions (apart from light) may also influence this pathway, since nitrogen limitation may act synergistically with irradiance to increase CEF-PSII (Wagner et al. 2016).

Ultimately, cellular metabolism requires that the carbon fixation pathway must interact with other electron-consuming processes. Electrons drive reductive assimilation of sulphate and nitrogen compounds, and reductive biosynthesis of proteins, nucleic acids and particularly lipids, leading to a concurrent increase in K_C. Nitrogen is the second-most abundant constituent of phytoplankton dry biomass after carbon, often requiring the reductive assimilation of inorganic nitrogen from an external source (Anderson, 1995), with an associated assimilatory reductant cost that increases roughly in parallel with the oxidation state of the available N-source; Organic N< NH_4^+< N_2< NO_2^- < NO_3^-. The most reduced inorganic form, NH_4^+ is assimilated into biomass at the expense of only ~2 e^- $[mol\ N]^{-1}$ and 1 ATP, whilst NO_3^- requires a further investment of 8 mol e^- $[mol\ N]^{-1}$ for reduction to the level of NH_4^+ prior to assimilation (Timmermans et al. 1994). Utilising atmospheric N_2 is very costly, and to do so diazotrophs must invest a minimum of 5 e^- $[mol\ N]^{-1}$, plus at least 16 mol ATP $[mol\ N]^{-1}$ (Postgate, 1974; Scherer et al. 1988). Raising the substantial ATP capital needed to assimilate N_2 inevitably comes at a cost to the coupling between ETR_{PSII} and CO_2 uptake. In fact, this has been proposed as the mechanism to explain why N_2-fixing cyanobacteria fail to dominate in hypertrophic lakes where self-shading limits light-availability, and thus the means to generate sufficient ATP to sustain high diazotrophic growth rates (Zevenboom and Mur, 1980). Similarly, the assimilation of sulphur into organic metabolites is also a metabolically expensive process (Takahashi et al. 2011), requiring that the sulphate anion is activated by ATP sulfurylase before it can be reduced to sulphite at the total cost of 2 e^- $[mol\ S]^{-1}$and 1 ATP (Giordano et al. 2005), prior to further reduction to the level of organic-S at the expense of 6 further e^- $[mol\ S]^{-1}$ during biosynthesis. Whether

cells that require N- and S-rich compounds to maximise competitive success thus inherently exhibit a higher K_C is as yet untested.

Other notable processes that may account for the divergence of ETR_{PSII} from C-fixation include "enhanced dark" respiration and photorespiration, although it is unclear how significant the latter is for marine phytoplankton due to their development of carbon-concentrating mechanisms (CCMs), evolved primarily to avoid RuBisCO-oxygenation events (see Beardall, 1989). Claquin et al. (2004) demonstrated that light-enhanced respiration in the diatom *Cylindrotheca* was primarily due to Mehler-type reactions and that photorespiration *per se* played only a minor role. More research is, however, required to unlock the relevance of photorespiration in regulating the flow of electrons to carbon for algae where RuBisCO shows a poor CO_2/O_2 discrimination, notably the form II RuBisCO of dinoflagellates (e.g. Brading et al. 2013).

Finally, phytoplankton can release variable, but often large, amounts of dissolved organic carbon (DOC) to the environment, thereby altering the ratio of ETR_{PSII} to retained fixed C. Such excreted DOC can often be missed when the particulate fraction of C-fixation alone is measured, and thus dependant on the methodology employed. Extracellular DOC release is a normal function of phytoplankton cells, representing: metabolic waste, cellular communication, chemoattractants, chemical defence and substrate acquisition (Carlson, 2002). This release of DOC broadly scales with total productivity in marine systems, where it averages 13% of PP (Baines and Pace, 1991) but can reach as high as 80% (Lancelot, 1983), possibly increasing significantly during periods of environmental stress (Leboulanger et al. 1998; Bertilisson et al. 2005). Whilst it is yet to be conclusively shown which environmental factor(s) primarily influence DOC release (Carlson, 2002), studies have demonstrated a link between irradiance and DOC production (Panzenböck, 2007; Cherrier, 2015).

Collectively, these processes influence the ratio between gross O_2 evolution and ETR_{PSII} relative to the concurrent retained fixed C (i.e. K_C), operating on different timescales (see Fig. 6.2). However controlled laboratory or field experiments needed to unravel the nature and magnitude of the various pathways have rarely been performed for phytoplankton (but see Roberty et al. 2014; Kana, 1992, 1993; Fisher and Halsey, 2016). Consequently, we have as yet a poor understanding of how non-C-fixing pathways, or indeed extracellular release of DOC, influence K_C across taxonomic groups and/or growth conditions.

6.6 Evolutionary (taxonomic) divergence

Variability in FRRf-based K_C has also been frequently considered at a taxonomic level, across both phytoplankton cultures (Fujiki et al. 2007; Suggett et al. 2009; Brading et al. 2013), and natural populations (Moore et al. 2006; Suggett et al. 2006, Robinson et al. 2014). Variance of K_C relative to taxa present is perhaps unsurprising considering that phytoplankton have evolved over long geological timescales across a broad range of environments (Simon et al. 2009). This is reflected in their elemental composition, with field observations of C:N:P stoichiometry deviating significantly from the canonical "Redfield ratio" of 106:16:1 (Redfield, 1934), across latitudinal environmental gradients (Martiny et al. 2013). A recent meta-analysis by Finkel et al. (2016) identified taxon-specific differences in the macromolecular pools of proteins, lipids and carbohydrates across marine and freshwater phytoplankton which is consistent with the observed variability in C:N. Due to the energetic and reductant cost involved in assimilating N (discussed in Section 6.5), and the differences in reductant requirements to generate retained proteins, lipids and carbohydrates, it could therefore be expected that differences in C:N ratio across taxa ultimately translate into species-specific differences in K_C.

Furthermore, taxonomically distinct groups of phytoplankton have adopted very different strategies of photosynthetic energy harvesting and utilisation (Lavaud et al. 2007; Halsey et al. 2014). For example, diatoms express a high capacity for NPQ relative to other taxa (Ruban et al. 2004) through an energy-dependent mechanism (qE) that diverts excess excitation energy away from PSII before it enters the ETC (Lavaud et al. 2007). In this instance, lowering excitation pressure upon PSII (Li et al. 2009) alleviates potential demand for dynamic AEF processes that could otherwise increase K_C. Other taxonomic groups have smaller amplitudes of qE (chlorophytes, cryptophytes) or analogous quenching mechanisms (cyanobacteria, Kiriloviski 2007, 2015; Gorbunov et al. 2011), potentially leaving a greater burden for AEFs to dissipate excess excitation energy after it has been delivered to the ETC via PSII, thus increasing K_C. The proportionality between measured changes in NPQ and downregulation of the effective absorption cross-section of PSII (σ_{PSII}) can vary with taxa and conditions (Koblizek et al. 2001). Environmental conditions that ultimately select for different taxa can therefore potentially explain spatial or temporal variance in K_C (e.g. Suggett et al. 2006; Lawrenz et al. 2013; Robinson et al. 2014; Zhu et al. 2017).

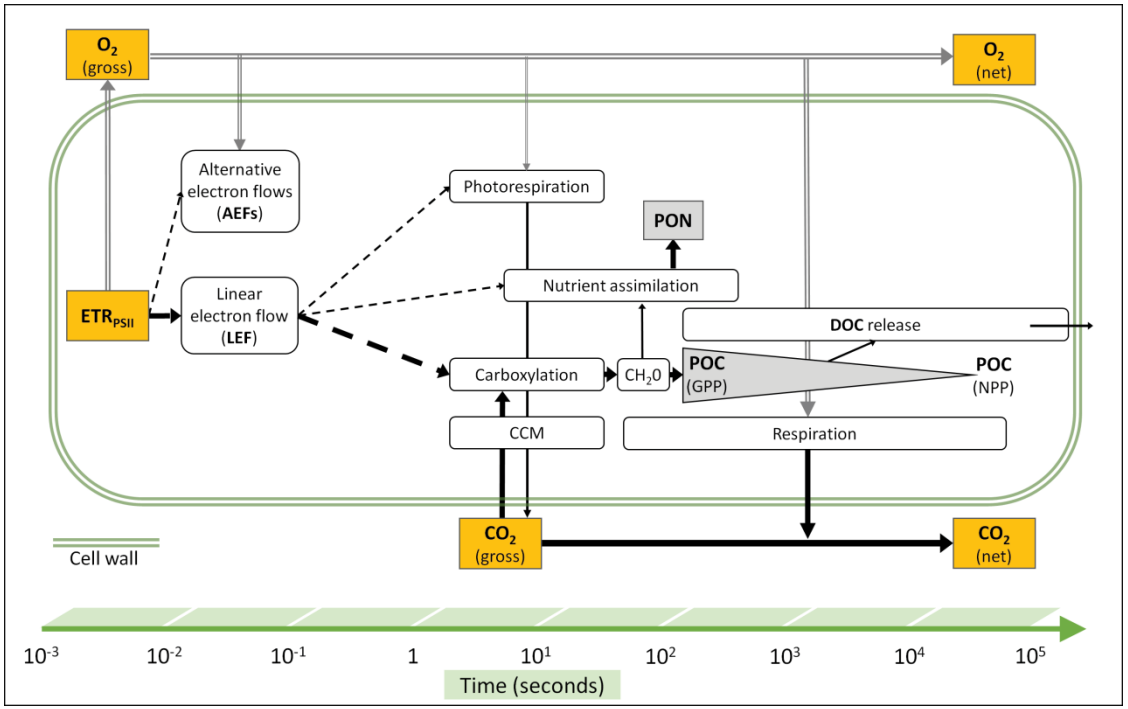

Figure 6.2 Simplified, conceptual summary highlighting the fluxes of the three major photosynthetic currencies (gold boxes) within a photosynthetic cell: electrons (ETRPSII – dashed lines), oxygen (double gray lines) and carbon (solid black) over a timescale from µs to hours/days, with the direction of arrows indicating production (arrow head: source) and consumption (arrow tail: sink). Major and minor pathways are indicated by thick and thin lines respectively. Particulate organic nitrogen (PON) and particulate organic carbon (POC) are indicated by the grey shapes. The direction of the grey triangle (POC) reflects that the fraction of POC measured by 14C-incorporation retained decreases over time due to respiration, as the photosynthetic rate captured transitions from gross to net primary production (GPP and NPP) with increasing incubation length (e.g. from minutes to hours).

Whilst the capacities and extents to which specific AEFs regulate photosynthesis across phytoplankton taxa is still poorly resolved, some evidence exists to suggest that certain pathways are particularly important for certain phytoplankton groups. Flavoproteins (Flv) have recently been identified as mediating electron flows direct to oxygen from PSII in cyanobacteria, and from PSI to oxygen in all tested photoautotrophs except angiosperms (Allahverdiyeva et al. 2015; Ilík et al. 2017). Such Flv flows appear particularly important during transitions from dark to light, when electron transport transiently outpaces the regulatory induction of carbon fixation. We can therefore hypothesize that Flv-mediated pseudo-cyclic flows might raise K_C under fluctuating light regimes in rapidly mixing waters (see Hoppe et al. 2015). In another example, PTOX appears important for the picocyanobacteria (*Synechococcus* and especially *Prochlorococcus,* Berg et al. 2011) and the prasinophyte, *Ostreococcus* (Mackey et al. 2008), allowing these taxa to sustain high ETR_{PSII} and hence presumably high ATP generation rates under conditions where the acceptor-side of PSI is heavily impaired under iron-limitation, or under high light, thereby minimising the potential for photoinhibition. Because cyanobacteria numerically dominate oligotrophic waters (Partensky et al. 1999), the PTOX pathway can account for a significant proportion of total PSII electron flow in these regions (Bailey et al. 2008; Cardol et al. 2011). Thus, measured K_C values in low-nutrient, oligotrophic regions are expected to sit towards the higher end of the range reported (Lawrenz et al. 2013). Even within the same genus, alternate photosynthetic strategies across environmental niches can have markedly different implications for K_C; for example, the prasinophyte *Ostreococcus tauri* preferentially employs a dynamic qE mechanism to sustain growth rates under very high light (1500 μmol photons m^2 s^{-1}) (Cardol et al. 2008), whilst the low-light adapted *O. tauri* strain RCC809 mainly utilises PTOX (or analogous midstream-oxidase

pathways) to limit photoinhibition and generate ATP under saturating light (Six et al. 2008), thus adopting a strategy with a higher K_C. Taxa-specific differences in extracellular DOC release have also been reported by Becker et al. (2014) who found that total percentage of fixed carbon released as DOC ranged from 5-25% across 4 species of marine phytoplankton, yet found limited variability between conspecific strains for each group (three diatoms and one cyanobacterium). Wider variability in extracellular DOC release across a broader range of taxa or conditions seems plausible, if as yet unproven, with potentially significant implications for the determination of K_C, depending upon whether C-uptake is measured as particulate, or total organic carbon (i.e. POC vs. TOC).

Ultimately, variance of K_C across taxa likely reflects fundamental differences in lifestyle strategies, which have evolved to maintain photosynthetic fitness in terms of requirements for both reductant (NADPH) and energy (ATP) in order to successfully compete in different environmental niches. These variations in strategies may also extend to CO_2 assimilation itself. Notably, geologically-older taxa such as cyanobacteria may need to expend more ATP and reductant to fuel carbon concentration mechanisms (CCMs, in the form of carboxysomes) to compensate for RuBisCO that has (i) lower catalytic efficiency (Badger et al. 1998) or (ii) lower affinity for CO_2 compared to more recently-evolved phytoplankton groups such as diatoms (see Tortell, 2000). Diverse CCMs incur a metabolic cost to the cell through ATP consumption, dissipation of chemiosmotic potential or cyclic electron flows (Raven et al. 2014), and hence may be expected to exert a taxa-specific influence upon K_C.

Within laboratory studies, diatoms, the most recently evolved major phytoplankton taxon, typically exhibit K_C values within the lower range of reported values (Suggett et

al. 2009; Hoppe et al. 2015; Chapter 3, but see also Hughes et al. in press., Chapter 2). Many of the lowest reported values for K_C in the field (i.e. <4 mol e^- [mol C]$^{-1}$) originate from cyanobacterial-dominated communities (Robinson et al. 2014), which might reflect the distinct macromolecular composition of these prokaryotes compared to eukaryotes (Finkel et al. 2016). With the limited data to date it is hard to infer the extent to which K_C variability can be attributed to fundamental taxonomic divergence across groups versus physiological plasticity (see Suggett et al. 2009). We do know that environmental variability including rapidly fluctuating light, nutrients and temperature conditions results in the allocation of carbon and photosynthetically-derived reductant and energy to a range of metabolic pathways to balance cell maintenance and growth with resource availability and acquisition (Halsey et al. 2014; Fisher and Halsey, 2016); thus, it seems conceivable to expect K_C to exhibit considerable plasticity in response to local environmental conditions, irrespective of whether the community assemblage (taxonomy) changes, but this notion clearly warrants future targeted testing.

Lack of K_C data with which to reconcile true variance across taxa and conditions is of course further compounded by methodological inconsistencies associated with ETR_{PSII} and CO_2-uptake determinations. In particular, values of K_C less than the "theoretical minimum" of 4 (see Table 6.2) are reported frequently (~30% across FRRf datasets; Robinson et al. 2014), and are difficult to reconcile on a physiological level with the oxygenic photosynthetic pathway (Fig. 6.1) (see Suggett et al. 2009a). Resolving the nature and extent of photoheterotrophic metabolism may be a key, but as yet unexplored, process driving these values of K_C below the theoretical minimum. In order to robustly advance programs seeking to better resolve K_C, we next highlight likely sources of error associated with over- and under-estimation of ETR_{PSIIs} and/or CO_2-uptake rates.

6.7 Construction of *Absolute* Rates of Electron Transport (ETR_{PSII})

Absolute electron transport rates are commonly calculated from a simple mathematical construct: the product of light intensity, how much of this light is absorbed by PSII and the proportion of this absorbed light subsequently used for photochemistry. In the case of FRRf-based measurements, an ETR is retrieved for each induction normalized per unit PSII reaction centre (ETR_{PSII}) as,

$$E \cdot \sigma_{PSII}' \cdot F_q'/F_v' \quad [1]$$

where E, σ_{PSII}', and F_q'/F_v' are terms for irradiance, the PSII functional absorption coefficient (the prime notation denotes that this measurement is performed under actinic light) and the PSII operating efficiency. Equation 1 is equivalent to,

$$E \cdot \sigma_{LHII} \cdot F_q'/F_m' \quad [2]$$

where σ_{LHII} is the PSII absorption coefficient (since σ_{PSII} is the product of σ_{LHII} and the PSII maximum quantum yield, F_v/F_m), and F_q'/F_m' is the PSII photochemical efficiency otherwise termed ϕ_{PSII} (Oxborough et al. 2012). None-the-less, equations 1 and 2 yield ETR_{PSII} per unit PSII reaction centre, and thus must further account for the number of PSII reaction centres per unit volume of (sea)water, [RCII], to scale ETR_{PSII} to a more ′ecologically meaningful′ productivity rate per unit volume of water (see Suggett et al. 2009a),

$$E \cdot a_{LHII} \cdot \phi_{PSII} = E \cdot \sigma_{PSII} \cdot (F_v/F_m)^{-1} \cdot [RCII] \cdot F_q'/F_m' \quad [3]$$

Irradiance and ϕ_{PSII} are both subject to measurement error (see Huot and Babin, 2010; Silsbe et al. 2015), yet conventionally it is the parameterisation of a_{LHII} which has introduced the largest source of error into estimates of ETR_{PSII}. Much of this uncertainty

arises from the need to quantify PSII reaction centres per unit volume of (sea)water, [RCII]. Direct measurement of [RCII] is conventionally performed using laborious O_2 flash-yield methodology (e.g. Falkowski et al. 1981), requiring highly concentrated biomass (to >1 g m^3 Chl-*a*) and considerable operator effort rendering this largely impractical for studies of natural communities (Moore et al. 2006; Suggett et al. 2006; Oxborough et al. 2012). Instead, many studies have assumed a constant ratio between the number of Chl-*a* and PSII units (n_{PSII}), thus relying upon ancillary measurements of Chl-*a* to estimate PSII per unit volume. Values for n_{PSII} of 500 mol Chl-*a* $RCII^{-1}$ for eukaryotes and 300 mol Chl-*a* $RCII^{-1}$ for prokaryotes have commonly been applied by oceanographers (Suggett et al. 2010); however, evidence indicates that this constant is unlikely to hold true across phytoplankton taxa or growth conditions (Suggett et al. 2004, 2011; Silsbe et al. 2015; but see Suggett et al. 2006). Indeed, use of n_{PSII} has been identified as the major uncertainty in estimates of ETR_{PSII} (Robinson et al. 2009). Parameterisation of a_{LHII} usually incorporates a measurement of σ_{PSII} (unless using the "absorption" algorithm of Oxborough et al. 2012), which is spectrally-weighted to the FRRf excitation LED and therefore requires a correction factor to account for the spectral quality of the ambient light driving photosynthesis versus the spectral quality of the natural light field and the absorbance spectra of the cells (see Suggett et al. 2001). Such corrections require knowledge of lamp and absorbance spectra thereby limiting the autonomous nature of past FRRf-derived PP determinations (Suggett et al. 2010; but see Suggett et al. 2006). However, new multi-wavelength fluorometers enable construction of fluorescence-excitation spectra for any given sample, allowing for correction factors to be applied with relative ease (Silsbe et al. 2015; Szabo et al. 2014).

The major bottleneck associated with how variance of [RCII] contributes to that of ETR_{PSII} using FRRf may be overcome by the development of a fluorescence-based

algorithm by Oxborough et al. (2012). Their approach requires a one-time calibration of the FRRf instrument to return independent determinations of [RCII] purely from FRRf-derived parameters, specifically the PSII minimal fluorescence yield (F_0) and σ_{PSII}. The Oxborough et al. (2012) algorithm has been evaluated for natural communities and laboratory culture under steady-state growth (Oxborough et al. 2012; Silsbe et al. 2015), and applied to examine ETR_{PSII} (Robinson et al. 2014; Hoppe et al. 2015; Suggett et al. 2015). This approach is attractive since it simply requires a fluorometer pre-calibrated to [RCII] content (Oxborough et al. 2012; Robinson et al. 2014; Silsbe et al. 2015), which could simply involve cross-instrument calibrations with known differences in excitation power (Oxborough et al. 2012). A major constraint to widespread application at present is whether and how this approach will apply under certain specific physiological conditions such as iron-limitation (Greene et al. 1992; Schrader et al. 2011) or photoinhibition (see Murphy et al. 2017). In particular, the presence of fluorescent pigment complexes, which are not energetically coupled to PSII (notably under iron-limitation, Behrenfeld et al. 2006; Schrader et al. 2011; Ryan-Keogh et al. 2012; Macey et al. 2014) would result in a significant overestimation of [RCII]. As such, a rigorous assessment of the $[RCII]^{(FRRf)}$ algorithm robustness in the field under various environmental regimes is an important step towards understanding the environmental confines under which $[RCII]_{[FRRf]}$ (and therefore absolute ETR_{PSII}) can be confidently estimated via a calibrated FRRf. Such an evaluation has recently been performed in N-limited coastal waters (Hughes et al. in press., Chapter 2), and for N-replete phytoplanlton cultures (Chapter 3) but should also be extended to the laboratory, incorporating a wide diversity of strains, conditions and physiological states to place better confidence intervals on field measurements of [RCII] (Murphy et al. 2017).

Interestingly, Schuback et al. (2015, 2016) recently demonstrated that variability in K_C /[RCII], i.e. the relationship between ETR_{PSII} and C fixation, under iron-limited conditions was correlated with an FRRf-based proxy for NPQ, specifically the normalised Stern-Volmer coefficient (NPQ_{NSV}) (see McKew et al. 2013). Their approach therefore maintains [RCII] as a constant. However, recent work suggests that [RCII] may indeed be highly-variable in response to relief from N-limitation (Hughes et al. in press., Chapter 2). Such empirical relationships provide promise for the predictability of, RCII and/or K_C variability within certain environments, but would require further testing (e.g. Zhu et al. 2016) to determine how/when they may be applied, and therefore should be incorporated routinely into future data-collection campaigns for evaluation purposes. Ultimately, it may prove to be the case that a combination of approaches is required to accurately predict K_C across global scales, likely depending upon the system in question. Given that both the approaches of Oxborough et al. (2012) and Schuback et al. (2015) consider variance of [RCII] via inherent FRRf-measured parameters, it may be possible to begin this process by re-evaluating past FRRf data sets.

6.8 Determination of CO_2-uptake

Regardless of the photosynthetic currency in question, it is useful to define three components of primary production that can be estimated from measurements in closed systems (Cullen, 2001): Gross Primary Production (GPP), the rate of photosynthesis not reduced for losses to excretion and respiration, Net Primary Production (NPP), where GPP is adjusted for excretion and respiration, and Net Community Production (NCP), where NPP is adjusted for respiration losses by heterotrophic microorganism and metazoan respiration. FRRf-based ETR_{PSII} measures represent a true GPP (electron

generation at PSII through water-splitting) and thus places an upper bound on photosynthetic reductant and energy generation. CO_2-fixation measurements on the other hand may represent any one of these definitions depending on the time-scale with which these measurements are made (Milligan et al. 2015). Importantly, coupling between GPP, NPP and NCP will not be constant where changes to prevailing environmental conditions and taxa moderate the efficiency with which CO_2 is assimilated. Consequently, K_C may be more appropriately defined as $K_{C\,[GPP]}$, $K_{C\,[NPP]}$ etc., and a first step means to provide direct physiological information on the importance of alternative electron flows and respiratory losses; we return to this point later.

Carbon radio- (^{14}C), and more recently stable- (^{13}C), isotope labelled bicarbonate methods are commonly viewed as the gold-standard of phytoplankton productivity measurements since they directly track "CO_2-uptake", and thus the benchmark against which other techniques are commonly evaluated (see Table 6.4). Nonetheless, the ^{14}C method, in particular, has faced considerable methodological scrutiny since its introduction (see Longhurst et al. 1995; Melrose et al. 2006; Marra, 2009), prompting Longhurst et al. (1995) to wryly observe, "Rarely, in fact, can a technique have been so persistently criticised, but so consistently used". A special conference was organized by Williams et al. (2008) to celebrate the developments 50 years after the introduction of the ^{14}C-technique; however, nearly a decade on from this, many of the methodological concerns highlighted by Longhurst et al. (1995) persist, particularly in the complex relationship between incubation time and the subsequent cellular residency and metabolic processing of fixed carbon. Theoretically, short-term incubations that allow little time for fixed carbon to be respired or excreted (released as DOC) should approximate GPP, whereas longer (e.g. dawn-dusk) incubations inherently allow for a

proportion of any fixed-^{14}C to be lost to respiration, such that measurements over a full diel cycle tend to best approximate NPP (Dring and Jewson, 1982). In this context, we strictly define NPP as GPP minus light-enhanced mitochondrial respiration and photorespiration (as per Halsey and Jones, 2015), reflecting production rates predominately from the photosynthetic activity of the microbial population. Furthermore, the CO_2 assimilated must be strictly defined as that contributing to new particulate production versus that excreted as DOC, where in the latter case it may be reincorporated either by heterotrophic bacteria or mixotrophic phytoplankton. As such,

$$NPP = GPP - R_{LIGHT + DARK} \quad [4]$$

$$NPP_{PARTICULATE} = NPP - DOC_{EXCRETED} \quad [5]$$

Laboratory experiments regularly show GPP to be on average 3-fold higher than NPP, with a range of 1.2 to 7 fold (see Halsey and Jones, 2015), and therefore K_C (ETR_{PSII}/CO_2-uptake) increases with incubation length as CO_2-uptake transitions from GPP to NPP, with this transition time influenced by both, species, and the dominant growth phase of the population (Lopez-Sandoval et al. 2014). However, differentiation between short and long incubations (supposedly capturing GPP and NPP respectively) is not always clear-cut, as demonstrated by a series of illustrative papers by Halsey et al. (2010, 2011, 2013). Even very short incubations (20 min – 1 h) can yield a variable CO_2-uptake rate somewhere between GPP and NPP, influenced by cellular growth rate-dependent differences in the lifetimes of newly-fixed carbon (Halsey et al. 2011, 2013); such studies neatly demonstrate the rate and extent with which GPP-derived energy and reductant are used to fuel cellular maintenance. Specifically, when the marine chlorophyte *Dunaliella tertiolecta* was maintained under steady-state, nitrogen limited growth (0.12 day^{-1}), newly-fixed carbon predominantly in the form of glyceraldehyde 3-

phosphate (GAP), was rapidly catabolised for cellular processes over a 20 min incubation, yielding a CO_2-uptake rate reflective of NPP. Conversely, at a higher, N-replete growth rate (1.2 day^{-1}) newly-fixed carbon, was instead, invested into longer-lived polysaccharides which have a turnover time of ~4-6 hr, thereby accumulating up to 3 times more radio-labelled carbon during the same incubation period (i.e. closer to GPP). For another marine diatom, *Chaetoceros muelleri* we similarly show here that 30 min carbon uptake rates decrease linearly (by a factor of 3.5) with decreasing growth rate and merge with NPP at very low growth rates (~0.025 day^{-1}) imposed by severe nitrate limitation (Fig. 6.3).

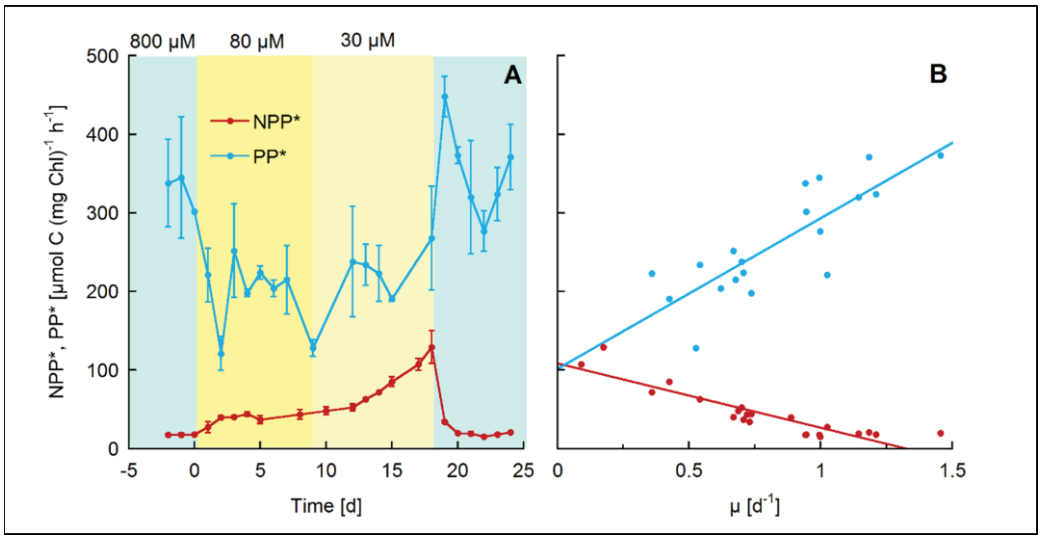

Figure 6.3 (A) Chlorophyll-specific C-fixation rates determined from 24 hr incubations with ^{13}C representing net primary productivity (NPP*) and from short term (30 min) incubations with ^{14}C representing (PP*) in the marine diatom *Chaetoceros muelleri* (CCAP 1010/3) grown in duplicate semi-continuous batch cultures with daily dilutions (according to their 24 h growth rates) at a continuous growth irradiance of 180 µmol quanta m^{-2} s^{-1} throughout a transient change in NO_3^- availability. Cultures acclimated to NO_3^- replete conditions (800 µM NO_3^-) were driven into non-steady state NO_3^- limitation of 80 µM (NO_3^-) on day 0, followed by the initiation of severe NO_3^- stress (30 µM NO_3^-) on day 9 and a recovery period with fully NO_3^- replete medium starting on day 18. Error bars are standard deviations of 2 independent replicate cultures. (B) Dependency of NPP* and PP* on their corresponding cell specific growth rates. The extrapolated regression lines of NPP* (= -81.9x + 109, r2 = 0.811) and PP* (=192x – 102, r2 = 0.683) intercept one another at 0.025 d^{-1} and 106 µmol C (mg Chl)$^{-1}$ h^{-1}.

Furthermore, unlike the studies of Halsey et al. (2010, 2011, 2014, 2015; Felcmanová et al. 2017) that utilised steady-state chemostat-grown cultures, chlorophyll normalized NPP in non-steady state phytoplankton is not constant, rather it declines linearly with increasing growth rate. Therefore, the variation among growth rate, NPP and short-term C-uptake across different phytoplankton taxa remains to be fully understood through further study.

Considerable methodological uncertainty may therefore be introduced when K_C is derived from incubation lengths where it is not possible to determine exactly where a given CO_2-uptake rate sits on the ′sliding scale′ from GPP to NPP (Milligan et al. 2015). This holds particularly true for natural phytoplankton communities where growth rates can be highly variable and impractical to quantify. Most studies seeking to derive K_C values from natural communities have done so using incubation lengths of 1-4 hr upon the assumption that the measured CO_2-uptake rates represent GPP (Lawrenz et al. 2013), and less commonly from longer (12-24 hr) incubations aiming to measure NPP rates (Zhu et al. 2016, 2017). Given our relatively new insights into the blurred boundaries between GPP and NPP during short incubations, it raises the obvious question: is it even possible to estimate GPP in the field using conventional "short-term" incubations, or is this an inherently flawed approach? To answer this, we compared ^{14}C-uptake rates obtained from 2 hr, versus 12hr incubations, using natural samples from a coastal reference station (Port Hacking, NSW, Australia) over an 18-month period. The reasonable equivalency between rates (Slope: 0.902, $R^2 = 0.871$, Fig. 6.4) provides compelling evidence that 2hr incubations do not reliably determine GPP for field samples, but are actually close to NPP.

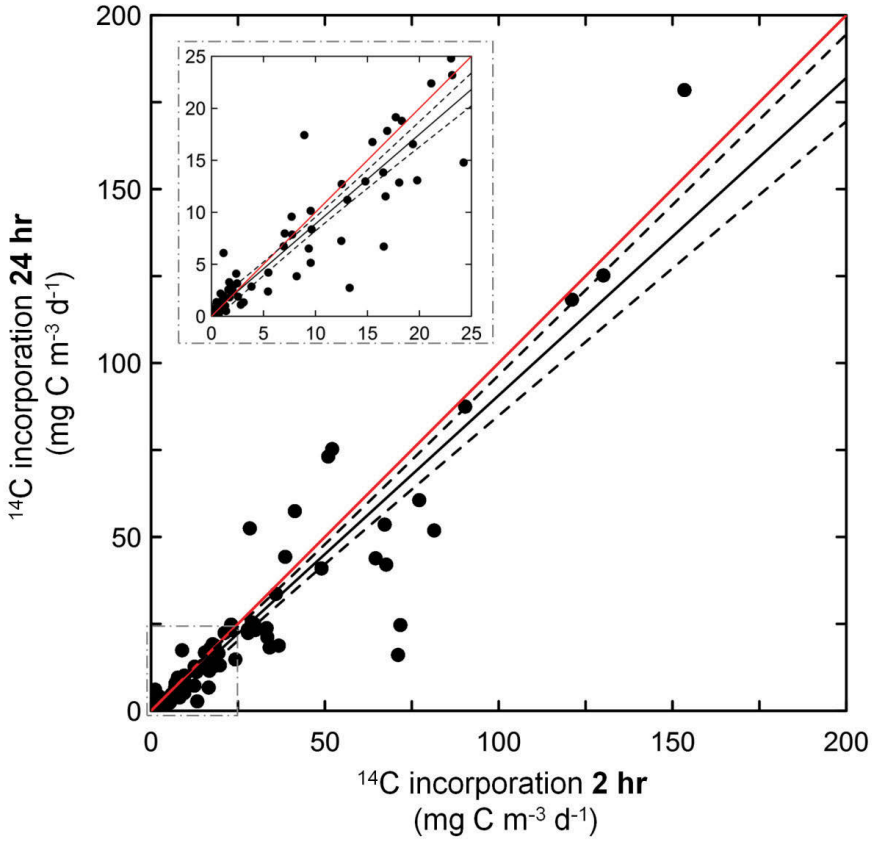

Figure 6.4 Comparison of C-fixation rates derived from both short (2 hr) and long (24 hr) 14C-incorporation incubations (250 ml), performed ex-situ following JGOFS protocols (Knapp et al. 1996). Data represents samples collected from natural phytoplankton assemblages (Port Hacking 100 m coastal reference station, NSW, Australia: 34.120ºS 151.224ºE) over a period of 18 months (April 2014 – September 2015). Linear regression generated r2 values of 0.86 (slope: 0.88). Breakout panel (inset, dashed grey lines) is used to provide clearer visualisation of lower values (0-25 mg C m-3 d-1). Black dashed lines show 95% confidence interval, whilst the solid red line represents a theoretical 1:1 relationship..

Clearly the use of short (in this context defined as 1-4 hr), and inconsistent, incubation lengths limits our ability to reconcile the observed variability of K_C for natural assemblages across broad spatial scales (Lawrenz et al. 2013). With inherent uncertainty surrounding the CO_2-uptake rates generated by incubation lengths within this timeframe, we ask whether future efforts should instead focus on deriving $K_{C\ [NPP]}$ where NPP can perhaps be measured with more confidence than GPP, e.g. in the case of Fig. 6.4, 2 hr would seem appropriate but clearly this would unlikely commonly apply

across systems and taxa. At this stage, we would propose that additional research is needed to determine the "sweet spot" in terms of incubation lengths long enough to reliably capture NPP, but not so long as to introduce sizeable artefacts arising from bottle effects, particularly under irradiance levels conducive to photoinhibition. Tentative evidence would suggest that an incubation length of ~6 hr may yield a CO_2-uptake rate equivalent to NPP independent of growth rate (Halsey et al. 2013), but further evaluation of both laboratory cultures and natural communities is still needed. The priority here is to ensure that by advocating lengthier incubation times we do not induce variability in K_C due to bottle-effects, which outweighs the current variability arising from the uncertainty of the balance between GPP and NPP captured by shorter incubation times. Unless we can overcome our ability to retrieve GPP from ^{14}C in the field, this may be the most currently desirable means to begin to better standardise data sets. Alternatively, additional experimentation could be performed to evaluate exactly where a given measured CO_2-uptake rate derived from short-term incubations falls on the spectrum between GPP and NPP (as per Halsey et al. 2010, 2011, 2014, 2015; Felcmanová et al. 2017).

Similarly, for consistency, future laboratory studies investigating K_C should be mindful of the broader limitations of resolving GPP, such that measurements from phytoplankton cultures can directly inform observations from the field (NPP). This is not to say that GPP should not be the target of laboratory studies. Indeed, developing an understanding of the mechanisms regulating K_C will require systematically tracking the flow of energy through various photosynthetic currencies (ETR_{PSII}, O_2 and CO_2-uptake), which is only feasible under controlled laboratory settings that track CO_2 uptake (GPP) into assimilation (NPP) and ultimately growth. Regardless, it is important that future

studies use terminology, e.g. $K_{C\,[GPP]}$ or $K_{C\,[NPP]}$ to clearly identify the ′carbon currency′ used.

Finally, characterisation of either particulate, or total organic carbon fixed (i.e. POC vs. TOC) will also affect the measured value of K_C. Usually for oceanographic studies, radiolabelled-samples are passed through filters to trap phytoplankton cells (representing POC), thus missing the variable fraction of radiolabelled-carbon that may have been released extracellularly as DOC.

6.9 A roadmap towards widespread implementation of FRRf for PP

A clear long-term goal for the growing number of FRRf practitioners and data-user communities is to be in a position where we possess sufficiently broad, high-quality, datasets that allow us to reconcile natural variability of K_C over space and time. Developments in technology and approach provide a roadmap towards this goal. The short-term priority must be to limit, or compensate for, methodological inconsistencies that have consistently plagued FRRf and carbon fixation datasets to date (see Table 6.5), allowing us to confidently and consistently, *measure* ′real′ variability of K_C across natural assemblages. Unquestionably, applying ′easy to fix′ sources of error must be central to study design and execution. For example, lack of spectral corrections of antennae sizes (e.g. Suggett et al. 2001, 2004), sample blanks and/or instrument corrections (e.g. Laney 2003; Laney et al. 2008) can introduce up to 100% error and thus are a first order priority.

Table 6.5 Methodological issues associated with FRRf measurements and recommended solutions/best practice.

Issue	Methodological Challenge	"Best-Practice" Solution
Spectral weighting of σ_{PSII}	σ_{PSII} is derived from FRRf excitation LED (e.g. 450nm) and must be scaled to phytoplankton absorption spectrum	Spectrally correct σ_{PSII} from Particulate absorption spectra (Pabs) measurements, or fluorescence excitation spectra (Flu-ex)
Spectral correction of actinic light source(s)	Differences in spectral output between actinic light sources used for FRRf and ^{14}C incubations must be corrected-for.	Use light source with very similar spectral output for ETR and ^{14}C incubations or: Spectrally correct PAR data from Pabs/Flu-ex or: Measure ETR and ^{14}C-uptake simultaneously under the same actinic source (e.g. Suggett et al. 2009)
Quantification of RCII	Proportion of functional PSII reaction centres [RCII] must be quantified/estimated to derive absolute ETR_{PSII}	Fluorometers should be calibrated to derive fluorescence-based $[RCII]_{[FRRF]}$ (Oxborough et al. 2012). Further validation of $[RCII]_{[FRRF]}$ against [RCII] from O_2 flash-yields needed. Continued evaluation of empirical approaches (Schuback et al. 2013)
Subtraction of baseline fluorescence (blank)	Baseline fluorescence from dissolved organic material may contaminate FRRf signal. Issue is exacerbated when fluorescence yield is low (e.g. low biomass regions). Leads to underestimation of ϕ_{PSII}	Baseline fluorescence (0.2µm filtered seawater) should be subtracted from discrete samples. During continuous/standalone profiling, baseline fluorescence should be periodically subtracted (recommended minimum twice-daily)
Calculation of ETR	Several equations/algorithms exist for which to calculate ETRs (see Fig. 6.5).	Use consistent approach to constructing ETRs to aid inter-comparison of datasets. Note: As ETRs can usually be re-calculated retrospectively from fluorescence variables, comparison between algorithms could be included in future publications to evaluate their relative performance
Underestimation of ETRs for cyanobacterial-dominated assemblages	Single-wavelength (blue LED) may fail to drive complete PSII reaction centre closure for communities dominated by cyanobacteria	Use multi-spectral fluorometers for communities known to be cyanobacteria-dominated. If constrained to using single-LED fluorometer induction data, quality-control fluorescence induction data periodically to check PSII-saturation is occurring.
Duration of photosynthesis-irradiance (PE) curves	Variable duration and number of light-steps may return variable paramaterisation of: α, ETR_{max} and therefore Ek (calculated as ETR_{max}/α)	Standardise exposure time and number of light-steps for PE-curves where possible. Ensure sufficient low-light steps to accurately derive α. Use sufficient irradiance to saturate photosynthesis (to reliably derive ETR_{max}).
Standardisation of single-turnover protocols	Variable instrument protocols	Maximise signal-to-noise ratio by using sufficient FRRf sequence acquisitions per measurement (especially for low-biomass). Clearly report instrument protocols used.
Variable Terminology	Inconsistent use of FRRf-related terminology within the literature	Adopt universal, recommended terminology

Based on Section 6.8, evidence would suggest we rapidly transition *towards preferentially longer incubations* that consistently estimate CO_2-uptake rates reflecting NPP using protocols that minimize bottle artefacts like photoacclimation, whilst simultaneously ensuring that routine ancillary measurements are collected to inform the key environmental drivers of K_C (see Table 6.6). However, in order to transition to longer incubations that are consistently reflecting some ′steady state′ NPP (Milligan et al. 2015), this will require intensification of studies that integrate time-resolved measurements of CO_2-fixation – an approach that will not be trivial for natural communities where biomass remains low. Photoacclimation might be avoided by mimicking vertical mixing through the mixed layer by using programmable LED light sources, but how well this can be achieved to mimic real-world complex physically dynamic regimes will first require much improved understanding of light-field regulation. *Adoption of clear and standardised terminology when reporting key parameters* (for both ETR_{PSII} and CO_2-uptake) will reduce methodological ambiguity and facilitate inter-comparison across datasets. Furthermore, calibration of fluorometers to measure $[RCII]^{[FRRf]}$ as per Oxborough et al. (2012) should also be considered a central step prior to FRRf-based campaigns. On this note, there are numerous approaches to constructing an absolute ETR_{PSII} (see Fig. 6.5), but as yet their relative performance has not been well scrutinised (but see Oxborough et al. 2012; Robinson et al. 2014; Silsbe et al. 2015). However, *reducing uncertainties in fluorescence yields and how they robustly scale to effective quantum yields*, e.g. re-adsorption of emitted fluorescence and interference from other pigments such as phycobilins, will be needed to reach this goal. Making these steps routine components of future studies, or of retrospective re-calculations of existing datasets, would allow us to determine which

algorithm is most broadly applicable, or if specific algorithms perform better under certain environmental or taxonomic conditions.

Table 6.6 Recommended ancillary measurements for future K_C campaigns. Measurements have been divided into essential and desirable for field studies (targeting CO_2-uptake rates representing NPP) and laboratory studies (CO_2-uptake rates equivalent to both GPP and NPP). No recommendation is given for measuring CO2-uptake reflecting GPP in the field, reflecting the methodological uncertainty involved: see **Section 6.5**).

	Field (natural assemblages)	Laboratory Studies	
	$K_{C\,[NPP]}$	$K_{C\,[GPP]}$ (<20 min)	$K_{C\,[NPP]}$ (8-12 hr)
Essential	PAR(λ)	PAR(λ)	PAR(λ)
	Nutrients (N, P, Si)	Temperature	Temperature
	Temperature	Salinity	Salinity
	Salinity	NPQ_{NSV}	NPQ_{NSV}
	NPQ_{NSV}	Blank Fluorescence (blank)	Blank Fluorescence (blank)
	Blank Fluorescence	Pabs <u>or</u> flu-ex	Pabs <u>or</u> flu-ex
	Particulate absorption spectra (Pabs) <u>or</u> Fluorescence excitation spectra (flu-ex)	Growth Rate	DIC
	Chl-*a*	DIC	
	Day length		
	Incubation PAR spectra		
	Dominant Taxa		
Desirable	Detailed Taxonomy (e.g. DNA or microscopy) Flow-cytometry	Cell volume	Cell volume
	Pigment quantification (via High Performance Liquid Chromatography)	POC:PON:POP	POC:PON:POP
	Size-fractionated Chl-a	DOC	DOC
	Dissolved organic carbon (DIC)	Nutrients (N, P, Si)	(N, P, Si)
	POC:PON		

Table 6.7 Construction of vETRPSII according to commonly-used algorithms from published studies, together with units and key information pertaining to each algorithm. All vETRs follow the same theoretical construct: $ETR_{PSII} = E \bullet a_{LHII} \bullet \Phi PSII$ but require unit correction factors to derive appropriate units, along with spectral correction).

ETR Algorithm	SI Units	Key Notes
1) Fixed n_{PSII}		
$E \cdot \sigma_{PSII} \cdot n_{PSII} \cdot [\text{Chl-}a] \cdot (F_v/F_m)^{-1} \cdot F_q'/F_m' \cdot \Phi_{RC}$	mol e^- (mg Chl-*a*) s^{-1}	Requires assumption of number of PSII units per unit Chl-*a* (n_{PSII}, mol RCII [mol Chl-a]$^{-1}$). Values of **0.002** for eukaryotes and **0.003** for prokaryotes are often used.
2) Direct [RCII] measurement		
$E \cdot \sigma_{PSII} \cdot [\text{RCII}] \cdot (F_v/F_m)^{-1} \cdot F_q'/F_m' \cdot \Phi_{RC}$	mol e^- m^{-3} s^{-1}	Requires use of O_2 flash-yield system to measure [RCII].
3) FRRf-based $[RCII]^{(FRRf)}$ algorithm		
$E \cdot \sigma_{PSII} \cdot [\text{RCII}]^{(FRRf)} \cdot (F_v/F_m)^{-1} \cdot F_q'/F_m' \cdot \Phi_{RC}$	mol e^- m^{-3} s^{-1}	Requires calibrated fluorometer to retrieve $[RCII]^{(FRRf)}$.
4) Absorption algorithm		
$E \cdot \frac{F_m \cdot F_o'}{F_m - F_o} \cdot \frac{K_R}{E_{LED}} \cdot F_q'/F_m' \cdot \Phi_{RC}$	mol e^- m^{-3} s^{-1}	No measurement of σ_{PSII} is required to calculate ETR. Requires calibrated fluorometer to derive K_R.
5) ETR on a per RCII basis		
$E \cdot \sigma_{PSII} \cdot (F_v/F_m)^{-1} \cdot F_q'/F_m' \cdot \Phi_{RC}$	mol e^- mol RCII^{-1} s^{-1}	Estimates rates of charge separation in functional RCIIs, but does not quantify total RCII content.

In the mid-term, field-studies can begin a process of algorithm evaluation *assessing the robustness of* more semi-empirical/theoretical (Oxborough et al. 2012) and empirical (Schuback et al. 2015, 2016) approaches to quantify K_C, across a range of biogeographical provinces. During this validation process, we can continue to evolve region-specific empirical models to predict K_C (as per Lawrenz et al. 2013), which *needs critical support from laboratory screening of* K_C under a diverse selection of taxa/strains and growth conditions to tease apart the respective influence of environment and taxonomy upon K_C. For field-based studies it is critical to also measure phytoplankton functional type data (HPLC pigment and flow cytometry) or use microscopy to resolve community composition. In addition to collecting data to support empirical modelling of K_C, it is critical that *we exploit functional genomic tools to develop a mechanistic understanding of electron allocation informed by taxonomic differences in genomic capacities, and in parallel use (meta) transcriptomic and metabolomic tools to improve our understanding of physiologically variable changes in*

metabolism (driven by potential changes in electron allocations and changes in nutrient acquisition strategies such as mixotrophy) within a taxon or community (e.g. Wu et al. 2014; Zorz et al. 2015). Membrane Inlet Mass Spectrometry (MIMS)-based O_2 dynamic measurements, which can unambiguously resolve water-splitting in parallel with transcriptomics and metabolomics to quantify presence of key markers for alternate electron fluxes could be used to mechanistically "deconstruct" K_C for key taxa or oceanographic regions. Very few studies have yet attempted to directly quantify the proportion of electrons being diverted into one or more AEFs (e.g. Bailey et al. 2008) relative to carbon fixation to explain variability of K_C, and this remains a fundamental knowledge gap. Whilst AEFs have been examined using photosynthetic pathway inhibitors to isolate specific electron pathways (e.g. as per Lewitus and Kana, 1995; Mackey et al. 2008; Ralph et al. 2010; but also see Roberty et al. 2014), *functional genomics platforms would enable these pathways to be examined as an operational network* using flux balance models.

As we begin to generate high-quality datasets, *the establishment of a centralised data repository (or at least ensure data is collected according to SOPs and subsequently made publically accessible) dedicated to FRRf-based campaigns* would bring significant added value to datasets and offer considerable research benefits to the wider community. Firstly, by integrating data into a centralised location, disparities in methodology used to derive K_C can be documented and accounted-for.

Secondly, the accessibility of multiple, quality-controlled datasets from global studies could be a game-changer for modellers of global PP, providing a central resource for data to feed directly into algorithm development and subsequent ground-truthing. NPP (using ^{14}C) global data sets have been the backbone of ever-improved algorithms to

retrieve high resolution marine productivity patterns from satellites (e.g. Saba et al. 2011). However, models that are built around ETR_{PSII}, GPP, and energy and reductant usage, would offer a new platform to understand the role of the oceans in global bio-energetic fluxes. Thirdly, and perhaps most critically, this repository (and its applications) would provide capacity to evolve over time to keep pace with technical developments. For example, archiving of fluorescence induction curves, rather than just key FRRf parameters extracted by any one physiological model, allows the potential for the retrospective application of future FRRf-based algorithm developments, or $[RCII]_{[FRRf]}$ calibration to historical datasets.

In conclusion, we are closer than ever in positioning ourselves to confidently evaluate the accuracy of fluorometric assessment coupled with CO_2-uptake. This can only happen if we can effectively use the growing global pool of FRRf platforms to generate sufficient datasets that allow us to (i) understand and model the critical photosynthetic conversion factor, the "electron requirement for carbon fixation", K_C; and (ii) develop new conceptual understanding of electrons as drivers of biological metabolism and associated biogeochemical cycles, and hence a relevant currency outright for MPP. The likelihood of such a scenario would be greatly increased by a more coherent and methodologically consistent research approach from the FRRf-community, to systematically address the important gaps in knowledge that still hinder our current understanding of K_C variability and complexity. In reviewing current gaps in knowledge and advances, we offer a research roadmap to realise this vision (Fig. 6.6). As part of this progression, we as a community must overcome long-held views of carbon as *the* currency of primary productivity, to enable progression towards complimentary mechanistic frameworks to capitalise on ever growing datasets of photosynthetic electron transfer, the fundamental driver of aquatic biogeochemical cycles.

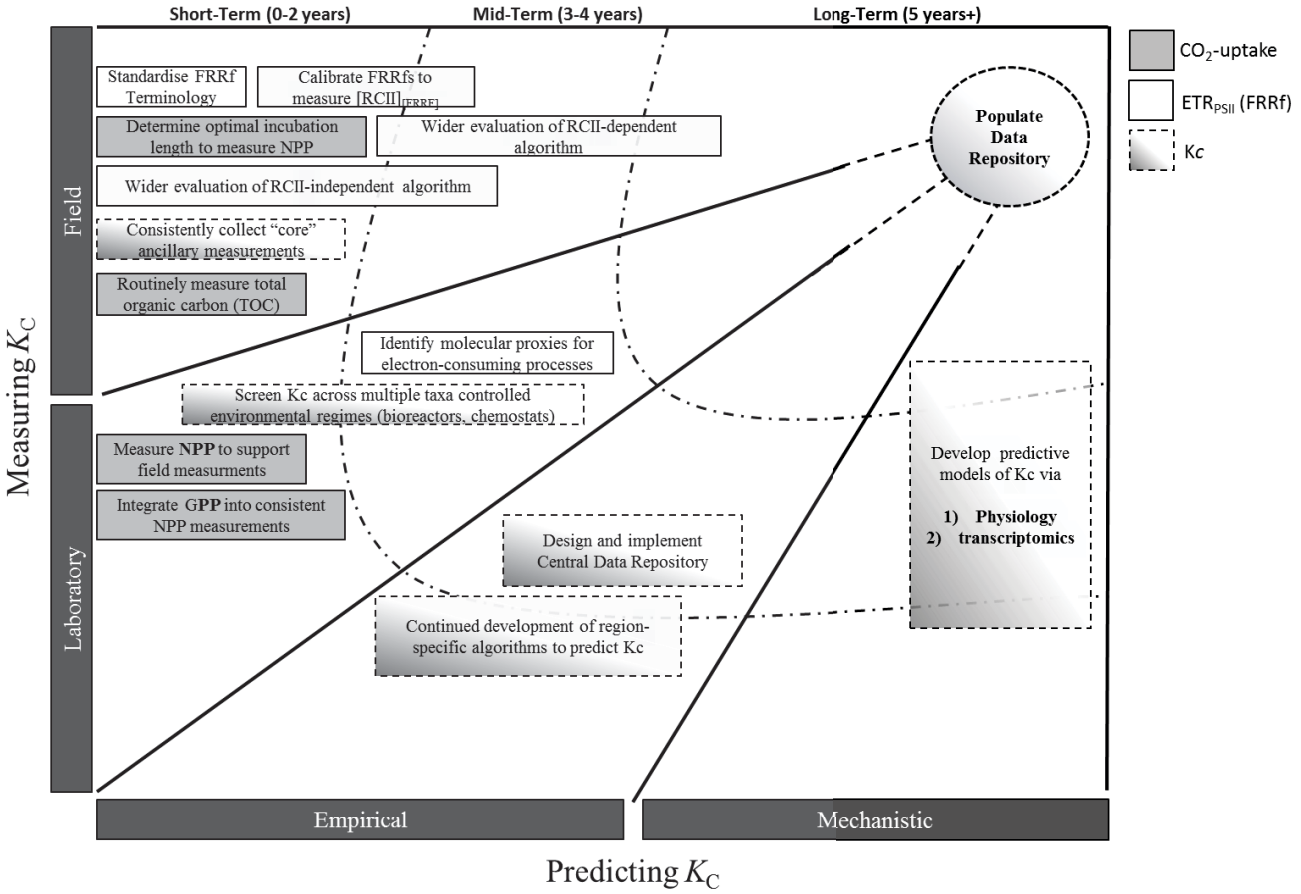

Figure 6.5 Roadmap for improving Fast Repetition Rate fluorometry (FRRf)-based estimates of primary productivity, focussing upon developing our predictive capability for the critical photosynthetic "exchange rate", K_C. Short-long term research objectives are outlined for laboratory and field measurements of both ETR_{PSII} and CO_2-uptake rates, together with recommended steps towards modelling K_C both empirically and mechanistically. The roadmap culminates in the long-term objective of populating a centralised data repository which would provide a dedicated resource from which to "ground-truth" satellite-based models of primary productivity.

6.10 Acknowledgements

We wish to acknowledge invaluable discussions across the peer community in distilling the concepts presented here; in particular, we thank John Raven, Dave Hutchins, Max Gorbunov, Yannick Huot. The contribution of DJS was supported by an ARC Future Fellowship (FT130100202, and input of MD and DJS enhanced through involvement with an ARC Linkage Infrastructure, Equipment and Facilities project LE160100146 led by David Antoine). Work of EL was funded by a FP7-PEOPLE-2013-IEF Marie Curie Fellowship (PIEF-GA-2013-630023). Data presented in Fig. 6.5 was supported by the CSIRO Marine and Coastal Carbon Biogeochemistry Cluster and Australia′s Integrated Marine Observing System (IMOS).

6.11 References

Allahverdiyeva, Y., J. Isojärvi, P. Zhang, and E.-M. Aro. 2015. Cyanobacterial oxygenic photosynthesis is protected by flavodiiron proteins. Life 5(1): 716-743.

Allen, A. E. and others. 2008. Whole-cell response of the pennate diatom *Phaeodactylum tricornutum* to iron starvation. Proc. Natl. Acad. Sci. U. S. A. 105(30): 10438-10443.

Allen, J. F. 2003. Cyclic, pseudocyclic and noncyclic photophosphorylation: new links in the chain. Trends Plant Sci. 8(1): 15-19.

Anderson, L. A. 1995. On the hydrogen and oxygen content of marine phytoplankton. Deep Sea Res., Part I. 42(9): 1675-1680.

Asada, K. 1999. The Water-water cycle in chloroplasts: Scavenging of active oxygens and dissipation of excess photons. Annu. Rev. Plant Physiol. Plant Mol. Biol. 50: 601-639.

Badger, M. R., T. J. Andrews, S. Whitney, M. Ludwig, D. C. Yellowlees, W. Leggat, and G. D. Price. 1998. The diversity and coevolution of RuBisCO, plastids, pyrenoids, and chloroplast-based CO_2-concentrating mechanisms in algae. Can. J. Bot. 76(6): 1052-1071.

Bailey, S. and others. 2008. Alternative photosynthetic electron flow to oxygen in marine *Synechococcus*. Biochim. Biophys. Acta, Bioenerg. 1777(3): 269-276.

Baines, S. B., and M. L. Pace. 1991. The production of dissolved organic matter by phytoplankton and its importance to bacteria: patterns across marine and freshwater systems. Limnol. Oceanogr. 36(6): 1078-1090.

Beardall, J. 1989. Photosynthesis and photorespiration in marine phytoplankton. Aquat. Bot. 34(1): 105-130.

Becker, J., P. Berube, C. Follett, J. Waterbury, S. Chisholm, E. Delong, and D. Repeta. 2014. Closely related phytoplankton species produce similar suites of dissolved organic matter. Front. Microbiol. 5(111). doi.org/10.3389/fmicb.2014.00111.

Behrenfeld, M. J., K. H. Halsey, and A. J. Milligan. 2008. Evolved physiological responses of phytoplankton to their integrated growth environment. Philos. Trans. R. Soc., B 363(1504): 2687-2703.

Behrenfeld, M. J., and Z. S. Kolber. 1999. Widespread iron limitation of phytoplankton in the South Pacific Ocean. Science 283(5403): 840-843.

Behrenfeld, M. J., O. Prasil, Z. S. Kolber, M. Babin, and P. G. Falkowski. 1998. Compensatory changes in photosystem II electron turnover rates protect photosynthesis from photoinhibition. Photosynth. Res. 58(3): 259-268.

Behrenfeld, M. J., K. Worthington, R. M. Sherrell, F. P. Chavez, P. Strutton, M. Mcphaden, and D. M. Shea. 2006. Controls on tropical Pacific Ocean productivity revealed through nutrient stress diagnostics. Nature 442(7106): 1025-1028.

Berg, G. M., J. Shrager, G. Van Dijken, M. M. Mills, K. R. Arrigo, and A. R. Grossman. 2011. Responses of psbA, hli and ptox genes to changes in irradiance in marine *Synechococcus* and *Prochlorococcus*. Aquat. Microb. Ecol. 65(1): 1-14.

Bertlisson, S., O. Berglund, M. J. Pullin, and S. W. Chisholm. 2005. Release of dissolved organic matter by *Prochlorococcus*. Vie et Milieu 55(3-4): 225-232.

Brading, P., M. E. Warner, D. J. Smith, and D. J. Suggett. 2013. Contrasting modes of inorganic carbon acquisition amongst *Symbiodinium* (Dinophyceae) phylotypes. New Phytol. 200(2): 432-442.

Campbell, D. A., and E. Tyystjärvi. 2012. Parameterization of photosystem II photoinactivation and repair. Biochim. Biophys. Acta, Bioenerg. 1817(1): 258-265.

Cardol, P. and others. 2008. An original adaptation of photosynthesis in the marine green alga Ostreococcus. Proc. Natl. Acad. Sci. 105(22): 7881-7886.

Cardol, P., G. Forti, and G. Finazzi. 2011. Regulation of electron transport in microalgae. Biochim. Biophys. Acta, Bioenerg. 1807(8): 912-918.

Cardol, P., G. Gloire, M. Havaux, C. Remacle, R. Matagne, and F. Franck. 2003. Photosynthesis and state transitions in mitochondrial mutants of *Chlamydomonas reinhardtii* affected in respiration. Plant Physiol. 133(4): 2010-2020.

Carlson, C. A. 2002. Production and removal processes, p. 91-151. In D. A. Hansell and C. A. Carlson [eds.], Biogeochemistry of marine dissolved organic matter. Academic Press.

Chavez, F. P., M. Messié, and J. T. Pennington. 2011. Marine primary production in relation to climate variability and change. Annu. Rev. Mar. Sci. 3: 227-260.

Cherrier, J., S. Valentine, B. Hamill, W. H. Jeffrey, and J. F. Marra. 2015. Light-mediated release of dissolved organic carbon by phytoplankton. J. Mar. Syst. 147: 45-51.

Claquin, P., J.-C. Kromkamp, and V. Martin-Jezequel. 2004. Relationship between photosynthetic metabolism and cell cycle in a synchronized culture of the marine alga *Cylindrotheca fusiformis* (Bacillariophyceae). Eur. J. Phycol. 39: 33–41.

Corno, G., R. M. Letelier, M. R. Abbott, and D. M. Karl. 2006. Assessing primary production variability in the North Pacific Subtropical Gyre: a comparison of fast repetition rate fluorometry and ^{14}C measurements. J. Phycol. 42(1): 51-60.

Cournac, L., E.-M. Josse, T. Joët, D. Rumeau, K. Redding, M. Kuntz, and G. Peltier. 2000. Flexibility in photosynthetic electron transport: a newly identified chloroplast oxidase involved in chlororespiration. Philos. Trans. R. Soc., B 355(1402): 1447-1454.

Cullen, J. 2001. Primary production methods. Mar. Ecol.: Prog. Ser. 52(77): 2277-2284.

Delong, E. F., and O. Beja. 2010. The light-driven proton pump proteorhodopsin enhances bacterial survival during tough times. PLoS Biol. 8(4): e1000359.

Dring, M. J., and D. H. Jewson. 1982. What does ^{14}C uptake by phytoplankton really measure? A theoretical modelling approach. Proc. R. Soc. Lond. [Biol]. 214(1196): 351-368.

Falkowski, P., and Z. Kolber. 1995. Variations in chlorophyll fluorescence yields in phytoplankton in the world oceans. Funct. Plant Biol. 22(2): 341-355.

Falkowski, P. G., Y. Fujita, A. Ley, and D. Mauzerall. 1986. Evidence for Cyclic Electron Flow around Photosystem II in *Chlorella pyrenoidosa.* Plant Physiol. 81(1): 310-312.

Falkowski, P. G., T. G. Owens, A. C. Ley, and D. C. Mauzerall. 1981. Effects of growth irradiance levels on the ratio of reaction centers in two species of marine phytoplankton. Plant Physiol. 68(4): 969-973.

Felcmanová, K., M. Lukeš, E. Kotabová, E. Lawrenz, K. H. Halsey, and O. Prášil. 2017. Carbon use efficiencies and allocation strategies in *Prochlorococcus marinus* strain PCC 9511 during nitrogen-limited growth. Photosynth. Res. 134(1): 71-82.

Finkel, Z. V., M. J. Follows, J. D. Liefer, C. M. Brown, I. Benner, and A. J. Irwin. 2016. Phylogenetic diversity in the macromolecular composition of microalgae. PloS one 11(5): e0155977.

Fisher, N. L., and K. H. Halsey. 2016. Mechanisms that increase the growth efficiency of diatoms in low light. Photosynth. Res. 129(2): 183-197.

Flameling, I. A., and J. Kromkamp. 1998. Light dependence of quantum yields for PSII charge separation and oxygen evolution in eucaryotic algae. Limnol. Oceanogr. 43(2): 284-297.

Foyer, C. H., M. Lelandais, and K. J. Kunert. 1994. Photooxidative stress in plants. Physiol. Plant. 92(4): 696-717.

Fujiki, T., T. Hosaka, H. Kimoto, T. Ishimaru, and T. Saino. 2008. *In situ* observation of phytoplankton productivity by an underwater profiling buoy system: use of fast repetition rate fluorometry. Mar. Ecol.: Prog. Ser. 353: 81-88.

Fujiki, T., T. Suzue, H. Kimoto, and T. Saino. 2007. Photosynthetic electron transport in *Dunaliella tertiolecta* (Chlorophyceae) measured by fast repetition rate fluorometry: relation to carbon assimilation. J. Plankton Res. 29(2): 199-208.

Genty, B., J.-M. Briantais, and N. R. Baker. 1989. The relationship between the quantum yield of photosynthetic electron transport and quenching of chlorophyll fluorescence. Biochim. Biophys. Acta, Gen. Sub 990(1): 87-92.

Giordano, M., A. Norici, and R. Hell. 2005. Sulfur and phytoplankton: acquisition, metabolism and impact on the environment. New Phytol. 166(2): 371-382.

Gorbunov, M. Y., and P. G. Falkowski. 2004. Fluorescence induction and relaxation (FIRe) technique and instrumentation for monitoring photosynthetic processes and primary production in aquatic ecosystems. In: *Photosynthesis: Fundamental Aspects to Global Perspectives-Proc. 13th International Congress of Photosynthesis*, 1029-1031.

Gorbunov, M. Y., Z. S. Kolber, and P. G. Falkowski. 1999. Measuring photosynthetic parameters in individual algal cells by Fast Repetition Rate fluorometry. Photosynth. Res. 62(2): 141-153.

Gorbunov, M. Y., Z. S. Kolber, M. P. Lesser, and P. G. Falkowski. 2001. Photosynthesis and photoprotection in symbiotic corals. Limnol. Oceanogr. 46(1): 75-85.

Gorbunov, M. Y., F. I. Kuzminov, V. V. Fadeev, J. D. Kim, and P. G. Falkowski. 2011. A kinetic model of non-photochemical quenching in cyanobacteria. Biochim. Biophys. Acta, Bioenerg. 1807(12): 1591-1599.

Greene, R. M., R. J. Geider, Z. Kolber, and P. G. Falkowski. 1992. Iron-induced changes in light harvesting and photochemical energy conversion processes in eukaryotic marine algae. Plant Physiol. 100(2): 565-575.

Grossman, A. R., K. R. Mackey, and S. Bailey. 2010. A perspective on photosynthesis in the oligotrophic oceans: hypotheses concerning alternate routes of electron flow. J. Phycol. 46(4): 629-634.

Halsey, H. K., J. A. Milligan, and J. M. Behrenfeld. 2014. Contrasting strategies of photosynthetic energy utilization drive lifestyle strategies in ecologically important picoeukaryotes. Metabolites 4(2): 260-280.

Halsey, K. H., and B. M. Jones. 2015. Phytoplankton strategies for photosynthetic energy allocation. Annu. Rev. Mar. Sci. 7: 265-297.

Halsey, K. H., A. J. Milligan, and M. J. Behrenfeld. 2010. Physiological optimization underlies growth rate-independent chlorophyll-specific gross and net primary production. Photosynth. Res. 103(2): 125-137.

Halsey, K. H., A. J. Milligan, and M. J. Behrenfeld. 2011. Linking time-dependent carbon-fixation efficiencies in *Dunaliella tertiolecta* (chlorophyceae) to underlying metabolic pathways. J. Phycol. 47(1): 66-76.

Halsey, K. H., R. T. O'malley, J. R. Graff, A. J. Milligan, and M. J. Behrenfeld. 2013. A common partitioning strategy for photosynthetic products in evolutionarily distinct phytoplankton species. New Phytol. 198(4): 1030-1038.

Hancke, K., T. Dalsgaard, M. K. Sejr, S. Markager, and R. N. Glud. 2015. Phytoplankton productivity in an Arctic Fjord (West Greenland): estimating electron requirements for carbon fixation and oxygen production. PloS One 10(7): e0133275.

Heber, U. 2002. Irrungen, Wirrungen? The Mehler reaction in relation to cyclic electron transport in C3 plants. Photosynth. Res. 73(1): 223-231.

Helman, Y., D. Tchernov, L. Reinhold, M. Shibata, T. Ogawa, R. Schwarz, I. Ohad, and A. Kaplan. 2003. Genes encoding A-type flavoproteins are essential for photoreduction of O_2 in Cyanobacteria. Curr. Biol. 13(3): 230-235.

Hoppe, C. J. M., L.-M. Holtz, S. Trimborn, and B. Rost. 2015. Ocean acidification decreases the light-use efficiency in an Antarctic diatom under dynamic but not constant light. New Phytol. 207(1): 159-171.

Hughes, D.J., Varkey, D., Doblin, M.A., Ingleton, T., Mcinnes, A., Ralph, P.J., van Dongen-Vogels, V and D.J Suggett. 2018. Impact of nitrogen availability upon the electron requirement for carbon fixation in Australian coastal phytoplankton communities (In Press). Limnol. Oceanogr. DOI: 10.1002/lno.10814

Huner, N. P., G. Öquist, and F. Sarhan. 1998. Energy balance and acclimation to light and cold. Trends Plant Sci. 3(6): 224-230.

Huot, Y., and M. Babin. 2010. Overview of fluorescence protocols: theory, basic concepts, and practice, p. 31-74. In D. Suggett, O. Prášil and M. Borowitzka [eds.], Chlorophyll a fluorescence in aquatic sciences: Methods and applications. Springer.

Ilík, P. and others. 2017. Alternative electron transport mediated by flavodiiron proteins is operational in organisms from cyanobacteria up to gymnosperms. New Phytol. 214(3):97-972.

Kana, T. M. 1992. Relationship between photosynthetic oxygen cycling and carbon assimilation in *Synechococcus* WH7803 (Cyanophyta). J. Phycol. 28(3): 304-308.

Kana, T. M. 1993. Rapid oxygen cycling in *Trichodesmium thiebautii*. Limnol. Oceanogr. 38(1): 18-24.

Kirilovsky, D. 2007. Photoprotection in cyanobacteria: the orange carotenoid protein (OCP)-related non-photochemical-quenching mechanism. Photosynth. Res. 93(1-3): 7.

Kirilovsky, D. 2015. Modulating energy arriving at photochemical reaction centers: orange carotenoid protein-related photoprotection and state transitions. Photosynth. Res. 126(1): 3-17.

Klughammer, C., and U. Schreiber. 2008. Complementary PS II quantum yields calculated from simple fluorescence parameters measured by PAM fluorometry and the Saturation Pulse method. PAM Application Notes 1(2).

Koblížek, M., D. Kaftan, and L. Nedbal. 2001. On the relationship between the non-photochemical quenching of the chlorophyll fluorescence and the Photosystem II light harvesting efficiency. A repetitive flash fluorescence induction study. Photosynth. Res. 68(2): 141-152

Kolber, Z., and P. G. Falkowski. 1993. Use of active fluorescence to estimate phytoplankton photosynthesis *in situ*. Limnol. Oceanogr. 38(8): 1646-1665.

Kolber, Z., J. Zehr, and P. Falkowski. 1988. Effects of growth irradiance and nitrogen limitation on photosynthetic energy conversion in photosystem II. Plant Physiol. 88(3): 923-929.

Kolber, Z. S., R. T. Barber, K. H. Coale, S. E. Fitzwateri, R. M. Greene, K. S. Johnson, S. Lindley, and P. G. Falkowski. 1994. Iron limitation of phytoplankton photosynthesis in the equatorial Pacific Ocean. Nature 371(6493): 145-149.

Kolber, Z. S., O. Prášil, and P. G. Falkowski. 1998. Measurements of variable chlorophyll fluorescence using fast repetition rate techniques: defining methodology and experimental protocols. Biochim. Biophys. Acta, Bioenerg. 1367(1–3): 88-106.

Krall, J. P., and G. E. Edwards. 1992. Relationship between photosystem II activity and CO_2 fixation in leaves. Physiol. Plant. 86(1): 180-187.

Kramer, D. M., G. Johnson, O. Kiirats, and G. E. Edwards. 2004. New fluorescence parameters for the determination of Q_A redox state and excitation energy fluxes. Photosynth. Res. 79(2): 209-218.

Kromkamp, J. C., N. A. Dijkman, J. Peene, S. G. Simis, and H. J. Gons. 2008. Estimating phytoplankton primary production in Lake IJsselmeer (The Netherlands) using variable fluorescence (PAM-FRRF) and C-uptake techniques. Eur. J. Phycol. 43(4): 327-344.

Kromkamp, J. C., and R. M. Forster. 2003. The use of variable fluorescence measurements in aquatic ecosystems: differences between multiple and single turnover measuring protocols and suggested terminology. Eur. J. Phycol. 38(2): 103-112.

Lancelot, C. 1983. Factors affecting phytoplankton extracellular release in the Southern Bight of the North Sea. Mar. Ecol.: Prog. Ser. 12(2): 115-121.

Laney, S. 2003. Assessing the error in photosynthetic properties determined with Fast Repetition Rate fluorometry. Limnol. Oceanogr. 48(6): 2234-2242.

Laney, S. R., and R. M. Letelier. 2008. Artifacts in measurements of chlorophyll fluorescence transients, with specific application to fast repetition rate fluorometry. Limnol. Oceanogr. Methods 6: 40-50.

Lavaud, J. 2007. Fast regulation of photosynthesis in diatoms: mechanisms, evolution and ecophysiology. Funct. Plant Sci. Biotechnol. 1: 267-287.

Lavaud, J., R. F. Strzepek, and P. G. Kroth. 2007. Photoprotection capacity differs among diatoms: Possible consequences on the spatial distribution of diatoms related to fluctuations in the underwater light climate. Limnol. Oceanogr. 52(3): 1188-1194.

Lavaud, J., H. J. Van Gorkom, and A.-L. Etienne. 2002. Photosystem II electron transfer cycle and chlororespiration in planktonic diatoms. Photosynth. Res. 74(1): 51-59.

Lawrenz, E. and others. 2013. Predicting the electron requirement for carbon fixation in seas and oceans. PLoS One 8(3): e58137.

Laws, E. A. 1991. Photosynthetic quotients, new production and net community production in the open ocean. Deep Sea Res., Part I. 38(1): 143-167.

Leboulanger, C., V. Martin-Jézéquel, C. Descolas-Gros, A. Sciandra, and H. J. Jupin. 1998. Photorespiration in continuous culture of *Dunaliella tertiolecta* (Chlorophyta): relationships between serine, glycine, and extracellular glycolate. J. Phycol. 34(4): 651-654.

Lewitus, A. J., and T. M. Kana. 1995. Light respirtion in six estuarine phytoplankton species: contrasts under photoautotrophic nd mixotrophic growth conditions. J. Phycol. 31(5): 754-761.

Li, Z., S. Wakao, B. B. Fischer, and K. K. Niyogi. 2009. Sensing and responding to excess light. Annu. Rev. Plant Biol. 60: 239-260.

Lin, H., F. I. Kuzminov, J. Park, S. Lee, P. G. Falkowski, and M. Y. Gorbunov. 2016. The fate of photons absorbed by phytoplankton in the global ocean. Science 351(6270): 264-267.

Longhurst, A., S. Sathyendranath, T. Platt, and C. Caverhill. 1995. An estimate of global primary production in the ocean from satellite radiometer data. J. Plankton Res. 17(6): 1245-1271.

López-Sandoval, D. C., T. Rodríguez-Ramos, P. Cermeño, C. Sobrino, and E. Marañón. 2014. Photosynthesis and respiration in marine phytoplankton: Relationship with cell size, taxonomic affiliation, and growth phase. J. Exp. Mar. Biol. Ecol. 457: 151-159.

Macey, A., T. Ryan-Keogh, S. Richier, C. Moore, and T. Bibby. 2014. Photosynthetic protein stoichiometry and photophysiology in the high latitude North Atlantic. Limnol. Oceanogr. 59(6): 1853-1864.

Mackey, K. R. M., A. Paytan, A. R. Grossman, and S. Bailey. 2008. A photosynthetic strategy for coping in a high-light, low-nutrient environment. Limnol. Oceanogr. 53(3): 900-913.

Makino, A., C. Miyake, and A. Yokota. 2002. Physiological Functions of the water–water cycle (Mehler Reaction) and the Cyclic Electron Flow around PSI in rice leaves. Plant Cell Physiol. 43(9): 1017-1026.

Marra, J. 2009. Net and gross productivity: weighing in with ^{14}C. Aquat. Microb. Ecol. 56(2-3): 123-131.

Martiny, A., J. A. Vrugt, F. W. Primeau, and M. W. Lomas. 2013. Regional variation in the particulate organic carbon to nitrogen ratio in the surface ocean. Global Biogeochem. Cycles 27(3): 723-731.

Mckew, B. A. and others. 2013. The trade-off between the light-harvesting and photoprotective functions of fucoxanthin-chlorophyll proteins dominates light acclimation in *Emiliania huxleyi* (clone CCMP 1516). New Phytol. 200(1): 74-85.

Melrose, D. C., C. A. Oviatt, J. E. O'reilly, and M. S. Berman. 2006. Comparisons of fast repetition rate fluorescence estimated primary production and ^{14}C uptake by phytoplankton. Mar. Ecol.: Prog. Ser. 311: 37-46.

Milligan, A. J., K. H. Halsey, and M. J. Behrenfeld. 2015. Advancing interpretations of 14C-uptake measurements in the context of phytoplankton physiology and ecology. J. Plankton Res. 37(4): 692-698.

Miyake, C. 2010. Alternative Electron Flows (Water–Water Cycle and Cyclic Electron Flow around PSI) in photosynthesis: molecular mechanisms and physiological functions. Plant Cell Physiol. 51(12): 1951-1963.

Miyake, C., and M. Okamura. 2003. Cyclic Electron Flow within PSII protects PSII from its photoinhibition in thylakoid membranes from spinach chloroplasts. Plant Cell Physiol. 44(4): 457-462.

Miyake, C., K. Yonekura, Y. Kobayashi, and A. Yokota. 2002. Cyclic electron flow within PSII functions in intact chloroplasts from spinach leaves. Plant Cell Physiol. 43(8): 951-957.

Moore, C. M. and others. 2003. Physical controls on phytoplankton physiology and production at a shelf sea front: a fast repetition-rate fluorometer based field study. Mar. Ecol.: Prog. Ser. 259: 29-45.

Moore, C. M., D. J. Suggett, A. E. Hickman, Y.-N. Kim, J. F. Tweddle, J. Sharples, R. J. Geider, and P. M. Holligan. 2006. Phytoplankton photoacclimation and photoadaptation in response to environmental gradients in a shelf sea. Limnol. Oceanogr. 51(2): 936-949.

Morris, J. J., Z. I. Johnson, M. J. Szul, M. Keller, and E. R. Zinser. 2011. Dependence of the cyanobacterium *Prochlorococcus* on hydrogen peroxide scavenging microbes for growth at the ocean's surface. PloS One 6(2): e16805.

Murphy, C. D. and others. 2017. Quantitating active Photosystem II reaction center content from fluorescence induction transients. Limnol. Oceanogr.: Methods 15(1): 54-69.

Oxborough, K., C. M. Moore, D. J. Suggett, T. Lawson, H. G. Chan, and R. J. Geider. 2012. Direct estimation of functional PSII reaction center concentration and PSII electron flux on a volume basis: a new approach to the analysis of Fast Repetition Rate fluorometry (FRRf) data. Limnol. Oceanogr.: Methods 10(3): 142-154.

Panzenböck, M. 2007. Effect of solar radiation on photosynthetic extracellular carbon release and its microbial utilization in alpine and Arctic lakes. Aquat. Microb. Ecol. 48(2): 155-168.

Partensky, F., W. R. Hess, and D. Vaulot. 1999. *Prochlorococcus*, a marine photosynthetic prokaryote of global significance. Microbiol. Mol. Biol. Rev. 63(1): 106-127.

Peltier, G., D. Tolleter, E. Billon, and L. Cournac. 2010. Auxiliary electron transport pathways in chloroplasts of microalgae. Photosynth. Res. 106(1): 19-31.

Postgate, J. R. 1974. New advances and future potential in biological nitrogen fixation. J. Appl. Bacteriol. 37(2): 185-202.

Prasil, O., Z. Kolber, J. A. Berry, and P. G. Falkowski. 1996. Cyclic electron flow around photosystem II in vivo. Photosynth. Res. 48(3): 395-410.

Raateoja, M., J. Seppälä, and P. Ylöstalo. 2004. Fast repetition rate fluorometry is not applicable to studies of filamentous cyanobacteria from the Baltic Sea. Limnol. Oceanogr. 49(4): 1006-1012.

Ralph, P. J., C. Wilhelm, J. Lavaud, T. Jakob, K. Petrou, and S. A. Kranz. 2010. Fluorescence as a tool to understand changes in photosynthetic electron flow regulation, p. 75-89. In D. Suggett, O. Prášil and M. Borowitzka [eds.], Chlorophyll a fluorescence in aquatic sciences: Methods and applications. Springer.

Raven, J. A., J. Beardall, and M. Giordano. 2014. Energy costs of carbon dioxide concentrating mechanisms in aquatic organisms. Photosynth. Res. 121(2-3): 111-124.

Redfield, A. C. 1934. On the proportions of organic derivatives in sea water and their relation to the composition of plankton. University Press of Liverpool.

Roberty, S., B. Bailleul, N. Berne, F. Franck, and P. Cardol. 2014. PSI Mehler reaction is the main alternative photosynthetic electron pathway in *Symbiodinium* sp., symbiotic dinoflagellates of cnidarians. New Phytol. 204(1): 81-91.

Robinson, C., D. J. Suggett, N. Cherukuru, P. J. Ralph, and M. A. Doblin. 2014. Performance of Fast Repetition Rate fluorometry based estimates of primary productivity in coastal waters. J. Mar. Syst. 139: 299-310.

Royer, S. J., A. S. Mahajan, M. Galí, E. Saltzman, and R. Simó. 2015. Small-scale variability patterns of DMS and phytoplankton in surface waters of the tropical and subtropical Atlantic, Indian, and Pacific Oceans. Geophys. Res. Lett. 42(2): 475-483.

Ruban, A., J. Lavaud, B. Rousseau, G. Guglielmi, P. Horton, and A.-L. Etienne. 2004. The super-excess energy dissipation in diatom algae: comparative analysis with higher plants. Photosynth. Res. 82(2): 165-175.

Ryan-Keogh, T. J. and others. 2013. Spatial and temporal development of phytoplankton iron stress in relation to bloom dynamics in the high-latitude North Atlantic Ocean. Limnol. Oceanogr. 58(2): 533-545.

Ryan-Keogh, T. J., A. I. Macey, A. M. Cockshutt, C. M. Moore, and T. S. Bibby. 2012. The cyanobacterial chlorophyll-binding-protein IsiA acts to increase the in vivo effective absorption cross-section of PSI under iron limitation. J. Phycol. 48(1): 145-154.

Saba, V. and others. 2011. An evaluation of ocean color model estimates of marine primary productivity in coastal and pelagic regions across the globe. Biogeosciences 8:489-503.

Scherer, S., H. Almon, and P. Böger. 1988. Interaction of photosynthesis, respiration and nitrogen fixation in cyanobacteria. Photosynth. Res. 15(2): 95-114.

Schrader, P. S., A. J. Milligan, and M. J. Behrenfeld. 2011. Surplus photosynthetic antennae complexes underlie diagnostics of iron limitation in a cyanobacterium. PLoS One 6(4): e18753.

Schreiber, U., U. Schliwa, and W. Bilger. 1986. Continuous recording of photochemical and non-photochemical chlorophyll fluorescence quenching with a new type of modulation fluorometer. Photosynth. Res. 10(1): 51-62.

Schuback, N., M. Flecken, M. T. Maldonado, and P. D. Tortell. 2016. Diurnal variation in the coupling of photosynthetic electron transport and carbon fixation in iron-limited phytoplankton in the NE subarctic Pacific. Biogeosciences 13(4): 1019-1035.

Schuback, N., C. J. Hoppe, J. É. Tremblay, M. T. Maldonado, and P. D. Tortell. 2017. Primary productivity and the coupling of photosynthetic electron transport and carbon fixation in the Arctic Ocean. Limnol. Oceanogr. 62: 898-921.

Schuback, N., C. Schallenberg, C. Duckham, M. T. Maldonado, and P. D. Tortell. 2015. Interacting effects of light and iron availability on the coupling of photosynthetic electron transport and CO_2-assimilation in marine phytoplankton. PLoS One 10(7): e0133235.

Silsbe, G. M. and others. 2015. Toward autonomous measurements of photosynthetic electron transport rates: An evaluation of active fluorescence-based measurements of photochemistry. Limnol. Oceanogr.: Methods 13(3): 138-155.

Simon, N., A.-L. Cras, E. Foulon, and R. Lemée. 2009. Diversity and evolution of marine phytoplankton. C. R. Biol. 332(2–3): 159-170.

Six, C., Z. V. Finkel, F. Rodriguez, D. Marie, F. Partensky, and D. A. Campbell. 2008. Contrasting photoacclimation costs in ecotypes of the marine eukaryotic picoplankter *Ostreococcus*. Limnol. Oceanogr. 53(1): 255-265.

Slawyk, G., Y. Collos, and J. C. Auclair. 1977. The use of the ^{13}C and ^{15}N isotopes for the simultaneous measurement of carbon and nitrogen turnover rates in marine phytoplankton. Limnol. Oceanogr. 22(5): 925-932.

Smyth, T. J., K. L. Pemberton, J. Aiken, and R. J. Geider. 2004. A methodology to determine primary production and phytoplankton photosynthetic parameters from Fast Repetition Rate Fluorometry. J. Plankton Res. 26(11): 1337-1350.

Steeman-Nielsen, E. 1952. The use of radioactive carbon (C^{14}) for measuring organic production in the sea. ICES J. Mar. Sci. 18(2): 117-140.

Steglich, C., M. Futschik, T. Rector, R. Steen, and S. W. Chisholm. 2006. Genome-wide analysis of light sensing in *Prochlorococcus*. J. Bacteriol. 188(22): 7796-7806.

Suggett, D., G. Kraay, P. Holligan, M. Davey, J. Aiken, and R. Geider. 2001. Assessment of photosynthesis in a spring cyanobacterial bloom by use of a fast repetition rate fluorometer. Limnol. Oceanogr. 46(4): 802-810.

Suggett, D. J., S. Goyen, C. Evenhuis, M. Szabó, D. T. Pettay, M. E. Warner, and P. J. Ralph. 2015. Functional diversity of photobiological traits within the genus *Symbiodinium* appears to be governed by the interaction of cell size with cladal designation. New Phytol. 208(2): 370-381.

Suggett, D. J., S. C. Maberly, and R. J. Geider. 2006. Gross photosynthesis and lake community metabolism during the spring phytoplankton bloom. Limnol. Oceanogr. 51(5): 2064-2076.

Suggett, D. J., H. L. Macintyre, and R. J. Geider. 2004. Evaluation of biophysical and optical determinations of light absorption by photosystem II in phytoplankton. Limnol. Oceanogr.: Methods 2(10): 316-332.

Suggett, D. J., H. L. Macintyre, T. M. Kana, and R. J. Geider. 2009. Comparing electron transport with gas exchange: parameterising exchange rates between alternative photosynthetic currencies for eukaryotic phytoplankton. Aquat. Microb. Ecol. 56(2-3): 147-162.

Suggett, D. J., C. M. Moore, A. E. Hickman, and R. J. Geider. 2009. Interpretation of fast repetition rate (FRR) fluorescence: signatures of phytoplankton community structure versus physiological state. Mar. Ecol.: Prog. Ser. 376: 1-19.

Suggett, D. J., K. Oxborough, N. R. Baker, H. L. Macintyre, T. M. Kana, and R. J. Geider. 2003. Fast repetition rate and pulse amplitude modulation chlorophyll a fluorescence measurements for assessment of photosynthetic electron transport in marine phytoplankton. Eur. J. Phycol. 38(4): 371-384.

Suggett, D. J., O. Prášil, and M. A. Borowitzka. 2010. Chlorophyll a fluorescence in aquatic sciences: methods and applications. Springer.

Szabó, M. and others. 2014. Photosynthetic acclimation of *Nannochloropsis oculata* investigated by multi-wavelength chlorophyll fluorescence analysis. Bioresour. Technol. 167: 521-529.

Takahashi, H., S. Kopriva, M. Giordano, K. Saito, and R. Hell. 2011. Sulfur assimilation in photosynthetic organisms: molecular functions and regulations of transporters and assimilatory enzymes. Annu. Rev. Plant Biol. 62: 157-184.

Timmermans, K., W. Stolte, and H. D. Baar. 1994. Iron-mediated effects on nitrate reductase in marine phytoplankton. Mar. Biol. 121(2): 389-396.

Tortell, P. D. 2000. Evolutionary and ecological perspectives on carbon acquisition in phytoplankton. Limnol. Oceanogr. 45(3): 744-750.

Trampe, E. C. L., P. J. Hansen, and M. Kühl. 2015. A comparison of photosynthesis measurements by O_2 evolution, ^{14}C assimilation and variable chlorophyll fluorescence during light acclimatization of the diatom *Coscinodiscus granii*. Algae 30(2): 103-119.

Vass, I. 2011. Role of charge recombination processes in photodamage and photoprotection of the photosystem II complex. Physiol. Plant. 142(1): 6-16.

Wagner, H., T. Jakob, A. Fanesi, and C. Wilhelm. 2017. Towards an understanding of the molecular regulation of carbon allocation in diatoms: the interaction of energy and carbon allocation. Phil. Trans. R. Soc. B 372(1728): 20160410.

Wagner, H., T. Jakob, J. Lavaud, and C. Wilhelm. 2016. Photosystem II cycle activity and alternative electron transport in the diatom *Phaeodactylum tricornutum*

under dynamic light conditions and nitrogen limitation. Photosynth. Res. 128(2): 151-161.

Waring, J., M. Klenell, U. Bechtold, G. J. C. Underwood, and N. R. Baker. 2010. Light-induced responses of oxygen photoreduction, reactive oxygen species production and scavenging in two diatom species. J. Phycol. 46(6): 1206-1217.

Williams, P. 1993. Chemical and tracer methods of measuring plankton production. ICES Mar. Sci. Symp. 197: 20-36.

Williams, P. J. L. B., D. N. Thomas, and C. S. Reynolds. 2008. Phytoplankton productivity: carbon assimilation in marine and freshwater ecosystems. John Wiley and Sons.

Wu, Y., J. Jeans, D. J. Suggett, Z. V. Finkel, and D. A. Campbell. 2014. Large centric diatoms allocate more cellular nitrogen to photosynthesis to counter slower RUBISCO turnover rates. Front. Mar. Sci. 1: 68.

Zehr, J. P., and R. M. Kudela. 2009. Photosynthesis in the Open Ocean. Science 326(5955): 945-946.

Zevenboom, W., and L. R. Mur. 1980. N_2-fixing cyanobacteria: why they do not become dominant in Dutch, hypertrophic lake, p. 123-130. In J. Barica and L. R. Mur [eds.], Hypertrophic ecosystems. Springer.

Zhu, Y., J. Ishizaka, S. C. Tripathy, S. Wang, Y. Mino, T. Matsuno, and D. J. Suggett. 2016. Variation of the photosynthetic electron transfer rate and electron requirement for daily net carbon fixation in Ariake Bay, Japan. J. Oceanogr. 72(5): 761-776.

Zhu, Y., J. Ishizaka, S. C. Tripathy, S. Wang, C. Sukigara, J. Goes, T. Matsuno, and D. J. Suggett. 2017. Relationship between light, community composition, and the electron requirement for carbon fixation in natural phytoplankton assemblages of the East China Sea. Mar. Ecol.: Prog. Ser. doi.org/10.3354/meps1231.

Zorz, J. K., J. R. Allanach, C. D. Murphy, M. S. Roodvoets, D. A. Campbell, and A. M. Cockshutt. 2015. The RUBISCO to photosystem II ratio limits the maximum photosynthetic rate in picocyanobacteria. Life 5(1): 403-417.